



National Library  
of Canada

Bibliothèque nationale  
du Canada

Canadian Theses Service    Service des thèses canadiennes

Ottawa, Canada  
K1A 0N4

## NOTICE

The quality of this microform is heavily dependent upon the quality of the original thesis submitted for microfilming. Every effort has been made to ensure the highest quality of reproduction possible.

If pages are missing, contact the university which granted the degree.

Some pages may have indistinct print especially if the original pages were typed with a poor typewriter ribbon or if the university sent us an inferior photocopy.

Reproduction in full or in part of this microform is governed by the Canadian Copyright Act, R.S.C. 1970, c. C-30, and subsequent amendments.

## AVIS

La qualité de cette microforme dépend grandement de la qualité de la thèse soumise au microfilmage. Nous avons tout fait pour assurer une qualité supérieure de reproduction.

S'il manque des pages, veuillez communiquer avec l'université qui a conféré le grade.

La qualité d'impression de certaines pages peut laisser à désirer, surtout si les pages originales ont été dactylographiées à l'aide d'un ruban usé ou si l'université nous a fait parvenir une photocopie de qualité inférieure.

La reproduction, même partielle, de cette microforme est soumise à la Loi canadienne sur le droit d'auteur, SRC 1970, c. C-30, et ses amendements subséquents.

UNIVERSITY OF ALBERTA

THE MEASUREMENT OF COCURRENT AND COUNTERCURRENT RELATIVE  
PERMEABILITIES AND THEIR USE TO ESTIMATE GENERALIZED  
RELATIVE PERMEABILITIES

BY

ABDALLA ALI MANAI

A THESIS

SUBMITTED TO THE FACULTY OF GRADUATE STUDIES AND RESEARCH  
IN PARTIAL FULFILLMENT OF THE REQUIREMENTS FOR THE DEGREE  
OF MASTER OF SCIENCE

IN

PETROLEUM ENGINEERING

DEPARTMENT OF MINING, METALLURGICAL AND PETROLEUM  
ENGINEERING

EDMONTON, ALBERTA

SPRING, 1991



National Library  
of Canada

Bibliothèque nationale  
du Canada

Canadian Theses Service    Service des thèses canadiennes

Ottawa, Canada  
K1A 0N4

The author has granted an irrevocable non-exclusive licence allowing the National Library of Canada to reproduce, loan, distribute or sell copies of his/her thesis by any means and in any form or format, making this thesis available to interested persons.

The author retains ownership of the copyright in his/her thesis. Neither the thesis nor substantial extracts from it may be printed or otherwise reproduced without his/her permission.

L'auteur a accordé une licence irrévocable et non exclusive permettant à la Bibliothèque nationale du Canada de reproduire, prêter, distribuer ou vendre des copies de sa thèse de quelque manière et sous quelque forme que ce soit pour mettre des exemplaires de cette thèse à la disposition des personnes intéressées.

L'auteur conserve la propriété du droit d'auteur qui protège sa thèse. Ni la thèse ni des extraits substantiels de celle-ci ne doivent être imprimés ou autrement reproduits sans son autorisation.

ISBN 0-315-00022-4

Canada

UNIVERSITY OF ALBERTA

RELEASE FORM

NAME OF AUTHOR: Abdalla Ali Manai

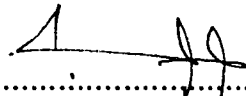
TITLE OF THESIS: The Measurement of Cocurrent and  
Countercurrent Relative Permeabilities and Their  
Use to Estimate Generalized Relative  
permeabilities

DEGREE FOR WHICH THESIS WAS PRESENTED : MASTER OF SCIENCE

YEAR THE DEGREE WAS GRANTED : SPRING, 1991

Permission is hereby granted to THE UNIVERSITY OF ALBERTA LIBRARY to reproduce single copies of this thesis and to lend or sell such copies for private, scholarly or scientific research purposes only.

The author reserves other publication rights, and neither the thesis nor extensive extracts from it may be printed or otherwise reproduced without the author's written permission.

(SIGNED)  .....

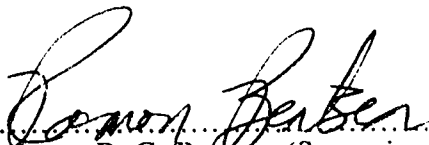
PERMANENT ADDRESS:


MIZDA,  
LIBYA

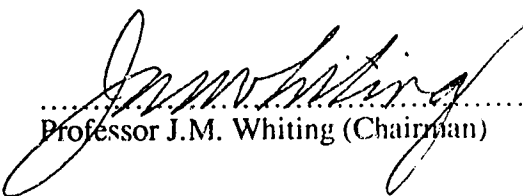
DATED : *February 25, 1991*

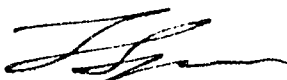
UNIVERSITY OF ALBERTA  
FACULTY OF GRADUATE STUDIES AND RESEARCH

The undersigned certify that they have read, and recommend to the Faculty of Graduate Studies and Research, for acceptance, a thesis entitled "**The Measurement of Cocurrent and Countercurrent Relative Permeabilities and Their Use to Estimate Generalized Relative Permeabilities**" submitted by **Abdalla Ali Manai** in partial fulfillment of the requirements for the degree of **Master of Science in Petroleum Engineering**.

  
.....  
Professor R. G. Beetsen (Supervisor)

  
.....  
Professor A.K. Ambastha

  
.....  
Professor J.M. Whiting (Chairman)

  
.....  
Professor T.J.T. Spanos (External Examiner)

DATED : *February 18, 1991*

*TO*  
*"THE LITTLE CANDLES"*

## ABSTRACT

Countercurrent flow can take place in a number of different situations including gravity drainage and spontaneous imbibition. Some questions have arisen with respect to using cocurrent relative permeabilities to predict countercurrent flows in such situations.

In the case of coupled, two-phase flow of fluids in porous media, the governing equations may be written to show that there are four independent generalized relative permeability curves which have to be measured separately. In order to specify these four curves at a specific saturation, it is necessary to conduct two types of flow experiments. The two types of flow experiment used in this study are cocurrent and countercurrent, steady-state relative permeability experiments.

Steady-state flow experiments involving cocurrent and countercurrent flow of oil and water were performed on horizontal, unconsolidated porous media confined with a rectangular, laminated fibreglass coreholder. Pressures were found to be distributed linearly in both cocurrent and countercurrent flow experiments. Saturations were found to be constant along the core in both types of experiment. The countercurrent relative permeability curves were found to be always less than the cocurrent curves. The inlet capillary pressure for countercurrent flow was found to be, within experimental error, the same as that for cocurrent flow.

Moreover, it is shown that it is possible to define the four generalized relative permeability curves in terms of conventional cocurrent and countercurrent relative permeabilities for each phase. It is demonstrated that a given generalized phase relative permeability falls between the conventional, cocurrent relative permeability for that phase, and that for countercurrent flow of the same phase. Also, it is suggested that the conventional relative permeability for a given phase can be interpreted as arising out of the

effects of two types of viscous drag: that due to the flow of a given phase over the solid surfaces in the porous medium and that due to momentum transfer across phase 1-phase 2 interfaces in the porous medium. The magnitude of viscous coupling is significant, contributing at least 14-16 % to the total conventional cocurrent relative permeability for both phases. Finally, it is shown that the nontraditional generalized relative permeabilities which arise out of viscous drag effects can not equal one another, even when the interfacial tension is allowed to go zero.



## ACKNOWLEDGEMENTS

I wish to express my sincere gratitude and thanks to my supervisor Dr. Ramon G. Bentsen for his guidance and assistance during the course of this study. My thanks go also to the teaching, administrative and technical staff of the Department of Mining, Metallurgical and Petroleum Engineering. I must, however, single out Mr. Bob Smith for his help in setting up the experimental apparatus, and Mr. Jacques Gibeau for his extensive technical help.

I would like to express my appreciation to the Natural Sciences and Engineering Research Council of Canada for the financial assistance which made this study possible.

Special thanks are extended to Mrs. Barbara Bentsen, who painstakingly reviewed the manuscript. I also take this opportunity to thank my friends in Calgary and Edmonton for their generosity, understanding and patience especially at those times when I insisted that my thesis be the topic of the day.

Finally, my very special thanks and gratitude go to those loved ones in Mizda (Libya), whose constant encouragement, good wishes and sacrifices have contributed immensely towards the successful completion of this study.

*A. A. M.*

## TABLE OF CONTENTS

Chapter	Page
1. INTRODUCTION .....	1
2. LITERATURE REVIEW.....	3
2.1 BASIC THEORY.....	3
2.1.1 Historical Background .....	3
2.1.2 Two-Phase Flow.....	4
2.1.3 Hysteresis of Relative Permeabilities.....	7
2.1.4 Capillary Pressure .....	8
2.1.4.1 Laboratory Measurements of Capillary Pressure .....	9
2.1.4.1.1 Desaturation or Displacement Method .....	10
2.1.4.1.2 Mercury-Injection Method.....	10
2.1.4.1.3 Centrifuge Method .....	10
2.1.4.1.4 Dynamic Method .....	10
2.1.4.1.5 Evaporation Method.....	11
2.2 Factors Affecting Relative Permeabilities.....	11
2.2.1 Saturation .....	12
2.2.2 Porous Media Characteristics.....	13
2.2.3 Interfacial tension .....	14
2.2.4 Viscosity .....	15
2.2.5 Initial Water Saturation.....	16
2.2.6 Temperature .....	16
2.2.7 Flow Rate and Pressure.....	17
2.3 Measurement of Relative Permeability.....	19
2.3.1 Mathematical Models.....	20

2.3.1.1	Network Models.....	20
2.3.1.2	Capillary Models.....	20
2.3.1.3	Statistical Models.....	20
2.3.1.4	Empirical Models.....	21
2.3.2	Field Performance.....	21
2.3.3	Laboratory Methods.....	22
2.3.3.1	Capillary Pressure Methods.....	22
2.3.3.2	Centrifuge Methods.....	22
2.3.3.3	Unsteady-State Methods.....	22
2.3.3.4	Steady-State Methods.....	25
2.3.3.4.1	Hassler Method.....	25
2.3.3.4.2	Penn-State Method.....	26
2.3.3.4.3	Stationary Fluid Method.....	26
2.3.3.4.4	Hafford Method.....	27
2.3.3.4.5	Dispersed Feed Method.....	27
2.4	Countercurrent Flow.....	28
2.5	Saturation Measurement Techniques.....	31
2.5.1	External Techniques.....	31
2.5.2	<i>In situ</i> Techniques.....	32
2.5.2.1	Resistivity Technique.....	32
2.5.2.2	X-ray Absorption Technique.....	33
2.5.2.3	Optical Technique.....	33
2.5.2.3	Microwave Attenuation Technique.....	33
3.	STATEMENT OF THE PROBLEM.....	35
4.	THEORY.....	36
4.1	Fluid Flow Equations.....	36
4.1.1	Basic Motion Equations.....	36

4.1.2	Generalized Flow Equations.....	38
4.1.2.1	Relationship between $k_{r12}$ and $k_{r21}$ .....	46
4.2	Microwave Theory .....	47
4.2.1	Dielectric Properties .....	48
4.2.2	Optical Properties .....	50
4.2.3	Physical Properties .....	54
4.2.4	Estimation of Water Saturation.....	57
5.	EXPERIMENTAL EQUIPMENT AND PROCEDURE.....	60
5.1	Description of the Experimental Apparatus.....	60
5.1.1	Microwave Instrumentation.....	60
5.1.2	Fluid Injection System and Pressure Measuring Devices .....	64
5.1.3	Data Acquisition and Storage.....	65
5.1.3.1	Multiprogrammer .....	66
5.1.3.2	Multiprogrammer Interface.....	66
5.2	Experimental Procedure .....	67
5.2.1	Core Preparation Procedure .....	67
5.2.2	Cocurrent Flow Experiments.....	70
5.2.3	Countercurrent Flow Experiments.....	72
6.	RESULTS AND DISCUSSION .....	73
6.1	Introduction .....	73
6.2	Data Analysis .....	73
6.3	Results.....	78
6.4	Discussion of Results.....	102
6.4.1	Core preparation .....	102
6.4.2	Relative Permeability Curves.....	109
6.4.3	Inlet Capillary Pressure .....	113
6.4.4	Generalized Relative Permeabilities.....	114

7. SUMMARY AND CONCLUSIONS .....	117
8. SUGGESTIONS FOR FUTURE STUDY.....	119
REFERENCES .....	120
APPENDIX A	
Programs for Data Acquisition and Retrieval.....	126
APPENDIX B	
Data Conditioning Procedure and Some Experimental Results and Figures.....	170
APPENDIX C	
Typical Routines for Fitting of Experimental Data and Values of Parameters Obtained from Fitting the Data. ....	183

## LIST OF TABLES

Table	Page
5.1 Physical Dimensions of Coreholder .....	69
6.1 Fluid Properties at 22°C.....	74
6.2 Core and Fluid Properties.....	79
B.1 Results of Cocurrent Flow Experiments (Set I).....	171
B.2 Results of Countercurrent Flow Experiments (Set I).....	172
B.3 Results of Cocurrent Flow Experiments (Set II).....	173
B.4 Results of Countercurrent Flow Experiments (Set II).....	174
B.5 Relative Permeabilities and Capillary Pressure for Cocurrent Flow (Set I).....	175
B.6 Relative Permeabilities and Capillary Pressure for Cocurrent Flow (Set II).....	176
B.7 Relative Permeabilities and Capillary Pressure for Countercurrent Flow (Set I).....	177
B.8 Relative Permeabilities and Capillary Pressure for Countercurrent Flow (Set II).....	178
C.1 Parameters Obtained From Fitting of Water Cocurrent Relative Permeability.....	187
C.2 Parameters Obtained From Fitting of Water Countercurrent Relative Permeability .....	187
C.3 Parameters Obtained From Fitting of Oil Cocurrent Relative Permeability .....	188
C.4 Parameters Obtained From Fitting of Oil Countercurrent Relative Permeability .....	188
C.5 Parameters Obtained From Fitting of Ratio of Cocurrent Flow Rates.....	189
C.6 Parameters Obtained From Fitting of Ratio of Countercurrent Flow Rates.....	189
C.7 Parameters Obtained From Fitting Cocurrent Ratio of Pressure Gradients .....	190

C.8	Parameters Obtained From Fitting Countercurrent Ratio of Pressure Gradients.....	190
C.9	Parameters Obtained From Fitting Inlet Capillary Pressure.....	191

## LIST OF FIGURES

Figure	Page
4.1 Dielectric Constants for Dipolar Liquid with Single Relaxation Time, $\tau$ , (after Parsons).....	51
4.2 Loss Factors for Some Pure Liquids (after Parsons).....	55
4.3 Loss Factors for Aqueous Salt Solutions (after Parsons).....	56
5.1 Schematic Diagram of the Cocurrent Experimental Apparatus .....	61
5.2 Schematic Diagram of the Countercurrent Experimental Apparatus .....	62
5.3 Schematic Diagram of Microwave Instrumentation.....	63
6.1 Dynamic Water Saturation Profiles during Cocurrent Flow (Experiment No. 1).....	80
6.2 Dynamic Water Saturation Profiles during Cocurrent Flow (Experiment No. 2).....	81
6.3 Dynamic Water Saturation Profiles during Countercurrent Flow (Experiment No. 13) .....	82
6.4 Dynamic Water Saturation Profiles during Countercurrent Flow (Experiment No. 14) .....	83
6.5 Pressure Profiles during Cocurrent Flow (Experiment No. 1).....	84
6.6 Pressure Profiles during Cocurrent Flow (Experiment No. 2).....	85
6.7 Pressure Profiles during Countercurrent Flow (Experiment No. 13) .....	87
6.8 Pressure Profiles during Countercurrent Flow (Experiment No. 14) .....	88
6.9 Ratios of Pressure Gradients between Water and Oil for Cocurrent and Countercurrent Flow (Set I).....	89
6.10 Ratios of Pressure Gradients between Water and Oil for Cocurrent and Countercurrent Flow (Set II) .....	90



6.11	Comparison of Measured and Fitted Relative Permeabilities for Cocurrent and Countercurrent Flow (Set I) .....	91
6.12	Comparison of Measured and Fitted Relative Permeabilities for Cocurrent and Countercurrent Flow (Set II) .....	92
6.13	Comparison of Measured and Fitted Flow Rate Ratios for Cocurrent and Countercurrent Flow (Set I) .....	93
6.14	Comparison of Measured and Fitted Flow Rate Ratios for Cocurrent and Countercurrent Flow (Set II) .....	94
6.15	Inlet Capillary Pressure-Saturation Curves for Cocurrent and Countercurrent Flow (Set I) .....	96
6.16	Inlet Capillary Pressure-Saturation Curves for Cocurrent and Countercurrent Flow (Set II) .....	97
6.17	Comparison of Normalized Relative Permeabilities for Cocurrent and Countercurrent Flow (Set I) .....	98
6.18	Comparison of Normalized Relative Permeabilities for Cocurrent and Countercurrent Flow (Set II) .....	99
6.19	Permeability Coefficients (Set I) .....	100
6.20	Permeability Coefficients (Set II) .....	101
6.21	Comparison of Relative Permeabilities for Cocurrent and Countercurrent Flow with Generalized Relative Permeabilities (Set I) .....	103
6.22	Comparison of Relative Permeabilities for Cocurrent and Countercurrent Flow with Generalized Relative Permeabilities (Set II) .....	104
6.23	Relative Viscous Drag Coefficients (Set I) .....	105
6.24	Relative Viscous Drag Coefficients (Set II) .....	106
6.25	Relative Viscous Coupling Effect (Set I) .....	107
6.26	Relative Viscous Coupling Effect (Set II) .....	108

6.27	Ratio of Relative Permeabilities (Set I).....	111
6.28	Ratio of Relative Permeabilities (Set II).....	112
B.1	Conditioned Pressure Profiles during Cocurrent Flow (Experiment No. 1).....	179
B.2	Conditioned Pressure Profiles during Cocurrent Flow (Experiment No. 2).....	180
B.3	Conditioned Pressure Profiles during Countercurrent Flow (Experiment No. 13) .....	181
B.4	Conditioned Pressure Profiles during Countercurrent Flow (Experiment No. 14) .....	182

## NOMENCLATURE

$a$	parameter in Equation (6.6)
$a_1, a_2$	parameters in Equations (6.1) and (6.3), respectively
$a_3, a_4$	parameters in Equation (6.5)
$a_5$	parameter in Equation (6.9)
$a^*$	parameter in Equation (6.8)
$a_1^*, a_2^*$	parameters in Equations (6.2) and (6.4), respectively
$a_3^*, a_4^*$	parameters in Equation (6.7)
$A$	system cross-sectional area, $m^2$ [ft <sup>2</sup> ]
$A_{ls}$	lump sum absorbance due to core material, sand and oil, mW
$A_{st}$	total absorbance, mW
$A_w$	absorbance due to water, mW
$b_1, b_2$	parameters in Equations (6.1) and (6.3), respectively
$b_3, b_4$	parameters in Equation (6.5)
$b_5$	parameter in Equation (6.9)
$b_1^*, b_2^*$	parameters in Equations (6.2) and (6.4), respectively
$b_3^*, b_4^*$	parameters in Equation (6.7)
$B$	constant of absorbance in Equation (4.69)
$c$	velocity of light, m/s [ft/sec]
$c_1, c_2$	parameters in Equations (6.1) and (6.3), respectively
$c_3, c_4$	parameters in Equation (6.5)
$c_5$	parameter in Equation (6.9)
$c_1^*, c_2^*$	parameters in Equations (6.2) and (6.4), respectively
$c_3^*, c_4^*$	parameters in Equation (6.7)
$C$	concentration of absorber
$d_5$	parameter in Equation (6.9)

D	instantaneous electric displacement
$D_{max}$	maximum instantaneous electric displacement
E	instantaneous field strength
$E_i$	maximum electric field strength
$E_{max}$	maximum instantaneous field strength
f	frequency of microwave signals, Hz
$f_v$	volume fraction of absorber
$f_w$	fractional flow of water
$f_2$	empirically determined function of saturation in Equation (4.50)
g	acceleration due to gravity, $m/s^2$ [ft/sec <sup>2</sup> ]
$\vec{g}$	acceleration due to gravity vector, $m/s^2$ [ft/sec <sup>2</sup> ]
$g_{11}, g_{12}, g_{21}, g_{22}$	permeability coefficients
h	thickness of system, m [ft]
$h_1, h_2$	hydrostatic heads at the inlet and outlet, respectively, of the sand filter, m [ft]
i	$\sqrt{-1}$
$I_i$	incident microwave power, mW
$I_o$	attenuated microwave power, mW
k	extinction coefficient
$k_o$	effective permeability to oil, $m^2$ [darcy]
$k_{oiw}$	effective permeability to oil at initial water saturation, $m^2$ [darcy]
$k_{ro}, k_{ro}^*$	cocurrent and countercurrent oil relative permeabilities, respectively
$(k_{ro})_n, (k_{ro}^*)_n$	cocurrent and countercurrent oil normalized relative permeabilities, respectively
$k_{rv1}, k_{rv2}$	relative viscous coupling effects of phase 1 and phase 2, respectively
$k_{rw}, k_{rw}^*$	cocurrent and countercurrent water relative permeabilities, respectively

$(k_{rw})_n, (k_{rw}^*)_n$	cocurrent and countercurrent water normalized relative permeabilities, respectively
$k_{r11}$	generalized relative permeability of phase 1
$k_{r12}$	relative viscous drag of phase 1 due to phase 2
$k_{r21}$	relative viscous drag of phase 2 due to phase 1
$k_{r22}$	generalized relative permeability of phase 2
$k_{v1}, k_{v2}$	viscous coupling effects of phase 1 and phase 2, respectively, m <sup>2</sup> [darcy]
$k_w$	effective permeability to water, m <sup>2</sup> [darcy]
$k_{wor}$	effective permeability to water at residual oil saturation, m <sup>2</sup> [darcy]
$k_1, k_1^*$	cocurrent and countercurrent effective permeabilities to phase 1, respectively, m <sup>2</sup> [darcy]
$k_{11}$	generalized permeability of phase 1, m <sup>2</sup> [darcy]
$k_{12}$	viscous drag of phase 1 due to phase 2, m <sup>2</sup> [darcy]
$k_2, k_2^*$	cocurrent and countercurrent effective permeabilities to phase 2, respectively, m <sup>2</sup> [darcy]
$k_{21}$	viscous drag of phase 2 due to phase 1, m <sup>2</sup> [darcy]
$k_{22}$	generalized permeability of phase 2, m <sup>2</sup> [darcy]
$K$	absolute permeability, m <sup>2</sup> [darcy]
$K_a$	molar absorption coefficient
$K_{wa}$	extinction coefficient of water
$K_1$	proportionality factor in Equation (2.1)
$L$	length of system, m [ft]
$n$	index of refraction
$n^*$	complex index of refraction
$N_c$	capillary number
$P$	pressure, kPa [psi]

$P_c$	capillary pressure, kPa [psi]
$P_{nwt}$	pressure in non-wetting phase, kPa [psi]
$P_o$	pressure in oil phase, kPa [psi]
$P_{o1}, P_{o2}$	inlet and outlet pressures in oil phase, respectively, kPa [psi]
$P_{cin}, P_{cin}^*$	cocurrent and countercurrent inlet capillary pressures, respectively, kPa [psi]
$P_r$	power, mW
$P_w$	pressure in water phase, kPa [psi]
$P_{wt}$	pressure in wetting phase, kPa [psi]
$P_{w1}, P_{w2}$	inlet and outlet pressures in water phase, respectively, kPa [psi]
$P_1, P_1^*$	cocurrent and countercurrent pressures in phase 1, respectively, kPa [psi]
$P_2, P_2^*$	cocurrent and countercurrent pressures in phase 2, respectively, kPa [psi]
$q$	volumetric flow rate, m <sup>3</sup> /s [ft <sup>3</sup> /sec]
$q_o, q_o^*$	cocurrent and countercurrent oil flow rates, respectively, m <sup>3</sup> /s [ft <sup>3</sup> /sec]
$q_w, q_w^*$	cocurrent and countercurrent water flow rates, respectively, m <sup>3</sup> /s [ft <sup>3</sup> /sec]
$q_1, q_1^*$	cocurrent and countercurrent flow rates for phase 1, respectively, m <sup>3</sup> /s [ft <sup>3</sup> /sec]
$\vec{q}_1$	flow rate vector for phase 1, m <sup>3</sup> /s [ft <sup>3</sup> /sec]
$q_2, q_2^*$	cocurrent and countercurrent flow rates for phase 2, respectively, m <sup>3</sup> /s [ft <sup>3</sup> /sec]
$\vec{q}_2$	flow rate vector for phase 2, m <sup>3</sup> /s [ft <sup>3</sup> /sec]
$R_{12}, R_{12}^*$	ratios of pressure gradients in cocurrent and countercurrent flow, respectively

$s$	path of flow
$S$	normalized water saturation
$S_w$	water saturation
$S_{wi}$	initial water saturation
$S_w^*$	specific water saturation
$t$	time, sec
$v$	apparent velocity, m/s [ft/sec]
$v_{os}$	apparent velocity of oil phase along flow path $s$ , m/s [ft/sec]
$v_{ox}$	apparent velocity of oil phase along $x$ -axis, m/s [ft/sec]
$v_{ws}$	apparent velocity of water phase along flow path $s$ , m/s [ft/sec]
$v_{pr}$	velocity of propagation, m/s [ft/sec]
$v_{wx}$	apparent velocity of water phase along $x$ -axis, m/s [ft/sec]
$V$	volume of core holder, $m^3$ [ft <sup>3</sup> ]
$x, y, z$	coordinate axes
$\delta$	phase angle, radians [degrees]
$\epsilon$	dielectric constant
$\epsilon'$	real part of dielectric constant
$\epsilon''$	imaginary part of dielectric constant
$\theta$	angle between the positive $s$ direction and the horizontal, radians [degrees]
$\mu$	viscosity, Pa.s [cp]
$\mu_o, \mu_w$	oil and water viscosities, respectively, Pa.s [cp]
$\mu_1, \mu_2$	phase 1 and phase 2 viscosities, respectively, Pa.s [cp]
$\xi$	dimensionless distance (normalized distance), $x/L$
$\pi$	3.14159.....
$\rho$	density, $kg/m^3$ [gm/cm <sup>3</sup> ]
$\rho_o, \rho_w$	oil and water densities, respectively, $kg/m^3$ [gm/cm <sup>3</sup> ]

$\rho_1, \rho_2$	phase 1 and phase 2 densities, respectively, $\text{kg/m}^3$ [ $\text{gm/cm}^3$ ]
$\sigma$	interfacial tension, $\text{mN/m}$ [ $\text{dyne/cm}$ ]
$\tau$	relaxation time, sec
$\phi$	porosity
$\Phi$	potential, $\text{N.m/kg}$ [ $\text{lb}_f\text{-ft/lb}_m$ ]
$\Phi_o, \Phi_w$	potentials in oil phase and water phase, respectively, $\text{N.m/kg}$ [ $\text{lb}_f\text{-ft/lb}_m$ ]
$\rightarrow$	vector notation
$\nabla$	gradient operator



## 1. INTRODUCTION

Oil is a major source of energy in today's world. Efficient recovery of oil requires a better understanding of fluid behavior in reservoir rocks. Fluid transport through porous media is a complicated phenomenon and fluid flow in reservoir rocks cannot be described by theory alone.

Relative permeability is one of the more important properties needed to describe the movement of fluid through oil reservoir rocks. Consequently, the prediction of oil production from a reservoir requires measurement of the relative permeability curves. Many techniques are available to estimate relative permeabilities for oil/water systems. Among these techniques, laboratory measurement of relative permeabilities is considered to be the most reliable. Despite the relatively longer time they require, the steady-state methods are believed to be the most reliable techniques against which all other methods are compared. This is because steady-state techniques use the fewest assumptions. Thus, they provide more accurate relative permeability data. Moreover, they cover a wider range of saturation levels.

It has been a customary practice to conduct relative permeability measurements for cocurrent flow only and then use the relative permeability data to represent the relative permeability for oil/water systems in oil reservoir rocks.

The imbibition process, or the spontaneous flow of fluids in porous media under the effect of capillary pressure gradients, occurs wherever there exists, in permeable rock, capillary pressure gradients which are not balanced by opposing pressure gradients. While imbibition plays a very important role in the recovery of oil from normal reservoirs, imbibition might be the dominant displacement mechanism in water-flood reservoirs characterized by drastic variation in permeability, such as in fractured-matrix reservoirs. In a water-wet, fractured-matrix reservoir, water will be imbibed from fractures into the

matrix with a countercurrent expulsion of oil into the fractures. The relative permeability characteristics in countercurrent flow may be different from the characteristics of relative permeability in cocurrent flow and the use of cocurrent flow relative permeability to represent countercurrent flow relative permeability is questionable. Thus, there is a need to investigate both the similarities and the dissimilarities between cocurrent flow and countercurrent flow relative permeabilities. Another important characteristic is capillary pressure. The concern here is whether the capillary pressure-saturation curve is the same in both cocurrent and countercurrent flow.

The effect of viscosity and viscosity ratio on two-phase relative permeabilities has been a concern in reservoir-engineering-related literature for a long time. This issue is controversial. Some researchers have concluded that viscosity ratio has no influence on relative permeability, while others have suggested that viscosity and viscous coupling have an effect on relative permeability. These differences led some researchers to question the validity of the intuitive extension of Darcy's law for single-phase flow to two-phase flow. Such concerns have led researchers to derive the equations governing two-phase flow, through volume averaging, from the basic laws of physics. On the basis of such theoretical analyses, four generalized relative permeabilities have been proposed. These generalized relative permeabilities make it clear that viscosity, viscous coupling and viscous drag influence relative permeability characteristics. However, it is emphasized that there is a great need for experimental data to establish how much effect viscosity ratio has on relative permeability and how much viscous coupling occurs when two immiscible fluids are flowing through the interstices of porous media. Furthermore, experimental data are required to assist in describing how the generalized relative permeabilities differ from conventional relative permeabilities.

## 2. LITERATURE REVIEW

### 2.1 BASIC THEORY

#### 2.1.1 Historical Background

In 1865, Henry Darcy [1] conducted a series of experiments on the downward flow of water through filter sands, whereby he established that the rate of flow of water through the filter bed was directly proportional to the area of the sand and to the difference between the fluid heads at the inlet and outlet faces of the bed, and inversely proportional to the length of the bed, or, described analytically, as

$$q = K_1 A (h_1 - h_2) / L \quad (2.1)$$

The above relationship, appropriately, soon became known as Darcy's law. Darcy's experiments were confined to the flow of water through sand packs which were 100% saturated with water. Later, it was determined that Darcy's law could be modified to describe the flow of fluids other than water, and that the proportionality factor,  $K_1$ , could be replaced by  $K/\mu$ , where  $K$ , the permeability, is a property of the porous medium which can be defined as a measure of the porous medium's ability to transmit fluids [2]. With this modification, Darcy's law may be written in a more general form as

$$q = \frac{K A \Delta P}{\mu L} \quad (2.2)$$

Despite the fact that Darcy's law was an empirical relationship, many researchers

have attempted to deduce its theoretical basis, or, more generally, to derive the equations of motion in porous media. Hubbert [3] was the first to recognize that any attempt to derive Darcy's law should be based on Newton's second law of motion and the fundamental equation of Navier and Stokes for the motion of viscous fluid. Prager [4] used a variational approach to construct an equation for the permeability for an isotropic medium in terms of a function describing the geometry of the pore space. Raats and Klute [5] utilized the theory of mixtures to develop the macroscopic equations of continuity and motion. Slattery [6] and Whitaker [7] were able to complete the analysis begun by Hubbert, once the volume averaging theorems were developed in 1967. They averaged the Navier-Stokes equation over a representative volume of a porous medium and arrived at the motion equation for the general case of an anisotropic medium. Neuman [8] also constructed Darcy's law for anisotropic media from the Navier-Stokes equation using a formal averaging procedure which considers the permeability tensor to be symmetric. De la Cruz and Spanos [9] undertook a new approach to the use of local volume averaging to describe the flow of multiphase fluid phases. A detailed review of some of these and other related works is available in Scheidegger [10] and Bear [11].

### **2.1.2 Two-Phase Flow**

The law of simultaneous flow of two immiscible fluids in porous media can be obtained by assuming that a porous medium which contains more than one fluid has an effective permeability to each fluid present at a given cross-section of the porous medium. In 1936, Wyckoff and Botset [12] studied experimentally the steady flow of two-phase mixtures through unconsolidated sands. They found that the apparent (effective) permeability of the medium to the other component is variable and depends, in a complex manner, on the relative concentration of the two components. They argued that Darcy's law can be extended to describe the flow of two immiscible fluids flowing simultaneously through a porous medium as follows:

$$q_1 = \frac{k_1 A \Delta P_1}{\mu_1 L} \quad (2.3)$$

and

$$q_2 = \frac{k_2 A \Delta P_2}{\mu_2 L} \quad (2.4)$$

On the basis of the experiments of Wyckoff and Botset, Muskat and Meres [13] formulated differential equations governing the steady-state flow of fluids through porous media. Using Muskat and Meres' solution, Darcy's law was written in a more generalized form for the oil and water phases as

$$q_o = -\frac{k_o A}{\mu_o} \cdot \left( \frac{dP_o}{ds} - \rho_o g \frac{dz}{ds} \right) \quad (2.5)$$

and

$$q_w = -\frac{k_w A}{\mu_w} \cdot \left( \frac{dP_w}{ds} - \rho_w g \frac{dz}{ds} \right) \quad (2.6)$$

The effective permeabilities are the composite effect of pore geometry, wettability, fluid distribution, and saturation history [14]. If one defines relative permeability as the ratio of effective permeability to the absolute permeability, Equations (2.5) and (2.6) may be restated as follows:

$$q_o = -\frac{k_{ro} KA}{\mu_o} \cdot \left( \frac{dP_o}{ds} - \rho_o g \frac{dz}{ds} \right) \quad (2.7)$$

and

$$q_w = -\frac{k_{rw} KA}{\mu_w} \cdot \left( \frac{dP_w}{ds} - \rho_w g \frac{dz}{ds} \right) \quad (2.8)$$

In the early 1950's, several studies were carried out to identify fluid-flow patterns during two-phase flow through porous media. Two-phase flows were observed microscopically in flow cells containing glass beads, or thin sections of reservoir rock. In the microscopic experiments, the two fluids flow simultaneously at constant overall rates. Chatenever and Calhoun [15] visually investigated the mechanisms of fluid behavior in porous media. They observed channel flow in which transport was effected through stable networks of interconnecting channels. As the saturation of one phase increases, the widths of channels containing that phase increase. Multiphase flow occurs through a series of continuous but tortuous channels. Each phase flows through its own channels. As a consequence, there must be one or more continuous flow paths in the pore space from one end of the porous medium to another for a phase to flow. That is to say, for a specified rock and fluid phase, minimum saturations are required for the wetting phase and the non-wetting phase to flow in a two-phase system under an applied pressure gradient. As the saturation of a phase decreases, the cross-sectional area of the channel of the phase tends to decrease; and as the saturation becomes discontinuous, the flow of the phase ceases [16]. In other words, the effective permeability of a phase is a function of the saturation, varying from zero when the phase is immobile at residual saturation (discontinuous) to maximum when the other phase or phases are at their residual saturations.

The effort of researchers to generalize Darcy's law to two-phase flow has continued. Recently, Whitaker [17] extended the method of volume-averaging to describe immiscible flow of two fluids in a rigid porous medium. Kalaydjian [18] used mass- and momentum-balance equations to arrive at a macroscopic description of two-phase flow in a porous medium. Spanos *et al.* [19] presented a set of equations to describe multi-phase flow of oil and water in a homogeneous water-wet medium. They argued that the generalization of Darcy's law using volume-averaging was an improvement over Muskat and Meres' equations because it describes correctly multi-dimensional flows. That is,

Muskat and Meres' equations are valid only for one-dimensional flow.

When viscous coupling is included in the analysis, four generalized permeabilities, rather than the usual two permeabilities, are required to describe two-phase flow. Although several investigators have indicated that the measurement of the generalized permeabilities is not a simple matter, there is a need to measure these four generalized permeabilities experimentally. However, no experimental study has yet been conducted to estimate the four generalized permeability curves [17].

### 2.1.3 Hysteresis of Relative Permeabilities

In spite of the fact that the concept of channel flow of each fluid phase establishing its own channels of flow through a porous medium makes the flow description easy, it is questionable because one of the fluids preferentially wets the porous medium and tends to spread on or adhere to the solid surfaces surrounding the non-wetting phase. The fluid flow processes under consideration are irreversible; therefore, they are inherently path dependent. One consequence is that the equilibrium states approached in one direction can be different from those approached in another [20]. This phenomenon is called hysteresis. Moreover, relative permeability measurements are dependent on saturation level and since many interstitial fluid distributions are possible for each level of saturation, depending on the direction of saturation change, different values of relative permeability versus saturation may be obtained. That is to say, relative permeability curves obtained for imbibition (increase in wetting phase saturation) may be different from those for drainage (reduction of wetting phase saturation). Many investigators [21,22,23] reported that because the wetting phase relative permeability is a function of its own saturation, it was not likely to show any hysteresis effect. The non-wetting phase, however, is affected by the direction of the saturation change. During the imbibition process, lower relative permeabilities are obtained at any saturation. This behavior may be explained as follows. In the imbibition process, more and more non-wetting phase becomes disconnected, and as a consequence,

bypassing in the larger capillaries takes place [24], while in the drainage process, all the non-wetting phase remains continuous. Morrow *et al.* [25] argued that any small decrease in relative permeability because of an increase in the contact angle may be due to the curvature relaxation at the fluid-fluid interface, and such a phenomenon is saturation dependent. In a later study, McCaffery and Bennion [26] found no significant history dependence in relative permeability curves under strongly wet conditions. As the contact angle was increased, a consistent shift in relative permeability of both phases was found for a porous medium with an initial irreducible saturation of the displacing phase. In drainage experiments, they observed that relative permeability curves were little affected when the contact angle varied from 180 degrees to 90 degrees. They showed that the sensitivity of relative permeability relations to contact angle changes was strongly affected by the saturation history of the core.

#### 2.1.4 Capillary Pressure

Capillary pressure in porous media can be defined simply [14] as the pressure difference existing across the interface separating two immiscible fluids, one of which wets the surface of the rock in preference to the other. The capillary pressure is expressed generally as the pressure in the non-wetting phase minus the pressure in the wetting phase, and so is commonly a positive value, and thus can be written as follows :

$$P_c = P_{nwt} - P_{wt} \quad (2.9)$$

or for a porous medium which is preferentially water wet, capillary pressure can be defined as the pressure in the oil phase minus the pressure in the water phase, or

$$P_c = P_o - P_w \quad (2.10)$$

The above relationship was reported originally by Leverett [27] in 1941. He stated that



since the water and oil are separated by curved interfaces the pressures in the two phases are not in general equal in the same plane normal to  $v$ . As a reasonable simplification, Leverett assumed that this pressure differential between the fluids is  $P_c$ , the capillary pressure. He concluded that the pressure gradients in the two fluids are related by a quantity which, according to the above assumption, is a function of saturation gradient and saturation only.

Capillary pressure depends upon several factors, notably : i) texture and wettability of the porous medium, ii) the interfacial tension between the fluids, and iii) saturation distribution of the fluids and the manner in which the saturations were attained. Thus, for a given pair of immiscible fluids in a particular porous medium, capillary pressure is a unique function of fluid saturation. However, hysteresis in capillary pressure is usually observed upon change in saturation direction. Hysteresis was observed by Leverett [27] in his pioneering work in 1941 in which he presented both drainage and imbibition capillary pressure curves obtained using unconsolidated sand .

#### **2.1.4.1 Laboratory Measurements of Capillary Pressure**

Leverett [27] used long sand tubes in conducting his capillary pressure experiments, and because core samples are often small and are not available in continuous lengths sufficiently long to carry out the drainage process, it would not be possible to use such a method to obtain capillary pressure characteristics. Since then several methods have been proposed by other investigators.

Amyx *et al.* [28] classified these methods into five categories. These categories are : i) the desaturation or displacement process, ii) the mercury-injection method, iii) the centrifuge method, iv) the dynamic capillary-pressure method, and v) the evaporation method.

#### **2.1.4.1.1 Desaturation or Displacement Method**

This method, well known as the restored-state method, was presented by Bruce and Welge [29] in 1947. The method utilizes a permeable membrane with a uniform pore-size distribution such that the displacing fluid will not penetrate the diaphragm until a certain threshold (displacing) pressure is applied. This pressure is increased by small increments and the core is allowed to reach equilibrium at each pressure level before calculating the wetting phase saturation corresponding to each point defining the capillary pressure curve.

#### **2.1.4.1.2 Mercury-Injection Method**

Purcell [30] introduced this method in 1949. In this method, the time needed to construct the capillary pressure curve is greatly reduced because equilibrium is attained rapidly; and a higher pressure range can be covered since a membrane is not required. The procedure calls for injecting mercury into an evacuated core sample under pressure and calculating the saturation of the mercury, the non-wetting fluid, at each applied pressure, and thus the capillary pressure curve is obtained.

#### **2.1.4.1.3 Centrifuge Method**

In 1951, Slobod *et al.* [31] reported a detailed experimental study to determine capillary pressure characteristics using the centrifuge method. In this technique, the core sample is rotated at different speeds causing an increase in the gravitational force, and by converting the speed of rotation into force units and by measuring the fluid saturation, the capillary pressure data is obtained in a very short time.

#### **2.1.4.1.4 Dynamic Method**

This technique was used first by Brown [32] in 1951. He measured the pressure in each phase of two fluids flowing simultaneously at steady state. He used special wetted disks that allowed the hydraulic pressure transmission of only the desired phase. The

difference between the measured pressures of the two phases is the dynamic capillary pressure at a specific saturation, and by changing the saturation, through varying the flow rates ratio, a complete dynamic capillary curve is established.

#### **2.1.4.1.5 Evaporation Method**

In 1951, Messer [33] proposed this technique which involves continuously monitoring the decrease in weight due to the evaporation of fluids in a core sample initially saturated with 100% of the wetting fluid.

In summary, capillary pressure curves are of great use in the petroleum industry. They are used to determine fluid distributions in porous media, measure saturations, study wettability, and to measure the connectedness of the pores in the formation. They also represent an experimental correlation of the pressure difference between two phases at equilibrium in a porous medium, and they even can be used as additional information to study the homogeneity of the formation. Thus, it is important to construct the capillary pressure curves. Among the briefly mentioned methods to measure capillary pressure data, the restored-state method, even though it is time consuming, is considered to be the standard method in that actual wetting conditions are met (oil and water are used). On the other hand, the dynamic method gives more reliable results as capillary pressure curves are established under dynamic conditions.

## **2.2 Factors Affecting Relative Permeabilities**

Relative permeabilities are necessary to describe the flow of more than one phase in a porous network. Relative permeability is primarily dependent on saturation. Relative permeability for a fluid phase should be unity if the fluid phase is the only phase present within the porous medium. In the presence of another phase, the relative permeability for one phase decreases as its saturation decreases and as the other phase's saturation

increases; however, the sum of the relative permeabilities for the two phases is almost always less than unity because of interference between the two phases sharing flow channels. This interference is due to a number of reasons. These reasons are [34]: i) part of the pore channels available for flow of a fluid may be reduced in size by the other fluid present in the rock; ii) immobilized droplets of one fluid may completely plug some constrictions in a pore channel through which another fluid would otherwise flow; iii) some pore channels may become effectively plugged by diverse capillary forces if the pressure gradient is too low to push an interface through a constriction; and iv) groups of globules that are clustered together may be trapped, since the grain configuration allows fluid to flow around the trapped globules without developing a pressure gradient sufficient to move them.

To fully understand the relative permeability curves, it is essential to understand the factors that affect the relative permeability characteristics; these are a combination of both fluid and porous medium characteristics. These factors are discussed in the following sections.

### 2.2.1 Saturation

For a fluid to flow in a porous medium, its phase should be continuous. At low saturations of the phase that preferentially wets the porous medium, the wetting phase forms rings around the grain contact points that are separate from one another and thus pressure cannot be transmitted through them. Above the critical saturation (the irreducible wetting phase saturation), the wetting phase is mobile, and as its saturation increases, the wetting phase relative permeability increases. As the saturation of the wetting phase further increases, the non-wetting phase breaks down and becomes a discontinuous phase at the critical non-wetting phase saturation (non-wetting residual saturation). Several studies have been conducted to investigate the dependence of relative permeability on saturation. Leverett and Lewis [21] studied this phenomenon in consolidated sand, and

they indicated that for strongly water wet sands, the permeability to the wetting phase is strictly a function of water saturation. On the other hand, Caudle *et al.* [35] showed that the non-wetting phase relative permeability depends on the wetting, as well as the non-wetting, phase saturation for strongly water-wet systems. However, in oil-wet systems, Emmett *et al.* [36] found that the oil-phase relative permeability is dependent solely upon its own saturation, while in water-wet rocks, the oil-phase relative permeability depends on both water and oil saturation.

### 2.2.2 Porous Media Characteristics

Relative permeability curves vary from formation to formation, and even from one portion to another of a heterogeneous formation. Corey and Rathjens [37] investigated the effect of heterogeneity on drainage gas-oil relative permeability and found that the relative permeability for flow parallel to the bedding plane was greater than that for flow perpendicular to the bedding plane. Huppler [38] numerically investigated the effects of core heterogeneities on relative permeability and concluded that relative permeability of composite core varies appreciably when the sections are arranged in different orders. Many investigators have studied the effect of consolidation of sands on relative permeability and noted that the saturation range for a mobile fluid phase is wider in unconsolidated rock than in consolidated rock [34]. While several researchers found that gas-oil fluid behavior of consolidated sandstone is qualitatively similar to that of unconsolidated sand, Naar *et al.* [39] have shown that the relative permeability of unconsolidated sand differs qualitatively and quantitatively from that of consolidated sand. It is important to know the structure of the pore geometry of porous media by evaluating the behavior of fluid flowing through it. Fatt [40] used a structural model to investigate the dynamic properties of networks and concluded that the relative permeability of porous media is a direct consequence of the network structure. Leverett [41] showed that relative permeability of unconsolidated sand to an oil-water mixture is related to the

pore size distribution. Morgan and Gordon [42] studied the effect of pore geometry and surface area on water-oil relative permeability and concluded that formations with large pores (small surface areas) have low irreducible water saturations, and thus have a relatively large pore space available for fluids to flow.

### 2.2.3 Interfacial tension

Interfacial tension,  $\sigma$ , is the force per unit length existing at fluid-fluid and fluid-solid interfaces. Moreover, it is the force responsible for retention of a residual saturation in porous media. Leverett [41] described a small but definite effect of interfacial tension. He reported a tendency for relative permeability, in a water/oil system in consolidated sands, to increase about 20 to 30% if  $\sigma$  was decreased from 24 mN/m (24 dyne/cm) to 5 mN/m (5 dyne/cm). Muskat [2] concluded that there is influence of interfacial tension within the range of 27 to 72 mN/m (dyne/cm) on gas-liquid relative permeability. Owens and Archer [43] observed no effect of interfacial tension on either the water-oil relative permeability of a water-wet rock or the gas-oil relative permeability of an oil-wet rock. On the other hand, several investigators observed a reduction in residual oil saturation at low values of interfacial tension. Moore and Slobod [44] found a reduction in the water-flood residual oil saturation of a water-wet core at lower values of interfacial tension. Talash [45] reported some relative oil and water permeability curves for various low-tension formations. He observed an increase in the relative permeability curves for both phases with a decrease in interfacial tension at a given water saturation. Amaefule and Handy [46] investigated the effect of low interfacial tensions on relative oil/water permeabilities of consolidated porous media. They used both steady- and unsteady-state displacement methods to generate relative permeability curves. They observed that the relative permeabilities for both phases increased with decreasing interfacial tension. Bardon and Longeron [47] studied the influence of low interfacial tensions on relative permeability in vapor-liquid systems. They found through numerical simulation that relative permeability

is strongly affected by  $\sigma$ , especially when it is lower than 0.02 mN/m. They concluded that at a very low value of interfacial tension ( $\sigma = 0.001$  mN/m), the relative permeabilities can be represented by two lines with a slope of one in the relative permeability diagram. However, Bardon and Longeron stated that the prediction for very low values of interfacial tension was more difficult.

#### 2.2.4 Viscosity

The effect of viscosity and viscosity ratio is a controversial subject among researchers, and thus some examples from both sides of the controversy will be mentioned. Many investigators consider the relative permeability curves to be independent of the viscosities of both immiscible phases. Leverett [41] found no systematic deviations of relative permeability due to viscosity variations. Sandberg *et al.* [48] reported that relative permeability curves of a uniformly saturated core are independent of the oil viscosity in the range of 0.398 to 1.683 cp. Donaldson *et al.* [49] concluded that the relative permeability is independent of viscosity as long as the wettability of the porous medium is preserved.

On the other hand, many other investigators carried out experimental work and concluded that relative permeability was dependent on viscosity. Hassler *et al.* [50] observed that lower gas relative permeability values were associated with lower oil viscosity, but they concluded that the variation in relative permeability could not be described by a single factor varying with oil viscosity. Morse *et al.* [51] concluded that relative permeability increased with an increase of the viscosity ratio. Odeh [52] reported that the non-wetting phase relative permeability increases with an increase in viscosity ratio. However, he concluded that the wetting phase relative permeability is not affected by variation in viscosity ratio. Lefebvre du Prey [53] found that the endpoint relative permeability of the wetting phase increases as the viscosity ratio increases, while the endpoint relative permeability of the non-wetting phase decreases.

However, because of the diverse opinions of various investigators concerning the

influence of viscosity on relative permeability, Honarpour *et al.* [34] suggested that more reliable data can be obtained if laboratory relative permeability experiments are conducted with fluids which are similar in viscosity to the reservoir fluids.

### 2.2.5 Initial Water Saturation

The initial (irreducible, connate, interstitial) water saturation is the water saturation present in the reservoir at discovery. Caudle *et al.* [35] investigated the influence of initial water saturation on relative permeability characteristics. They found that the initial water saturation affects both the starting points and the shape of relative permeability curves. Craig [14] concluded that up to 20% of the connate water saturation in oil-wet cores had no effect on oil-water relative permeabilities. However, in water-wet cores, the connate water saturation had a definite effect upon the relative permeability characteristics; therefore, the amount of water present at the start of a relative permeability measurement should closely approximate the reservoir connate water saturation.

### 2.2.6 Temperature

Despite the contradiction among the studies carried out to investigate the effect of temperature on relative permeability, most of them showed that with increasing temperature, irreducible water saturation increased and residual oil saturation decreased. Almost all the studies were performed by dynamic displacement, and the change in relative permeability characteristics, in those studies so indicated, was attributed indirectly to temperature (change in wettability, interfacial tension, and viscosity ratio). Edmondson [54] reported that the relative permeability ratio decreased with temperature at high water saturations, but increased with temperature at low saturations.

Poston *et al.* [53] observed no influence on the relative permeability ratio curve. Lo and Mungan [56], who conducted the only steady-state study, found that temperature affected relative permeabilities when using white oils, but observed no effect on relative



permeability curves when using tetradecane. Miller and Ramey [57] performed dynamic displacement experiments at elevated temperatures on unconsolidated and consolidated sands. They indicated that essentially no changes with temperature were observed in either residual saturations or relative permeability relationships. However, they concluded that some previous results may have been affected by a combination of laboratory-scaling phenomena and measurement difficulties; that is to say, temperature effects observed may have been affected by viscous instabilities, capillary end effects, and/or difficulties in maintaining material balance. However, Maini and Batycky [58] reported that temperature influences both the endpoint saturation and the shape of the relative permeabilities curves.

### **2.2.7 Flow Rate and Pressure**

The effect of pressure and flow rate is another controversial issue in reservoir engineering. Some investigators attribute relative permeability changes, that appear to be due to changes in displacement pressure and pressure gradient, to the boundary effect in laboratory experiments. Others believe that the effect of displacement pressure and pressure gradient may be due to the changes imposed on viscosity, interfacial tension, and other fluid or rock properties. It is essential to understand boundary effects in the laboratory tests. Boundary effect or end effect is attributed to a discontinuity in capillary properties of a core at the time of relative permeability measurement. In the laboratory experiments in which two immiscible fluids are flowed through a porous medium, there exists a saturation discontinuity at the outflow face. This discontinuity exists because the fluids pass from a region of finite capillary pressure in the sample to a region of zero capillary pressure (atmospheric pressure). The capillary forces existing in the core tend to prevent the wetting phase from leaving the sample, which results in the saturation of the wetting phase being maintained at a higher level near the outflow end of the core than throughout the remainder of the core. The accumulation of the wetting phase at the outflow face of the sample creates a saturation gradient along the sample which disturbs the relative

permeability measurements. That is to say, in a water-wet core, water accumulates at the outflow end of the core which causes a reduction in capillary pressure. The water will not leave the sample until the capillary pressure is overcome and the residual oil saturation, at the outflow face of the core, is reached; and thus estimation of the relative permeability based on the average saturation is erroneous, since the relative permeability varies due to the saturation gradient caused by the accumulation of the wetting phase at the outflow end of the core.

It should be mentioned that the boundary effect is a laboratory phenomenon. In reservoir rock, the capillary forces act uniformly in all directions, and thus negate each other. Hassler *et al.* [50] and Leverett and Lewis [21] attributed the observed changes in relative permeability to an end effect. Osoba *et al.* [59], Richardson *et al.* [60], and Sandberg *et al.* [61] observed no effect of flow rate on the relative permeability characteristics as long as a saturation gradient is not introduced into the sample by inertial forces. In other words, the flow rate is not so high that inertial effects become important. A later study by Ehrlich and Crane [62] concluded that both imbibition and drainage relative permeability were independent of flow rate. However, Wyckoff and Botset [12] indicated that the liquid and gas relative permeabilities were dependent on flow rate when the two phases flowed under the same pressure gradient. Morse *et al.* [51] found that relative permeability was dependent on flow rate.

Several authors studied the effect of the ratio of viscous forces to capillary forces. This ratio is known as the capillary number ( $N_C$ ). It is difficult to deduce which factor in the capillary number affects the relative permeability. However, Lefebvre du Prey [52] found that the relative permeability was a function of velocity ( $v$ ), through the ratio ( $\sigma \cos \theta / \mu v$ ), when the viscous forces predominate. Fulcher *et al.* [63] concluded that while the wetting phase (brine) relative permeability was a function of the capillary number, the non-wetting phase (oil) relative permeability was a function of interfacial tension and viscosity variables individually, rather than a function of the capillary number. Moreover,

they noted no velocity effects on the relative permeabilities.

For the effects of displacement pressure and pressure gradient, Wyckoff and Botset [12] and Leverett [41] found that these factors had a slight influence on the relative permeability characteristics. Pirson [64] indicated that the relative permeability in an imbibition cycle is affected by pressure gradient. However, Muskat [2] concluded that the gas and oil relative permeabilities of consolidated sands were independent of differential pressure changes. Delclaud [65] observed no effect of displacement pressure on the relative permeability.

It has been suggested that the most convenient way to minimize the boundary effect is the adjustment of capillary forces to insignificant values, as compared to the viscous forces. This can be achieved by a flow rate adjustment. However, the adjusted rate must be low enough so that the inertial forces are insignificant. Another convenient way of minimizing the boundary effect at the outflow end of a core is to use a more viscous oil in a long core.

In summary, many studies have been carried out to investigate the effects of different factors on relative permeability characteristics. In addition to those factors mentioned in this section, other factors are density of the fluid, an immobile third phase, and a trapped gas. Most researchers agree that these three factors have no significant effect on the relative permeability curves. However, the influence of any the factors mentioned above may be ambiguous, and it seems that the best way to obtain reliable relative permeability data is to make the conditions, under which the experiment is performed, as similar as possible to those of the reservoir porous medium.

### **2.3 Measurement of Relative Permeability**

Laboratory measurement methods are the most reliable sources of relative permeability data. However, there are several techniques available for estimation of relative

permeabilities. These techniques can be classified into three categories: i) mathematical models; ii) field performance; and iii) laboratory methods.

### **2.3.1 Mathematical Models**

These models are used to estimate relative permeability, not as a substitute for a laboratory measurement, but rather to extrapolate limited laboratory data. Since these models are beyond the scope of this study, they will be mentioned briefly in the following sections.

#### **2.3.1.1 Network Models**

These models are useful for understanding fluid behavior. They are usually based on the modeling of fluid flow in porous media using a network of electric resistors as an analog computer [34]. Relative permeability equations are formulated for a porous system in terms of porosity and a capillary pressure desaturation curve. These models are based on the assumption that a porous medium consists of a bundle of capillaries in order to apply Darcy's law and Poiseuille's equations in their derivations. In these models, the tortuosity concept is used to account for the tortuous path of the flow channels, as opposed to the concept of capillary tubes [66,67].

#### **2.3.1.2 Capillary Models**

Capillary models are also based on modeling of a porous medium by a bundle of capillary tubes of various diameters. Purcell [30] was among the first authors to develop an equation to compute the wetting-phase relative permeability in terms of porosity and a capillary pressure desaturation curve.

#### **2.3.1.3 Statistical Models**

Statistical models have also been used to describe the randomness of pore-size

distribution in porous media. They are also based on the bundle of capillary tubes system with various diameters distributed randomly. The system is described as being divided into a large number of thin slices by planes perpendicular to the axes of the tubes. However, these models ignore the interconnectivity of the pores in the formation.

#### **2.3.1.4 Empirical Models**

These models are based on empirical relationships describing relative permeabilities which are obtained by experimental measurements. These models are useful approximations to overcome the difficulties involved in the laboratory measurement.

It should be mentioned that the numerical simulator has become a valuable tool in reservoir engineering. It uses a history matching-technique to match production data. It involves assuming a set of relative permeability curves and matching the observed production and pressure data with that generated by solution of a finite difference approximation to the Buckley-Leverett equations.

#### **2.3.2 Field Performance**

Relative permeability data can be obtained from the production performance of a reservoir and its fluid properties. This process involves utilization of field data to calculate the relative permeability ratio of gas to oil by means of Darcy's law. Pressure-transient analysis is another means for determining the *in situ* effective permeability. It should be noted that the agreement between the experimentally measured relative permeabilities and those obtained from production data is generally poor. The core on which relative permeability is measured may not be representative of the reservoir. Relative permeability calculations from field performance give average values affected by pressure and saturation gradients, saturation variations in stratified reservoirs, and differences in stages of depletion [68].

### **2.3.3 Laboratory Methods**

Relative permeabilities can be measured in the laboratory by four methods. These methods are as follows: i) capillary pressure methods; ii) centrifuge methods; iii) unsteady-state methods; and v) steady-state methods

#### **2.3.3.1 Capillary Pressure Methods**

These techniques are usually used for small cores with low permeability, on which flow tests are impractical to perform. The capillary pressure techniques are developed to calculate relative permeabilities for drainage processes, where a non-wetting phase (gas) displaces a wetting phase (oil or water), and thus this technique is often used for gas-oil or gas-water systems. Equations have been developed to estimate relative permeability from capillary pressure data. Notable among them are those equations presented by Purcell [30] in 1949 and Fatt and Dykstra [69] in 1951.

#### **2.3.3.2 Centrifuge Methods**

These techniques utilize cores uniformly saturated with one or two fluids. Fluid production from these cores is monitored throughout the experiment. These methods, despite their lesser use, have some advantages over the other laboratory means in that they are faster than the steady-state methods, and they overcome the viscous fingering problems that may be encountered in the dynamic methods. However, they suffer from capillary end effects. Slobod *et al.* [31] first presented a mathematical technique to estimate relative permeability characteristics using a centrifuge. In 1983, O'Mera and Lease [70] developed an automated technique for measuring relative permeability using a centrifuge.

#### **2.3.3.3 Unsteady-State Methods**

These methods are known also as external-drive techniques. They are also called displacement methods because they involve displacing one fluid by another. Relative

permeability is calculated from the production data. Although these methods are faster than steady-state methods and relative permeability data can be obtained in a lesser time than that of steady-state methods, the mathematical analysis of the unsteady-state technique is more tedious. The unsteady-state basic theory was developed by Buckley and Leverett [71] in 1942. Based on the Buckley-Leverett frontal advance, Welge [72] presented a method to compute the average saturation and the oil recovery, and to obtain the ratio of relative permeabilities by knowing the fractional recovery of one fluid phase. Johnson *et al.* [73] extended the work of Welge to develop a method, known as the JBN method, to estimate the individual relative permeabilities.

Following the work of Johnson *et al.*, several authors proposed techniques to estimate the relative permeabilities from displacement data. These techniques are based on the same principle and most of them deal with either making the calculations less tedious, or obtaining more precise results. Jones and Roszelle [74] presented a graphical technique for estimating individual phase relative permeabilities. Sarma and Bentsen [75] extended the work of Jones and Roszelle. They took proper account of the constants of integration for the two differential equations describing the system, and thus they were able to obtain improved functional forms for smoothing cumulative oil and pressure drop histories. However, the use of external drive methods is limited to displacements in which the assumptions underlying Buckley-Leverett theory are met. In other words, it is important that the fluids used in these displacement experiments be incompressible and immiscible, and that the porous media be homogeneous and isotropic.

Finally, the application of external drive techniques requires that the flow be neither unsteady nor unstable, and that the saturation profiles be monotonic [76]. Moreover, the external drive methods suffer from several limitations. Several authors pointed out these limitations [77,73,75]. These methods require numerical or graphical differentiation of experimental data, and thus inaccuracies in data measurement become amplified by the process of differentiation. Another limitation is that these methods use the breakthrough

point as a very important parameter. Consequently, the slightest delay in observing this point may cause erroneous results. Moreover, because of discontinuities in saturation which may exist at the inlet and outlet ends of the core, the difference between the pressures measured externally at the inlet and outlet ends of the core may not be representative of the actual (internal) pressure drop across the core.

Another technique using the displacement method to obtain relative permeability data is the so-called dynamic method. This method is claimed to be applicable to measure relative permeabilities in a truly dynamic system under all flow conditions. Islam and Bentsen [23] related the fraction of flow to the pressure gradient by means of the differential form of Darcy's law to obtain a dynamic estimate of the effective permeability. This method requires measurement of both saturation and pressure profiles during displacement with respect to time and space. They showed that while the dynamic method gave relative permeabilities similar to those of JBN method during stabilized and stable displacement, the discrepancy between relative permeabilities from these two methods was significant when the displacement was unstabilized or unstable. However, Islam and Bentsen [23] neglected the saturation change and thus the capillary pressure in calculating the effective permeability of oil. Sarma and Bentsen [78] carried out the analysis from a Lagrangian rather than an Eulerian point of view. That is to say, they focussed on a specific saturation profile rather than a specific location along the core. They were able to estimate the flow fraction ( $f_w$ ) as a function of saturation. They demonstrated that it is acceptable to use equilibrium capillary pressure data to predict the pressure difference between oil and water in a dynamic displacement, provided the displacement is stable. Sarma and Bentsen [78] included the pressure gradient in the analysis and they concluded that unstabilized displacement data may be used to generate relative permeability curves over the entire saturation range of interest.



### 2.3.3.4 Steady-State Methods

In the steady-state methods, two different fluids are injected simultaneously at fixed and known flow rates or pressure for extended periods of time to reach equilibrium (inflow equals outflow and/ or the pressure drop across the core reaches a constant value and the saturation becomes invariant with time). Once steady-state (equilibrium) is reached, the flow rates and the pressure drop across the core are measured and used in Darcy's law to calculate the effective permeability for each phase at a particular saturation. The saturation may be obtained by either external or *in situ* techniques. The external techniques include material balance, gravimetric and extraction methods, while the *in situ* techniques include electric resistivity measurement, X-ray absorption, and microwave attenuation.

Despite the fact that the steady-state methods are time consuming, they are considered as the standard techniques against which all other methods are compared in that the steady-state techniques use the fewest assumptions, and thus they provide more reliable relative permeability data and they cover a wider range of saturation levels. Several steady-state methods have been proposed. They essentially follow the above description of the technique. However, they vary in the method of establishing capillary equilibrium between fluids and reducing or minimizing the boundary or end effects, and in the manner in which the two fluids are introduced into the core. These methods are discussed in the following sections.

#### 2.3.3.4.1 Hassler Method

As noted in Osoba *et al.* [59], this steady-state technique to measure relative permeability was developed originally by Hassler in 1944. The method was later modified by several investigators. The Hassler method produces good results for strongly wet cores. The apparatus involves installing a semipermeable membrane at each end of the measuring assembly. The purpose of these two membranes is to keep the fluid phases separated at both ends of the core, while both phases flow simultaneously through the core.

The pressure is measured separately in each fluid phase through a semipermeable barrier. This technique minimizes the capillary end effect by providing a uniform saturation throughout the length of the sample. The capillary pressures at boundary ends of the core can be made equal by equalizing the pressure gradients in the two fluid phases, through adjusting the flow rate of the non-wetting phase.

#### **2.3.3.4.2 Penn-State Method**

Morse *et al.* [51] presented this method in 1947. As for the previous method, several authors modified the technique described by Morse *et al.* Among those authors are Caudle *et al.* [35], Osoba *et al.* [59] and Geffen *et al.* [79]. In this technique, the core sample to be tested is mounted between two rock samples which are similar to the test sample. This set-up has two advantages, which are reducing the boundary effects and allowing mixing of the two fluid phases before they enter the test sample. In this procedure, one starts by saturating the sample with one fluid phase and adjusting the flow rate of this phase through the sample until a preselected pressure gradient is obtained. Then the second phase is injected at a low flow rate and the rate of the first phase is reduced slightly so that the pressure differential across the core remains constant. When equilibrium is reached, the two rates are recorded and the saturation of each phase is determined. After the fluid saturation in the core has been determined, the core assembly is reassembled and the procedure is repeated at a higher flow rate for the second phase until the complete relative permeability curve has been established. This steady-state technique can be used to measure relative permeability for either the imbibition or the drainage process, and it can be applied to both liquid-liquid and gas-liquid systems.

#### **2.3.3.4.3 Stationary Fluid Method**

This technique was described by Leas *et al.* [80] in 1950. The method then was improved by Osoba *et al.* [59]. In this technique, one measures permeability to gas with the

liquid phase held stationary within the core by capillary forces. The liquid phase is held stationary within the core by flowing the gas at very low rates so the liquid is not displaced, or by means of barriers which are permeable to gas but not to the liquid. The technique can be used to measure liquid permeability as well. Rapoport and Leas [66] used semipermeable barriers which held the gas phase stationary while allowing the liquid phase to flow. Relative permeability to gas determined by the stationary fluid method was in good agreement with values measured by other steady-state techniques. However, relative permeability to gas obtained by the stationary method was generally lower than other methods in the region of equilibrium gas saturation [59]. Moreover, this technique is considered to be unrealistic, since all mobile fluids are not permitted to flow simultaneously during the test [34].

#### **2.3.3.4.4 Hafford Method**

This method was described by Richardson *et al.* [60] in 1952. In this technique, the non-wetting fluid is injected directly into the sample and the wetting phase is injected into the sample through a semipermeable disc that allows only the wetting phase to pass. The central portion of the semipermeable disc is isolated from the remainder of the disc by a small metal sleeve. The central portion is used to measure the pressure in the wetting phase at the inlet end of the core. The pressure in the non-wetting phase is measured through a standard pressure tap machined into the Lucite surrounding the core. The pressure difference between the wetting and the non-wetting phase is a measure of the capillary pressure in the sample at the inflow end. The design of the apparatus of this technique allows investigation of boundary effects at the inlet of the core. The boundary effect can be minimized by using a high flow rate.

#### **2.3.3.4.5 Dispersed Feed Method**

Richardson *et al.* [60] also designed this steady-state method to measure relative

permeability. The dispersed feed method is similar to the Hafford and single-core methods. In this technique, the wetting fluid enters the test sample by first passing through a dispersing section. The dispersing section is made of porous material similar to the test sample. Moreover, in contrast to the Hafford device, the dispersing section does not contain a device for measuring the input pressure of the wetting fluid. The porous material, which in some cases has been made of the same core material as the sample, distributes the wetting phase so that the wetting fluid enters the test sample more or less uniformly over the inlet face. The non-wetting phase is introduced into the radial grooves which are machined into the outlet face of the dispersing section, at the junction between the displacing material and the test sample. Again, errors due to the boundary effect are made insignificant by using high rates of flow.

#### 2.4 Countercurrent Flow

Even though countercurrent flow phenomena were recognized early in reservoir engineering, these phenomena have received little treatment in the petroleum-related literature. The imbibition process of spontaneous flow of fluids in reservoir rock under a capillary pressure gradient was described by Buckley and Leverett [71], and Leverett *et al.* [81] in 1942. In reservoir rock, if capillary equilibrium is maintained, the water saturation in a coarse sand will increase gradually with a rise in the water table. As the water saturation in an adjacent coarse sand increases, a tight lens will imbibe water and expel oil, both by absorbing water at the bottom and expelling oil at the top, and by countercurrent flow of water and oil over the entire surface of the lens [71].

While imbibition plays a major part in the recovery of oil from normal reservoirs, imbibition might be the dominant displacement process in water flooding in fractured-matrix reservoirs. In water-wet fractured-matrix reservoirs, water will be imbibed from fractures into the matrix with a countercurrent expulsion of oil into the fractures [82]. Moreover, in fractured reservoirs, each block produces its oil almost independently from

its neighbors under the combined effect of gravity and capillarity. Spontaneous imbibition is a specific flow because it involves both cocurrent and countercurrent flows in proportions that depend on the ratio of gravity to capillary forces and on the boundary conditions. Countercurrent imbibition differs from cocurrent imbibition because of its lower kinetics, smoother water front, and slightly lower ultimate oil recovery [83].

The main concern for a long time has been the similarity and/or dissimilarity between the cocurrent and countercurrent flow mechanisms. More precisely, the question is whether it is acceptable to use relative permeability curves which were obtained for cocurrent flow to represent relative permeability saturation relationships for countercurrent flow.

In 1962, Templeton *et al.* [84] performed vertical countercurrent flow experiments on a 4-ft sandpacked tube. The two phases were pumped through until a reasonably uniform saturation was achieved, which was measured using the resistivity technique. Their results indicated that the capillary pressure saturation function and the relative permeability saturation functions changed during segregation. Templeton *et al.* concluded that Darcy's equations, modified for each phase, are valid generally for countercurrent flow.

In 1964, Blair [82] presented numerical solutions of the equations describing the imbibition of water and the countercurrent flow of oil in porous rocks. Calculations were made for imbibition of water into both linear and radial systems. These calculations were made based on the assumption that imbibition in the linear systems took place through one open, or permeable, face of the porous medium, while in the radial systems, water was assumed to be imbibed inward from the outer radius. The results of the calculations showed the variations in the imbibition of water caused by such factors as a change in viscosity of the oil and changes in the rock properties. Blair argued that his results demonstrated the value of his calculation method for studying imbibition phenomena, including the shapes of saturation and pressure profiles. However, Blair realized that his

theoretical calculations needed the support of laboratory imbibition experiments.

In 1966, Lelievre [85] applied the steady-state method for measuring cocurrent and countercurrent liquid-liquid relative permeabilities. He indicated that the relative permeability values of countercurrent flow were less than those of cocurrent flow. Lelievre found that the difference between cocurrent and countercurrent water relative permeabilities was always more than 25% for non-wetting phase saturations higher than 50%, while the oil relative permeabilities differed by more than 35% when the non-wetting phase saturation was higher than 20%.

In a later study, Lefebvre du Prey [86] investigated the validity of using laboratory experiments to scale gravity and capillarity, the two active forces in the recovery process from matrix blocks in fissured reservoirs. His imbibition tests showed a great discrepancy among the scaled recovery curves corresponding to different block sizes. The results created doubts about the use of tests on small samples to obtain recovery curves of blocks in a reservoir, even when the ratio of lengths is small. Lefebvre du Prey concluded that the conventional mathematical formulation was not applicable due to the following reasons : i) the formulation of the imbibition problem by the macroscopic equations generally accepted for displacement is not correct because relative permeabilities are valid when fluids are moving in the same direction, but cannot be used to describe imbibition when countercurrent flows are observed; ii) the actual boundary conditions on the porous medium side may be different from one block to another; iii) local heterogeneities are not scaled up when block sizes vary; and iv) instability may appear.

In 1986, Hamon and Vidal [87] conducted experimental and numerical studies to investigate the validity of the prediction of reservoir matrix-blocks performance from water-oil imbibition tests on small samples. They numerically reproduced relative permeabilities of countercurrent flow experiments with the standard relative permeability curves determined from a cocurrent unsteady-state waterflood. They used a synthetic porous medium having low permeability. However, Hamon and Vidal reported that a poor

reproducibility was obtained for some countercurrent flow tests on the light synthetic porous medium. They also observed a large lag between the time when water flowed through the core outlet end and the time when imbibition started.

Recently, Bourbiaux and Kalaydjian [83] carried out an experimental study of cocurrent and countercurrent flows on a vertical core sample. They used an X-ray absorption method to measure the fluids' saturations. They found that the relative permeabilities of countercurrent flow were about 30% less than the conventional cocurrent flow relative permeabilities, and the oil recovery from countercurrent flow was less than that of cocurrent flow. They concluded that Darcy's law is valid to describe the countercurrent flow.

It is clear from the relatively few studies in the literature that cocurrent and countercurrent flow are different in their mechanisms and consequently the use of the cocurrent relative permeability curves to describe countercurrent flow is questionable.

## **2.5 Saturation Measurement Techniques**

Relative permeability is a strong function of saturation. The quality of relative permeability curves depends on the accuracy of saturation measurement. There are two approaches to saturation determination. These two approaches are i) external techniques; and ii) *in situ* techniques.

### **2.5.1 External Techniques**

These techniques provide an average saturation value and do not reveal the saturation profile. Some of the methods used are the gravimetric method in which the saturation is obtained from the weight difference of the core before and during the test, and the extraction method in which the water saturation is inferred from distillation and extraction. In both methods, the core has to be removed from the core holder, subjecting it to saturation changes. The most-used method in the external techniques is the material

balance method, in which the saturation is obtained indirectly by measuring fluid production. The cumulative injection and production fluid volumes are measured and the difference is assumed to be retained in the sample. This method is subject to serious errors, especially when the pore volume of the core is small, because of the presence of dead volume in the system, fluid separation problems, and evaporation losses [68].

### **2.5.2 *In situ* Techniques**

In these methods, the fluid saturations inside the core are measured directly, without disturbing the fluid distribution. They provide saturation profiles and they are more accurate and reliable than external techniques. In the *in situ* techniques, a known stimulus is applied to the fluid in the core, and the resultant response is measured. The fluid saturation is then determined by referring to a pre-established calibration curve. The following are the most popular *in situ* techniques.

#### **2.5.2.1 Resistivity Technique**

This method is one of the oldest methods used for determining *in situ* saturation in a core sample. This technique utilizes the difference in brine and hydrocarbon resistivity to determine the fluid saturation. This method requires that the distilled water be replaced by brine to make the water conductive. The technique involves measuring the resistivity between two points (electrodes) in the sample and deducing the fluid saturation from this measurement. Although the resistivity technique is considered to be an *in situ* technique, it estimates only saturations that are a kind of integrated average between two fixed points (electrodes). A continuous saturation profile would not be achieved by increasing the number of electrodes; but, rather, this increase would cause interference between adjacent electrodes, and the estimated fluid saturation values would not represent the actual local saturations.



### **2.5.2.2 X-ray Absorption Technique**

In this technique, fluid saturation profiles are obtained along the length of the core. This method involves recording continuously the intensity of the X-ray beam that is transmitted through the core. By measuring the input and output intensities and relating them to a reference intensity of the X-ray beam that is transmitted by a known aqueous solution, the saturation of the aqueous solution can be determined. This technique involves the hazard of using X-rays. Another disadvantage of this method is that it requires adding a foreign material. The water has to be doped with Sodium Iodide, or Iodo-Benzene has to be added to the liquid hydrocarbon, which may affect the fluid properties. Moreover, the saturation profiles measured by the X-ray absorption method are not single-valued and involve some hysteresis effects [88], both of which make obtaining accurate relative permeability data questionable.

### **2.5.2.3 Optical Technique**

This technique requires the use of a transparent model. Fluid saturation profiles can be obtained by making use of the light absorption properties of the fluids. Oil has no photometric absorption, and light absorption depends solely on the quantity of water. Thus, water saturation can be determined along the length of the core. However, 1% (by weight) Cobalt-Chloride needs to be added to the water to color it blue [89]. This method is capable of generating continuous saturation profiles, but it, as does the X-ray absorption method, involves doping the water with a foreign substance. Moreover, the reported saturation profiles as determined by the optical method are not of good quality.

### **2.5.2.3 Microwave Attenuation Technique**

This method involves making use of the strong absorption of microwave radiation by water. Hydrocarbon and sand are nearly transparent compared with water.

In 1975, Parsons [90] used the selective absorption of electromagnetic radiation to

measure fluid saturation. Since then the microwave attenuation technique has become the most popular method for measuring fluid saturation. This technique is considered to be superior because it overcomes the difficulties that the other techniques suffer from, in that the microwave technique does not require adding a foreign material, and the continuous fluid saturation profiles generated by this method are of good reliability and high quality.

It should be mentioned that, in recent years, multidimensional scanning techniques, such as computerized tomography (CT) scan and nuclear magnetic resonance, have been used for relative permeability measurements to obtain additional diagnostic information about rock heterogeneity and saturation distribution .

### 3. STATEMENT OF THE PROBLEM

Understanding the mechanisms of fluid behavior in reservoir rocks is of great importance in optimizing the production of hydrocarbons from such rocks. Relative permeability characteristics play a vital role in describing fluid behavior in the porous medium. Thus, obtaining reliable and accurate relative permeability data, which can be used to verify two-phase flow theory, is a key factor in understanding better the flow of fluids in petroleum reservoir rocks.

Fractured reservoirs contain a substantial share of the oil reserves in the world. Production of oil from these reservoirs is accomplished by imbibition under the combined effect of gravity and capillarity.

As the literature review in the previous chapter revealed, there are a vast number of studies pertaining to relative permeability for cocurrent flow, but only a very few devoted to the study of relative permeability characteristics for countercurrent flow which are believed to account for a substantial part of the fluid behavior in fractured reservoirs.

In the present work, an attempt is made to study cocurrent and countercurrent flow by constructing the relative permeability curves for both flows. The steady-state method is used to investigate the similarity or dissimilarity of the relative permeability characteristics between cocurrent and countercurrent flow. Furthermore, the generalized relative permeabilities are investigated and compared with the conventional relative permeabilities.

An attempt is made also to determine the capillary pressure under dynamic conditions, since dynamic capillary pressure is more reliable and it describes the actual capillary pressure under dynamic flow conditions in porous media. Moreover, an attempt is made to investigate the inlet capillary pressure in countercurrent flow.

## 4. THEORY

### 4.1 Fluid Flow Equations

#### 4.1.1 Basic Motion Equations

If one considers flow in the direction  $s$ , where  $\theta$  is the angle between the positive  $s$  direction and the horizontal, then the force potential, such that flow will occur from higher values of potential to lower values, may be defined as [3]

$$\Phi = -gz \cos\theta + \int_{P_1}^{P_2} \frac{dP}{\rho} \quad (4.1)$$

Equation (4.1) can be rewritten as

$$\frac{d\Phi}{ds} = -g \cos\theta \frac{dz}{ds} + \frac{1}{\rho} \frac{dP}{ds} \quad (4.2)$$

provided the density of the fluid is independent of pressure (incompressible fluid). If one is measuring pressures in the water phase, then it is essential to assume that the fluids are being injected on the water side of the interface. For this case

$$\frac{d\Phi_w}{ds} = -g \cos\theta \frac{dz}{ds} + \frac{1}{\rho_w} \frac{dP_w}{ds} \quad (4.3)$$

and for the oil phase one can write,

$$\frac{d\Phi_o}{ds} = -g \cos\theta \frac{dz}{ds} + \frac{1}{\rho_o} \frac{dP_o}{ds} \quad (4.4)$$

The generalized Darcy's law for the water phase can be written

$$v_{ws} = -\frac{k_w \rho_w}{\mu_w} \left[ -g \cos\theta \frac{dz}{ds} + \frac{1}{\rho_w} \frac{dP_w}{ds} \right] \quad (4.5)$$

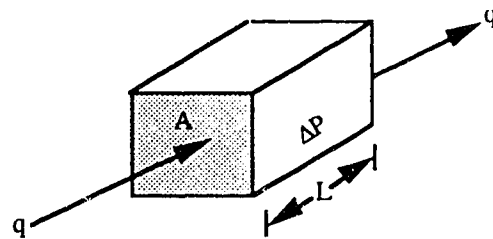
and, similarly, for the oil phase, it can be written

$$v_{os} = -\frac{k_o \rho_o}{\mu_o} \left[ -g \cos\theta \frac{dz}{ds} + \frac{1}{\rho_o} \frac{dP_o}{ds} \right] \quad (4.6)$$

If one considers horizontal steady-state flow in a block of a porous medium with cross

sectional area  $A$ , and length  $L$ , and if the flow is only horizontal, then  $\frac{dz}{ds} = 0.0$ ,  $\frac{dP_w}{ds} = \frac{dP_w}{dx}$ ,

$\frac{dP_o}{ds} = \frac{dP_o}{dx}$ , and Equation (4.5) reduces to



$$v_{wx} = -\frac{k_w}{\mu_w} \frac{dP_w}{dx} = \frac{q_w}{A} \quad (4.7)$$

and Equation (4.6) reduces to

$$v_{ox} = -\frac{k_o}{\mu_o} \frac{dP_o}{dx} = \frac{q_o}{A} \quad (4.8)$$

Integrating Equation (4.7) between the limits 0 and L in x and  $P_{w1}$  and  $P_{w2}$  where  $P_{w1}$  is the pressure at the inflow face and  $P_{w2}$  is the pressure at the outflow face,

$$q_w = \frac{k_w A (P_{w1} - P_{w2})}{\mu_w L} = \frac{k_w A \Delta P_w}{\mu_w L} \quad (4.9)$$

Similarly one can show that

$$q_o = \frac{k_o A (P_{o1} - P_{o2})}{\mu_o L} = \frac{k_o A \Delta P_o}{\mu_o L} \quad (4.10)$$

#### 4.1.2 Generalized Flow Equations

De la Cruz and Spanos [9] have shown, through volume averaging, that the generalized equations for the flow of two continuous phases are given by

$$\mu_1 \left[ \frac{1}{k_{11}} \bar{q}_1 - \frac{1}{k_{12}} \bar{q}_2 \right] = -\bar{\nabla} P_1 + \rho_1 \bar{g} \quad (4.11)$$

and

$$\mu_2 \left[ \frac{1}{k_{22}} \bar{q}_2 - \frac{1}{k_{21}} \bar{q}_1 \right] = -\bar{\nabla} P_2 + \rho_2 \bar{g} \quad (4.12)$$

Here  $\mu_i$  is the viscosity,  $\bar{q}_i$  is the Darcy velocity (per unit area),  $P_i$  is the volume-averaged pressure within phase  $i$ ,  $\rho_i$  is the density of phase  $i$  ( $i = 1, 2$ ) and  $k_{ij}$  are the generalized permeabilities.

For a horizontal, one-dimensional system, Equations (4.11) and (4.12) may be rewritten as

$$\mu_1 \left[ \frac{1}{k_{11}} q_1 - \frac{1}{k_{12}} q_2 \right] = -\frac{\Delta P_1}{L} \quad (4.13)$$

and

$$\mu_2 \left[ \frac{1}{k_{22}} q_2 - \frac{1}{k_{21}} q_1 \right] = -\frac{\Delta P_2}{L} \quad (4.14)$$

Equations (4.13) and (4.14) contain four unknown functions of saturation, the generalized permeabilities  $k_{11}$ ,  $k_{22}$ ,  $k_{12}$  and  $k_{21}$ . In order to specify the four generalized permeabilities at a specific saturation, say  $S_w^*$ , it is necessary to conduct two flow experiments. One approach would be to conduct two steady-state, cocurrent flow experiments, each at a different ratio of rates. However, if one takes this approach, each ratio of rates will give rise to a different saturation. This problem can be resolved by undertaking one cocurrent and one countercurrent flow experiment.

If the quantities measured in the countercurrent, steady-state flow experiments are designated by an asterisk, the equations for the countercurrent flow case, in view of Equations (4.13) and (4.14), become

$$\mu_1 \left[ \frac{1}{k_{11}} q_1^* - \frac{1}{k_{12}} q_2^* \right] = -\frac{\Delta P_1^*}{L} \quad (4.15)$$

and

$$\mu_2 \left[ \frac{1}{k_{22}} \dot{q}_2 - \frac{1}{k_{21}} \dot{q}_1 \right] = -\frac{\Delta P_2^*}{L} \quad (4.16)$$

Equations (4.13) - (4.16) may be solved to yield

$$k_{11} = \frac{\frac{\dot{q}_1}{q_2} - \frac{\dot{q}_1}{q_2}}{\frac{1}{\mu_1} \left[ \frac{1}{q_2} \frac{\Delta P_1^*}{L} - \frac{1}{q_2} \frac{\Delta P_1}{L} \right]} \quad (4.17)$$

$$k_{22} = \frac{\frac{\dot{q}_2}{q_1} - \frac{\dot{q}_2}{q_1}}{\frac{1}{\mu_2} \left[ \frac{1}{q_1} \frac{\Delta P_2^*}{L} - \frac{1}{q_1} \frac{\Delta P_2}{L} \right]} \quad (4.18)$$

$$k_{12} = \frac{\frac{\dot{q}_2}{q_1} - \frac{q_2}{q_1}}{\frac{1}{\mu_1} \left[ \frac{1}{q_1} \frac{\Delta P_1^*}{L} - \frac{1}{q_1} \frac{\Delta P_1}{L} \right]} \quad (4.19)$$

and

$$k_{21} = \frac{\frac{\dot{q}_1}{q_2} - \frac{q_1}{q_2}}{\frac{1}{\mu_2} \left[ \frac{1}{q_2} \frac{\Delta P_2^*}{L} - \frac{1}{q_2} \frac{\Delta P_2}{L} \right]} \quad (4.20)$$



For experimental reasons, it is not possible to ensure that a cocurrent and its associated countercurrent flow experiment are conducted at exactly the same saturation. As a consequence, it is necessary to correlate the measured ratios of flow rates and pressure gradients against saturation. It is convenient, and insightful, to use the conventional two-phase flow equations for this purpose. The conventional, steady-state, cocurrent equations may be written as

$$q_1 = -\frac{k_1 \Delta P_1}{\mu_1 L} \quad (4.21)$$

and

$$q_2 = -\frac{k_2 \Delta P_2}{\mu_2 L} \quad (4.22)$$

while the conventional, steady-state, countercurrent flow equations may be written as

$$q_1^* = -\frac{k_1^* \Delta P_1^*}{\mu_1 L} \quad (4.23)$$

and

$$q_2^* = -\frac{k_2^* \Delta P_2^*}{\mu_2 L} \quad (4.24)$$

If Equations (4.21) through (4.24) are introduced into Equations (4.17) through (4.20), it may be shown, after some manipulation, that

$$k_{11} = \frac{\frac{k_1 \Delta P_1}{k_2 \Delta P_2} - \frac{k_1^* \Delta P_1^*}{k_2^* \Delta P_2^*}}{\frac{1}{k_2 \Delta P_2} - \frac{1}{k_2^* \Delta P_2^*}} \quad (4.25)$$

$$k_{22} = \frac{\frac{k_2 \Delta P_2}{k_1 \Delta P_1} - \frac{k_2^* \Delta P_2^*}{k_1^* \Delta P_1^*}}{\frac{1}{k_1 \Delta P_1} - \frac{1}{k_1^* \Delta P_1^*}} \quad (4.26)$$

$$k_{12} = \frac{\mu_1 \left[ \frac{k_2 \Delta P_2}{k_1 \Delta P_1} - \frac{k_2^* \Delta P_2^*}{k_1^* \Delta P_1^*} \right]}{\mu_2 \left[ \frac{1}{k_1^*} - \frac{1}{k_1} \right]} \quad (4.27)$$

and

$$k_{21} = \frac{\mu_2 \left[ \frac{k_1 \Delta P_1}{k_2 \Delta P_2} - \frac{k_1^* \Delta P_1^*}{k_2^* \Delta P_2^*} \right]}{\mu_1 \left[ \frac{1}{k_2^*} - \frac{1}{k_2} \right]} \quad (4.28)$$

At this point, it is convenient to introduce the definitions

$$R_{12} = \frac{\Delta P_1}{\Delta P_2} \quad (4.29)$$

and

$$R_{12}^* = -\frac{\Delta P_1^*}{\Delta P_2^*} \quad (4.30)$$

While it is assumed generally that  $R_{12} = 1.0$  [27], it is unknown what  $R_{12}^*$  should be.

If Equations (4.29) and (4.30) are introduced into Equations (4.25) through (4.28), it may be shown that

$$k_{r11} = g_{11}k_{r1} \quad (4.31)$$

$$k_{r22} = g_{22}k_{r2} \quad (4.32)$$

$$k_{r12} = \frac{\mu_1}{\mu_2} g_{12}k_{r2} \quad (4.33)$$

and

$$k_{r21} = \frac{\mu_2}{\mu_1} g_{21}k_{r1} \quad (4.34)$$

where

$$g_{11} = \frac{R_{12}^* \frac{k_1^*}{k_1} + R_{12} \frac{k_2^*}{k_2}}{R_{12}^* + R_{12} \frac{k_2^*}{k_2}} \quad (4.35)$$

$$g_{22} = \frac{R_{12}^* \frac{k_1^*}{k_1} + R_{12} \frac{k_2^*}{k_2}}{R_{12}^* \frac{k_1^*}{k_1} + R_{12}} \quad (4.36)$$

$$g_{12} = \frac{1}{R_{12} R_{12}^*} \frac{R_{12}^* \frac{k_1^*}{k_1} + R_{12} \frac{k_2^*}{k_2}}{1 - \frac{k_1^*}{k_1}} \quad (4.37)$$

and

$$g_{21} = \frac{R_{12}^* \frac{k_1^*}{k_1} + R_{12} \frac{k_2^*}{k_2}}{1 - \frac{k_2^*}{k_2}} \quad (4.38)$$

and where

$$k_{r11} = \frac{k_{11}}{K} \quad (4.39)$$

$$k_{r22} = \frac{k_{22}}{K} \quad (4.40)$$

$$k_{r12} = \frac{k_{12}}{K} \quad (4.41)$$

and

$$k_{r21} = \frac{k_{21}}{K} \quad (4.42)$$

Equation (4.13) may be rearranged to read

$$-\frac{\mu_1 q_1 L}{\Delta P_1} = k_{11} - \mu_1 \frac{k_{11}}{k_{12}} \frac{q_2 L}{\Delta P_1} \quad (4.43)$$

Introducing Equations (4.21) and (4.29) into Equation (4.43), it follows that

$$k_1 = k_{11} - \mu_1 \frac{k_{11}}{k_{12}} \frac{q_2 L}{R_{12} \Delta P_2} \quad (4.44)$$

Finally, upon introducing Equation (4.22) into Equation (4.44), it may be shown that

$$k_1 = k_{11} + \frac{\mu_1}{\mu_2} \frac{k_{11}}{k_{12}} \frac{k_2}{R_{12}} \quad (4.45)$$

The generalized permeability,  $k_{11}$ , represents the influence of the viscous drag of fluid 1 on the solid surfaces in the porous medium [19]. Moreover, as noted by Whitaker [17], the ratio  $k_{11}/k_{12}$  represents the influence of the viscous drag that exists between phase 1 and phase 2. Thus, in view of Equation (4.45), one can view the conventional permeability,  $k_1$ , as representing the influence of two types of drag: the first is that due to the flow of fluid 1 over the solid surfaces in the porous medium, and the second is that due to momentum transfer across the fluid 1-fluid 2 interfaces in the porous medium.

By introducing Equations (4.25) and (4.27) into Equation (4.45), it may be shown that

$$k_{r1} = k_{r11} + k_{rv1} \quad (4.46)$$

where

$$k_{rv1} = \frac{k_1 - k_1^*}{1 + \frac{R_{12} k_2^*}{R_{12}^* k_2}} \frac{1}{K} \quad (4.47)$$

Similarly, it may be shown that

$$k_{r2} = k_{r22} + k_{rv2} \quad (4.48)$$

where

$$k_{rv2} = \frac{k_2 - k_2^*}{1 + \frac{R_{12}^* k_1^*}{R_{12} k_1}} \frac{1}{K} \quad (4.49)$$

#### 4.1.2.1 Relationship between $k_{r12}$ and $k_{r21}$

No consensus exists in the literature [17,19,91,92] as to the proper relationship between the relative viscous drag coefficients,  $k_{r12}$  and  $k_{r21}$ . However, if it is assumed that only phase 1 contacts the porous matrix, it can be shown that [19]

$$\frac{\mu_2}{k_{r21}} - \frac{\mu_1}{k_{12}} = \frac{\sigma f_2}{\phi^2 S_1 (1 - S_1)} \quad (4.50)$$

where  $f_2$  is an empirically determined function of saturation.

Equation (4.50) can be rearranged, in view of Equations (4.41) and (4.42), to give

$$\frac{k_{r12}}{k_{r21}} = \frac{\mu_1}{\mu_2} + \frac{k_{12}}{\mu_2} \frac{\sigma f_2}{\phi^2 S_1 (1 - S_1)} \quad (4.51)$$

If  $\sigma$  is allowed to become zero, it follows that

$$\frac{k_{r12}}{k_{r21}} = \frac{\mu_1}{\mu_2} \quad (4.52)$$

On the other hand, if one divides Equation (4.33) by Equation (4.34), it can be shown, after some manipulation, that

$$\frac{k_{r12}}{k_{r21}} = \left( \frac{\mu_1}{\mu_2} \right)^2 \frac{1}{R_{12}R_{12}^*} \frac{k_2 - k_2^*}{k_1 - k_1^*} \quad (4.53)$$

It is important to note that, while Equation (4.51) is based on physics, Equation (4.53) is not. This is because Equation (4.53) is defined in terms of empirical relationships for the ratios of the pressure gradients,  $R_{12}$  and  $R_{12}^*$ , and for the effective permeabilities,  $k_1$ ,  $k_1^*$ ,  $k_2$  and  $k_2^*$ . As a consequence, some caution must be exercised when using Equation (4.53) to draw conclusions concerning the proper relationship between  $k_{r12}$  and  $k_{r21}$ .

## 4.2 Microwave Theory

Microwaves are electromagnetic radiation of smaller wavelengths (1 meter to 0.1 cm) in the frequency spectrum of 0.3 GHz to 300 GHz [90]. Using the microwave technique for measuring saturation profiles requires understanding the laws governing the microwave behavior of any material. Materials are classified based on their interactions with microwaves, and thus there are three basic types of materials: i) conductors; ii) insulators; and iii) dielectrics.

Conductors are opaque to microwaves; thus, they are used to contain and guide the microwaves. Insulators, on the other hand, are materials that transmit microwaves without any appreciable loss of power; that is to say, microwaves can travel across them without losing their strength. Consequently insulators are regarded as being "transparent" to microwaves. Dielectrics are the other type of materials which absorb microwaves. In other words, once they are exposed to the path of microwaves only a small part of them can

cross the material. Dielectrics are characterized by their low electrical conductivity in comparison to that of metal. However, dielectrics absorb microwaves in different proportions. Absorption of energy as electromagnetic radiation travels through dielectrics can be described in terms of either dielectric or optical phenomenon. The following theoretical discussion is condensed from Reference [90].

#### 4.2.1 Dielectric Properties

Dielectric permittivity is one of the principal factors which determines the propagation of electromagnetic waves in materials. When a material is placed in a static electric field, a redistribution of electric charges in the field occurs. This total polarization may be caused by several simultaneous effects:

- 1) The relative displacement of the negative electron cloud and the positive nucleus;
- 2) Displacement of atoms or ions;
- 3) Alignment with the field by molecules with permanent dipoles;
- 4) An interfacial polarization phenomenon in emulsions.

If the external field is removed, each polarization effect would return to its normal state within a given time. However, the time required to return to the normal state, often called the relaxation time, may be very short or very long depending on the nature of the electric field involved. For example, electron-cloud relaxation times are very short because of the small displacements and high electron mobility, while molecular dipole relaxation times are relatively longer because of the longer separation of charges and the local retardation of molecular reorientation.

If the external field is applied and removed alternately at a certain frequency, that is to say, the electric field is alternating, the electric charges would be set into alternating polarization and relaxation. Electromagnetic radiation, as an alternating field, would cause the electric charge displacement to oscillate with the electric field frequency. However, the two vectors may not match and may differ by some phase angle,  $\delta$ . Therefore, at any time,



the instantaneous field strength and electric displacement may be described by

$$E = E_{\max} \cos 2\pi ft \quad (4.54)$$

and

$$D = D_{\max} \cos(2\pi ft - \delta) \quad (4.55)$$

If  $\delta=0$ , then the displacement and the electric field strength would be in phase. The concept of a dielectric constant is introduced in order to compare the displacement with the electric field strength. The dielectric constant is defined by  $\epsilon = D/E$ . However, when  $\delta \neq 0$ , so that the  $D$  and  $E$  vectors are not collinear, the dielectric constant is considered in two parts. The first part

$$\epsilon' = \frac{D_{\max} \cos \delta}{E_{\max}} \quad (4.56)$$

represents the normal dielectric constant, or the proportionality constant, between  $E_{\max}$  and the component of  $D_{\max}$  that is in phase with the field. The other part

$$\epsilon'' = \frac{D_{\max} \sin \delta}{E_{\max}} \quad (4.57)$$

represents the loss factor, which is the ratio of the  $90^\circ$  out of phase part of  $D_{\max}$  to  $E_{\max}$ . These two terms,  $\epsilon'$  and  $\epsilon''$ , are usually considered as the real and imaginary dielectric constants. They are functions of the material, the environment, and the field frequency. These constants can be determined experimentally.

Because a moving or oscillating charge is an electric current, a power-dissipation equation may be derived from the expressions for electric field and current to give

$$P_r = \frac{1}{2} f E_{\max}^2 \epsilon'' \quad (4.58)$$

Further, if the dielectric molecules behave like a perfect capacitor, the displacement current would follow the field,  $\epsilon''$  would be zero, and the material would be transparent to the radiation. Thus, only the out-of-phase part of the displacement current contributes to energy that is absorbed and ultimately dissipated as heat.

At microwave frequencies, the dipole relaxation is responsible mainly for the energy-absorbing process. For dipolar materials, the dielectric constant would depend on frequency, as can be predicted from the expression for the two parts of the dielectric constant. How the two parts of the dielectric constant vary with frequency for a pure dipolar liquid is shown in Figure 4.1. As can be seen in this Figure, at very low frequencies, the dipole alignment can track exactly the field oscillation and therefore  $\epsilon'' = 0$  and  $\epsilon' = \epsilon_0$ , the static value. On the other hand, at very high frequencies, the field changes so rapidly with respect to the dipole's ability to keep in step that the dipole orientations practically become random and do not contribute to a displacement current. Once again  $\epsilon''$  becomes zero, but  $\epsilon'$  remains at the optical dielectric constant  $\epsilon_\infty$ . Between these two extremes, at intermediate frequencies, there is a broad band where the dipoles can not keep in step with the field, and therefore the loss factor  $\epsilon''$ , and thus the energy absorption, is a bell-shaped curve that can be characterized by a single relaxation time,  $\tau$ , associated with the  $\epsilon''$  peak.

#### 4.2.2 Optical Properties

When electromagnetic radiation travels through a medium that absorbs magnetic radiation energy, the maximum electric-field strength diminishes with distance. The instantaneous field strength can be described as a function of time and position in terms of

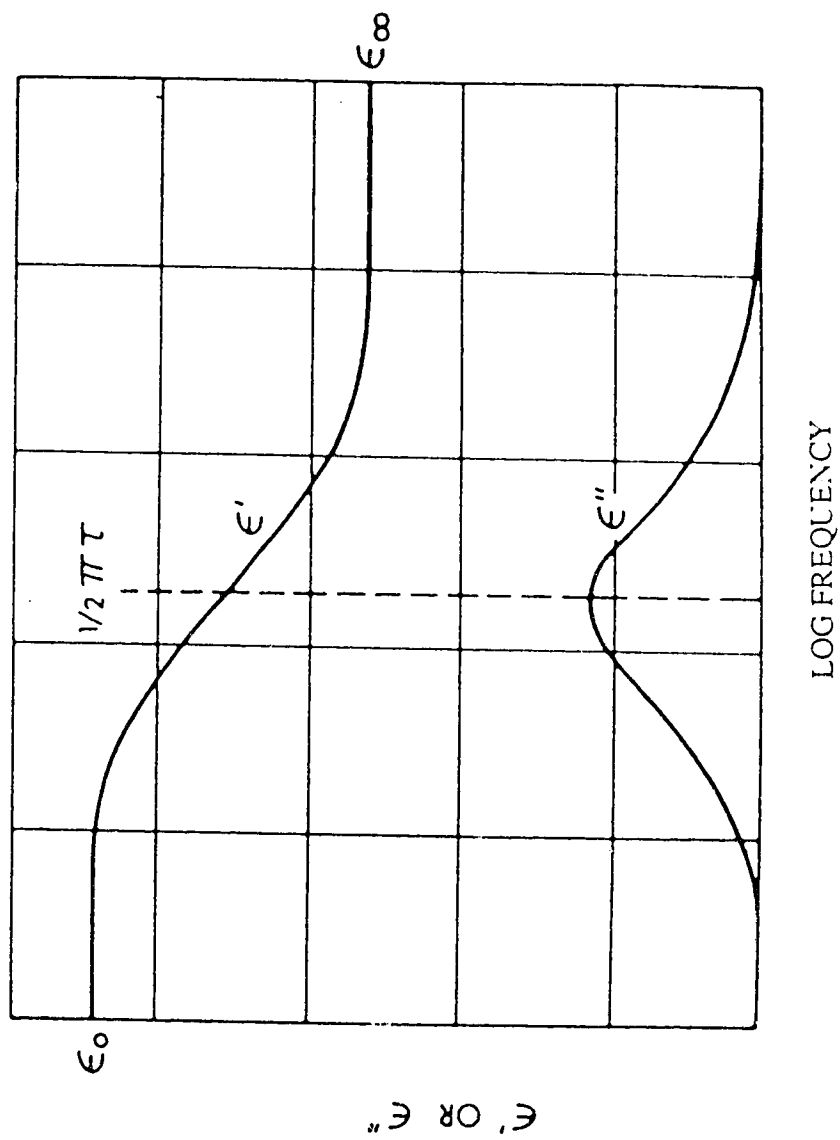


Figure 4.1 : Dielectric Constants for Dipolar liquid with Single Relaxation Time.  $\tau$  . ( after Parsons )

optical properties by the following relationship:

$$E(x,t) = E_0 \exp\left[-\frac{2\pi f k x}{c}\right] \exp\left[i2\pi f\left(t - \frac{nx}{c}\right)\right] \quad (4.59)$$

where

$E(x,t)$  = electric field strength at distance  $x$

and

$E_0$  = maximum electric field strength of the incident radiation (at  $x=0$ ).

In the above relationship, the first exponential term describes the absorption of energy as radiation passes through the medium. The extinction coefficient,  $k$ , is a characteristic of the particular medium. The second exponential term describes the sinusoidal variation of the field with time. Equation (4.59) can be simplified by introducing a complex index of refraction which can be defined as

$$n^* = n - ik \quad (4.60)$$

The velocity of propagation for a non-negative insulator is given by

$$v_{pr} = \frac{c}{\sqrt{\epsilon'}} = \frac{c}{n} \quad (4.61)$$

and thus, dielectric and optical treatments are made identical, and the complex dielectric constant,  $\epsilon^*$ , ( $\epsilon^* = \epsilon' - i\epsilon''$ ), and the complex refractive index are related by

$$\epsilon^* = n^{*2} \quad (4.62)$$

The above equation leads to the following relations among physically measurable quantities:

$$\epsilon' = n^2 - k^2 \quad (4.63)$$

and

$$\epsilon'' = 2nk \quad (4.64)$$

The Lambert absorption law is obtained by applying Equation (4.59) to the change in intensity of the radiation when it passes through some material. This familiar law states that, for homogeneous, multicomponent mixtures, each molecule contributes to the wave attenuation as if the other molecules were not present. Therefore, when the absorption ability of one species far overshadows the others (much larger extinction coefficient), then the total absorption in a sample is a direct function of the number of those molecules in the path of the electromagnetic radiation. Hence, the Beer-Lambert law

$$\frac{I_o}{I_i} = \exp(-K_s Ch) \quad (4.65)$$

or

$$\log \frac{I_o}{I_i} = A_{st} = -\frac{K_s Ch}{2.303} \quad (4.66)$$

where

$I_o$  = radiation intensity leaving the sample;

$I_i$  = radiation intensity entering the sample;

$K_s$  = molar absorption coefficient;

$C$  = concentration of absorption, molarity;

$h$  = thickness of the sample;

and

$A_{st}$  = absorbance of the system.

However, if more than one component in the mixture absorbs radiation in accordance with this law, the absorbances are additive.

Besides absorption phenomena, microwaves are subject to the usual optical laws of reflection, refraction, diffraction, and scattering. Microwaves have wave lengths relatively longer than ordinary light. Because the particle sizes of the components of the currently used experiments (sand grains, oil droplets, water droplets, microemulsions) are smaller than the wave length (approximately 1 cm for 27 GHz), the composite medium appears homogeneous to the microwaves.

#### **4.2.3 Physical Properties**

Most of the solids and gases have negligible loss factors at microwave frequencies. Even though some gas molecules have permanent dipoles (water vapor is a prime example), their low density makes the microwave absorption insignificant. On the other hand, the loss factor varies greatly for pure liquids.

The magnitude of the loss factor depends on both the molecular structure of the liquid and the temperature. Water, being a dipolar substance, strongly absorbs microwaves. A water molecule contains a positive and a negative charge. When an electric field is applied, molecules tend to align themselves in the direction of the applied field. If the frequency of the applied field is high enough (1 GHz to 120 GHz) that the dipolar molecules are no longer able to keep pace with changes of the applied field, a lag between dipolar rotation and change in the applied field occurs. As a consequence, the microwaves are attenuated and the dielectric under the applied field is heated. Dissolved salt content in the water may cause a change in the loss factor. However, the influence of dissolved salt in water is a second-order effect. The effects of temperature and dissolved salt content are depicted in Figures 4.2 and 4.3. As can also be seen in Figure 4.2, a majority of crude oil molecules are nonpolar and show extremely small microwave losses.

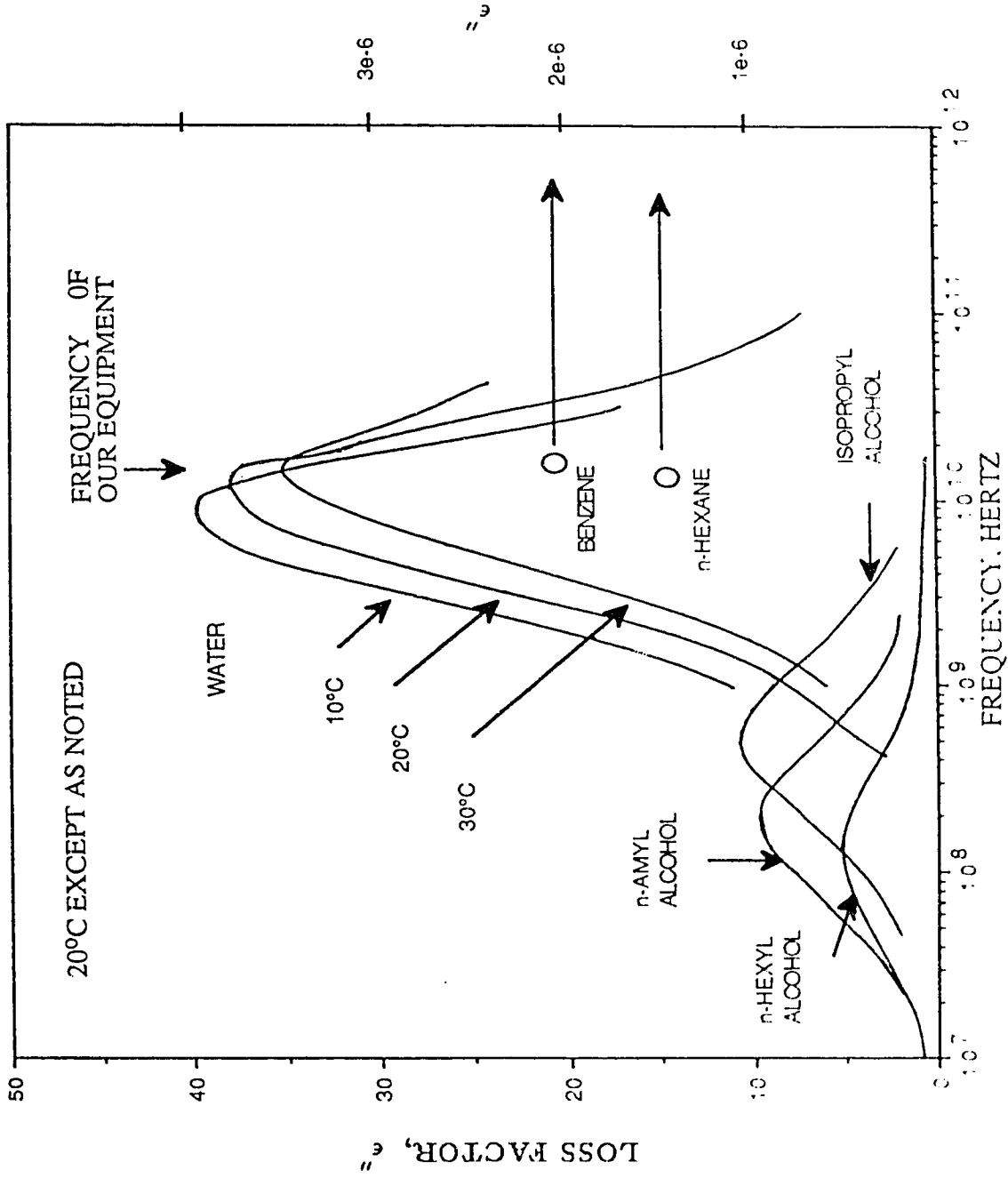


Figure 4.2 : Loss Factors for Some Pure Liquids. ( after Parsons )

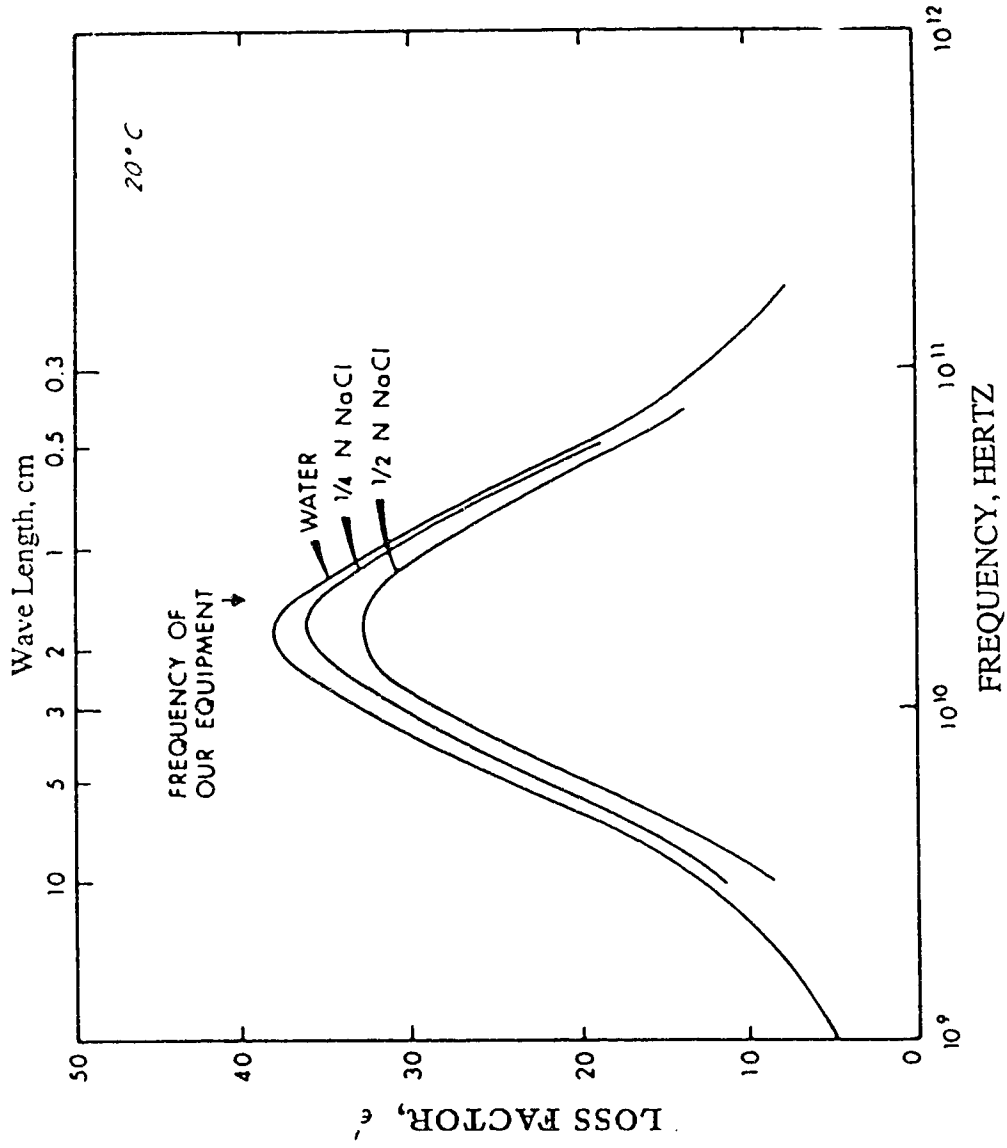


Figure 4.3 : Loss Factors for Aqueous Salt Solutions. ( after Parsons )



In this study, a microwave frequency of 27 GHz was chosen for the microwaves because maximum attenuation of the microwave signal by the water is achieved at this frequency. Thus, as the microwave travels across the coreholder, which contains sand and a mixture of water and oil, the loss factor of the water overshadows that of the oil, and the loss of energy may be attributed primarily to the water and partly to the coreholder material, sand, and oil which are considered nearly "transparent" to the microwaves.

#### 4.2.4 Estimation of Water Saturation

The amount of absorbance of microwaves as electromagnetic radiation travels through a homogeneous medium of thickness,  $h$ , (as explained previously) is dictated by the Beer-Lambert law (Equation 4.66).

When microwaves travel through a medium containing a solution, the attenuation of radiation through a given path length depends on the volume fraction of the solution. The molar absorption coefficient,  $K_a$ , can be defined as

$$K_a = \frac{4\pi f f_v k}{Cc} \quad (4.67)$$

where

$f$  = frequency of the microwave;

$f_v$  = volume fraction of absorber;

$C$  = concentration of absorber, molarity;

$c$  = velocity of light.

By combining Equations (4.66) and (4.67) one can show that

$$\log \frac{I_o}{I_i} = -\frac{4\pi h f f_v k}{2.303c} \quad (4.68)$$

If water were the only absorptive material in the system, then the theoretical relationship

between the microwave signal and the water saturation could be described as

$$\log \frac{I_o}{I_i} = A_w = -\frac{4\pi f K_{wa} h \phi S_w}{2.303c} = BS_w \quad (4.69)$$

However, as the fibreglass, sand, and oil also absorb part of the microwave signal, the absorbance of these materials must be taken into account. The over-all system may be considered to have two absorptive components: water and every thing else. In this regard, the absorbance due to materials other than water is determined experimentally. This absorbance not only accounts for the losses due to the coreholder, oil and sand, but also for other losses such as those due to reflection. One can express the total absorbance as

$$A_{st} = A_w + A_{ls} \quad (4.70)$$

where  $A_{st}$  is the total absorbance,  $A_w$  is the absorbance due to water, and  $A_{ls}$  is the absorbance due to other materials and factors. If one introduces Equation (4.70) into Equation (4.68), one may write

$$\log \frac{I_o}{I_i} = A_w + A_{ls} \quad (4.71)$$

Therefore

$$\log \frac{I_o}{I_i} = BS_w + A_{ls} \quad (4.72)$$

By scanning the core at two different water saturations, Equation (4.72) may be written for these water saturations; thus, parameters B and  $A_{ls}$  can be determined by solving the resulting equations simultaneously. Therefore, water saturation can be

estimated using the following equation

$$S_w = \frac{\left( \log \frac{I_o}{I_i} - A_b \right)}{B} \quad (4.73)$$

## 5. EXPERIMENTAL EQUIPMENT AND PROCEDURE

### 5.1 Description of the Experimental Apparatus

A schematic diagram of the equipment used in the experiments conducted to estimate relative permeabilities and dynamic capillary pressure in cocurrent flow is shown in Figure 5.1. The experimental set-up was modified slightly to study countercurrent flow. A schematic diagram of the equipment used in countercurrent flow experiments is presented in Figure 5.2. The experimental set-up was similar to the one used in a previous study [24]. The rectangular coreholder, of width 1.1 cm, height 5.65 cm, and total length 100 cm, was made of insulating-type fiberglass, because this material readily transmits microwaves and has a high strength.

The instruments, for this study, may be classified under the following categories:

- (1) microwave instrumentation;
- (2) fluid injection system and pressure measuring devices;
- (3) data acquisition and storage.

#### 5.1.1 Microwave Instrumentation

The microwave attenuation apparatus to estimate the dynamic water saturation can be simplified in that it consists of a stable source of microwaves and a detection system. The different components of the microwave system are shown in Figure 5.3. These units are:

1. klystron and power supply unit: to supply very stable single-phase, single-frequency microwave signals. The microwave generator has a frequency range of 26-30 GHz;
2. tuner: micrometer plungers in both the electrical and magnetic planes to fine-

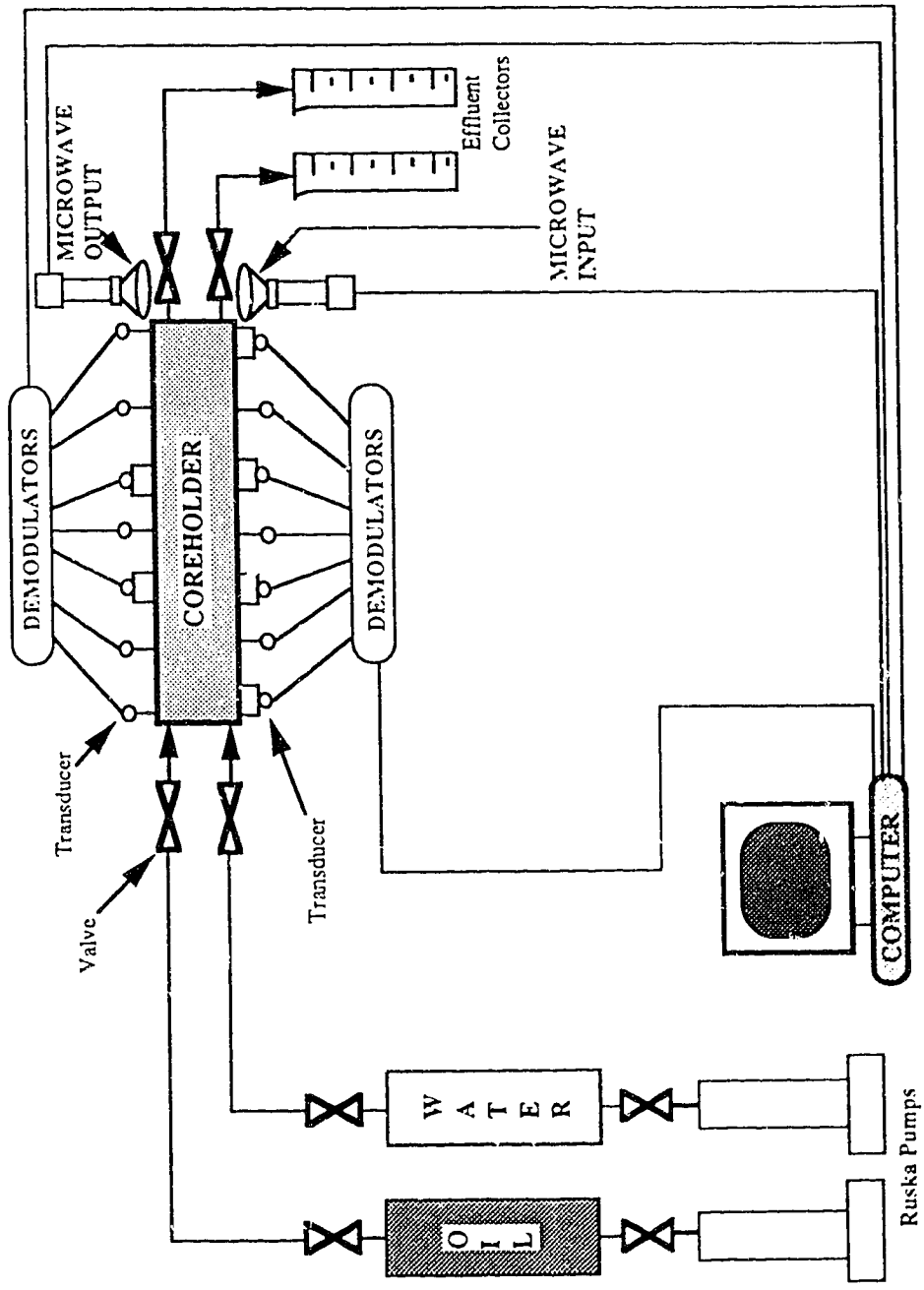


Figure 5.1 : Schematic Diagram of the Cocurrent Experimental Apparatus.

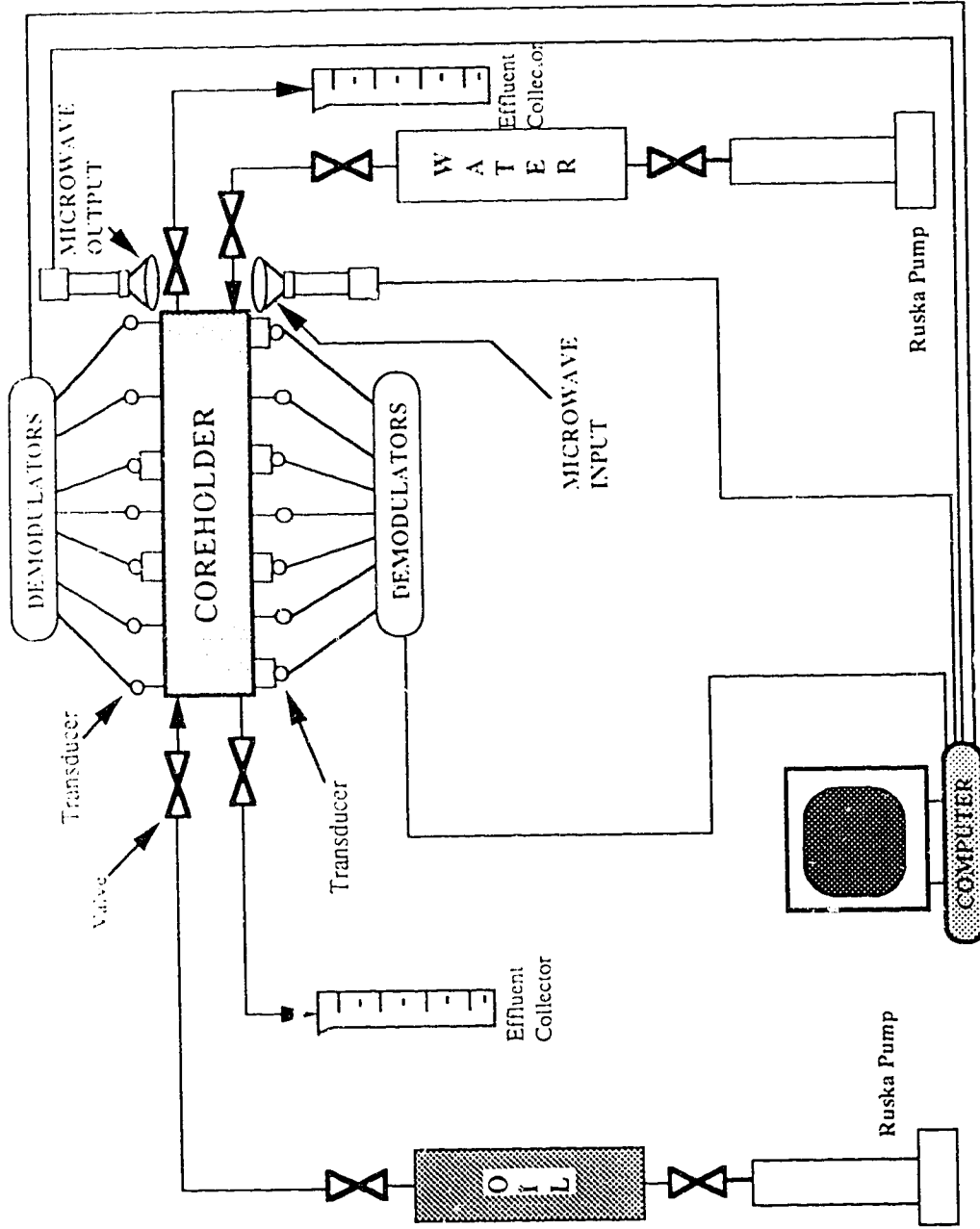


Figure 5.2 : Schematic Diagram of the Countercurrent Experimental Apparatus.

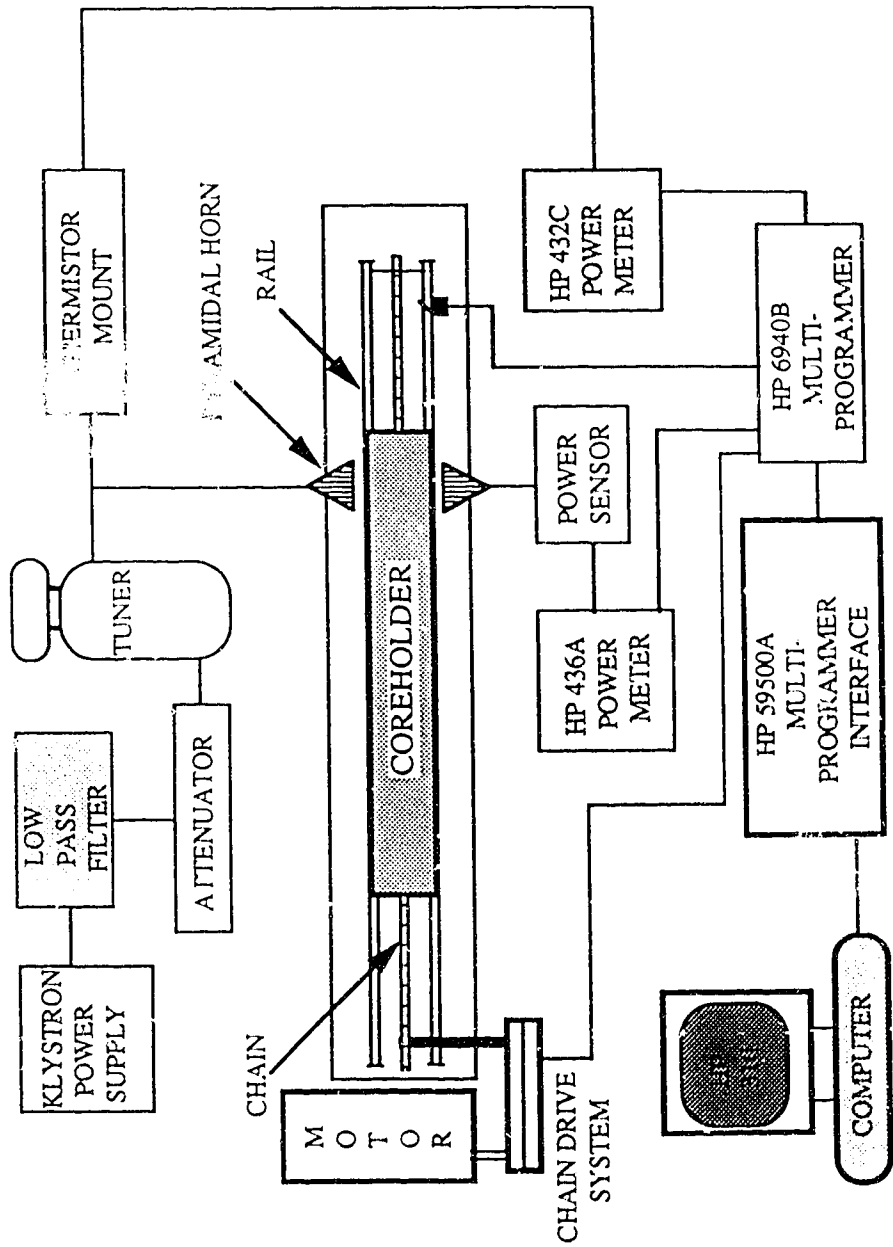


Figure 5.3 : Schematic Diagram of Microwave Instrumentation.

tune the microwave frequency;

3. attenuator: to regulate the microwave signal to any desired level;

4. pyramidal horns: two pyramidal horns with antennas were mounted on both sides of the core to facilitate transmitting and receiving of the microwave signals. Directional couplers were used along with the waveguides to attain proper alignment between the horns;

5. detecting meters: two power meters, one on each side of the coreholder, to measure microwave signals via power sensors. The power meter on the input side was an HP432C power meter and was used for measuring input power. The power meter on the output side was a digital power meter, HP436, which receives microwave signals via an HP8486 power sensor. The analogue microwave data were fed readily to the computer via the HP-IB using an HP-option 022 kit. Transmitted microwave signals at the other side of the coreholder were measured by a power sensor, HP-R8486A. This sensor is capable of measuring power in the range of 1 microwatt to 100 milliwatt in the frequency range of 26.5 GHz-40 GHz.

### **5.1.2 Fluid Injection System and Pressure Measuring Devices**

Two constant-rate Ruska pumps were used to inject fluids through the coreholder. One pump was used to inject water and the other was used to inject oil. The pumps were operated by shifting gears to obtain the desired flow rate. The fluid-containing cylinders of the two pumps were connected to the coreholder by flexible tygon tubing. The coreholder had two end caps. Each end cap had two fritted plates with an opening in each plate. One plate was made of an oil-wet material (Teflon) for injecting or producing oil, while the other plate was made of a water-wet material (fused glass beads) for injecting or producing water.

For pressure profile measurement along the length of the core, the coreholder had fourteen pressure-transducer taps; seven were located on the top and seven on the bottom



of the coreholder. The placement of the pressure transducers is depicted in Figures 5.1 and 5.2. Oil-wet fritted discs were mounted in the pressure-transducer taps located on the top of the coreholder, while water-wet fritted discs were mounted in those located on the bottom of the coreholder. Consequently, it was possible to measure the pressure in both the oil and the water at a given position along the length of the core. Two of the seven pressure transducers located on the top of the coreholder were used to measure differential pressures, and five pressure transducers were used to measure absolute pressure in the oil phase. Four of the seven pressure transducers located on the bottom of the coreholder were used to measure differential pressures, while the other three pressure transducers were used to measure absolute pressure in the water phase. The measurements taken using the differential pressure transducers were used to check the pressure gradients estimated using the absolute pressures. Data from the fourteen transducers were recorded automatically, via an interface, by an HP-310 computer, which acted as the controller. Moreover, a comprehensive interactive software package, which was modified from a software package developed for a previous study [24], enabled almost complete automation of the experimental runs and continuous data acquisition. The two Ruska pumps were the only two units not controlled by the computer. The program for monitoring and data sorting of the experimental runs is presented in Appendix A.

### 5.1.3 Data Acquisition and Storage

Acquisition and recording of microwave input and output power measurements and transducer pressure measurements were automated. Also, the scanning of the coreholder had to be automated. An HP-IB interface system was central to the data acquisition for the present study. The HP-IB interface is comprised of a multiprogrammer, HP6940B, and a multiprogrammer interface, HP59500A. An interface system performs three basic functions: i) talk; ii) listen; and iii) service request serial poll.

### 5.1.3.1 Multiprogrammer

The multiprogrammer, HP6940B, functioned as a multi-channel bi-directional interface between the controller (HP310 computer) and the other experimental devices to which command signals were sent and from which signals were received. Thus, it was regarded as the master control unit for bi-directional interfacing. Communication between the multiprogrammer and the external device was achieved via plugged-in input/output cards in the multiprogrammer. While data transfers between the multiprogrammer mainframe and input/output card were digital (twelve data bits), the transfers between the card and the external devices were either digital or analog (in the form of voltages or currents).

Data transfers from the controller to the multiprogrammer took the form of a sixteen-bit output word; while data transfers from the multiprogrammer to the computer took the form of a thirteen-bit (twelve data bits plus one status bit) word.

Communication between the multiprogrammer and the external devices was realized via the following cards: i) standard input; ii) remote/local; iii) logic and timing; iv) a scanner card capable of scanning 16 single-ended or eight differential voltages from the pressure transducers at very high speed; v) a digital output card to provide logic-level outputs to reflect the status of 12 programmed bits; vi) a high speed analog-to-digital converter card to provide high conversion speed and excellent accuracy; vii) a digital input card to receive 12 separate digital logic-level inputs from an external device; viii) a timer/spacer card to pace multiprogrammer I/O operations, and to generate accurate one-shot pulses; ix) unit select cards; and x) a voltage regulator card to provide isolated sources of  $\pm 15$  volt d.c. power which was required when the multiprogrammer used the high-speed A/D converter card.

### 5.1.3.2 Multiprogrammer Interface

The use of a multiprogrammer, HP59500A, enabled achieving bi-directional

operation of the multiprogrammer. Multiprogrammer HP59500A buffered and transmitted data and control signals between the HP-IB and the multiprogrammer. The multiprogrammer operations were initiated only when the HP59500A was listening. It converted the serial ASCII characters, both alpha and numeric, from the controller into a 16-bit word format required by the multiprogrammer. When the HP59500A talk address was received, the encoder translated the 15th bit into an octal digit and bits 11-0 to four octal digits.

The service request line was used by the HP59500A to indicate that the multiprogrammer required service. This service line was enabled whenever the multiprogrammer was operating in the timing mode. Consequently, it was set when the multiprogrammer completed an operation or requested an interruption of the current programming sequence. Control signals from the multiprogrammer, HP6940B, to HP59500A implemented the service request function.

Serial poll was a method used by the controller to determine which bus device had requested service. Thus, essentially, it consisted of interrogating bus devices in sequence, and then reading back a status byte from each device which was used to identify the devices requesting service. When addressed to talk in serial poll mode, the multiprogrammer interface, HP59500A, returned a status byte of 64 if it was requesting a service; if not, a status byte of zero was returned.

## **5.2 Experimental Procedure**

The experimental procedure can be divided into three distinct parts: i) core preparation; ii) cocurrent experiments; and iii) countercurrent experiments. Each part is described in detail in the following sections.

### **5.2.1 Core Preparation Procedure**

An unconsolidated porous medium was prepared by wet-packing the coreholder

with Ottawa Silica sand. The sand, 70-130 mesh as received from the suppliers, was sieved to obtain 80-120 mesh sand. In order to pack the core, the pressure transducer taps were fitted with dummy plugs. Then the coreholder, the physical dimensions of which are listed in Table 5.1, was suspended in a vertical position and filled partially with distilled water. Sand was dropped into the coreholder through a constant height of distilled water so as to have a water head on the top of the sand. The process was continued until the coreholder was filled with sand. The coreholder was vibrated overnight in a vertical position. Once the coreholder was packed, the end plate was put on the end of it. To this point, both end caps (preparation end caps) had one opening in each of them to enable estimation of rock properties and to establish irreducible water saturation. Then the coreholder was tested for leaks at a water pressure of 25 psi. The core was dried by passing compressed dry air through the core holder for about 24 hours. After drying the sample, a microwave scan at zero percent water saturation was obtained. The microwave response data at zero percent water saturation were stored for subsequent saturation calculations. The coreholder was weighed both empty and with dry sand in order to estimate the mass of the sandpack. Once a dry scan was taken, the packed core was attached to a vacuum pump and evacuated for 24 hours. Then the core was resaturated by imbibition of distilled water into the sand. Subsequently the pore volume of the sandpack was determined by a material balance calculation. The absolute permeability was then estimated using Darcy's law for several flow rates.

Once the core was saturated, a microwave scan was performed at 100% water saturation. Following the same procedure as for the dry scan, the microwave response data were recorded and stored by the computer. The sandpack with 100% water saturation was then allowed to sit for about twelve hours to render it water-wet.

For the microwave scans, the speed of the electric motor was adjusted so that the core travel time was that required for the computer to collect 100 data points (one datum point every cm). This adjustment was made for every run.

**Table 5.1: Physical Dimensions of Coreholder**

Width (cm)	Height (cm)	Total Length (cm)	Bulk Volume (cc)
1.1	5.65	100	621.5

To establish an irreducible water saturation,  $S_{wi}$ , an oilflood was conducted. A refined oil (MCT-5) was injected through the core at a constant flow rate for all the runs to avoid any effect of flow rate on the irreducible water saturation. The oilflood was continued until such time as the incremental recovery of water became essentially zero. This usually required the injection of about four pore volumes of oil. When the irreducible water saturation was reached, another microwave scan was taken and the microwave response data were stored for further analysis.

After establishing the irreducible water saturation, the effective oil permeability was determined using Darcy's law. This was accomplished by replacing two of the dummy plugs, one at the inlet and one at the outlet end, with pressure transducers, so that the total pressure drop across the core could be determined. Next, the remaining dummy plugs were removed so that the pressure transducers (with oil-wet or water-wet fritted discs) could be installed in the remaining taps. Also, the endcaps (preparation end caps) were replaced by two different endcaps (cocurrent or countercurrent flow end caps) which had two plates in each with an opening in each plate. One of these plates was oil-wet while the other was water-wet. To avoid entrapment of air [24] during the mounting of transducers and replacing endcaps, oil was circulated at a very slow rate while the transducers and the endcaps were being installed.

### 5.2.2 Cocurrent Flow Experiments

With the core at initial fluid saturation (irreducible water saturation), both fluids were injected simultaneously into the core in the same direction. Oil was injected through the oil-wet plate and the water through water-wet plate. The injection of the fluids was performed at a fixed ratio of the rates and it was continued until steady state was achieved. Usually injection was continued as long as the maximal allowable time. The maximal allowable time was dependent on the capacities of the cylinders of the Ruska pumps and the rate at which the fluid was being injected.

During the experiment, the core was scanned periodically by microwaves to obtain the dynamic water saturation along the core. The interval between the microwave scans was preselected on the basis of injection rate and duration of the run. At the same time pressure readings were obtained by the fourteen transducers. Thus, the scan profiles and pressure measurements were taken at the same point in time. However, the desired number of scans was introduced as input data in the computer program so that microwave scans could be made as often as one scan every fifteen seconds. During scanning, an interrupter box, controlled by the digital output card in the HP-IB, activated the piston of the air actuator valve, causing the piston to lock onto a chain driven at a constant rate by the electrical motor. Because this air actuator valve was fitted to the clamp holding the coreholder, it enabled the movement of the core on the rails between the two microwave antennas. Once the coreholder was scanned over its entire length, it hit the interrupter switch fitted in the rails. At this point, the piston of the air actuator valve was unlocked from the moving chain. The deadweight attached at the output-end side of the coreholder helped it roll back to its initial position. In order to avoid a fast and violent rollback, the dead weight was allowed to slide into a column of water which acted as a cushion and helped the coreholder to roll back gently and slowly. Fluid production was collected in two graduated cylinders placed at the outlet ends to provide a means to check the water saturation by material balance.

At the end of each experiment, data were analyzed, and only the portion of the results where steady state was established was retained. To minimize boundary effects, calculations were made as if the core were only 96 cm long, considering only the length between the two far transducers (each of which was 2 cm away from the end of the coreholder). Effective permeabilities of both oil and water at a specific saturation were determined using Darcy's law, and relative permeabilities were then obtained as the ratios between effective and absolute permeabilities.

Once the effective permeabilities at a certain saturation were determined, the

experimental apparatus was prepared for the next experiment, the ratio between the flow rates was changed, and the experiment was reconducted. The procedure was repeated until a complete set of imbibition relative permeabilities was obtained.

### **5.2.3 Countercurrent Flow Experiments**

Upon establishing the relative permeability curves for cocurrent flow, the end caps (cocurrent or countercurrent flow end caps) of the coreholder were replaced by the preparation end caps (with one opening in each end), while oil was circulated at a very low rate to avoid entrapment of air, as previously explained. The core was then reflooded with oil until irreducible water saturation was reestablished, in order to retain the properties of the sample so that the characteristics of cocurrent and countercurrent flow could be compared and studied. The pressure transducers were recalibrated to assure accurate pressure measurement.

Once the irreducible water saturation was recreated, the countercurrent flow end caps were replaced and a microwave scan was performed at the initial water saturation. Then the cylinders of the two Ruska pumps were connected to the coreholder. A ratio between the oil flow rate and water flow rate was chosen. Oil was injected into one end of the coreholder, while water was injected into the other end of the coreholder. As in the cocurrent experiments, microwave scans and pressure measurements were performed regularly throughout the experiment. At the end of the experiment, the effective permeabilities were calculated. Then the ratio of the flow rates was changed and the experiment was repeated until a complete set of imbibition relative permeabilities was obtained.



## 6. RESULTS AND DISCUSSION

### 6.1 Introduction

The steady-state flow experiments conducted in this study were carried out in water-wet unconsolidated sandpacks. Two sets of runs were conducted. In each set, the imbibition relative permeability and capillary pressure curves were constructed for cocurrent flow. The sandpack was reflooded with oil in order to attain the original core properties. Then the relative permeability and the inlet capillary pressure curves for the countercurrent flow were constructed. The hydrocarbon fluid used in this study was MCT-5. The properties of the water and oil used in the experiments are listed in Table 6.1.

### 6.2 Data Analysis

In order to solve for  $k_{r11}$ ,  $k_{r22}$ ,  $k_{r12}$  and  $k_{r21}$ , Equations (4.32), (4.34), (4.36) and (4.38) have to be solved at the same water saturation. Because there is no assurance this would occur experimentally, it is necessary to solve the above-mentioned equations numerically. That is to say, the experimentally obtained data have to be curve-fitted. Fitting the results obtained from the different experiments allowed evaluating the equations, and thus the variables, at the same water saturation without actually obtaining those results at the same water saturation.

To carry out a least-squares analysis, it is essential to specify a number of different "predictor" variables which can be used in the fitting equations. Once a specific set of "predictor" variables had been chosen, they were conditioned so as to be consistent with the equation they fit. Then the method of least squares was used to estimate the values of the parameters (coefficients) of the regression equation selected. This was repeated for a number of different regression equations. Then various statistical methods provided

**Table 6.1: Fluid Properties at 22°C**

Fluid System	Density (gm/cc)	Viscosity (cp)	Interfacial Tension (dync/cm)
1. Distilled Water	0.9982	1.0	-
2. MCT-5	0.8123	30.48	32.6

within the BMDP [93] program and SPSS-X [94] program, non-linear regression analysis packages available on the MTS at the University of Alberta, were used to select the best fitting equation.

First pressure data obtained experimentally by transducers were plotted versus dimensionless distance, and then the best straight line was obtained by using the method of least squares. Then the data were conditioned. This was done to utilize all of the data, to minimize experimental errors, and to make the data analysis consistent. The data conditioning procedure is explained in Appendix B. It should be noted here that the resulting pressure gradients after conditioning the data, were very close to those of the raw experimental data. This indicates that the measured data were of good quality; however, conditioning the data has enabled making the data analysis consistent. The ratio of the pressure gradient in the water phase to the pressure gradient in the oil phase, for both cocurrent and countercurrent flow,  $R_{12}$  and  $R_{12}^*$ , respectively, was plotted versus normalized water saturation, which was least-squares fitted in order to estimate the ratio of pressure gradients as a function of water saturation for both cocurrent and countercurrent flow.

For the relative permeabilities, Darcy's law was used to calculate the water and oil relative permeabilities using the measured data (except for the pressure data which were conditioned as stated above). This was done for both cocurrent and countercurrent flow. Relative permeability curves were constructed and then the data were fitted using the method of least squares. The water relative permeabilities were fitted as functions of water saturation using the following parametric equations:

$$k_{rw} = a_1(S_w - S_{wi}) + b_1(S_w - S_{wi})^2 + c_1(S_w - S_{wi})^3 \quad (6.1)$$

and

$$k_{rw}^* = a_1^*(S_w - S_{wi}) + b_1^*(S_w - S_{wi})^2 + c_1^*(S_w - S_{wi})^3 \quad (6.2)$$

Equations (6.1) and (6.2) were selected in the above specific forms so that both  $k_{rw}$  and  $k_{rw}^*$  would be equal to zero at initial water saturation ( $S_{wi}$ ). The oil relative permeabilities were also fitted as functions of water saturation using the following parametric equations:

$$k_{ro} = a_2(1 - S_{or} - S_w) + b_2(1 - S_{or} - S_w)^2 + c_2(1 - S_{or} - S_w)^3 \quad (6.3)$$

and

$$k_{ro}^* = a_2^*(1 - S_{or} - S_w) + b_2^*(1 - S_{or} - S_w)^2 + c_2^*(1 - S_{or} - S_w)^3 \quad (6.4)$$

Equations (6.3) and (6.4) were selected in the above specific forms so that both  $k_{ro}$  and  $k_{ro}^*$  would be equal to zero at residual oil saturation (at water saturation equal to  $1 - S_{or}$ ). The fitted relative permeabilities were then used to estimate  $k_{r11}$ ,  $k_{r22}$ ,  $k_{r12}$  and  $k_{r21}$  which were plotted versus water saturation.

It should be noted here that the ratios of flow rates were also fitted versus water saturation using the method of least squares. The parametric equation used to fit the ratio of flow rates for cocurrent flow was

$$\frac{q_w}{q_o} = R_{12} \frac{\mu_o}{\mu_w} \left( \frac{a_3(S_w - S_{wi}) + b_3(S_w - S_{wi})^2 + c_3(S_w - S_{wi})^3}{a_4(1 - S_{or} - S_w) + b_4(1 - S_{or} - S_w)^2 + c_4(1 - S_{or} - S_w)^3} \right) \quad (6.5)$$

where

$$R_{12} = a \frac{(S_w - S_{wi})}{(1 - S_{or} - S_{wi})} + 1 - a \quad (6.6)$$

Equation (6.6) is the least-squares fitting equation for the ratio of pressure gradients in the water phase to that in the oil phase for cocurrent flow.

The parametric equation used to fit the ratio of flow rates for countercurrent flow was

$$-\frac{q_w^*}{q_o^*} = R_{12}^* \frac{\mu_o}{\mu_w} \left( \frac{a_3^*(S_w - S_{wi}) + b_3^*(S_w - S_{wi})^2 + c_3^*(S_w - S_{wi})^3}{a_4^*(1 - S_{or} - S_w) + b_4^*(1 - S_{or} - S_w)^2 + c_4^*(1 - S_{or} - S_w)^3} \right) \quad (6.7)$$

where

$$R_{12}^* = a^* \frac{(S_w - S_{wi})}{(1 - S_{or} - S_{wi})} - (1 + a^*) \quad (6.8)$$

Equation (6.8) is the least-squares fitting equation for the ratio of pressure gradient in the water phase to that in the oil phase for countercurrent flow.

The inlet capillary pressure,  $P_{cin}$ , for cocurrent flow was calculated as the difference between the fitted pressure versus distance in the oil phase and that in the water phase at the inlet end of the core. For countercurrent flow, the inlet capillary pressure,  $P_{cin}^*$ , was calculated as the difference between the fitted inlet pressure in the oil phase and the fitted inlet pressure in the water phase (at the other end of the core). The inlet capillary pressure for both cocurrent and countercurrent flow was fitted using a modified form of an empirical equation used by Van Domselaar [95]. The equation was modified so that the capillary pressure would be equal to zero at residual oil saturation (at normalized water saturation of unity) which is the case for strongly water-wet rock. This modified parametric equation was

$$P_c = \frac{a_5 + b_5 - a_5 S - b_5 S^2}{1 + c_5 S + d_5 S^2} \quad (6.9)$$

where  $S$ , the normalized water saturation, is equal to  $(S_w - S_{wi}) / (1 - S_{or} - S_{wi})$ .

When polynomials are used to construct an approximating function, oscillations of the approximating functions may prove troublesome. To lessen the severity of the

problem, only polynomials of relatively low degree were used in the regression function.

When regression equations with internally consistent parameters had been obtained, Equations (6.1) through (6.4) were used to generate the relative permeability versus saturation curves. And Equation (6.9) was used to construct the static capillary pressure-saturation curve.

### 6.3 Results

In order to evaluate the approach suggested in this study, two sets of data were utilized. A summary of the core and fluid properties for each set is provided in Table 6.2 while summaries of the basic results observed from the two sets of experiments are listed in Tables B.1 through B.8 in Appendix B.

The values of the parameters obtained from fitting the data, relative permeabilities, flow rate ratios, pressure gradients ratios, and inlet capillary pressure, Equations (6.1) through (6.9), are reported in Appendix C. Also reported in Appendix C are the residual sum of squares and the estimated mean-square error for each of the data sets.

Water saturation was monitored throughout each experiment by scanning the core at equally divided periods of time. Water saturation was estimated using Equation (4.73). Then dynamic water saturation profiles versus distance were constructed. Typical water saturation profiles for cocurrent flow experiments are shown in Figures 6.1 and 6.2, respectively. For countercurrent flow experiments, typical water saturation profiles are shown in Figures 6.3 and 6.4, respectively.

Pressure measurement was performed at the same time the core was scanned by microwaves but, as stated earlier, only pressure measurement at a time when steady-state was accomplished was considered in data analysis. Pressure was plotted versus distance as it was measured during each experiment. Samples of pressure profiles for cocurrent flow experiments are shown in Figures 6.5 and 6.6. Then the pressure data were conditioned, as stated in the previous section. Examples of conditioned pressure profiles for cocurrent flow experiments are shown in Figures B.1 and B.2 in Appendix B. For

**Table 6.2: Core and Fluid Properties**

Set	Porosity (%)	Absolute Permeability (d)	$S_{wi}$ (%)	$k_{oiw}$ (d)	$S_{or}$ (%)	$k_{wor}$ (d)
I	35.80	20.50	9.00	17.50	18.00	4.31
II	35.36	20.40	9.50	16.80	17.50	4.20

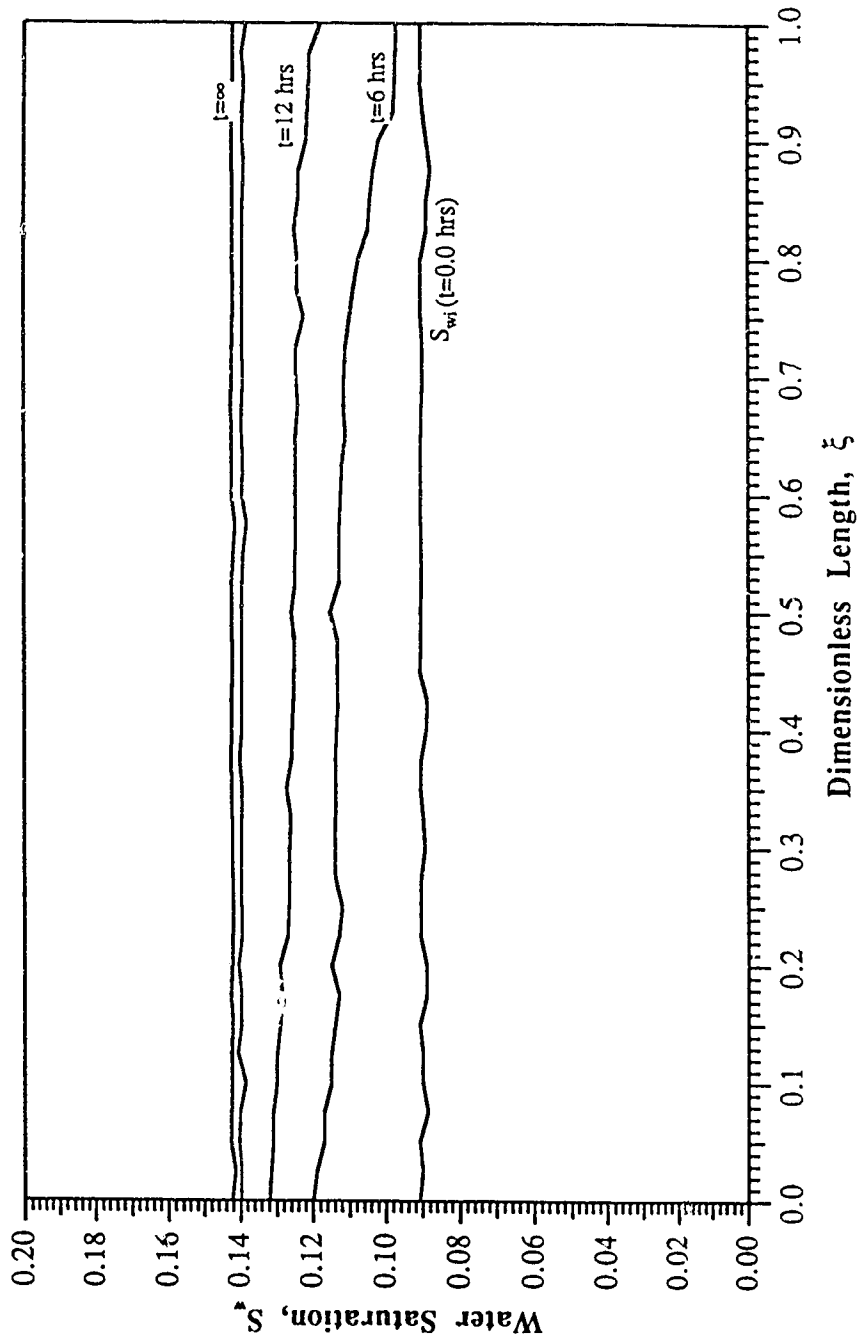


Figure 6.1 : Dynamic Water Saturation Profiles during Cocurrent Flow (Experiment No. 1)



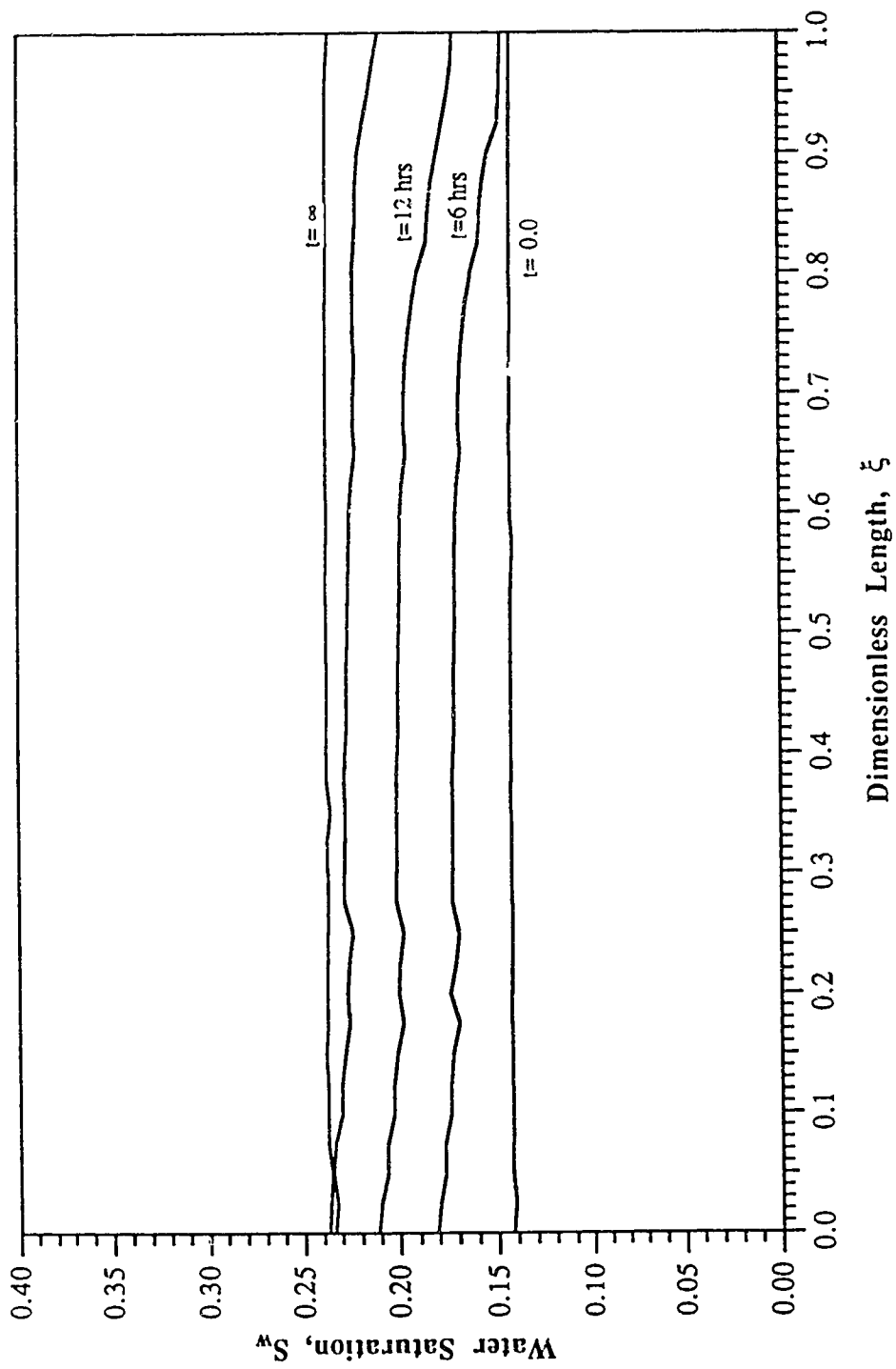


Figure 6.2 : Dynamic Water Saturation Profiles during Cocurrent Flow (Experiment No. 2)

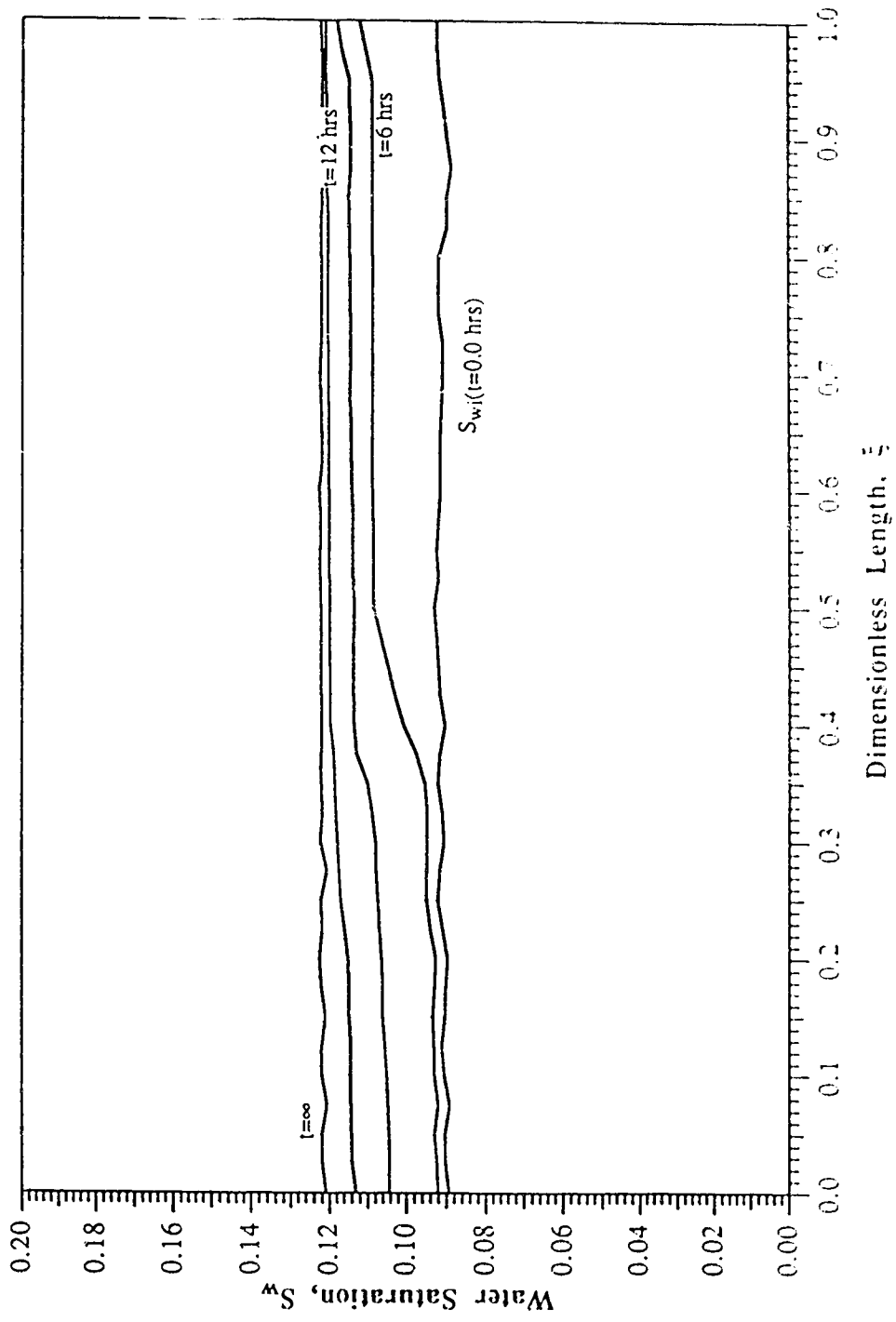


Figure 6.3 : Dynamic Water Saturation Profiles during Countercurrent Flow (Experiment No. 13)

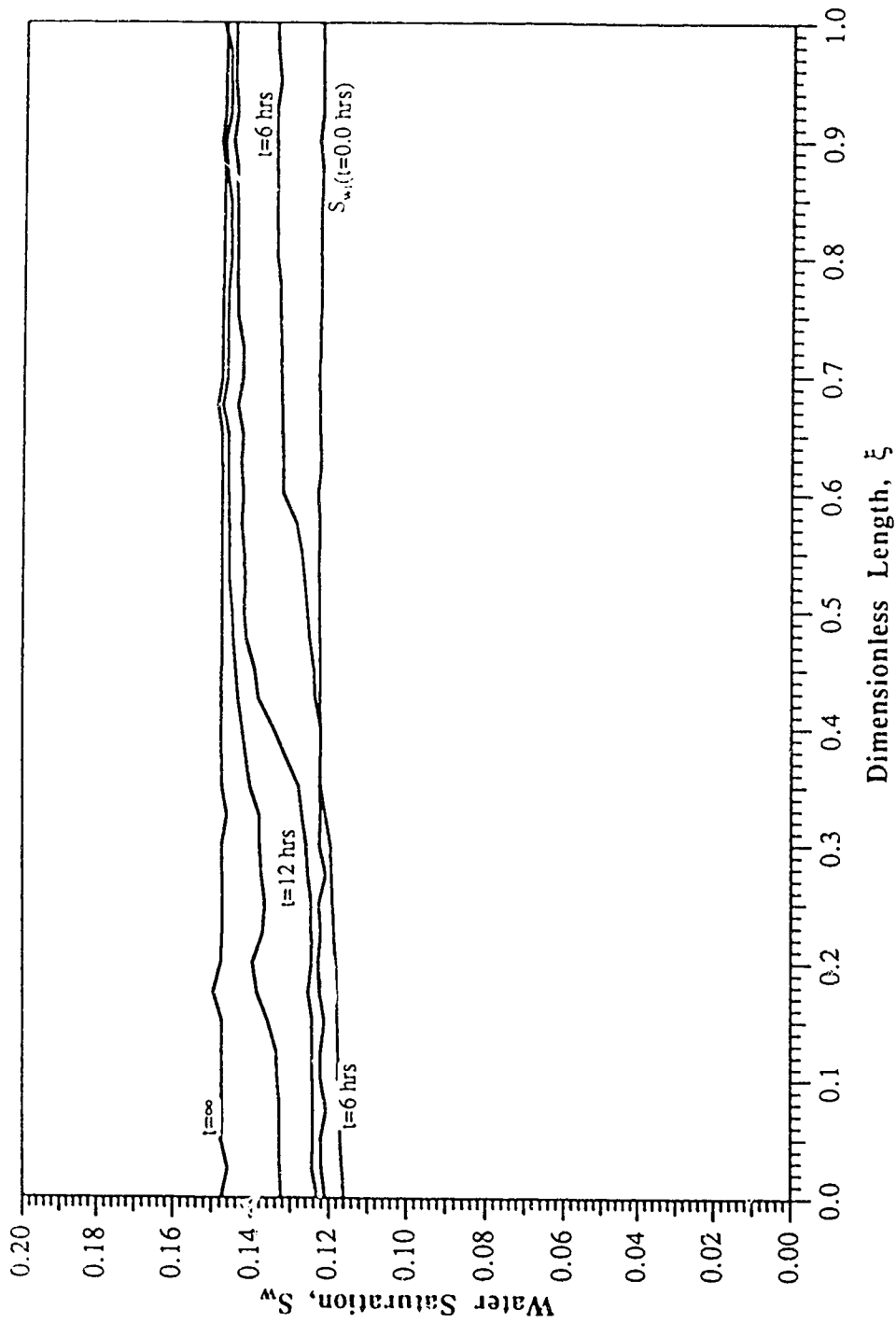


Figure 6.4: Dynamic Water Saturation Profiles during Countercurrent Flow (Experiment No. 14)

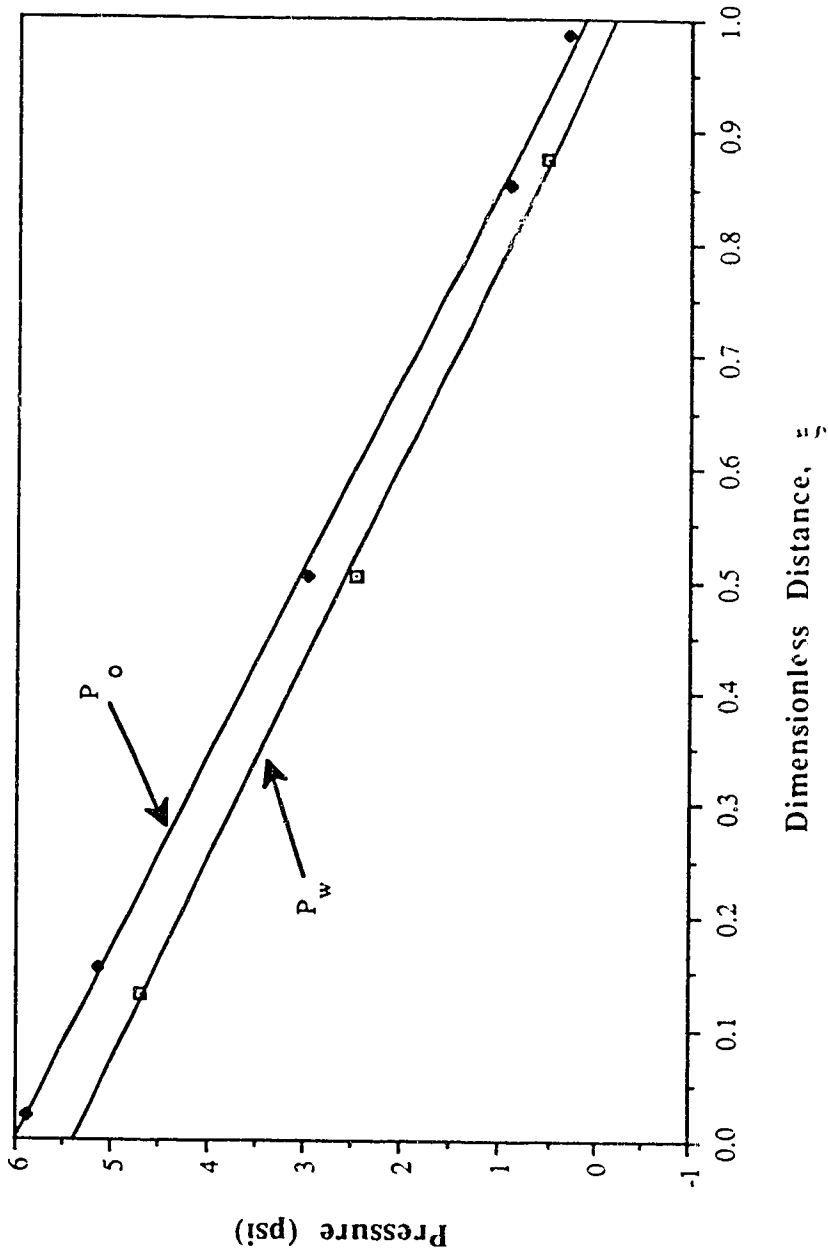


Figure 6.5 : Pressure Profiles during Cocurrent Flow (Experiment No. 1)

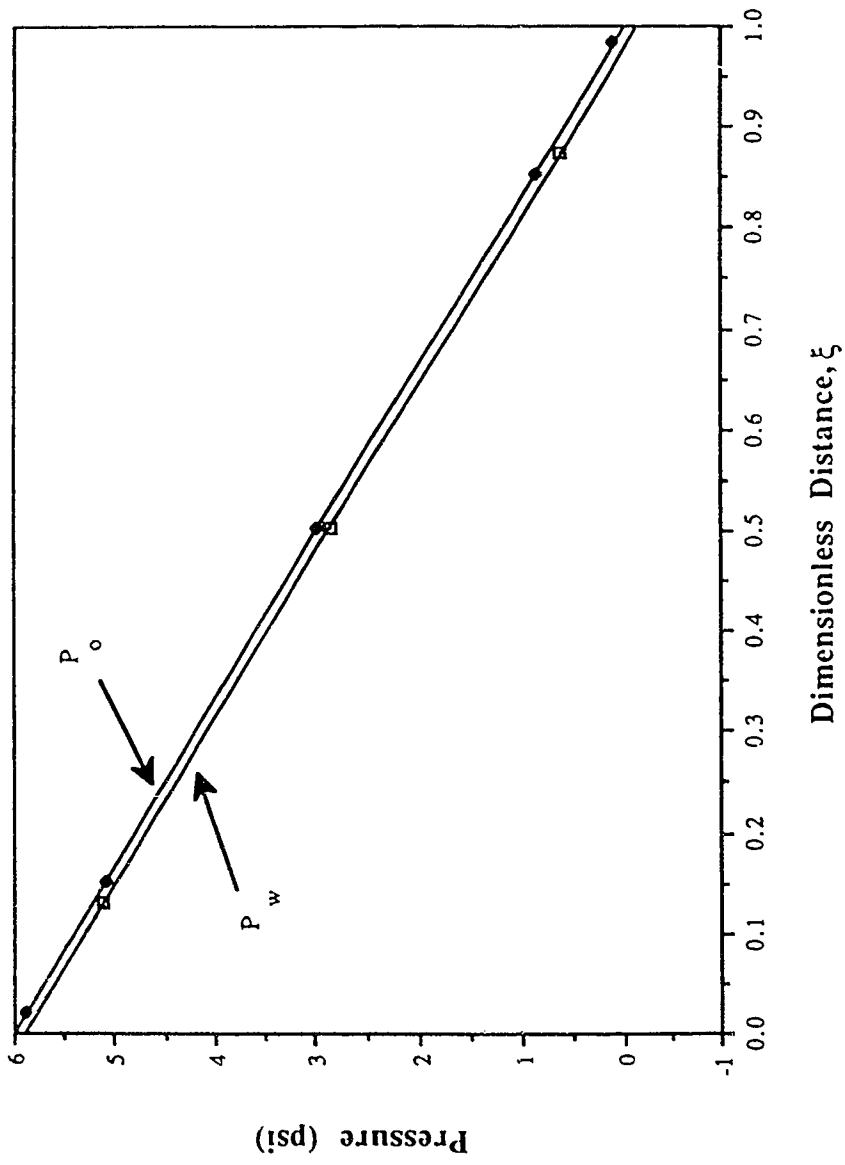


Figure 6.6 : Pressure Profiles during Cocurrent Flow (Experiment No. 2)

countercurrent flow experiments, samples of raw pressure profiles are provided in Figures 6.7 and 6.8, while conditioned pressure profiles are shown in Figures B.3 and B.4 in Appendix B.

A comparison of the pressure gradient in the water phase to that in the oil phase for both cocurrent and countercurrent flow showed that the pressure gradient in the water phase and the pressure gradient in the oil phase were not equal. The ratio of pressure gradients was plotted versus normalized water saturation. The ratio of the pressure gradient in the water phase to that in the oil phase for cocurrent flow,  $R_{12}$ , was fitted using Equation (6.6), while for countercurrent flow the ratio of pressure gradients,  $R_{12}^*$ , was fitted using Equation (6.8). Then the fitting equations were used to estimate the ratio of pressure gradients for Equations (6.5) and (6.7), and for the equations that are used to estimate the generalized relative permeabilities and their coefficients. The ratios of pressure gradients for Set I are shown in Figure 6.9, while those for Set II are shown in Figure 6.10.

Conventional relative permeabilities for cocurrent and countercurrent flow were calculated using the conditioned pressure data. For the two sets of experiments, the cocurrent and countercurrent relative permeabilities were plotted versus water saturation, along with the relative permeability curves constructed using Equations (6.1) through (6.4). The cocurrent and countercurrent relative permeability curves for the two sets are shown in Figures 6.11 and 6.12, respectively.

In order to compare flow rate ratios for cocurrent and countercurrent flow, the ratio of water flow rate to oil flow rate was plotted versus water saturation. Comparisons of measured and fitted flow rate ratios for cocurrent and countercurrent flow for the two sets of experiments are shown in Figures 6.13 and 6.14, respectively.

The pressure difference between the oil and the water did not appear to be constant along the core. For this reason the capillary pressure for cocurrent flow was measured at the inlet end of the core. This capillary pressure is called the cocurrent inlet capillary

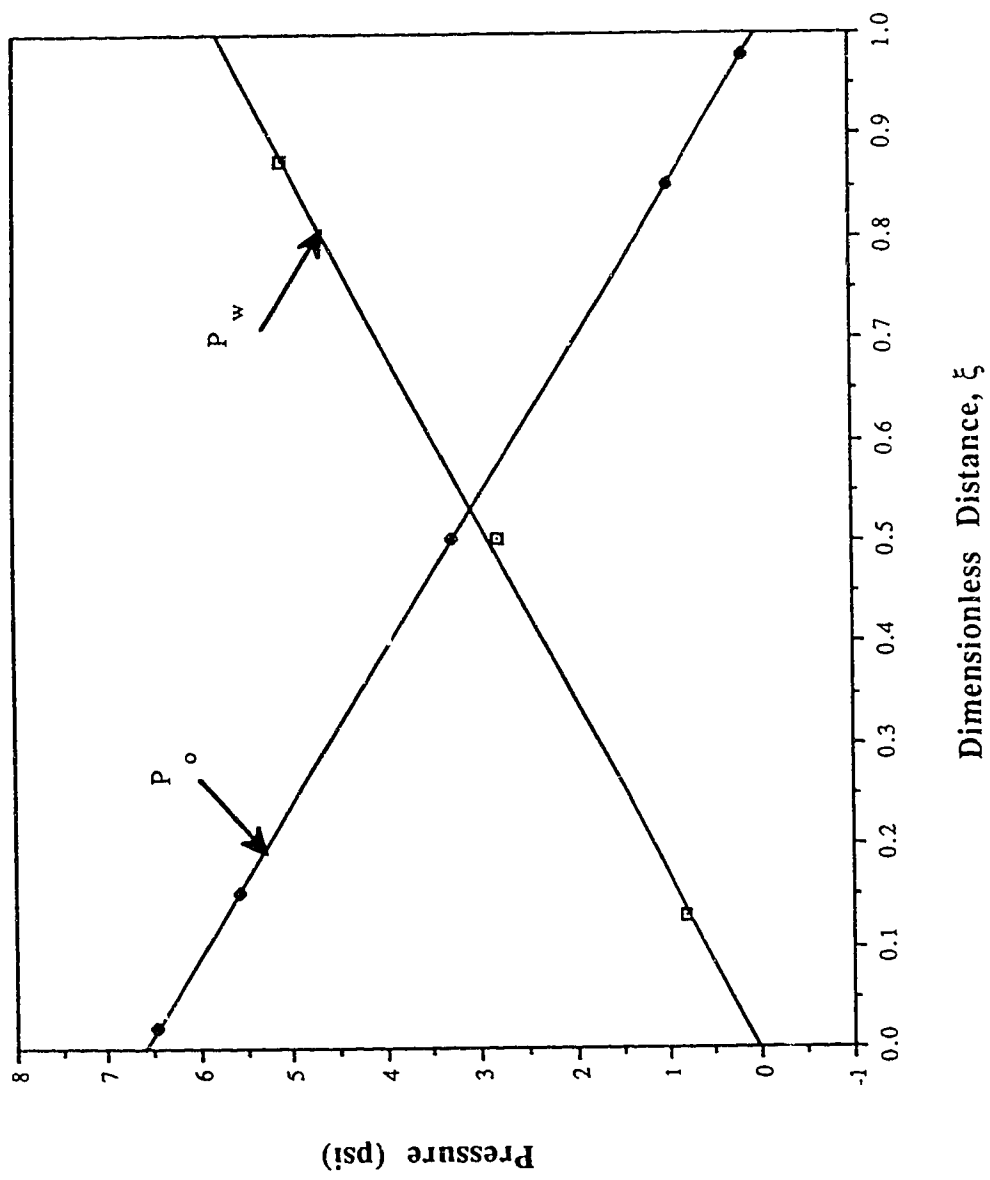


Figure 6.7 : Pressure Profiles during Countercurrent Flow (Experiment No. 13)

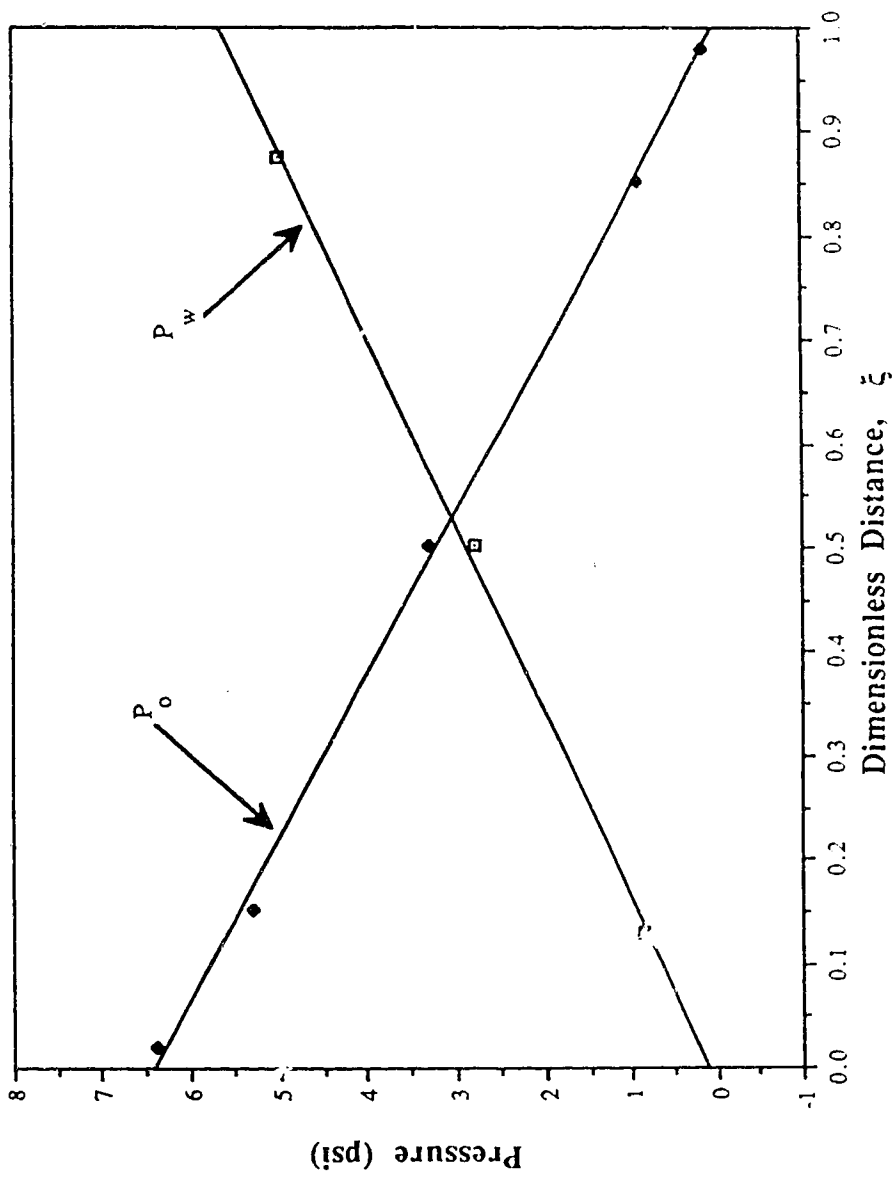


Figure 6.8 : Pressure Profiles during Countercurrent Flow (Experiment No. 14)



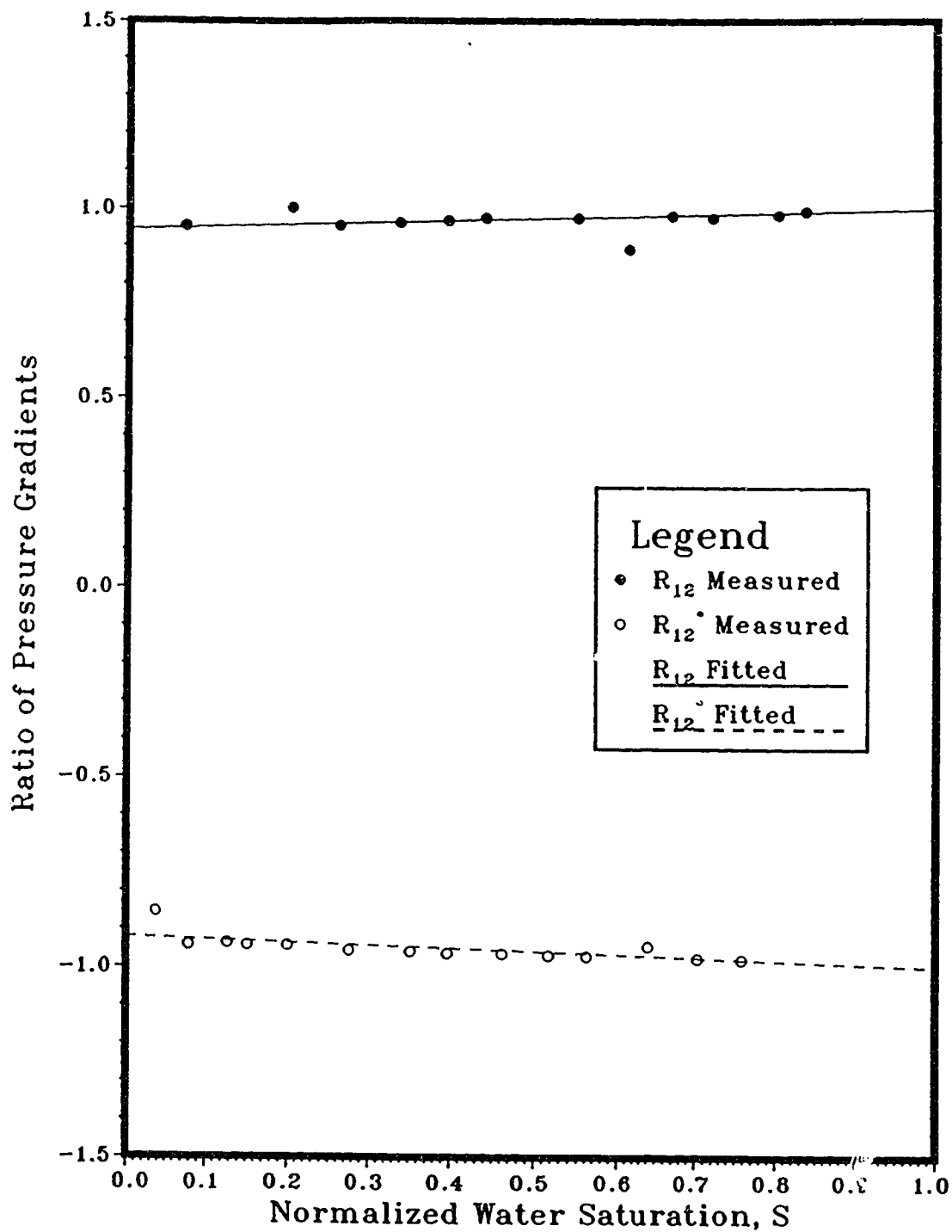


Figure 6.9 : Ratios of Pressure Gradients between Water and Oil for Cocurrent and Countercurrent Flow (Set I)

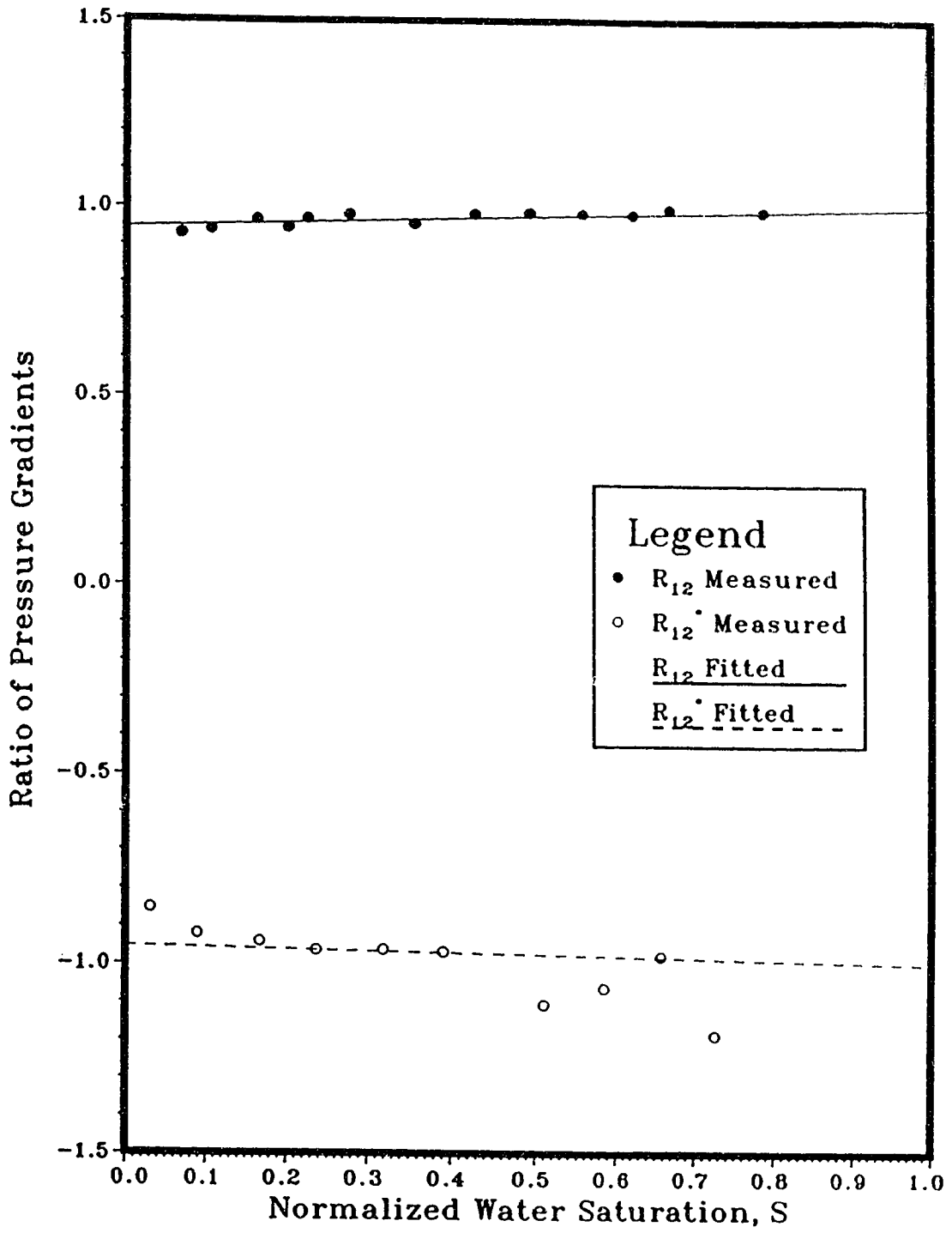


Figure 6.10 : Ratios of Pressure Gradients between Water and Oil for Cocurrent and Countercurrent Flow (Set II)

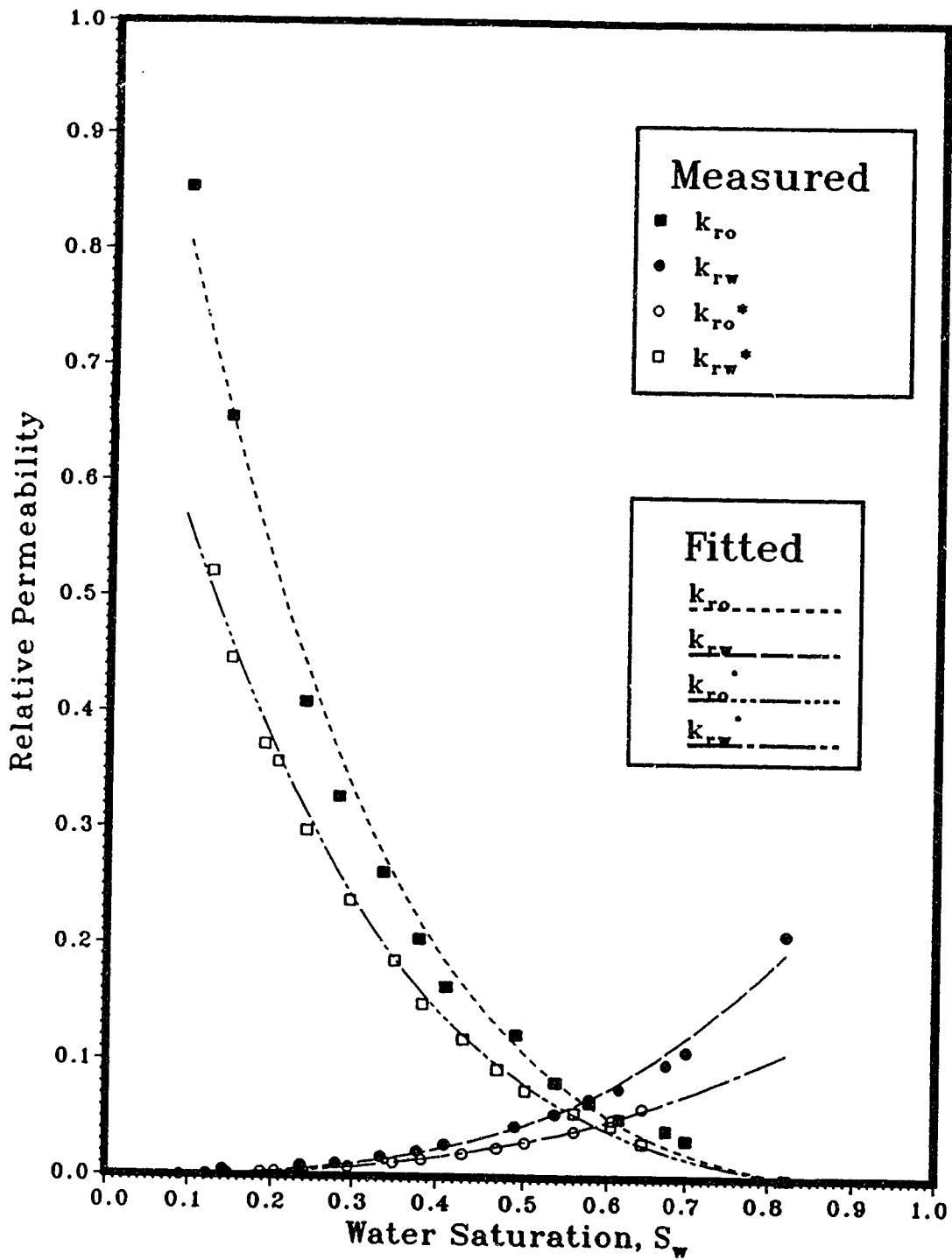


Figure 6.11 : Comparison of Measured and Fitted Relative Permeabilities for Cocurrent and Countercurrent Flow (Set I)

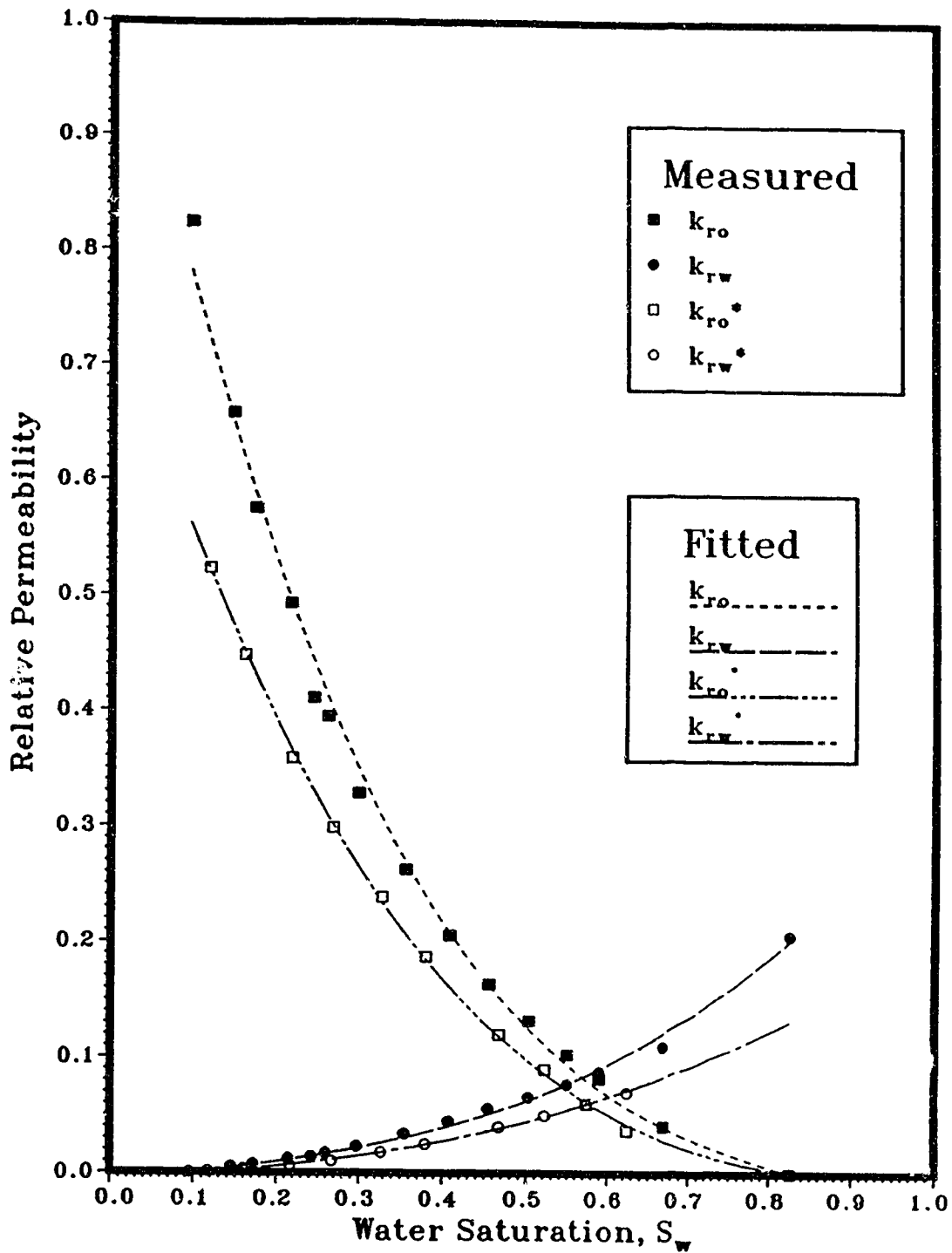


Figure 6.12 : Comparison of Measured and Fitted Relative Permeabilities for Cocurrent and Countercurrent Flow (Set II)

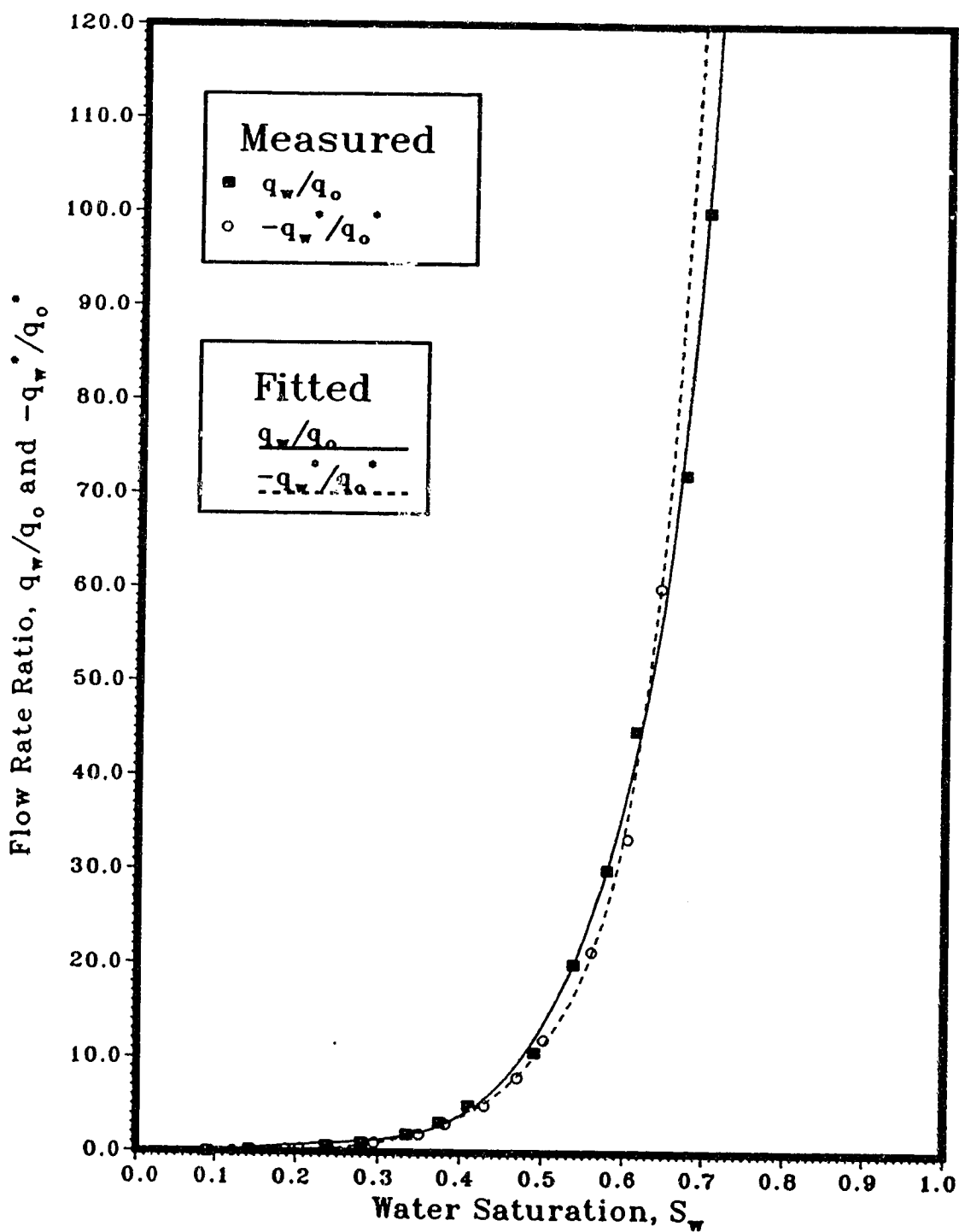


Figure 6.13 : Comparison of Measured and Fitted Flow Rate Ratios for Cocurrent and Countercurrent Flow (Set I)

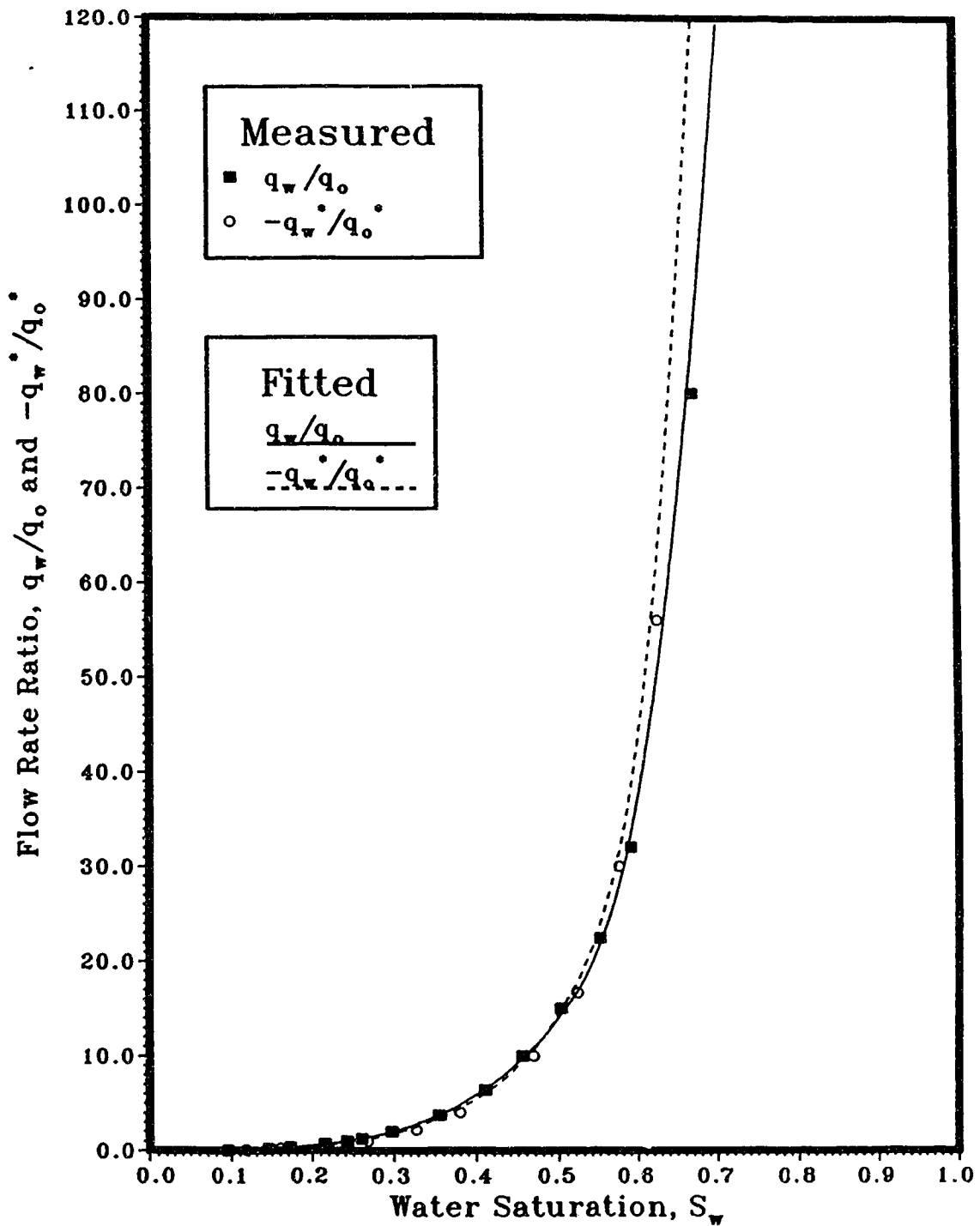


Figure 6.14 : Comparison of Measured and Fitted Flow Rate Ratios for Cocurrent and Countercurrent Flow (Set II)

pressure,  $P_{cin}$ . For countercurrent flow it is obvious that (see Figures 6.7 and 6.8) the pressure difference is not constant along the core. That is, the pressure in one phase decreased with distance, while the pressure in the other phase increased with distance. The capillary pressure in countercurrent flow, the countercurrent inlet capillary pressure,  $P_{cin}^*$ , was calculated as the difference between the pressure in the oil phase at the inlet end of the core and the pressure in the water phase at the other end of the core, the inlet end of the core for the water phase. Because the inlet capillary pressure for cocurrent flow was similar to that for countercurrent flow, they were both fitted using the same equation. The cocurrent inlet capillary pressure, countercurrent inlet capillary pressure, and the fitted inlet capillary pressure for Set I are shown in Figure 6.15, while those for Set II are shown in Figure 6.16.

The relative permeabilities were normalized in order to compare the curvature of the cocurrent and countercurrent relative permeabilities. Normalization of the relative permeabilities was accomplished by dividing the oil permeability by the end-point oil effective permeability (oil permeability at initial water saturation) and by dividing the water permeability by the end-point water effective permeability (water permeability at residual oil saturation). The normalized relative permeabilities are plotted versus normalized water saturation in Figures 6.17 and 6.18, respectively.

As noted in the literature review, measurement of the generalized relative permeabilities is not a simple matter. However, as has been shown in the theory section, the generalized relative permeabilities can be decomposed into permeability coefficients and relative permeabilities. This decomposition enables estimating the generalized relative permeabilities.

The permeability coefficients,  $g_{11}$ ,  $g_{22}$ ,  $g_{12}$  and  $g_{21}$ , were calculated using Equations (4.35) through (4.38). The permeability coefficients for Set I and Set II were plotted versus water saturation and they are presented in Figures 6.19 and 6.20, respectively.

The generalized relative permeabilities,  $k_{r11}$  and  $k_{r22}$ , were estimated using

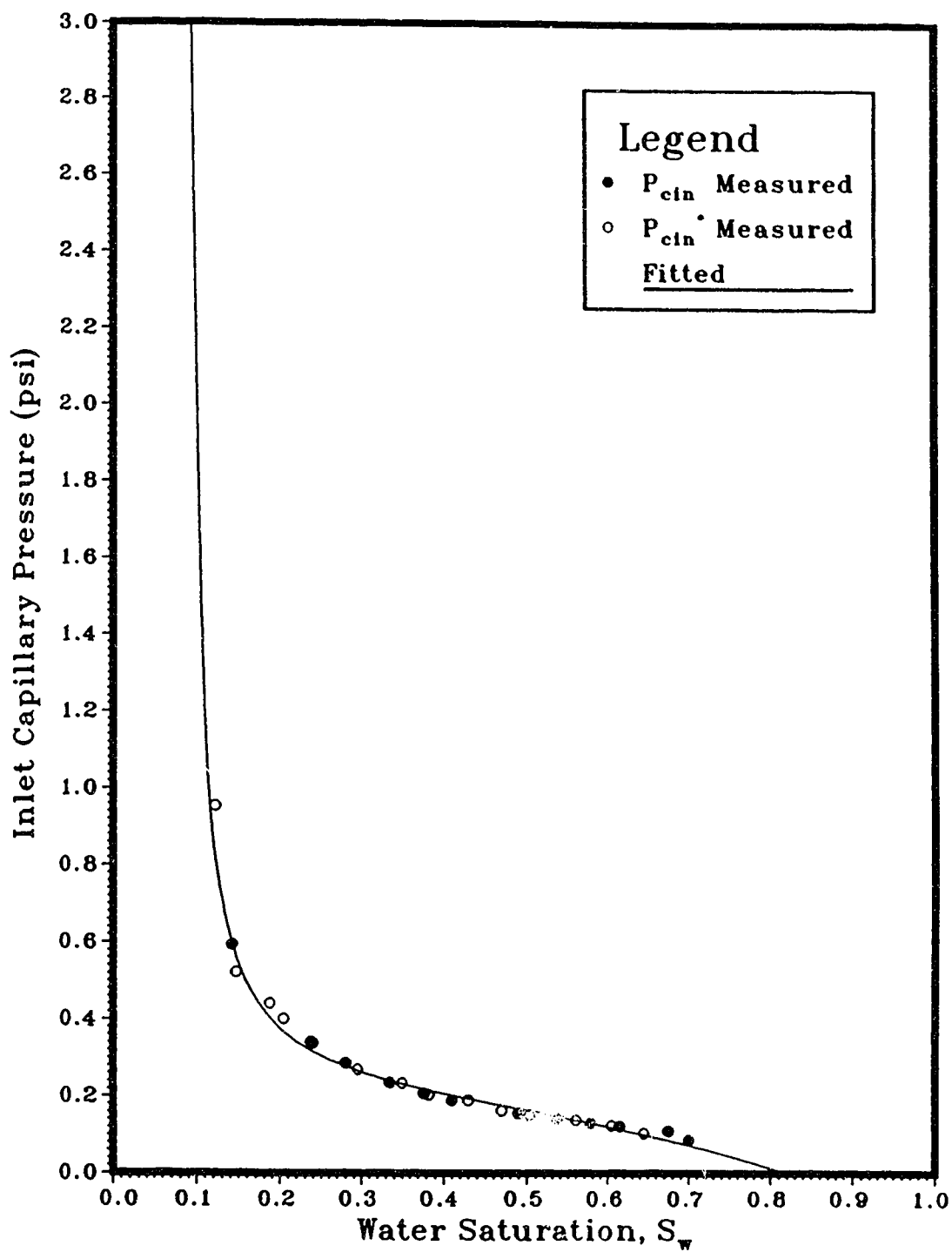


Figure 6.15 : Inlet Capillary Pressure-Saturation Curves for Cocurrent and Countercurrent Flow (Set I)



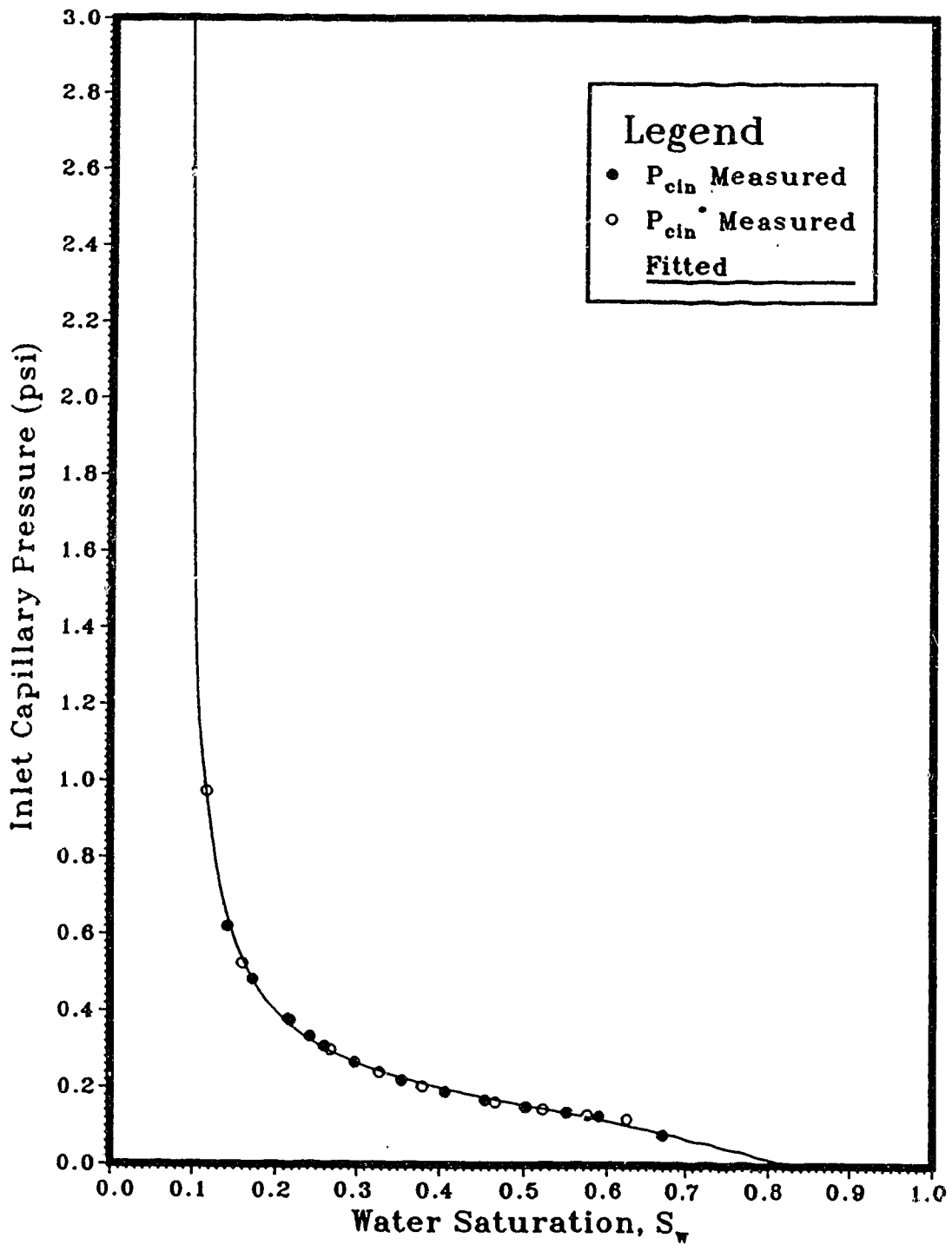


Figure 6.16 : Inlet Capillary Pressure-Saturation Curves for Cocurrent and Countercurrent Flow (Set II)

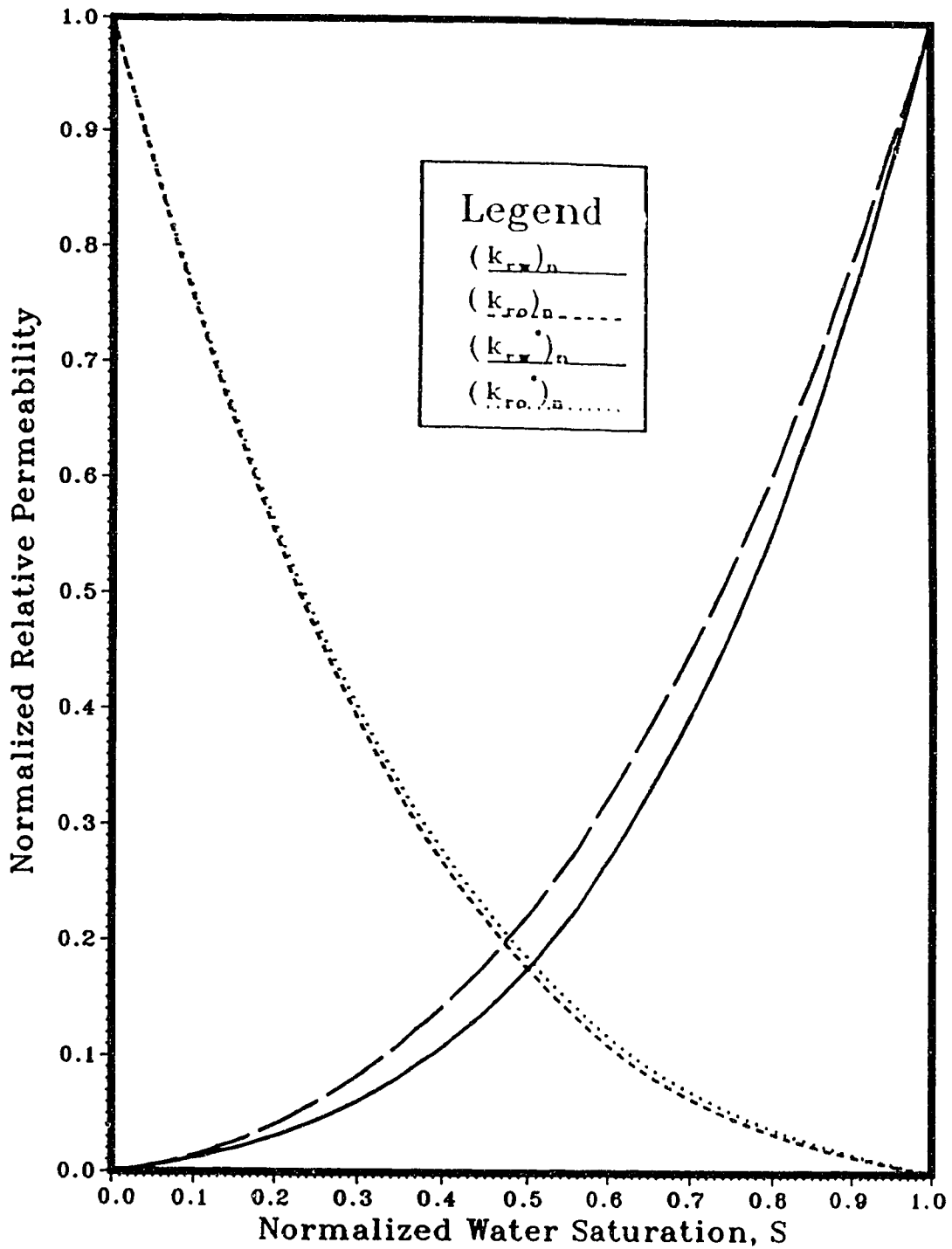


Figure 6.17 : Comparison of Normalized Relative Permeabilities for Cocurrent and Countercurrent Flow (Set I)

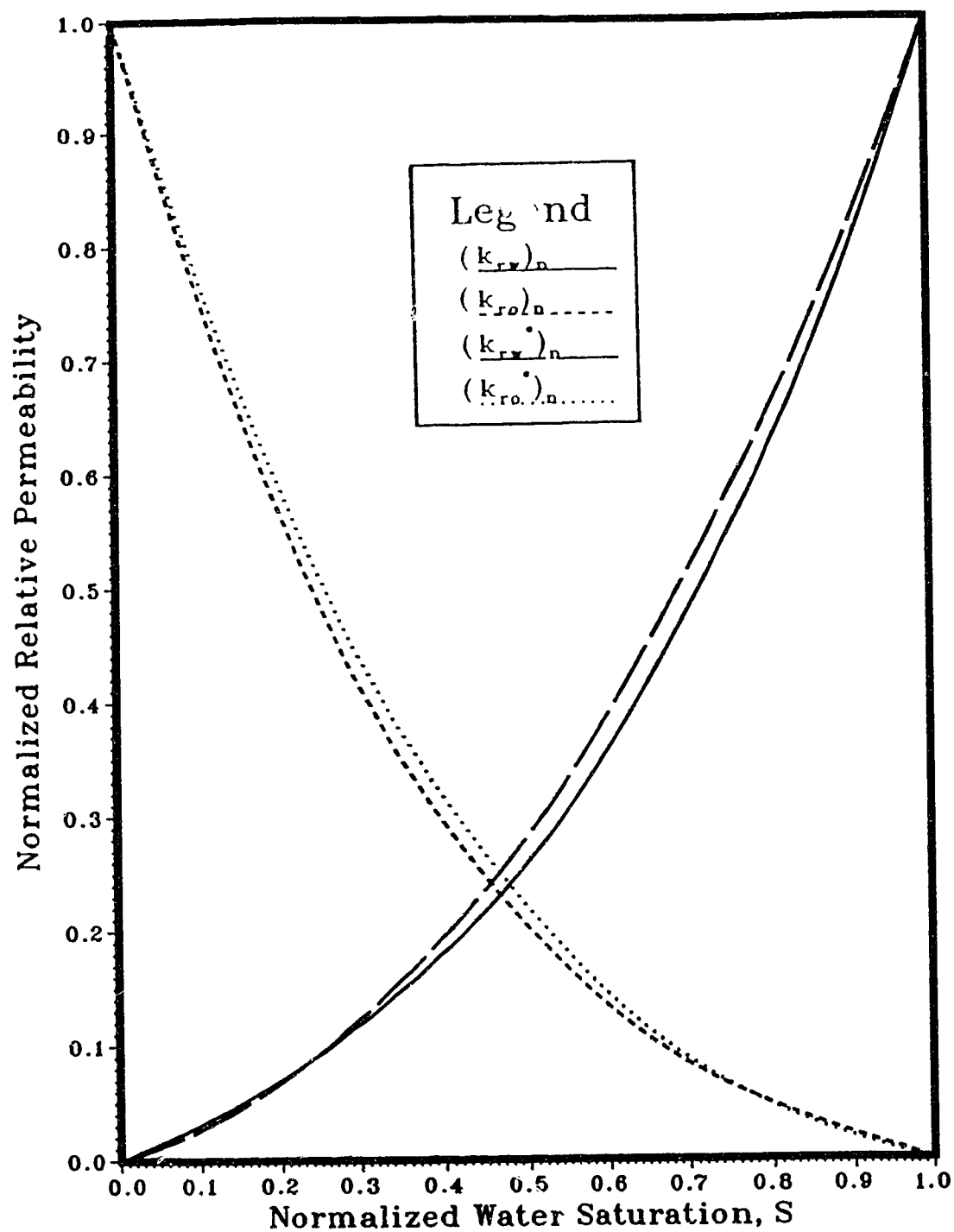


Figure 6.18 : Comparison of Normalized Relative Permeabilities for Cocurrent and Countercurrent Flow (Set II)

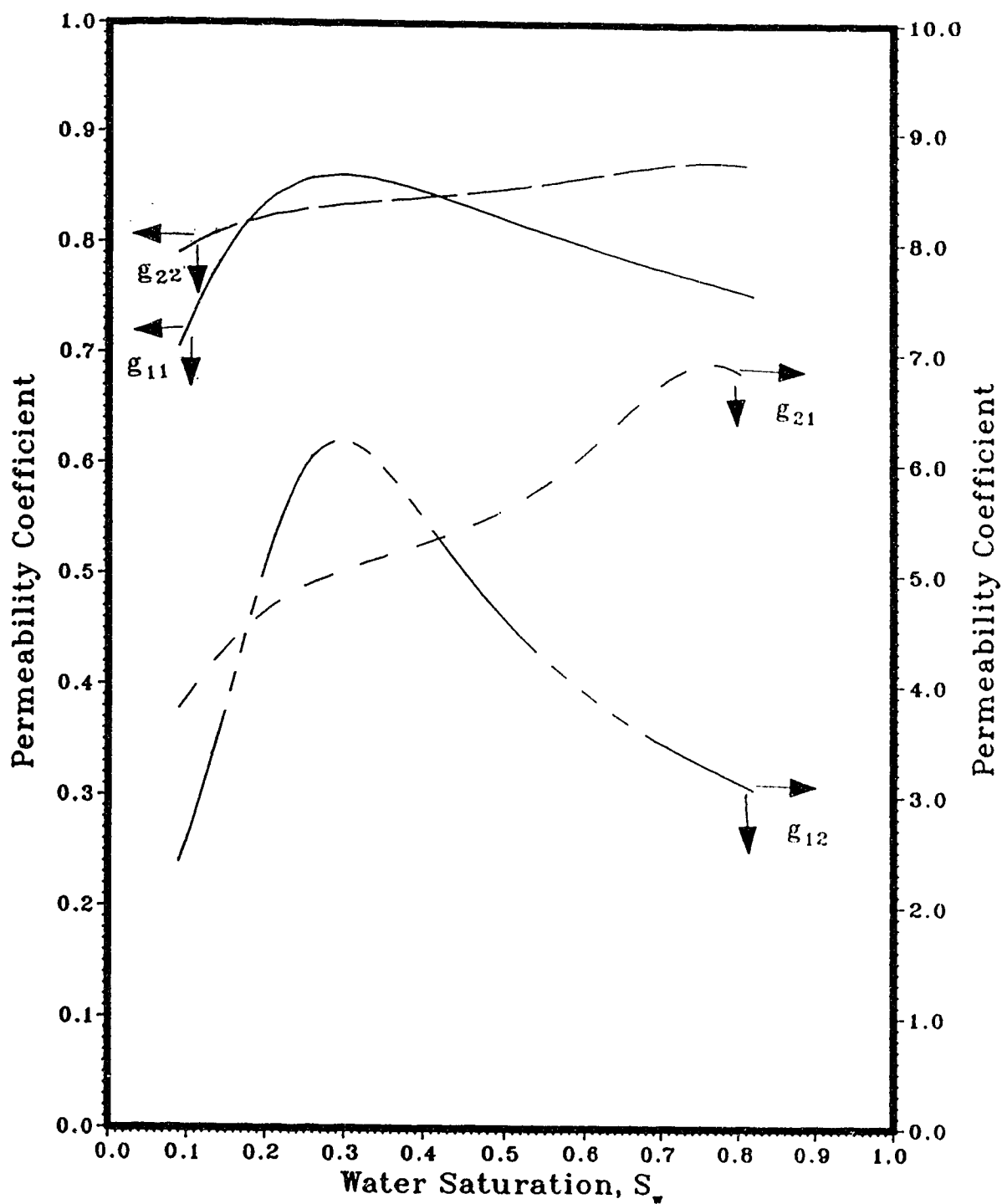


Figure 6.19 : Permeability Coefficients (Set I)

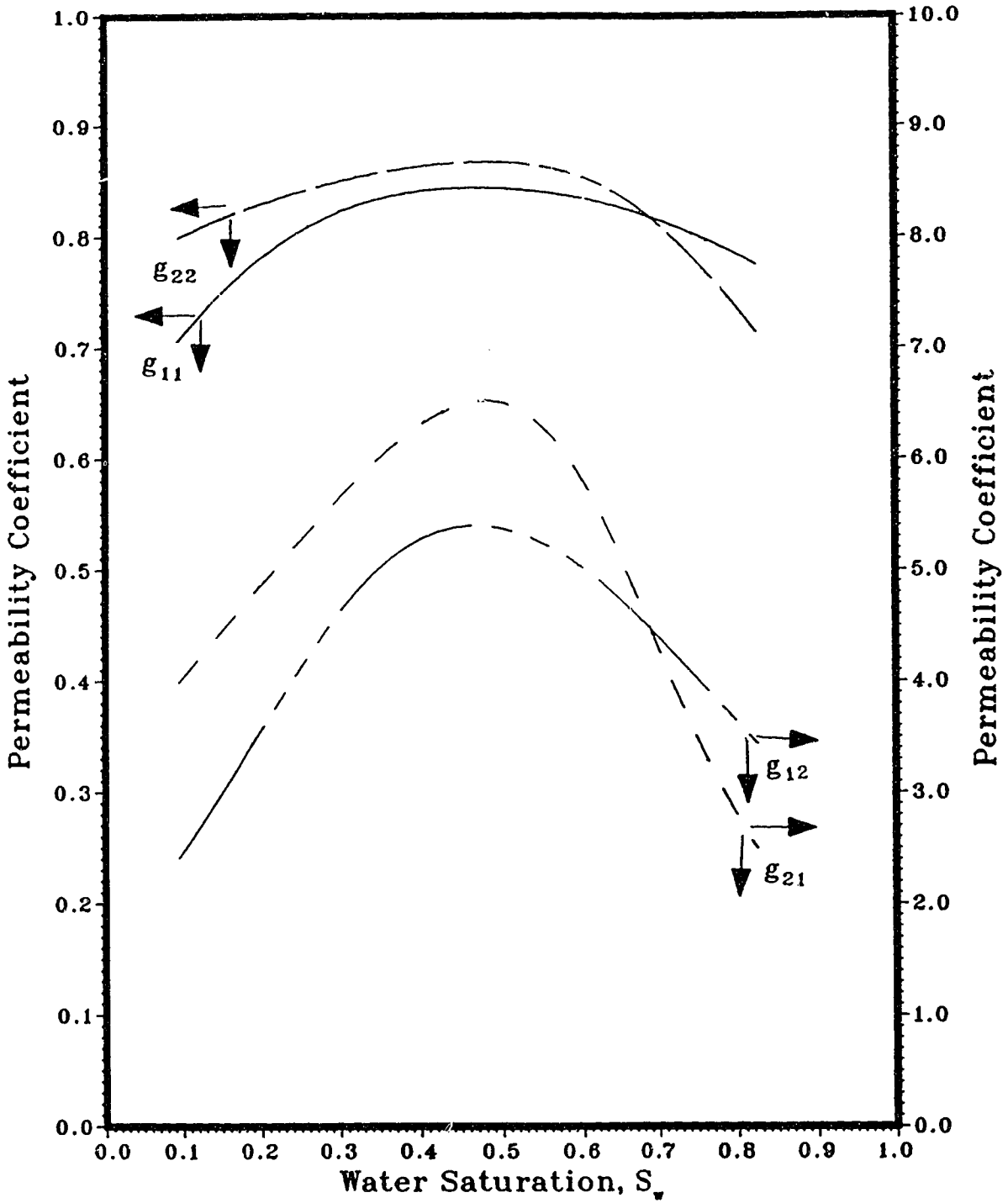


Figure 6.20 : Permeability Coefficients (Set II)

equations (4.31) and (4.32). They were found to take nearly the shape of the relative permeabilities; however, they lay between the cocurrent and countercurrent relative permeabilities. For the sake of comparison, the generalized relative permeabilities are plotted together with the fitted relative permeabilities for cocurrent and countercurrent flow in Figures 6.21 and 6.22, respectively.

Some of the few previous studies that dealt with generalized relative permeabilities suggested that the relative viscous drag coefficients,  $k_{r12}$  and  $k_{r21}$ , should be the same, provided that the viscosity ratio is unity. The permeability coefficients,  $g_{12}$  and  $g_{21}$ , were used to estimate  $k_{r12}$  and  $k_{r21}$  using Equations (4.33) and (4.34). Then the relative viscous drag coefficient-saturation curves were constructed. These curves are presented in Figures 6.23 and 6.24, respectively. It can be seen clearly from these figures that  $k_{r12}$  and  $k_{r21}$  have different shapes.

Finally, in order to appraise the contribution of momentum transfer across the water-oil (fluid 1-fluid 2) interfaces to conventional relative permeability, relative viscous coupling effects,  $k_{rv1}$  and  $k_{rv2}$ , were estimated using Equations (4.47) and (4.49), and they are plotted versus water saturation in Figures 6.25 and 6.26, respectively.

## 6.4 Discussion of Results

As has been indicated earlier, the purpose of this study was to evaluate the relative permeabilities of cocurrent and countercurrent flow, and the generalized relative permeabilities. In order to achieve a genuine evaluation, consistency was maintained throughout the experimental and evaluation procedure.

### 6.4.1 Core preparation

Porosities and absolute permeabilities for the two sets of experiments were similar. A flow rate of 200 cc/hr was used during the establishment of the irreducible (initial) water

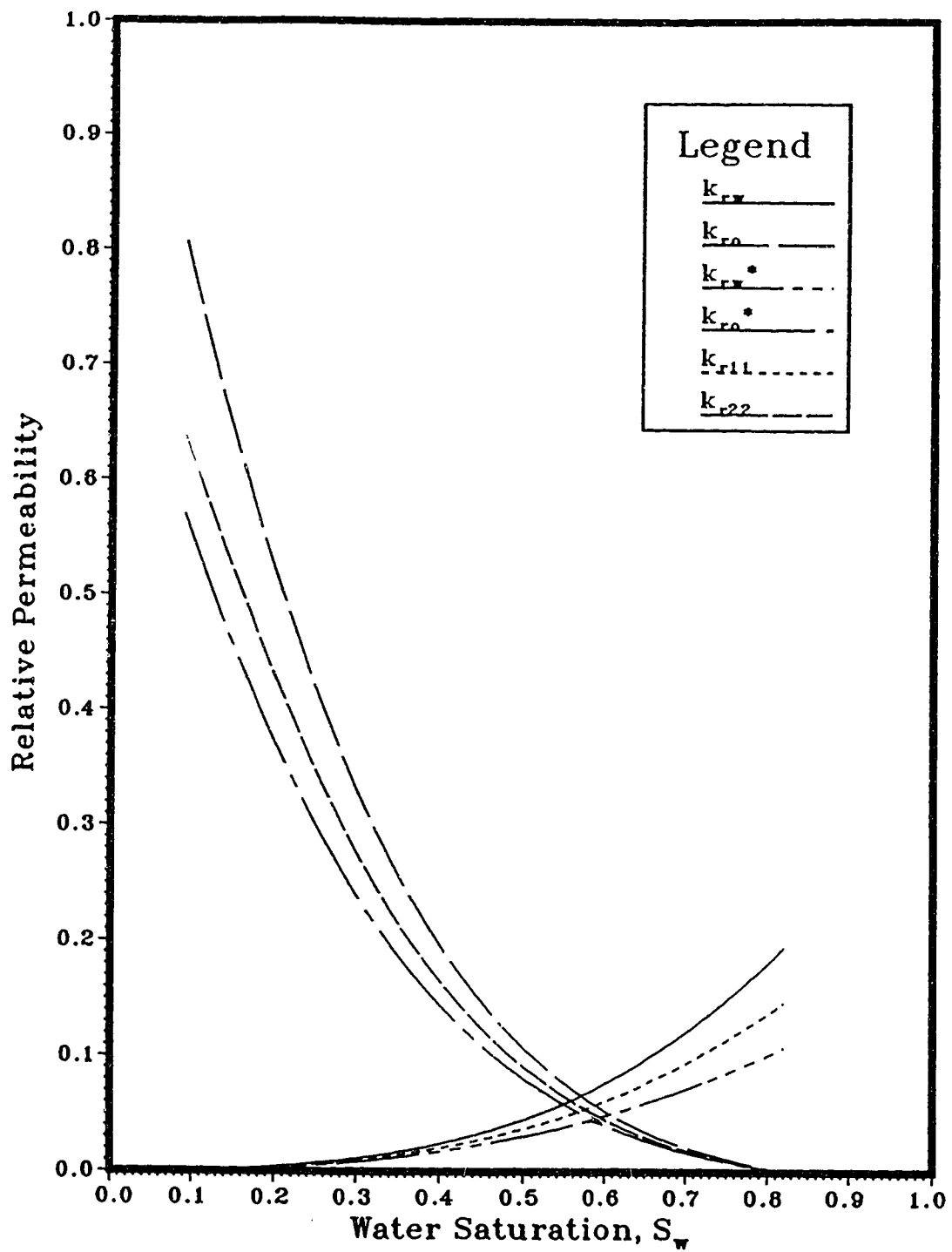


Figure 6.21 : Comparison of Relative Permeabilities for Cocurrent and Countercurrent Flow with Generalized Relative Permeabilities (Set I)

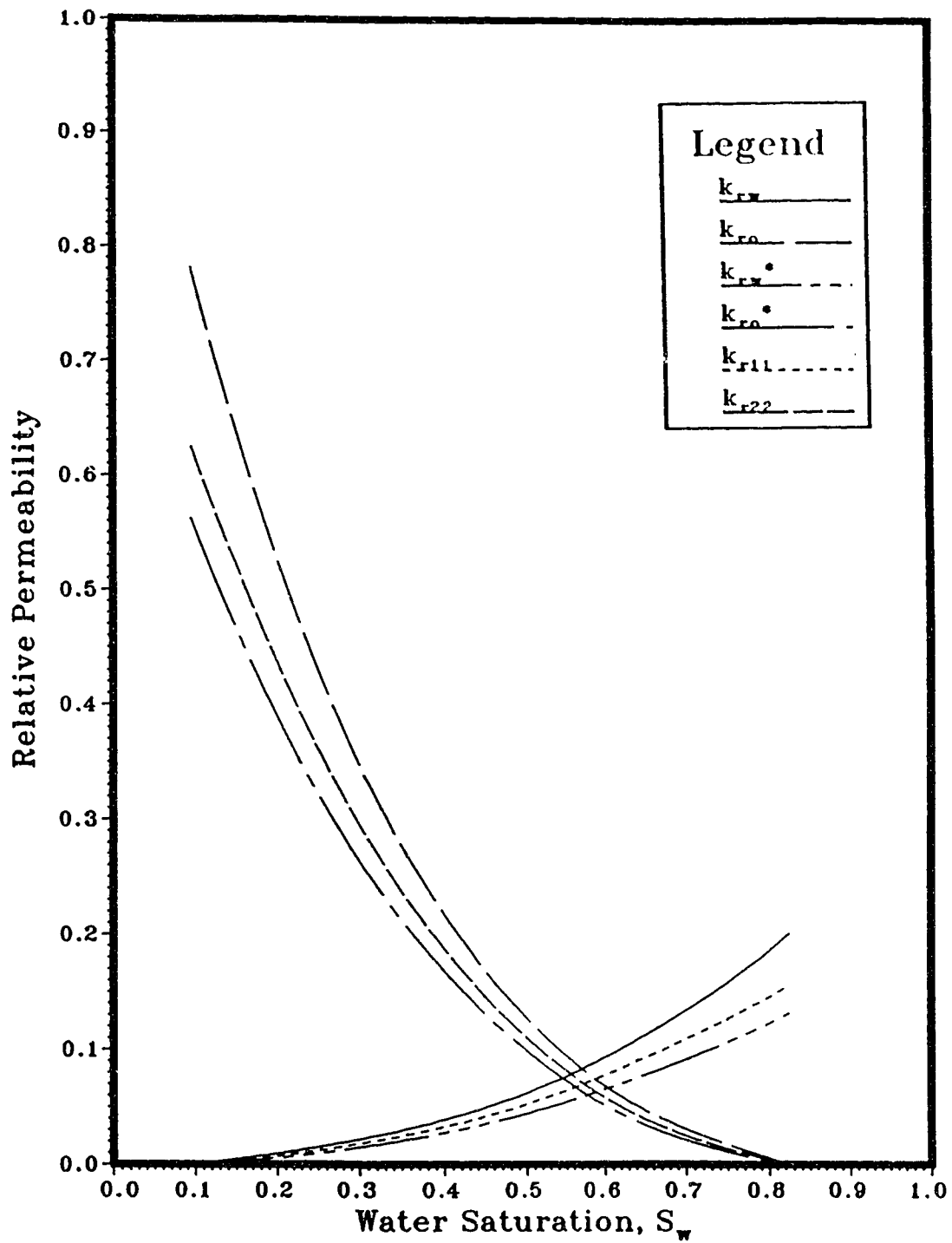


Figure 6.22 : Comparison of Relative Permeabilities for Cocurrent and Countercurrent Flow with Generalized Relative Permeabilities (Set II)



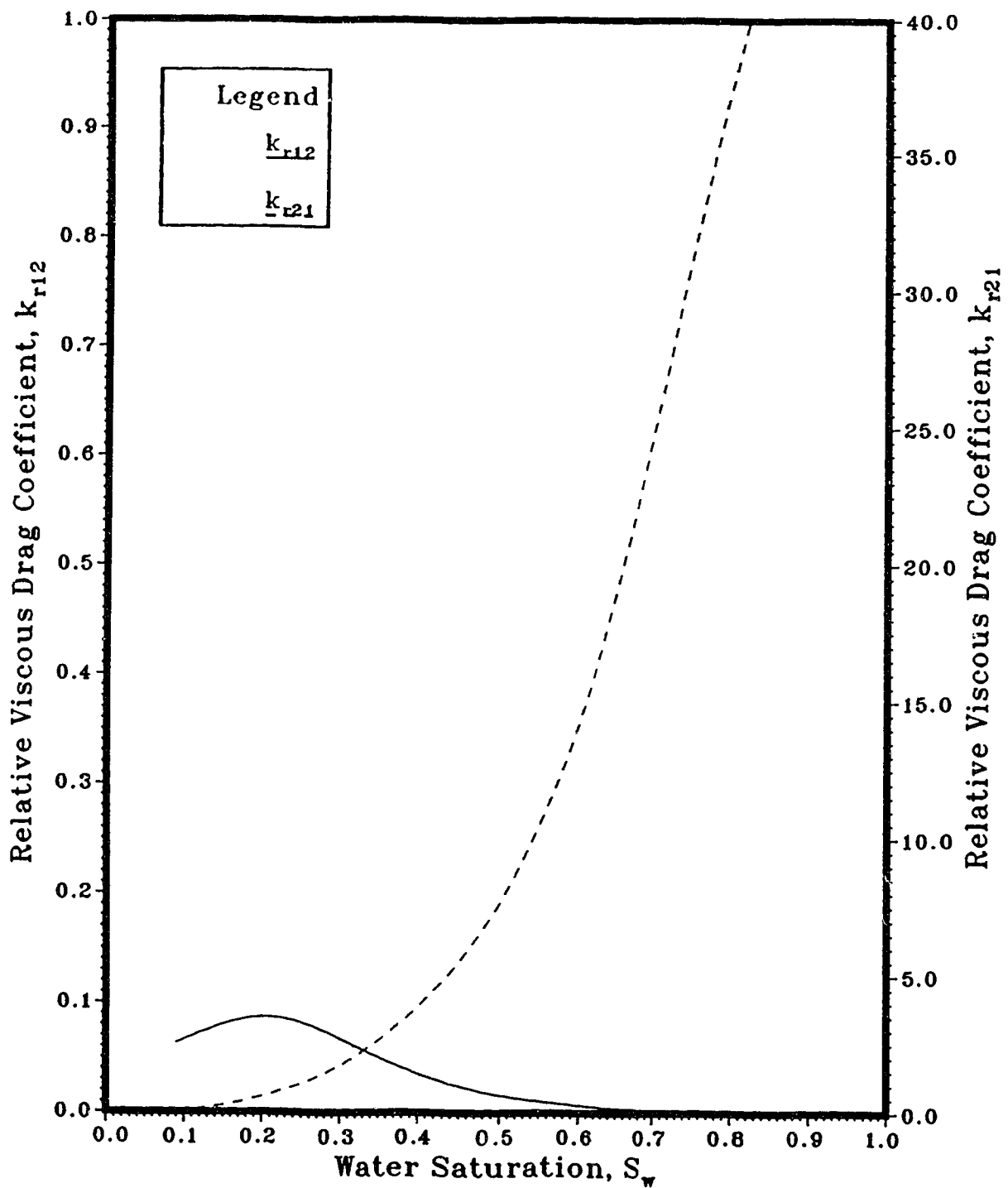


Figure 6.23 : Relative Viscous Drag Coefficients (Set I)

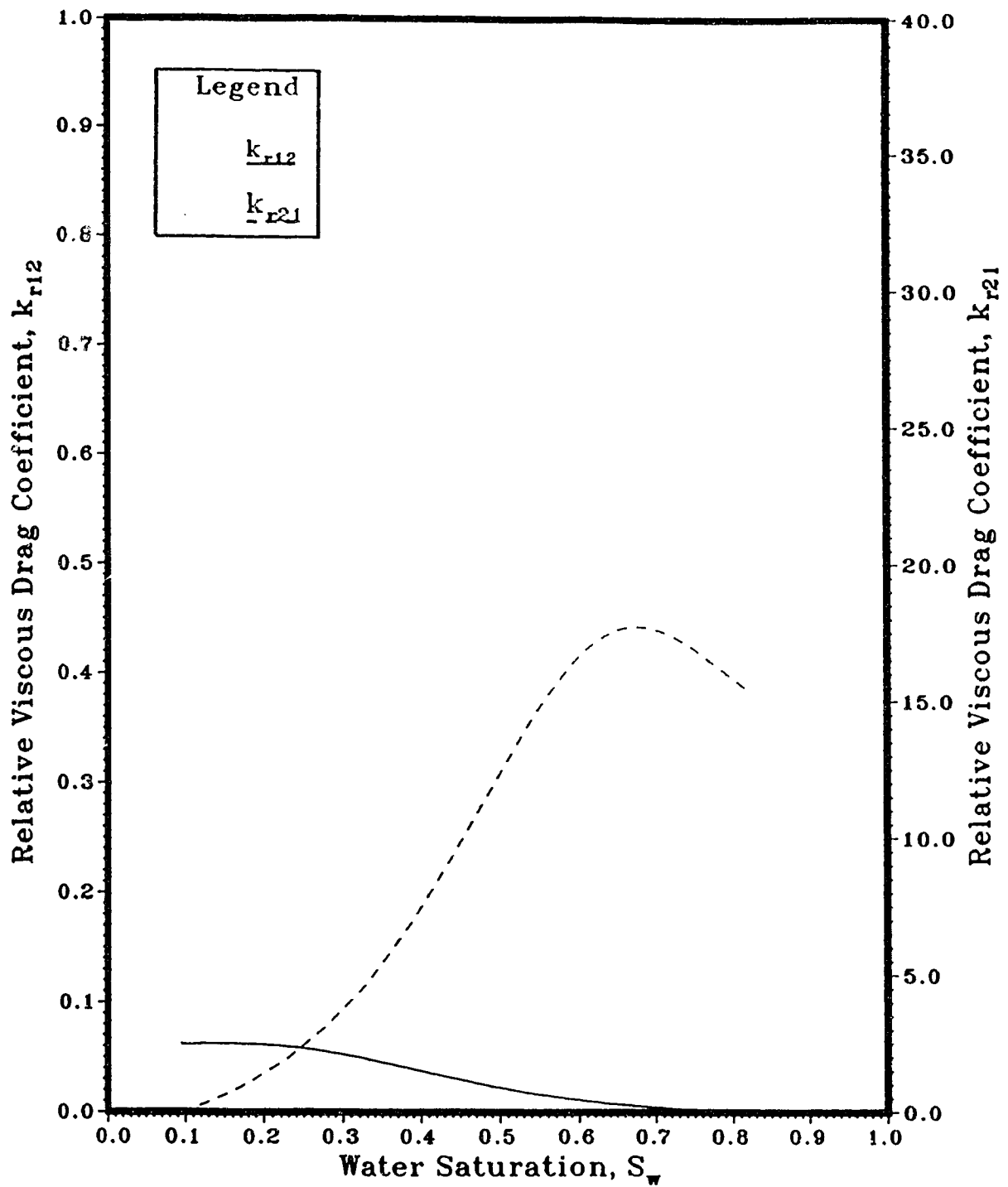


Figure 6.24 : Relative Viscous Drag Coefficients (Set II)

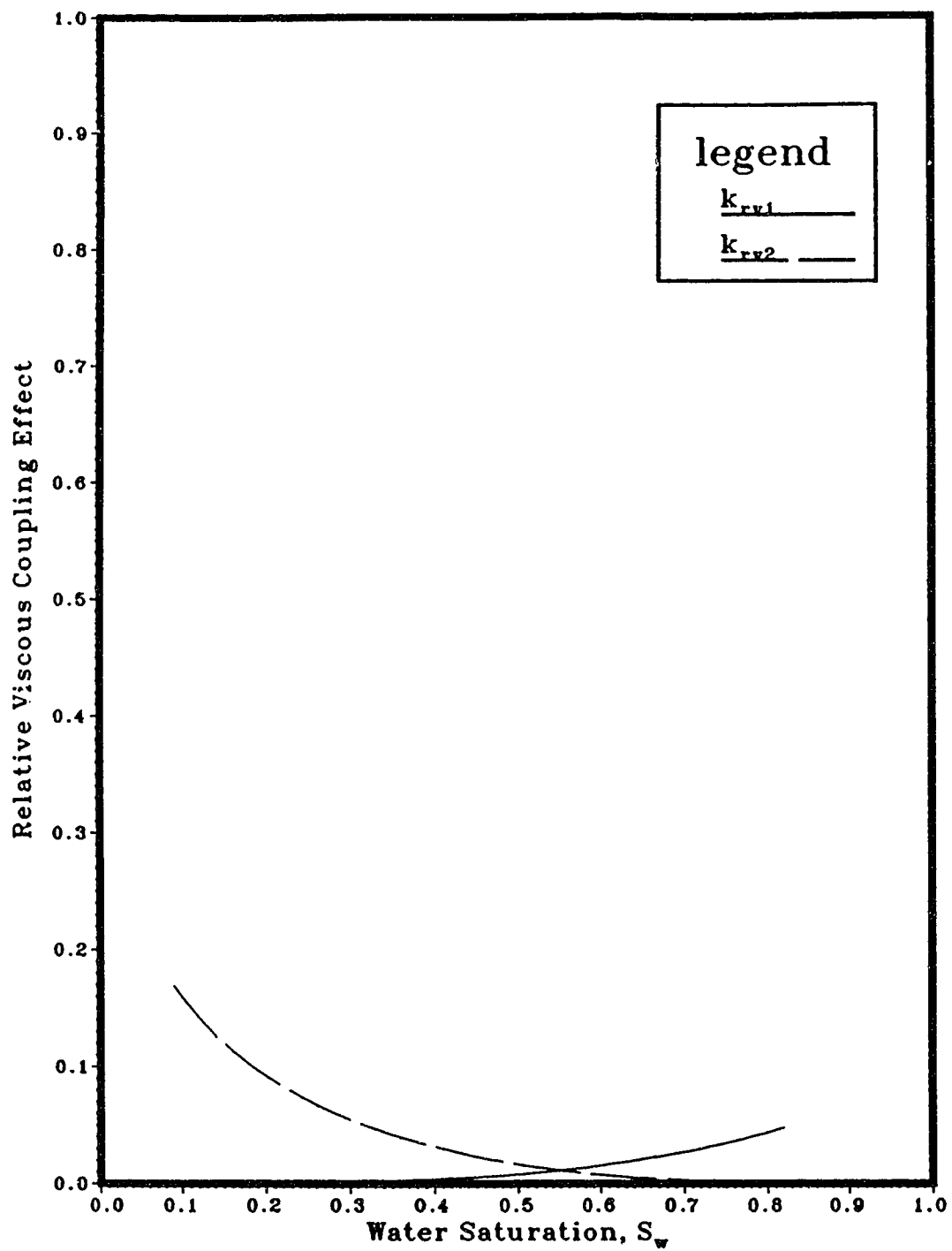


Figure 6.25 : Relative Viscous Coupling Effect (Set I)

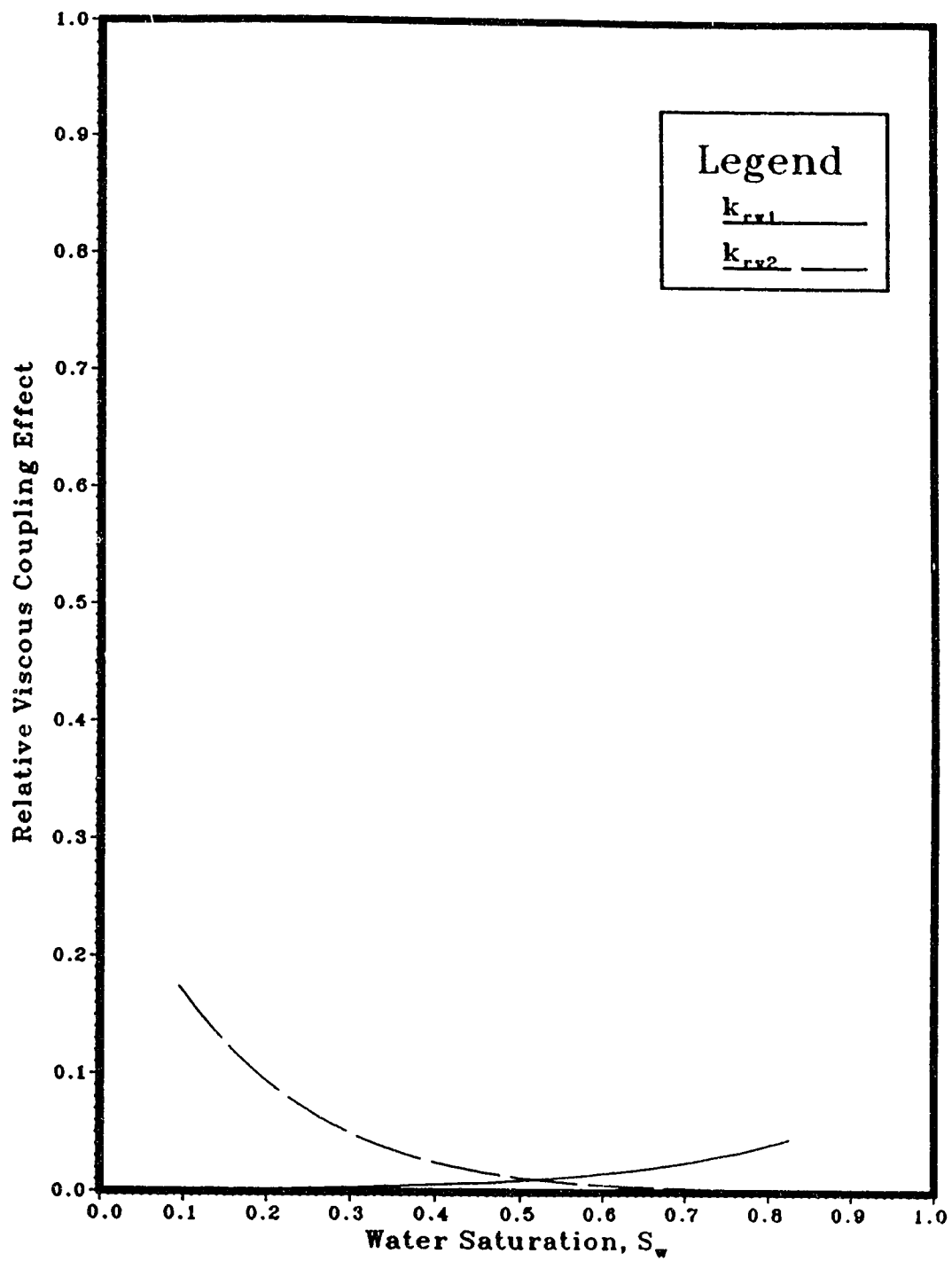


Figure 6.26 : Relative Viscous Coupling Effect (Set II)

saturation. A cumulative oil injection of about four pore volumes was needed to establish the initial water saturation. The values of initial water saturation for the two sets were very close to each other. This shows that a good reproducibility has been obtained in packing the core. Regarding the effective oil permeability at initial water saturation,  $k_{oiw}$ , the two sets of experiments showed very close agreement. Furthermore, rock and fluid properties were consistent with those in a previous study [14] in which the same coreholder, sand, and fluid system were used. It should be noted that the flow rate for establishing irreducible water saturation was kept constant for the two sets; therefore, any question of observing differences in  $k_{oiw}$  due to variations in oil flooding was eliminated.

#### 6.4.2 Relative Permeability Curves

The steady-state cocurrent relative permeability curves in Figures 6.11 and 6.12 exhibit the typical shape of water-wet steady-state relative permeability curves. For countercurrent flow, the kinetics were much slower than those of cocurrent flow. It took a longer time to achieve steady-state flow during countercurrent flow experiments than it did for the cocurrent flow experiments. The time required for the countercurrent experiments to reach steady-state was as long as one and one-half times that required for the cocurrent experiments. The difference in kinetics between cocurrent and countercurrent flow can be observed in the dynamic saturation profiles in Figures 6.1, 6.2, 6.3 and 6.4. For cocurrent flow, water saturation increased according to the imbibition process, while for countercurrent flow, water saturation decreased in the early stages of each experiment at the part of the core near the oil-injection inlet. However, later in the experiment the imbibition process was dominant, and as steady-state was approached the process was completely imbibition. The countercurrent flow relative permeability, for both water and oil, was less than the cocurrent flow relative permeability.

It should be noted here that because of establishing relative permeabilities at different water saturations, for cocurrent and countercurrent flow, exact comparisons

between the relative permeabilities were not possible and thus comparisons were made based on the fitted relative permeabilities. The comparison between cocurrent and countercurrent flow relative permeabilities was sensitive to the fitted relative permeability, especially at low values of the relative permeability. A better comparison could have been achieved if more measured data points were available which could have made the fitted relative permeabilities more representative and consistent, thus enabling a more precise comparison. In order to evaluate exactly the magnitude of the ratios of countercurrent flow relative permeabilities to cocurrent flow relative permeabilities, the ratios of water countercurrent flow relative permeability to water cocurrent relative permeability, and of oil countercurrent flow relative permeability to oil cocurrent flow relative permeability, are plotted versus saturation. These plots are presented in Figures 6.27 and 6.28, respectively. As can be seen from these figures, the oil countercurrent flow relative permeability was always less than the oil cocurrent relative permeability. Moreover, the relative difference, for both Set I and Set II, decreases from a value of about 30% at the irreducible water saturation to a value of about 26% at a water saturation of 55%. For saturations above 55% the relative difference for Set I continued to decrease to a minimum of 20% at  $1-S_{or}$ , while it increased to a maximum of 50% at  $1-S_{or}$ , for Set II. This difference in behavior between the two data sets at high water saturations is likely attributed to the difficulty in obtaining precise estimates of the oil relative permeabilities at high values of the water saturation. That is, small differences in the fitted equations for cocurrent, and countercurrent flow, result in large differences in the behavior of the ratio of the two curves.

The behavior of the water relative permeability curves was similar to that of the oil relative permeability curves in that the countercurrent curves were always less than cocurrent curves. For both data sets, the relative difference was about 47% at  $S_w=S_{wi}$ . However, for Set I, the relative difference decreased to a value of about 25% at  $S_w=28\%$  and then increased to a value of 42% at  $S_w=1-S_{or}$ , while for Set II, the relative difference decreased to a value of 30% at  $S_w=50\%$  and then increased to a value of 35% at  $S_w=1-S_{or}$ .

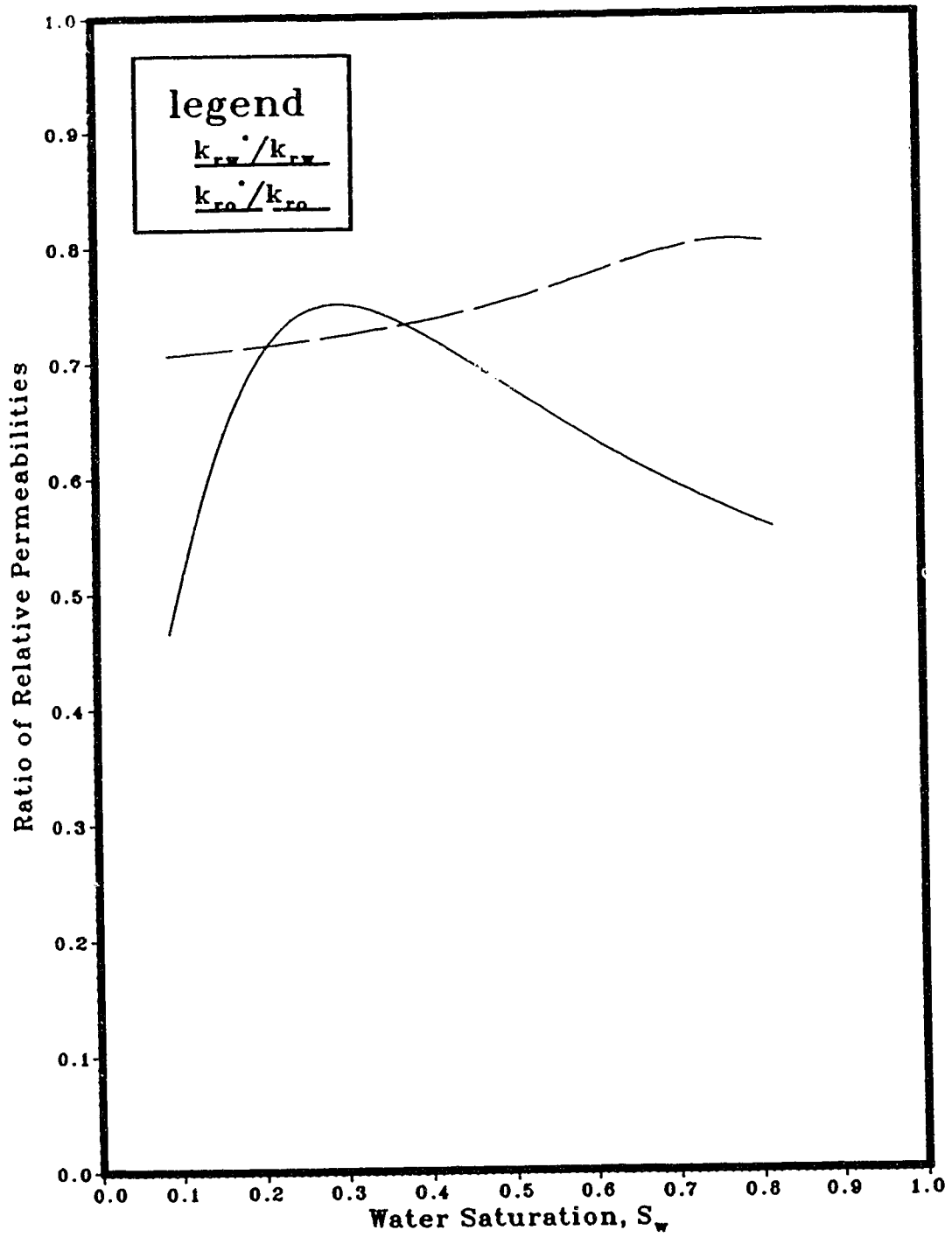


Figure 6.27 : Ratio of Relative Permeabilities (Set I)

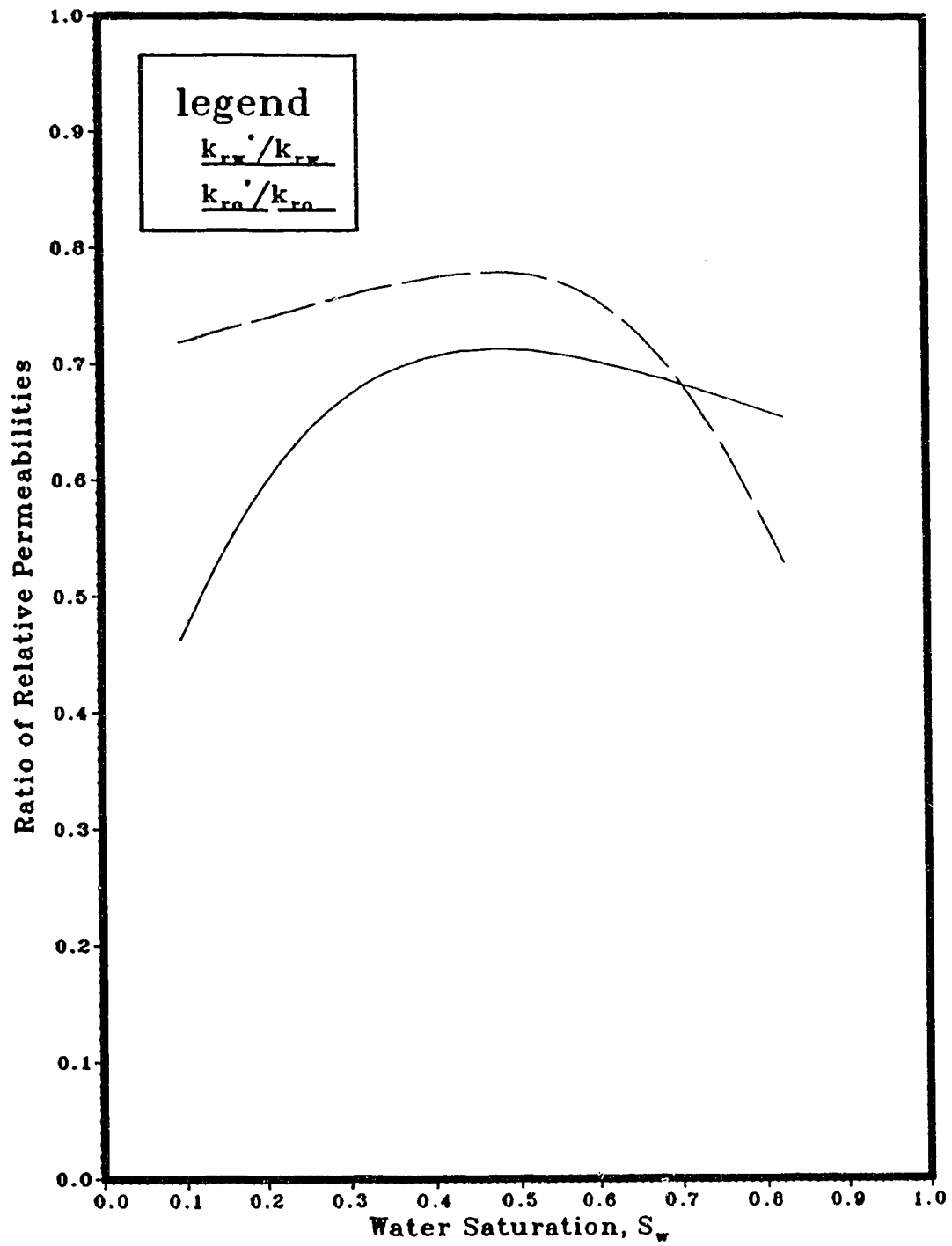


Figure 6.28 : Ratio of Relative Permeabilities (Set II)



Again this difference in behavior between the two data sets probably arose because of a lack of precision in the estimated values of relative permeability. However, the relative difference between water cocurrent flow relative permeability and countercurrent flow relative permeability was always greater than 25%, while the relative difference between oil cocurrent flow relative permeability and countercurrent flow relative permeability was always greater than 20%.

The above observations are consistent, in general, with the observations of previous studies that dealt with countercurrent flow, particularly with the study conducted by Lelievre [85] who found that countercurrent relative permeability values were less than cocurrent ones. He found that the difference between countercurrent and cocurrent oil relative permeabilities was more than 35% for nonwetting-phase saturations higher than 20%. These results are consistent also with the conclusions drawn by Bourbiaux and Kalaydjian [83] who stated that countercurrent relative permeabilities should be 30% less than cocurrent relative permeabilities.

The normalized cocurrent and countercurrent relative permeability curves for Set I and Set II are compared in Figures 6.17 and 6.18, respectively. As can be seen from these figures, the cocurrent relative permeability curves, for both the oil and water, fall below the countercurrent relative permeability curves. However, the magnitude of the difference between the cocurrent and countercurrent curves appears to be somewhat larger for the water relative permeability curves, as compared to the oil relative permeability curves. The cross-over of the water relative permeability curves at  $S=0.25$  in Figure 6.18 occurs probably because of a lack of precision in the estimated values of water relative permeabilities in the region of low water-saturation values. That is, such a cross-over likely would have been avoided, had more precise data been available in this region.

### 6.4.3 Inlet Capillary Pressure

As can be seen from Figures 6.15 and 6.16, there is close agreement between the

cocurrent inlet capillary pressure,  $P_{cin}$ , and the countercurrent inlet capillary pressure,  $P_{cin}^*$ . In these two figures, the similarity between cocurrent inlet capillary pressure and countercurrent inlet capillary pressure is strong enough that they can be fitted by the same curve. Because of the good agreement between cocurrent and countercurrent inlet capillary pressure curves, it is thought that the shapes of cocurrent and countercurrent inlet capillary pressure curves are the same. However, this conclusion requires further experimental verification.

#### 6.4.4 Generalized Relative Permeabilities

As indicated in Sections 4.1.2 and 6.3, the generalized relative permeability curves may be viewed as being proportional to the conventional relative permeability curves. The generalized relative permeabilities are decomposed into permeability coefficients and conventional relative permeabilities. In estimating the permeability coefficients,  $g_{11}$ ,  $g_{22}$ ,  $g_{12}$  and  $g_{21}$ , using Equations (4.35) through (4.38), the ratios of pressure gradients between water and oil,  $R_{12}$  and  $R_{12}^*$ , were included. As can be seen in Figures 6.9 and 6.10,  $R_{12}$  and  $R_{12}^*$  are dependent on saturation. Despite the fact that  $R_{12}$  and  $R_{12}^*$  are weak functions of saturation, both curves tend to approach unity as saturation approaches its maximal value (at residual oil saturation). Again, more experimental evidence is needed before a strong conclusion as to the behavior of the ratios of pressure gradients in both cocurrent and countercurrent flow can be drawn.

The permeability coefficients,  $g_{11}$ ,  $g_{22}$ ,  $g_{12}$  and  $g_{21}$ , in Set I, Figure 6.19, are slightly different from those in Set II, Figure 6.20, mainly because of the strong dependence of these permeability coefficients on the ratio of countercurrent flow relative permeabilities to cocurrent flow relative permeabilities. Thus a different ratio of relative permeabilities will lead to a difference in permeability coefficients.

The generalized water relative permeability,  $k_{r11}$ , curve lies between the water countercurrent flow and the water cocurrent flow relative permeability curves, while the oil

generalized relative permeability,  $k_{r22}$ , curve lies between the oil countercurrent flow and the oil cocurrent flow relative permeability curves. This can be seen clearly in Figures 6.21 and 6.22. If one adds the relative viscous effect,  $k_{rv1}$ , curves in Figures 6.25 and 6.26 to the water generalized relative permeability,  $k_{r11}$ , curves in Figures 6.21 and 6.22, respectively, one will arrive at the water cocurrent flow relative permeability,  $k_{rw}$ , curves in the latter Figures. The same is true with respect to the oil phase. This is the case, as noted previously in the section on theory, because the conventional effective permeability of the water-phase,  $k_w$ , or that of the oil phase,  $k_o$ , represents the influence of two types of drag: that due to the flow of the fluid itself over the solid surfaces in the porous medium,  $k_{11}$  and  $k_{22}$ , and that due to momentum transfer across the fluid-fluid interfaces in the porous medium,  $k_{v1}$  and  $k_{v2}$ . In other words, the conventional permeability for a fluid, say phase 1,  $k_1$ , is made up of its generalized permeability,  $k_{11}$ , and the viscous coupling effect,  $k_{v1}$ . The magnitude of the viscous coupling is significant, contributing at least 14-16 % (see Figures 6.21, 6.22, 6.25 and 6.26) to the total conventional cocurrent relative permeability for both phases. This can be seen also through Figures 6.19 and 6.20. In view of Equations (4.31), (4.32), (4.46) and (4.48), the magnitude of the viscous coupling effect is about 15% at intermediate water-saturation values (45-55% ) in Set II, and at water-saturation values of 20-30% in Set I; and it is higher at both lower and higher water-saturation values.

In terms of relative viscous drag coefficients,  $k_{r12}$  and  $k_{r21}$ , it should be noted that  $k_{r12}$  and  $k_{r21}$  are strong functions of the viscosity ratio between fluid 1 and fluid 2. Although the relative viscous drag coefficient to water,  $k_{r12}$ , is similar in both Set I and Set II, Figures 6.23 and 6.24, the shape of the relative viscous drag coefficient,  $k_{r21}$ , is different in Set I from that in Set II, Figures 6.23 and 6.24. This dissimilarity can be attributed to the difference in permeability coefficient,  $g_{21}$ , and hence to the difference in the ratio of relative permeabilities.

It can be seen clearly in Figures 6.23 and 6.24 that  $k_{r12}$  and  $k_{r21}$  are not the same. In

fact, there is a large difference between them. This difference is due mainly to the viscosity ratio ( $\mu_o/\mu_w = 30.48$  in this study). In order to investigate the shapes of  $k_{r12}$  and  $k_{r21}$  further, different viscosity ratios should be used in future studies. However, from the shapes of  $k_{r12}$  and  $k_{r21}$  in Figures 6.23 and 6.24, and in view of Equations (4.41) and (4.42), the shapes of  $k_{r12}$  and  $k_{r21}$  will be always different. These observations are consistent with the theoretical analysis presented by Whitaker [17]. The result is consistent also with the theoretical analysis presented by Spanos *et al.* [19] (see Equation (4.51)). However, Spanos *et al.* stated that the ratio between  $k_{r12}$  and  $k_{r21}$  becomes equal to the viscosity ratio if the interfacial tension is allowed to become zero (Equation (4.52)), and therefore  $k_{r12}$  and  $k_{r21}$  become the same at a viscosity ratio of one. However, with regard to the case of zero interfacial tension, Bardon and Longeron [47] concluded, as stated previously in Section 2.2.3, that the relative permeabilities,  $k_{r1}$  and  $k_{r2}$ , become straight lines of slope of one. If this conclusion is applied to Equation (4.53),  $k_{r12}$  and  $k_{r21}$  will still be different even at a viscosity ratio of one.

On the other hand, the above results are in disagreement with the analysis made by Kalaydjian [92] who concluded that the ratio between  $k_{r12}$  and  $k_{r21}$  is equal to the viscosity ratio in general and at any value of interfacial tension. It should be mentioned here that Rose [91] stated that equating  $k_{r12}$  and  $k_{r21}$  is to be avoided unless and until verified in the laboratory.

## 7. SUMMARY AND CONCLUSIONS

An evaluation of cocurrent and countercurrent imbibition flow mechanisms has been made. This was achieved first by manipulating the generalized equations for the flow of two continuous phases [9] to arrive at the defining equations for the generalized relative permeabilities, and second by performing two sets of flow experiments. In each set, cocurrent and countercurrent steady-state flow experiments were conducted. In every flow experiment, steady-state relative permeabilities were calculated using Darcy's law and inlet capillary pressure was estimated for both cocurrent and countercurrent flow. Generalized relative permeabilities and their coefficients were estimated using the fitted cocurrent and countercurrent relative permeability data.

Based on the experimental results presented herein, and keeping in mind that these results may apply only to the particular geometry and the sand-fluid system used in this study, the following conclusions may be drawn:

1. The method used in this study is simple, yet robust, in that it uses the same physical set-up for both cocurrent and countercurrent flow, and it can evaluate cocurrent and countercurrent flow with a good consistency.
2. Countercurrent flow differs from cocurrent flow because of its slower kinetics; that is, it takes a longer time for countercurrent flow to reach steady-state than it does for cocurrent flow.
3. Saturation is invariant with distance in both cocurrent and countercurrent, steady-state relative permeability flow experiments.
4. Pressure is distributed linearly in both cocurrent and countercurrent, steady-state relative permeability flow experiments.
5. Countercurrent flow relative permeabilities are less than cocurrent flow relative

permeabilities. The relative difference between water cocurrent flow relative permeability and water countercurrent flow relative permeability is always greater than 25%, while the relative difference between oil cocurrent flow relative permeability and oil countercurrent flow relative permeability is always greater than 20%.

6. On the basis of the above conclusion, the use of cocurrent flow relative permeabilities to describe relative permeabilities where countercurrent flow takes place is questionable.
7. The difference between cocurrent flow relative permeability and countercurrent flow relative permeability can be attributed to viscous coupling.
8. Conventional relative permeability can be seen as representing the influence of two types of drag: the first is that due to the flow of the fluid itself over the solid surfaces in the porous medium, the generalized relative permeability of the fluid; and the second is that due to momentum transfer across the fluid-fluid interfaces in the porous medium, the relative viscous coupling effect.
9. The magnitude of relative viscous coupling effect is significant, contributing at least 14-16 % to the total conventional cocurrent relative permeability.
10. Contrary to the suggestions of some of the previous studies, the relative viscous drag coefficients,  $k_{r12}$  and  $k_{r21}$ , Equations (4.41) and (4.42), were found to be unequal.
11. Because saturation is invariant with distance, and because pressure is distributed linearly in both phases, and because the slopes of the oil and water curves are different in sign, the difference in pressure between oil and water in countercurrent steady-state flow is not defined by capillary pressure. Thus the use of capillary pressure to define the difference in pressure between two phases flowing in a porous medium is suspect. Theoretical confirmation of this conclusion is required, before it can be accepted unequivocally.
12. The inlet countercurrent flow capillary pressure,  $P_{cin}^*$ , was found to be nearly the same as the inlet cocurrent flow capillary pressure,  $P_{cin}$ .

## 8. SUGGESTIONS FOR FUTURE STUDY

The experiments in this study were carried out using one pair of fluids having a viscosity ratio of 30.48. More experiments should be conducted with different viscosity ratios to investigate the effect of viscosity ratio on the relative viscous drag coefficients.

Although the experimental equipment used for this study is fairly accurate and reliable, there is some room for improvement in future studies. That is, in order to cover a wider range of flow rates, and consequently to investigate the effect of flow rate on the relative permeabilities, better pumps with a more flexible flow-rate range should be used. Moreover, the use of a more flexible flow-rate range would allow coverage of a wider range of saturation levels. This would lead to better precision and more accurate fitting of the relative permeability data. Hence, a better analysis of the generalized relative permeabilities would be achieved.

The end-caps used in this study were made of plexi-glass. It is recommended that the end-caps used in future studies be made of a stronger material so that they can withstand higher inlet pressures. This would enable flow experiments at higher flow rates. In terms of pressure measurement, an attempt should be made to use more accurate pressure-transducers to assure a precise and consistent pressure measurement along the core.

## REFERENCES

1. Darcy, H.: "Les Fontaines Publiques de la Ville de Dijon"; (In French), Victor Dalmont, Paris (1856).
2. Muskat, M.: *Physical Principles of Oil Production*; McGraw-Hill Book Co., Inc., New York (1949), Chapters 3 and 7.
3. Hubbert, M. K.: "Darcy's Law and the Field Equations of the Flow of Underground Fluids"; *Trans. AIME* (1956), Vol. 207, 222.
4. Prager, S.: "Viscous Flow Through Porous Media"; *Phys. of Fluids* (1961), 4, 1477.
5. Raats, P. A. C., and Klute, A.: "Transport in Soils: The Balance of Momentum"; *Soils Sci. Soc. Am. Proc.* (1968), 32, 452.
6. Slattery, J. C.: "Single-phase Flow Through Porous Media"; *AIChE J.* (1969), 15, 866.
7. Whitaker, S.: "Advances in Theory of Fluid Motion in Porous Media"; *Industr. Engin. Chem.* (1969), 61, 14.
8. Neuman, S. P.: "Theoretical Derivation of Darcy's Law"; *Acta. Mech.* (1977), 25, 153.
9. De la Cruz, V. and Spanos, T. J. T.: "Mobilization of Oil Ganglia"; *AIChE J.* (1983), Vol. 29 (5), 854.
10. Scheidegger, A. E.: *The Physics of Flow Through Porous Media*; University of Toronto Press, Toronto, Ontario (1960).
11. Bear, J.: *Dynamics of Fluids in Porous Media*; Elsevier, New York (1972).
12. Wyckoff, R. D. and Botset, H. G.: "The Flow of Gas-Liquid Mixtures Through Unconsolidated Sands"; *Physics* (1936), Vol. 7, 325.
13. Muskat, M. and Meres, M. W.: "The Flow of Heterogeneous Fluids Through Porous Media"; *Physics* (1936), Vol. 7, 346.
14. Craig, F. F., Jr.: *The Reservoir Engineering Aspects of Waterflooding*; Monograph Volume 3, Henry L. Doherty Series, Society of Petroleum Engineers of AIME, New York (1971), Chapter 2.
15. Chatenever, A. and Calhoun, J. C.: "Visual Examination of Fluid Behaviour in Porous Media"; *Trans. AIME*, Vol. 195, 149.
16. Willhite, G. P.: *Waterflooding*; Society of Petroleum Engineers, Richardson, TX (1986), Chapter 2.



17. Whitaker, S.: "Flow in Porous Media II: The Governing Equations for Immiscible, Two-Phase Flow"; *Transport in Porous Media* 1, (1986), 105.
18. Kalaydjian, F.: "A Macroscopic Description of Multiphase Flow in Porous Media Involving Spacetime Evolution of Fluid/Fluid Interface"; *Transport in Porous Media* 2, (1987), 537.
19. Spanos, T. J. T., de la Cruz, V., and Hube, J.: "An Analysis of the Theoretical Foundations of Relative Permeability Curves"; *AOSTRA Journal of Research*, 4 (1988), 181.
20. Rose, W.: *Relative Permeability*; Petroleum Production Handbook, SPE, Richardson, TX, (1987), Chapter 28.
21. Leverett, M. C. and Lewis, W. B.: "Steady Flow of Gas-Oil-Water Mixtures Through Unconsolidated Sands"; *Trans. AIME* (1942), Vol. 142, 107.
22. Schneider, F. N. and Owens, W. W.: "Steady-State Measurements of Relative Permeability for Polymer-Oil System"; SPE Paper No. 9408, Presented at the 55th Annual Tech. Conf. and Exhibition of SPE, Dallas, 1980.
23. Islam, M. R. and Bentsen, R. G.: "A Dynamic Method of Measuring Relative Permeability"; *J. Can. Pet. Tech.* (January-February, 1986), 39.
24. Sarma, H. K.: *A Study of the Impact of Instability*; Ph. D. Thesis, U of Alberta, (1988).
25. Morrow, N. C., Cram, P. C. and McCaffery, F. G.: "Displacement Studies in Dolomite with Wettability Control by Octanoic Acid"; *Soc. Pet. Eng. J.*, (August 1973), 221.
26. McCaffery, F. G. and Bennion, D. W.: "The Effect of Wettability on Two-Phase Relative Permeabilities"; *J. Can. Pet. Tech.* (October-December, 1974), 42.
27. Leverett, M. C.: "Capillary Behavior in Porous Solids"; *Trans. AIME* (1941), Vol. 142, 159.
28. Amyx, J. W., Bass, D. M. Jr., and Whiting, R. L.: *Petroleum Reservoir Engineering*; McGraw-Hill Book Co., New York (1960), Chapter 3.
29. Bruce, W. A. and Welge, H. J.: "The Restored-State Method for Determination of Oil and Connate Water"; *Drill. and Prod. Prac.*, API, Dallas (1947), 166.
30. Purcell, W. R.: "Capillary Pressures-Their Measurement Using Mercury and the Calculation of Permeability Therefrom"; *Trans. AIME* (1949), Vol. 186, 39.
31. Slobod, R. L., Chambers, A., and Prehn, W. L. Jr.: "Use of Centrifuge for Determining Connate Water, Residual Oil, and Capillary Pressure of Small Core Samples"; *Trans. AIME* (1951), Vol. 192, 127.
32. Brown, H. W.: "Capillary Pressure Investigations"; *Trans. AIME* (1951), Vol. 192, 67.

33. Messer, E. S.: "Interstitial Water Determination by an Evaporation Method"; *Trans. AIME* (1951), Vol. 192, 269.
34. Honarpour, M., Koederitz, L., and Harvey, A. H.: "*Relative Permeability of Petroleum Reservoir*"; CRC Press Inc., Boca Raton, FL (1986), Chapters 1 and 3.
35. Caudle, B. H., Slobod, R. L., and Brownscombe, E. R.: "Further Developments in the Laboratory Determination of Relative Permeability"; *Trans. AIME* (1951), Vol. 192, 145.
36. Emmett, W. R., Beaver, K. W., and McCalab, J. A.: "Little Buffalo Basin Tensleep Heterogeneity and its Influence on Drilling and Secondary Recovery"; *J. Pet. Tech.*, (February, 1971), 161.
37. Corey, A. T. and Rathjens, C. H.: "Effect of Stratification on Relative Permeability"; *Trans. AIME* (1956), Vol. 207, 358.
38. Huppler, J. D.: "Numerical Investigation of the Effects of Core Heterogeneities on Waterflood Relative Permeability"; *Soc. Pet. Eng. J.*, (October, 1970), 381.
39. Naar, J., Wygal, R. J., and Henderson, J. H.: "Imbibition Relative Permeability in Unconsolidated Porous Media"; *Trans. AIME* (1962), Vol. 225, 13.
40. Fatt, I.: "The Network Model of Porous Media III. Dynamic Properties of Networks with Tube Radius Distribution"; *Trans. AIME* (1956), Vol. 207, 164.
41. Leverett, M. C.: "Flow of Oil-Water Mixtures through Unconsolidated Sands"; *Trans. AIME* (1939), Vol. 132, 149.
42. Morgan, T. J. and Gordon, D. T.: "Influence of Pore Geometry on Water-Oil Relative Permeability"; *J. Pet. Tech.* (1970), 1199, 407.
43. Owens, W. W. and Archer, D. L.: "The Effect of Rock Wettability on Oil-Water Relative Permeability Relationships"; *Trans. AIME* (1971), Vol. 251, 873.
44. Moore, T. F. and Slobod, R. L.: "The Effect of Viscosity and Capillarity on the Displacement of Oil by Water"; *Prod. Mon.* (1956), Vol. 8, 20.
45. Talash, A. W.: "Experimental and Calculated Relative Permeability Data for Systems Containing Tension Additives"; SPE Paper No. 5810 Presented at the SPE Improved Oil Recovery Symposium, Tulsa, March 22-24, 1976.
46. Amaefule, J. O. and Handy, L. L.: "The Effect of Interfacial Tension on Relative Permeabilities of Consolidated Porous Media"; *Soc. Pet. Eng. J.* (1982), Vol. 273, 371.
47. Bardon, C. and Longeron, D. G.: "Influence of Very Low Interfacial Tensions on Relative Permeability"; *Soc. Pet. Eng. J.*, October, 1980, 391.
48. Sandberg, C. R., Gouney, L. S., and Suppel, R. F.: "Effect of Fluid Rate and Viscosity on Laboratory Determination of Oil-Water Relative Permeabilities"; *Trans. AIME* (1958), Vol. 213, 36.

49. Donaldson, E. C., Lorenz, P. B., and Thomas, R. D.: "The Effect of Viscosity and Wettability on Oil-Water Relative Permeability"; SPE Paper No. 1562 Presented at the SPE 41st Annual Meeting, Dallas, October 2-5, 1962.
50. Hassler, G. L., Rice, R. R., and Leeman, E. H.: "Investigation of Recovery of Oil from Sandstones by Gas-Drive"; *Trans. AIME* (1936), Vol. 118, 116.
51. Morse, R. A., Terwilliger, P. K., and Yuster, S. T.: "Relative Permeability Measurements on Small Core Samples"; *Oil and Gas J.*, August, 1947, 109.
52. Odeh, A. S.: "Effect of Viscosity Ratio on Relative Permeability"; *Trans. AIME* (1959), Vol. 216, 346.
53. Lefebvre du Prey, E. J.: "Factors Affecting Relative Permeabilities of Consolidated Porous Media"; *Soc. Pet. Eng. J.*, February, 1973, 39.
54. Edmondson, T. A.: "Effect of Temperature on Waterflooding"; *J. Can. Pet. Tech.*, (October-December, 1965), 236.
55. Poston, S. W., Ysrael, S., Hossain, A. K. H. S., Montgomery, E. F., III, and Ramey, H. J. Jr.: "The Effect of Temperature on Irreducible Water Saturation and Relative Permeability of Unconsolidated Sands"; *Soc. Pet. Eng. J.*, June, 1970, 171.
56. Lo, H. Y. and Mungan, N.: "Effect of Temperature on Water-Oil Relative Permeabilities in Oil-Wet and Water-Wet Systems"; SPE Paper No. 4505, Las Vegas, Nev., September 30, 1973.
57. Miller, M. A. and Ramey, H. J. Jr.: "Effect of Temperature on Oil/Water Relative Permeabilities of Unconsolidated and Consolidated Sands"; *Soc. Pet. Eng. J.*, (December, 1985), 945.
58. Maini, B. B. and Batycky, J.P.: "Effect of Temperature on Heavy-Oil/Water Relative Permeabilities in Horizontally and Vertically Drilled Core Plugs"; *J. Pet. Tech.* (August, 1985), 1500.
59. Osoba, J. S., Richardson, J. G., Kerver, J.K., Hafford, J. A., and Blair, P. M.: "Laboratory Measurements of Relative Permeability"; *Trans. AIME* (1951), Vol. 192, 47.
60. Richardson, J. G., Kerver, J. K., Hafford, J. A., and Osoba, J. S.: "Laboratory Determinations of Relative Permeability"; *Trans. AIME* (1952), Vol. 195, 187.
61. Sandberg, C. R., Gourney, L. S., and Suppel, R. F.: "Effect of Fluid Flow Rate and Viscosity on Laboratory Determination of Oil-Water Relative Permeabilities"; *Trans. AIME* (1958), Vol. 213, 36.
62. Ehrlich, R. and Crane, F. E.: "A Model for Two-Phase Flow in Consolidated Materials"; *Trans. AIME* (1969), Vol. 246, 221.
63. Fulcher, R. A., Jr., Turgay, E., and Stahl, C. D.: "Effect of Capillary Number and its Constituents on Two-Phase Relative Permeability Curves"; *Soc. Pet. Eng. J.* (1985), Vol. 279, I 249.

64. Pirson, S. J., Ed.: *Oil Reservoir Engineering*; McGraw-Hill Book, New York (1958), 68.
65. Delclaud, J. P.: "New Results on the Displacement of a Fluid by Another in a Porous Medium"; SPE Paper No. 4103 Presented at the SPE 47th Annual Meeting, San Antonio, Tex., 1972.
66. Rapoport, L. A. and Leas, W. J.: "Relative Permeability to Liquid-Gas System"; *Trans. AIME* (1951), Vol. 192, 83.
67. Naar, J. and Henderson, J. H.: "An Imbibition Model-Its Application to Flow Behavior and the Prediction of Oil Recovery"; *Trans. AIME* (1961), Vol. 222, 61.
68. Honarpour, M. and Mahmood, S. M.: "Relative-Permeability Measurements: An Overview"; *J. of Pet. Tech.*, (August, 1988), 53.
69. Fatt, I. and Dykstra, H.: "Relative Permeability Studies"; *Trans. AIME* (1951), Vol. 192, 41.
70. O'Mera, D. J., Jr., and Leas, W. O.: "Multiphase Relative Permeability Measurement Using an Automated Centrifuge"; SPE Paper No. 12128 Presented at the SPE 58th Annual Tech. Conf. and Exhibition, San Francisco, 1983.
71. Buckley, S. E. and Leverett, M. C.: "Mechanism of Fluid Displacement in Sands"; *Trans. AIME* (1942), Vol. 146, 107.
72. Welge, H. J.: "A Simplified Method for Computing Recovery by Gas or Water Drive"; *Trans. AIME* (1952), Vol. 195, 91.
73. Johnson, E. F., Bossler, D. P., and Neuman, V. O.: "Calculation of Relative Permeability from Displacement Experiments"; *Trans. AIME* (1959), Vol. 216, 370.
74. Jones, S. C. and Roszelle, W. O.: "Graphical Techniques for Determining Relative Permeabilities from Displacement Data"; *J. Pet. Tech.*, (May, 1978), 807.
75. Sarma, H. K. and Bentsen, R. G.: "A Method for Reducing Model Error when Estimating Relative Permeabilities from Displacement Data"; *J. of Pet. Sci. and Eng.*, (1989) Vol. 2, No. 4, 331.
76. Bentsen, R. G. and Saeedi, J.: "Liquid-Liquid Immiscible Displacement in Unconsolidated Porous Media"; *J. Can. Pet. Tech.* (January-March, 1981), Vol. 20, No. 1, 93.
77. Archer, J. S. and Wong, S. W.: "Use of a Reservoir Simulator to Interpret Laboratory Water Flooding Data"; *Soc. Pet. Eng. J.* (December, 1973), Vol. 13, No. 6, 343.
78. Sarma, H. K., and Bentsen, R. G.: "A New Method for Estimating Relative Permeabilities from Unstabilized Displacement Data", *J. Can. Pet. Tech.* (July-August, 1989), Vol. 28, No. 4, 118.
79. Geffen, T. M., Owens, W. W., Parrish, D. R., and Morse, R. A.: "Experimental Investigation of Factors Affecting Laboratory Relative Permeability Measurements";

- Trans. AIME* (1951), Vol. 192, 99.
80. Leas, W. J., Jenks, L.H., and Russell, C. D.: "Relative Permeability to Gas"; *Trans. AIME* (1950), Vol. 189, 65.
  81. Leverett, M. C., Lewis, W. B., and True, M. E.: "Dimensional Model Studies of Oil Field Behavior"; *Trans. AIME* (1942), Vol. 146, 175.
  82. Blair, P. M.: "Calculation of Oil Displacement by Countercurrent Water Imbibition"; *Soc. Pet. Eng. J.* (September, 1964), 195.
  83. Bourbiaux, B. and Kalaydjian, F.: "Experimental Study of Cocurrent and Countercurrent Flow in Natural Porous Media"; *Soc. Pet. Eng. J. (Res. Eng.)* (August, 1990), 363.
  84. Templeton, E. E., Nielsen, R. F., and Stahl, C. D.: "A Study of Gravity Counter Flow Segregation"; *Soc. Pet. Eng. J.* (June, 1962), 185.
  85. Lelievre, R. F.: *Etude d'écoulements disphasiques permanents a contre-courants en milieu poreux-comparaison avec les écoulements de meme sens*; (in French), Ph. D. Thesis, University of Toulouse (1966), 151.
  86. Lefebvre du Prey, E.: "Gravity and Capillary Effects on Imbibition in Porous Media"; *Soc. of Pet. Eng. J.* (June, 1978), 195.
  87. Hamon, G. and Vidal, J.: "Scaling-Up the Capillary Imbibition Process from Laboratory Experiments on Homogeneous and Heterogeneous Samples"; SPE Paper No. 15852 Presented at the SPE European Pet. Conf., London, (October 20-22, 1986).
  88. Islam, M. R.: *An Investigation on the Impact of Flow Regime on Effective Permeabilities*; M. Sc. Thesis, U of Alberta (1985).
  89. Hagoort, J.: "Displacement Stability of Water Drives in Water-Wet Connate Water Bearing Reservoirs"; *Soc. Pet. Eng. J.* (1974), Vol. 14(1), 63.
  90. Parsons, R. W.: "Microwave Attenuation-A New Tool for Monitoring Saturations in Laboratory Flooding Experiments"; *Soc. Pet. Eng. J.* (1974), Vol. 15(3), 302.
  91. Rose, W.: "Measuring Transport Coefficients Necessary for the Description of Coupled Two-Phase Flow of Immiscible Fluids in Porous Media"; *Transport in Porous Media* 3, (1988), 163.
  92. Kalaydjian, F.: "Origin and Quantification of Coupling Between Relative Permeabilities for Two-Phase Flows in Porous Media"; *Transport in Porous Media* 5, (1990), 215.
  93. BMDP Statistical Software Manual, Volume 2, University of California Press, Berkeley, California (1988).
  94. SPSS-X User's Guide, SPSS Inc. 444 North Michigan Avenue, Chicago (1988).
  95. Van Domselaar, H. R.: "An Exact Equation to Actual Saturations from Centrifuge Capillary Pressure Measurements"; *Rev. Tec. INTEVEP* (1984), Vol. 4 (1), 55.

## APPENDIX A: Programs for Data Acquisition and Retrieval

### A.1: Data Acquisition for microwave scan at constant saturation

```

10 !***** CONSCAN *****
20 !* THIS PROGRAM AND THE OTHER DATA ACQUISITION PROGRAMS *
30 !* WERE MODIFIED FROM THE PROGRAMS THAT WERE WRITTEN *
   !* ORIGINALLY BY SARMA (Ref. 24) *
40 !* PROGRAM FOR MICROWAVE DATA ACQUISITION *
50 !* SCANS MADE AT Sw=1 AND Swi FOR CONSTANTS CALCULATION *
60 !*****DIMENSIONALISING OF VARIABLES*****
70 OPTION BASE 1
80 INTEGER I,J,K,N,M,L
90 INTEGER Ii,Ik,Jj,Kk
100 DIM Ao$(2,100)[17]
110 DIM P(15)
120 DIM Power(2,100),Powin(2,100)
130 PRINTER IS 1
140 PRINT "PROGRAM CONSCAN: PERFORMS MICROWAVE SCANS AT
ENDPOINT Sws"
150 PRINT "Today is :",DATE$(TIMEDATE)
160 PRINT "Program Started @",TIME$(TIMEDATE)
170 !***** ASSIGNMENTS OF PERIPHERALS *****
180 ASSIGN @Multi TO 723
190 ASSIGN @Meter TO 713
200 Sc=9
210 CONTROL Sc,4;2+0+8+0
220 CONTROL Sc,5;3
230 CONTROL Sc,3;300
240 !***** ALLOCATE BYTES FOR STORAGE *****
250 Msus$=":CS80,700,0"
260 Pwr=101*8
270 Pr=15*8
280!***** ZEROING OF POWER METER *****
290 PRINT "PRESS SWITCH 1 IN POWER SUPPLY. TURN ON FAN. DO NOT
TURN ON SWITCH 2"
300 OUTPUT @Multi USING "#,K";"O040TG17TO260T"
310 REMOTE @Meter
320 CALL Zero_meter(@Meter)
330 BEEP
340 PRINT "COMPLETE MICROWAVE POWER SUPPLY AFTER STABLE ZERO,"
350 DISP "TURN ON SWITCH 2, THEN HIT CONTINUE "
360 PAUSE
370 !***** ALLOCATE FILE NAMES FOR POWER *****
380 INPUT "ENTER WATER SATURATION (FRACTION )",Sw
390 IF Sw<1 THEN GOTO 480
400 INPUT "FILENAME TO STORE OUTPUT POWER DATA (OP#S1)?",Name$
410 INPUT "DRIVE (ie. :,700,1) default current drive?",Msus$

```

```

420 Size_records=Pwr
430 No_records=2
440 ON ERROR GOSUB Createfile
450 ASSIGN @File11 TO Name$&Msus$
460 OFF ERROR
470 GOTO 550
480 INPUT "FILENAME TO STORE OUTPUT POWER DATA (OP#S2)?",Name$
490 INPUT "DRIVE (ie. :,700,1) default current drive?",Msus$
500 Size_records=Pwr
510 No_records=2
520 ON ERROR GOSUB Createfile
530 ASSIGN @File1 TO Name$&Msus$
540 OFF ERROR
550 IF Sw<1 THEN GOTO 640
560 INPUT "FILENAME TO STORE INPUT POWER DATA (IP#S1)?",Name$
570 INPUT "DRIVE (ie.:,700,1)default current drive?",Msus$
580 Size_records=Pwr
590 No_records=2
600 ON ERROR GOSUB Createfile
610 ASSIGN @File12 TO Name$&Msus$
620 OFF ERROR
630 GOTO 710
640 INPUT "FILENAME TO STORE INPUT POWER DATA (IP#S2)?",Name$
650 INPUT "DRIVE (ie.:,700,1)default current drive?",Msus$
670 No_cords=60
680 ON ERROR GOSUB Createfile
690 ASSIGN @File2 TO Name$&Msus$
700 OFF ERROR
710 OUTPUT @Multi USING "#,K";"O040TG17TO260T"
720 PRINTER IS 1
730 Day$=DATE$(TIMEDATE)
740 Tim$=TIME$(TIMEDATE)
750 PRINT "WHEN YOU ARE READY TO START, HIT CONTINUE"
760 PAUSE
770 !*****MICROWAVE SCAN*****
780 !*** PERFORM ONE SCAN OF RECEIVER AND TRANSMITER*****
790 IF Sw<1 THEN GOTO 820
800 J=1
810 GOTO 830
820 J=2
830 OUTPUT @Multi;"O0140T@7775T"
840 WAIT .1
850 OUTPUT @Multi;"O0140T@7777T"
860 FOR I=1 TO 100
870 Time1=TIMEDATE
880 OUTPUT @Multi USING "#,K";"O0240TKT"
890 OUTPUT @Multi USING "#,K";"JT"
900 ENTER @Multi;Ao$(J,I)
910 OUTPUT @Meter;"3A+I"
920 CALL Read_meter(@Meter,Power(J,I))
930 DISP I,Power(J,I),Ao$(J,I)
940 Time2=TIMEDATE
950 Time3=.10-(Time2-Time1)
960 WAIT Time3

```

```
970 NEXT I
980 OUTPUT @Multi;"00140T@7776T"
990 WAIT .01
1000 OUTPUT @Multi;"00140T@7777T"
1010 WAIT 10
1020 !** ***** CONVERSION ROUTINE FOR POWER HP 432C *****
1030 DISP "NOW DATA STORAGE BEGINS"
1040 FOR I=1 TO 100
1050   FOR Ik=1 TO 15
1060     P(Ik)=0
1070     NEXT Ik
1080     FOR K=1 TO 5
1090       C=VAL(Ao$(J,I)[K,K])
1100       IF C=0 THEN
1110         H1=0
1120         H2=0
1130         H3=0
1140       END IF
1150       IF C=1 THEN
1160         H1=0
1170         H2=0
1180         H3=1
1190       END IF
1200       IF C=2 THEN
1210         H1=0
1220         H2=1
1230         H3=0
1240       END IF
1250       IF C=3 THEN
1260         H1=0
1270         H2=1
1280         H3=1
1290       END IF
1300       IF C=4 THEN
1310         H1=1
1320         H2=0
1330         H3=0
1340       END IF
1350       IF C=5 THEN
1360         H1=1
1370         H2=0
1380         H3=1
1390       END IF
1400       IF C=6 THEN
1410         H1=1
1420         H2=1
1430         H3=0
1440       END IF
1450       IF C=7 THEN
1460         H1=1
1470         H2=1
1480         H3=1
1490       END IF
1500     IF K=1 THEN
```



```

1510     P(1)=H1
1520     P(2)=H2
1530     P(3)=H3
1540     END IF
1550     IF K=2 THEN
1560         P(4)=H1
1570         P(5)=H2
1580         P(6)=H3
1590     END IF
1600     IF K=3 THEN
1610         P(7)=H1
1620         P(8)=H2
1630         P(9)=H3
1640     END IF
1650     IF K=4 THEN
1660         P(10)=H1
1670         P(11)=H2
1680         P(12)=H3
1690     END IF
1700     IF K=5 THEN
1710         P(13)=H1
1720         P(14)=H2
1730         P(15)=H3
1740     END IF
1750     NEXT K
1760     Xa=0
1770     Ya=0
1780     Za=0
1790     Ra=0
1800     FOR K=3 TO 1 STEP -1
1810         Xa=Xa+P(K)*2^(3-K)
1820     NEXT K
1830     FOR K=7 TO 4 STEP -1
1840         Ya=Ya+P(K)*2^(7-K)
1850     NEXT K
1860     FOR K=11 TO 8 STEP -1
1870         Za=Za+P(K)*2^(11-K)
1880     NEXT K
1890     FOR K=15 TO 12 STEP -1
1900         Ra=Ra+P(K)*2^(15-K)
1910     NEXT K
1920     Tot=(Xa*1000+Ya*100+Za*10+Ra)/100
1930     IF Tot>12.0 THEN Tot=Tot-10.0
1940     Powin(J,I)=Tot
1950     Power(J,I)=ABS(Power(J,I))*1000.0
1960     NEXT I
1970     DISP J
1980     IF Sw<1 THEN GOTO 2020
1990     OUTPUT @File1;Power(*)
2000     OUTPUT @File2;Powin(*)
2010     GOTO 2040
2020     OUTPUT @File1;Power(*)
2030     OUTPUT @File2;Powin(*)
2040     DISP "DATA STORED"

```

```

2050 BEEP
2060 INPUT "DO YOU WANT HARD COPY mW PLOT ? ANSWER 1=YES
0=NO",Ipl
2070 IF Ipl=1 THEN DISP "CHANGE PAPER ON PLOTTER AND HIT CONTINUE:"
2080 IF Ipl=1 THEN PAUSE
2090 PEN 1
2100 GINIT
2110 IF Ipl<>1 THEN PLOTTER IS CRT,"INTERNAL"
2120 IF Ipl=1 THEN PLOTTER IS 705,"HPGL"
2130 GRAPHICS ON
2140 X_max=100*MAX(1,RATIO)
2150 Y_max=100*MAX(1,1/RATIO)
2160 LORG 6
2170 REM FOR I=-.3 TO .3 STEP .1
2180 MOVE X_gdu_max/2,Y_gdu_max
2190 LABEL USING ""mW vs X at constant Sw=""",2D.4D";Sw
2200 REM NEXT I
2210 DEG
2220 LDIR 90
2230 CSIZE 3
2240 MOVE 0,Y_gdu_max/2
2250 LABEL "Power (mW)"
2260 LORG 4
2270 LDIR 0
2280 MOVE X-gdu_max/2,0.7*Y_gdu_max
2290 LABEL "Length of Core"
2300 VIEWPORT .1*X_gdu_max,0.99*X_gdu_max,.15*Y_gdu_max,.9*Y_gdu_max
2310 FRAME
2320 WINDOW 0.,100,0.,MAX(Power(*))
2330 AXES 5.0,.05,0,0,5,5,2
2340 CLIP OFF
2350 CSIZE 2.5,.5
2360 LORG 6
2370 FOR I=0 TO 100 STEP 10
2380 MOVE I,-.1
2390 LABEL USING "#,K";I
2400 NEXT I
2410 LORG 8
2420 FOR I=0 TO MAX(Power(*))
2430 MOVE -.2,I
2440 LABEL USING "#,D.5D";I
2450 NEXT I
2460 PENUP
2470 FOR L=1 TO 100
2480 PLOT L,ABS(Power(J,L))
2490 NEXT L
2500 PENUP
2510 WAIT .1
2520 GRAPHICS OFF
2530 PEN 0
2540 BEEP
2550 IF Sw<1 THEN GOTO 2590
2560 DISP "YOU ARE DONE WITH MICROWAVE SCAN @ Sw=1.0"
2570 DISP "DISPLACE WATER WITH OIL TO CREATE Swi & PERFORM SCAN

```

```
FOR Swi"
2580 GOTO 2650
2590 DISP "YOU ARE DONE WITH MICROWAVE SCAN, @ Swi = ",Sw
2600 GOTO 2650
2610 !*****Creating Storage Files*****
2620 Createfile: REM
2630 CREAT BDAT Name$&Msus$,Size_records,No_records
2640 RETURN
2650 END
2660 SUB Zero_meter(@Meter)
2670 Rezero:OUTPUT @Meter,"Z1T"
2680 ENTER @Meter,Power
2690 IF ABS(Power)>2 THEN Rezero
2700 Unzero:OUTPUT @Meter,"3+AI"
2710 ENTER @Meter,Power
2720 IF Power>=84 THEN Unzero
2730 Preset:OUTPUT @Meter,"3A+I"
2740 SUBEND
2750 SUB Read_meter(@Meter,Power)
2760 ENTER @Meter,Power
2770 SUBEND
```

## A.2: Data Acquisition and Storage for Cocurrent Flow

```

10 !*****          COCURRENT.EX          *****
20 !*  PROGRAM FOR DATA ACQUISITION AND STORAGE FOR      *
30 !*  COCURRENT FLOW EXPERIMENTS                      *
40 !*  *
50 !*****
60 !*****DIMENSIONALISING OF VARIABLES*****
70 OPTION BASE 1
80 INTEGER I,J,K,N,M,L
90 INTEGER Ii,Ik,Jj,Kk
100 DIM A$(50)[17]
110 DIM Ao$(50,100)[17]
120 DIM Volt(50,14),P(50)
130 DIM V(14),Delp(50),P1(50),P2(50),Dlpw(50),P1w(50),P2w(50)
140 DIM T1(50),Tp(50),Tm(50),T2(50)
160 DIM Power(50,100),T7(50),Powin(50,100)
170 DIM T3(50),Pk1(50),Pk2(50),Delpk(50)
180
190 !*****          PUTTING APPROPRIATE FLAGS          *****
200 PRINTER IS 1
210 PRINT "Today is :",DATE$(TIMEDATE)
220 PRINT "Program Started @",TIME$(TIMEDATE)
230 !*****          ASSIGNMENTS OF PERIPHERALS          *****
240 ASSIGN @Multi TO 723
250 ASSIGN @Meter TO 713
260 Sc=9
270 CONTROL Sc,4;2+0+8+0
280 CONTROL Sc,5;3
290 CONTROL Sc,3;300
300 !*****          ALLOCATE BYTES FOR STORAGE          *****
310 Msus$=":CS80,700,0"
320 Pwr=101*8
330 Pr=15*8
340 !*****          ZEROING OF POWER METER          *****
350 PRINT "PRESS SWITCH 1 IN POWER SUPPLY. TURN ON FAN. DO NOT
TRUN ON SWITCH 2"
360 OUTPUT @Multi USING "#,K";"O040TG17TO260T"
370 REMOTE @Meter
380 CALL Zero_meter(@Meter)
390 BEEP
400 DISP "COMPLETE MICROWAVE POWER SUPPLY AFTER STABLE ZERO,
HIT CONTINUE"
410 PAUSE
420 !**** ALLOCATE FILE NAMES FOR POWER & PRESSURE DATA ****
430 INPUT "COCURRENT FLOW EXPERIMENT No.?",Run$
440 Ru=VAL(Run$)
450 INPUT "FILENAME TO STORE MICROWAVE OUTPUT POWER
DATA..(R#O)?",Name$
460 INPUT "DRIVE (ie :,700,1) default current drive?",Msus$
470 Size_records=Pwr

```

```

480 No_records=50
490 ON ERROR GOSUB Createfile
500 ASSIGN @File3 TO Name$&Msus$
510 OFF ERROR
520 INPUT "FILENAME TO STORE MICROWAVE INPUT POWER DATA ..
R#I)?",Name$
530 INPUT "DRIVE (ie :,700,1) default current drive?",Msus$
540 Size_records=Pwr
550 No_records=50
560 ON ERROR GOSUB Createfile
570 ASSIGN @File10 TO Name$&Msus$
580 OFF ERROR
590 INPUT "FILENAME TO STORE PRESSURE DATA ..(R#P)?",Name$
600 INPUT "DRIVE (ie :,700,1) default current drive?",Msus$
610 Size_records=Pr
620 No_records=50
630 ON ERROR GOSUB Createfile
640 ASSIGN @File4 TO Name$&Msus$
650 OFF ERROR
660 OUTPUT @Multi USING "#,K";"0040TG17TO260T"
670 FOR H=1 TO 14
680 OUTPUT @Multi USING "#,K";"FT"
690 ENTER @Multi;V(H)
700 V(H)=V(H)-10000
710 Octal$=VAL$(V(H))
720 V(H)=DVAL(Octal$,8)
730 IF V(H)>2047 THEN V(H)=V(H)-4096
740 V(H)=.005*V(H)
750 NEXT H
760 PRINT V(*)
780 INPUT "FILENAME FOR DATE AND TIME ..(R#D)?",Name$
790 INPUT "DRIVE (ie :,700,1) default current drive?",Msus$
800 Size_records=160
810 No_records=1
810 ON ERROR GOSUB Createfile
830 OFF ERROR
840 PRINTER IS 1
850 Day$=DATE$(TIMEDATE)
860 Tim$=TIME$(TIMEDATE)
870 Tst1=TIMEDATE
880 BEEP 81.38,10
890 INPUT "TOTAL VOLUME OF OIL TO BE PUMPED (IN CC)?",To
900 INPUT "TOTAL VOLUME OF WATER TO BE PUMPED (IN CC)?",Tw
910 INPUT "PUMP RATE OF OIL IN CC/HR?",Ro
920 INPUT "PUMP RATE OF WATER IN CC/HR?",Rw
930 Ot=To/Ro
940 Wt=Tw/Rw
950 IF Ot<=Wt THEN GOTO 980
960 Et=Wt*3600.0
970 GOTO 990
980 Et=Ot*3600.0
990 INPUT "No. OF SATURATION PROFILES ?",Nsat
1000 Nscan=Nsat+2
1010 Insat=(Et-((Nsat-1)*10.81))/(Nsat-1)

```

```

1020 Inprs=Insat
1030 PRINT "TIME FOR SATURATION PROFILE (seconds)",Insat
1040 PRINT "PRESSURE INETRVAL AFTER SCANNING PERIOD (seconds)",Inprs
1050 BEEP
1060 DISP "CHECK PUMP CONNECTIONS, WHEN YOU ARE READY HIT
CONTINUE"
1070 PAUSE
1080 Tst=TIMEDATE
1090 FOR J=3 TO Nscan
1100 !*****
1110 ! ***** PRESSURE DATA *****
1120 OUTPUT @Multi USING "#,K";"O040TG17TO260T"
1130 T1(J)=TIMEDATE-Tst
1140 FOR N=1 TO 14
1150 OUTPUT @Multi USING "#,K";"FT"
1160 ENTER @Multi;Volt(J,N)
1170 Volt(J,N)=Volt(J,N)-10000
1180 Octal$=VAL$(Volt(J,N))
1190 Volt(J,N)=DVAL(Octal$,8)
1200 IF Volt(J,N)>2047 THEN Volt(J,N)=Volt(J,N)-4096
1210 Volt(J,N)=.005*Volt(J,N)
1220 NEXT N
1230 !*****MICROWAVE SCAN*****
1240 T2(J)=TIMEDATE-Tst
1250 OUTPUT @Multi;"O0140T@7775T"
1260 WAIT .1
1270 OUTPUT @Multi;"O0140T@7777T"
1280 T8=TIMEDATE
1290 FOR I=1 TO 100
1300 Time1=TIMEDATE
1310 OUTPUT @Multi USING "#,K";"O0240TKT"
1320 OUTPUT @Multi USING "#,K";"JT"
1330 ENTER @Multi;Ao$(J,I)
1340 OUTPUT @Meter;"3A+I"
1350 CALL Read_meter(@Meter,Power(J,I))
1360 DISP I,Power(J,I),Ao$(J,I)
1370 Time2=TIMEDATE
1380 Time3=.10-(Time2-Time1)
1390 WAIT Time3
1400 NEXT I
1410 T9=TIMEDATE-T8
1420 OUTPUT @Multi;"O0140T@7776T"
1430 WAIT .01
1440 OUTPUT @Multi;"O0140T@7777T"
1450 DISP J,T9
1460 IF J=Nscan THEN GOTO 1500
1470 WAIT Insat
1480 NEXT J
1490 !*****
1500 DISP "NOW DATA STORAGE BEGINS"
1510 !***** CONVERSION OF THE mW DATA *****
1520 FOR J=3 TO Nscan
1530 FOR I=1 TO 100
15540 FOR Ik=1 TO 15

```

```
1550   P(Ik)=0
1560   NEXT Ik
1570   FOR K=1 TO 5
1580     C=VAL(AO$(J,I)|K,K|)
1590     IF C=0 THEN
1600       H1=0
1610       H2=0
1620       H3=0
1630     END IF
1640     IF C=1 THEN
1650       H1=0
1660       H2=0
1670       H3=1
1680     END IF
1690     IF C=2 THEN
1700       H1=0
1710       H2=1
1720       H3=0
1730     END IF
1740     IF C=3 THEN
1750       H1=0
1760       H2=1
1770       H3=1
1780     END IF
1790     IF C=4 THEN
1800       H1=1
1810       H2=0
1820       H3=0
1830     END IF
1840     IF C=5 THEN
1850       H1=1
1860       H2=0
1870       H3=1
1880     END IF
1890     IF C=6 THEN
1900       H1=1
1910       H2=1
1920       H3=0
1930     END IF
1940     IF C=7 THEN
1950       H1=1
1960       H2=1
1970       H3=1
1980     END IF
1990     IF K=1 THEN
2000       P(1)=H1
2010       P(2)=H2
2020       P(3)=H3
2030     END IF
2040     IF K=2 THEN
2050       P(4)=H1
2060       P(5)=H2
2070       P(6)=H3
2080     END IF
```

```

2090   IF K=3 THEN
2100     P(7)=H1
2110     P(8)=H2
2120     P(9)=H3
2130   END IF
2140   IF K=4 THEN
2150     P(10)=H1
2160     P(11)=H2
2170     P(12)=H3
2180   END IF
2190   IF K=5 THEN
2200     P(13)=H1
2210     P(14)=H2
2220     P(15)=H3
2230   END IF
2240   NEXT K
2250   Xa=0
2260   Ya=0
2270   Za=0
2280   Ra=0
2290   FOR K=3 TO 1 STEP -1
2300     Xa=Xa+P(K)*2^(3-K)
2310   NEXT K
2320   FOR K=7 TO 4 STEP -1
2330     Ya=Ya+P(K)*2^(7-K)
2340   NEXT K
2350   FOR K=11 TO 8 STEP -1
2360     Za=Za+P(K)*2^(11-K)
2370   NEXT K
2380   FOR K=15 TO 12 STEP -1
2390     Ra=Ra+P(K)*2^(15-K)
2400   NEXT K
2410   Tot=(Xa*1000+Ya*100+Za*10+Ra)/100
2420   IF Tot>12.0 THEN Tot=Tot-10.0
2430   Powin(J,I)=Tot
2440   Power(J,I)=ABS(Power(J,I))*1000.0
2450   NEXT I
2460   DISP J
2470   NEXT J
2480   OUTPUT @File3;T2(*),Power(*)
2490   OUTPUT @File10;T2(*),Powin(*)
2500   OUTPUT @File5;Day$,Tim$,Run$
2510   !*****
2520   !***** Conversion To Pressure from Volt.*****
2530   FOR J=3 TO Nscan
2540     Volt(J,1)=(Volt(J,1)-V(1))*7.5
2550     Volt(J,2)=(Volt(J,2)-V(2))*7.5
2560     Volt(J,3)=(Volt(J,3)-V(3))*5
2570     Volt(J,4)=(Volt(J,4)-V(4))*3.0
2580     Volt(J,5)=(Volt(J,5)-V(5))*5
2590     Volt(J,6)=(Volt(J,6)-V(6))*3.0
2600     Volt(J,7)=(Volt(J,7)-V(7))
2610     Volt(J,8)=(Volt(J,8)-V(8))*5
2620     Volt(J,9)=(Volt(J,9)-V(9))*7.5

```



```

2630 Volt(J,10)=(Volt(J,10)-V(10))*.5
2640 Volt(J,11)=(Volt(J,11)-V(11))*3.0
2650 Volt(J,12)=(Volt(J,12)-V(12))*.5
2660 Volt(J,13)=(Volt(J,13)-V(13))
2670 Volt(J,14)=(Volt(J,14)-V(14))*.5
2680 NEXT J
2690 WAIT .1
2700 OUTPUT @File4;T1(*),Volt(*)
2710 INPUT "DATA STORED. TYPE 1 IF PRINTOUTS OF PRESSURES
NEEDED",Ipr
2720 IF Ipr=1 THEN PRINTER IS 701
2730 IF Ipr=1 THEN OUTPUT 701;CHR$(27)&"&l1L"
2740 !*****
2750 !***** PRINTING RESULTS *****
2760 PRINT USING ""COCURRENT FLOW EXPERIMENT NUMBER
:"",DDD";Ru
2770 PRINT "DATE OF EXPERIMENT : ",Day$
2780 PRINT "SUMMARY OF PRESSURE DISTRIBUTION DURING THE RUN"
2790 PRINT "NOTE: Last column indicates dP(psi) across the core"
2800 PRINT "-----"
2810 PRINT " "
2820 FOR K=3 TO Nscan
2830 P1(K)=Volt(K,1)+2.0*(Volt(K,1)-Volt(K,2))/11.0
2840 P2(K)=Volt(K,7)-2.0*(Volt(K,6)-Volt(K,7))/11.0
2850 Delp(K)=P1(K)-P2(K)
2860 P1w(K)=Volt(K,9)+13*(Volt(K,9)-Volt(K,11))/36.5
2870 P2w(K)=Volt(K,13)-13*(Volt(K,11)-Volt(K,13))/36.5
2880 Dlpw(K)=P1w(K)-P2w(K)
2890 PRINT USING
"M4D.DD";Volt(K,1)Volt(K,2),Volt(K,3),Volt(K,4),Volt(K,5),Volt(K,6),Volt(K,7),Delp
(K)
2990 PRINT USING
"M4D.DD";Volt(K,8),Volt(K,9),Volt(K,10),Volt(K,11),Volt(K,12),Volt(K,13),Volt(K,1
4)
2910 NEXT K
2920 BEEP
2930 INPUT "DO YOU WANT HARD COPY PLOT (mW vs X)? 1=YES 0=NO",Ipl
2940 IF Ipl=1 THEN DISP "CHANGE PAPER ON PLOTTER AND HIT CONTINUE"
2950 IF Ipl=1 THEN PAUSE
2960 PEN 1
2970 GINIT
2980 IF Ipl<>1 THEN PLOTTER IS CRT,"INTERNAL"
2990 IF Ipl=1 THEN PLOTTER IS 705,"HPGL"
3000 GRAPHICS ON
3010 X_gdu_max=100*MAX(1,RATIO)
3020 Y_gdu_max=100*MAX(1,1/RATIO)
3030 LORG 6
3040 !FOR I=-.3 TO .3 STEP .1
3050 X_gdu_max/2,Y_gdu_max
3060 LABEL "Cocurrent RUN""",3D";Ru
3070 !NEXT I
3080 DEG
3090 LDIR 90
3100 CSIZE 3

```

```
3110 MOVE 0,Y_gdu_max/2
3120 LABEL "Power (mW)"
3130 LORG 4
3140 LDIR 0
3150 MOVE X_gdu_max/2,0.7*Y_gdu_max
3160 LABEL "Length of Core"
3170 VIEWPORT .1*X_gdu_max,.99*X_gdu_max,.15*Y_gdumax,.9*Y_gdu_max
3180 FRAME
3190 WINDOW 0.,100,0.,MAX(Power(*))
3200 AXES 5.0,.05,0,0,5,5,2
3210 CLIP OFF
3220 CSIZE 2.5,.5
3230 LORG 6
3240 FOR I=0 TO 100 STEP 10
3250 MOVE I,-.1
3260 LABEL USING "#,K";I
3270 NEXT I
3280 LORG 8
3290 FOR I=0 TO MAX(Power(*))
3300 MOVE -.2,I
3310 LABEL USING "#,D.5";I
3320 NEXT I
3330 PENUP
3340 FOR K=3 TO Nscan
3350 FOR L=1 TO 100
3360 PLOT L,ABS(Power(K,L))
3370 NEXT L
3380 PENUP
3390 WAIT .1
3400 NEXT K
3410 GRAPHICS OFF
3420 PEN 0
3430 BEEP
3440 INPUT "WANT HARD COPY PLOT (PRESSURE)? ANSWER 1=YES
0=NO",Ipl1
3450 IF Ipl1=1 THEN
3460 DISP "CHANGE PAPER ON PLOTTERT AND HIT CONTINUE"
3470 PAUSE
3480 END IF
3490 PEN 4
3400 GINIT
3510 IF Ipl1<>1 THEN PLOTTER IS CRT,"INTERNAL"
3520 IF Ipl1=1 THEN PLOTTER IS 705,"HPGL"
3530 GRAPHICS ON
3540 X_gdu_max=100*MAX(1,RATIO)
3550 Y_gdu_max=100*MAX(1,1/RATIO)
3560 LORG 6
3570 MOVE X_gdu_max/2,Y_gdu_max
3580 LABEL "Cocurrent RUN","",3D";Ru
3590 DEG
3600 LDIR 90
3610 CSIZE 3.5
3620 MOVE 0,Y_gdu_max/2
3630 LABEL "Pressure (psi)"
```

```
3640 LORG 4
3650 LDIR 0
3660 MOVE X_gdu_max/2,.07*Y_gdu_max
3670 LABEL "X-ducer Location in Core"
3680 VIEWPORT .1*X_gdu_max,.98*X_gdu_max,.15*Y_gdu_max,.9*Y_gdu_max
3690 FRAME
3700 WINDOW 1.,7,0.,MAX(Volt(*))
3710 AXES 1,0,5,0,0,1,5,5,2
3720 CLIP OFF
3730 CSIZE 2.5,.5
3740 LORG 6
3750 FOR I=1 TO 7
3760 MOVE I,-.1
3770 LABEL USING "#,K";I
3780 NEXT I
3790 LORG 8
3800 FOR I=0 TO MAX(Volt(*)) STEP 5
3810 MOVE -.1,I
3820 LABEL USING "#,DDD.DD";I
3830 NEXT I
3840 PENUP
3850 PEN 1
3860 FOR K=3 TO Nscan
3870 PLOT 1,Volt(K,1)
3880 PLOT 2,Volt(K,2)
3890 PLOT 4,Volt(K,4)
3900 PLOT 6,Volt(K,6)
3910 PLOT 7,Volt(K,7),2
3920 PENUP
3930 PEN 4
3940 WAIT 1
3950 PLOT 2,Volt(K,9)
3960 PLOT 4,Volt(K,11)
3970 PLOT 6,Volt(K,13),2
3980 WAIT .1
3990 PENUP
4000 NEXT K
4010 PEN 0
4020 GRAPHICS OFF
4030 BEEP
4040 INPUT "DO YOU WANT HARD COPY PLOT FOR dP? 1=Y 0=N ",Ip2
4050 IF Ip2=1 THEN DISP "CHANGE PAPER ON THE PLOTTER AND HIT
CONTINUE"
4060 IF Ip2=1 THEN PAUSE
4070 PEN 4
4080 GINIT
4090 IF Ip2<>1 THEN PLOTTER IS CRT,"INTERNAL"
4100 IF Ip2=1 THEN PLOTTER IS 705,"HPGL"
4110 GRAPHICS ON
4120 X_gdu_max=100*MAX(1,RATIO)
4130 Y_gdu_max=100*MAX(1,1/RATIO)
4140 LORG 6
4150 MOVE X_gdu_max/2,Y_gdu_max
4160 LABEL "DIFFERENTIAL PRESSURE = f(TIME)"
```

```
4170 DEG
4180 LDIR 90
4190 CSIZE 3.5
4200 MOVE 0,Y_gdu_max/2
4210 LABEL "Pressure (psi)"
4220 LORG 4
4230 LDIR 0
4240 MOVE X_gdu_max/2,.07*Y_gdu_max
4250 LABEL "Time (sec)"
4260 VIEWPORT .1*X_gdu_max,.98*X_gdu_max,.15*Y_gdu_max,.9*Y_gdu_max
4270 FRAME
4280 WINDOW 0.,MAX(T1(*)),0.,MAX(Volt(*))
4290 AXES 500.,5.0,0,0,5,5,2
4300CLIP OFF
4310 CSIZE 2.5,.5
4320 LORG 6
4330 FOR I=0 TO MAX(T1(*)) STEP 2000
4340 MOVE I,-.2
4350 LABEL USING "#,K";I
4360 NEXT I
4370 LORG 8
4380 FOR I=0 TO MAX(Volt(*)) STEP 10
4390 MOVE -.2,I
4400 LABEL USING "#,DDD.D";I
4410 NEXT I
4420 PENUP
4430 PEN 4
4440 FOR K=3 TO Nscan
4450 PLOT T1(K),Delp(K)
4460 NEXT K
4470 PEN 0
4480 GRAPHICS OFF
4490 DISPLAY "YOU ARE DONE WITH CURRENT FLOW EXPT. "
4500 GOTO 4550
4510 !***** Creating Storage Files *****
4520 Createfile: !
4530 CREAT BDAT Name$&Msus$,Size_records,No_records
4540 RETURN
4550 END
4560 SUB Zero_meter(@Meter)
4570 Rezero:OUTPUT @Meter;"Z1T"
4580 ENTER @Meter,Power
4590 IF ABS(Power)>2 THEN Rezero
4600 Unzero:OUTPUT @Meter;"3+AI"
4610 ENTER @Meter,Power
4620 IF Power>=84 THEN Unzero
4630 Preset:OUTPUT @Meter;"3A+I"
4640 SUBEND
4650 SUB Read_meter(@Meter,Power)
4660 ENTER @Meter,Power
4670 SUBEND
```

### A.3: Data Acquisition and Storage for Countercurrent Flow

```

10 !*****          COUNTERCURRENT.EX          *****
20 !*   PROGRAM FOR DATA AQUISITION & STORAGE FOR           *
30 !*   COUNTERCURRENT FLOW EXPERIMENTS                     *
40 !*                                                         *
50 !*                                                         *
60 !*****
70 !*****DIMENSIONALISINGOFVARIABLES*****
80 OPTION BASE 1
90  INTEGER I,J,K,N,M,L
100  INTEGER Ii,Ik,Jj,Kk
110  DIM A$(50)[17]
120  DIM Ao$(50,100)[17]
130  DIM Volt(50,14),P(50)
140  DIM V(14),Delp(50),P1(50),P2(50),Dlpw(50),P1w(50),P2w(50)
150  DIM T1(50),Tp(50),Tm(50)
160  DIM T2(50)
170  DIM Power(50,100),T7(50),Powin(50,100)
180  DIM T3(50),Pk1(50),Pk2(50),Delpk(50)
190
200!*****PUTTINGAPPROPRIATEFLAGS*****
210  PRINTER IS 1
220  PRINT "Today is :",DATE$(TIMEDATE)
230  PRINT "Program Started @",TIME$(TIMEDATE)
240!*****ASSIGNMENTSOFPERIPHERALS*****
250  ASSIGN @Multi TO 723
260  ASSIGN @Meter TO 713
270  Sc=9
280  CONTROL Sc,4;2+0+8+0
290  CONTROL Sc,5;3
300  CONTROL Sc,3;300
310!*****ALLOCATEBYTESFORSTORAGE*****
320  Msus$=":CS80,700,0"
330  Pwr=101*8
340  Pr=15*8
350!*****ZEROINGOFPOWERMETER*****
360  PRINT "PRESS SWITCH 1 IN POWER SUPPLY. TURN ON FAN. DO NOT
TRUN ON SWITCH 2"
370  OUTPUT @Multi USING "#,K";"O040TG17TO260T"
380  REMOTE @Meter
390  CALL Zero_meter(@Meter)
400  BEEP
410  DISP "COMPLETE MICROWAVE POWER SUPPLY AFTER STABLE ZERO,
HIT CONTINUE"
420  PAUSE
430!*****ALLOCATEFILENAMESFORPOWER&PRESSUREDATA*****
440  INPUT "COUNTERCURRENT FLOWW RUN No.?",Run$
450  Ru=VAL(Run$)

```

```

460 INPUT "FILENAME TO STORE MICROWAVE OUTPUT POWER DATA
.(R#O)?",Name$
470 INPUT "DRIVE (ie :,700,1) default current drive?",Msus$
480 Size_records=Pwr
490 No_records=50
500 ON ERROR GOSUB Createfile
510 ASSIGN @File3 TO Name$&Msus$
520 OFF ERROR
530 INPUT "FILENAME TO STORE MICROWAVE INPUT POWER DATA
.(R#I)?",Name$
540 INPUT "DRIVE (ie :,700,1) default current drive?",Msus$
550 No_records=Pwr
560 Size_records=50
570 ON ERROR GOSUB Createfile
580 ASSIGN @File10 TO Name$&Msus$
590 OFF ERROR
600 INPUT "FILENAME TO STORE EXPT. PRESSURE DATA ..(R#P)?",Name$
610 INPUT "DRIVE (ie :,700,1) default current drive?",Msus$
620 No_records=Pr
630 Size_records=50
640 ON ERROR GOSUB Createfile
650 ASSIGN @File4 TO Name$&Msus$
660 OFF ERROR
670 OUTPUT @Multi USING "#,K";"0040TG17TO260T"
680 FOR H=1 TO 14
690   OUTPUT @Multi USING "#,K";"FT"
700   ENTER @Multi;V(H)
710   V(H)=V(H)-10000
720   Octal$=VAL$(V(H))
730   V(H)=DVAL(Octal$,8)
740   IF V(H)>2047 THEN V(H)=V(H)-4096
750   V(H)=.005*V(H)
760 NEXT H
770 PRINT V(*)
780 INPUT "FILENAME FOR DATE AND TIME ..(R#D)?",Name$
790 INPUT "DRIVE (ie :,700,1) default current drive?",Msus$
800 No_records=160
810 Size_records=1
820 ON ERROR GOSUB Createfile
830 ASSIGN @File5 TO Name$&Msus$
840 OFF ERROR
850 PRINTER IS 1
860 Day$=DATE$(TIMEDATE)
870 Tim$=TIME$(TIMEDATE)
880 Tst1=TIMEDATE
890 BEEP 81.38,10
900 INPUT "TOTAL VOLUME OF OIL TO BE PUMPED (IN CC)?",To
910 INPUT "TOTAL VOLUME OF WATER TO BE PUMPED (IN CC)?",Tw
920 INPUT "PUMP RATE OF OIL IN CC/HR?",Ro
930 INPUT "PUMP RATE OF WATER IN CC/HR?",Rw
940 Ot=To/Ro
950 Wt=Tw/Rw
960 IF Ot<=Wt THEN GOTO 990
970 Et=Wt*3600.0

```

```

980 GOTO 1000
990 Et=Ot*3600.0
1000 INPUT "No. OF SATURATION PROFILES ?",Nsat
1010 Nscan=Nsat+2
1020 Insat=(Et-((Nsat-1)*10.81))/(Nsat-1)
1030 Inprs=Insat
1040 PRINT "SATURATION INTERVAL (seconds)",Insat
1050 PRINT "PRESSURE INETRVAL AFTER SCANNING PERIOD",Inprs
1060 BEEP
1070 DISP "CHECK PUMP CONNECTIONS, WHEN YOU ARE READY HIT
CONTINUE"
1080 PAUSE
1090 Tst=TIMEDATE
1100 FOR J=3 TO Nscan
1110 OUTPUT @Multi USING "#,K";"0040TG17TO260T"
1120 T1(J)=TIMEDATE-Tst
1130!*****PRESSUREDATA*****
1140 FOR N=1 TO 14
1150 OUTPUT @Multi USING "#,K";"FT"
1160 ENTER @Multi;Volt(J,N)
1170 Volt(J,N)=Volt(J,N)-10000
1180 Octal$=VAL$(Volt(J,N))
1190 Volt(J,N)=DVAL(Octal$,8)
1200 IF Volt(J,N)>2047 THEN Volt(J,N)=Volt(J,N)-4096
1210 Volt(J,N)=.005*Volt(J,N)
1220 NEXT N
1230!***** MICROWAVESCAN *****
1240 T2(J)=TIMEDATE-Tst
1250 OUTPUT @Multi;"00140T@7775T"
1260 WAIT .01
1270 OUTPUT @Multi;"00140T@7777T"
1280 T8=TIMEDATE
1290 FOR I=1 TO 100
1300 Time1=TIMEDATE
1310 OUTPUT @Multi USING "#,K";"00240TKT"
1320 OUTPUT @Multi USING "#,K";"JT"
1330 ENTER @Multi;Ao$(J,I)
1340 OUTPUT @Meter;"3A+I"
1350 CALL Read_meter(@Meter,Power(J,I))
1360 DISP I,Power(J,I),Ao$(J,I)
1370 Time2=TIMEDATE
1380 Time3=.10-(Time2-Time1)
1390 WAIT Time3
1400 NEXT I
1410 T9=TIMEDATE-T8
1420 OUTPUT @Multi;"00140T@7776T"
1430 WAIT .0
1440 OUTPUT @Multi;"00140T@7777T"
1450 DISP J,T9
1460 IF J=Nscan THEN GOTO 1500
1470 WAIT Insat
1480 NEXT J
1490!*****
1500 DISP "NOW DATA STORAGE BEGINS"

```

```
1510 !***** CONVERSION OF THE mW DATA *****
1520 FOR J=3 TO Nscan
1530   FOR I=1 TO 100
1540     FOR Ik=1 TO 15
1550       P(Ik)=0
1560     NEXT Ik
1570   FOR K=1 TO 5
1580     C=VAL(Ao$(J,I)[K,K])
1590     IF C=0 THEN
1600       H1=0
1610       H2=0
1620       H3=0
1630     END IF
1640     IF C=1 THEN
1650       H1=0
1660       H2=0
1670       H3=1
1680     END IF
1690     IF C=2 THEN
1700       H1=0
1710       H2=1
1720       H3=0
1730     END IF
1740     IF C=3 THEN
1750       H1=0
1760       H2=1
1770       H3=1
1780     END IF
1790     IF C=4 THEN
1800       H1=1
1810       H2=0
1820       H3=0
1830     END IF
1840     IF C=5 THEN
1850       H1=1
1860       H2=0
1870       H3=1
1880     END IF
1890     IF C=6 THEN
1900       H1=1
1910       H2=1
1920       H3=0
1930     END IF
1940     IF C=7 THEN
1950       H1=1
1960       H2=1
1970       H3=1
1980     END IF
1990     IF K=1 THEN
2000       P(1)=H1
2010       P(2)=H2
2020       P(3)=H3
2030     END IF
2040     IF K=2 THEN
```



```

2050     P(4)=H1
2060     P(5)=H2
2070     P(6)=H3
2080     END IF
2090     IF K=3 THEN
2100         P(7)=H1
2110         P(8)=H2
2120         P(9)=H3
2130     END IF
2140     IF K=4 THEN
2150         P(10)=H1
2160         P(11)=H2
2170         P(12)=H3
2180     END IF
2190     IF K=5 THEN
2200         P(13)=H1
2210         P(14)=H2
2220         P(15)=H3
2230     END IF
2240     NEXT K
2250     Xa=0
2260     Ya=0
2270     Za=0
2280     Ra=0
2290     FOR K=3 TO 1 STEP -1
2300         Xa=Xa+P(K)*2^(3-K)
2310     NEXT K
2320     FOR K=7 TO 4 STEP -1
2330         Ya=Ya+P(K)*2^(7-K)
2340     NEXT K
2350     FOR K=11 TO 8 STEP -1
2360         Za=Za+P(K)*2^(11-K)
2370     NEXT K
2380     FOR K=15 TO 12 STEP -1
2390         Ra=Ra+P(K)*2^(15-K)
2400     NEXT K
2410     Tot=(Xa*1000+Ya*100+Za*10+Ra)/100
2420     IF Tot>12.0 THEN Tot=Tot-10.0
2430     Powin(J,I)=Tot
2440     Power(J,I)=ABS(Power(J,I))*1000.0
2450     NEXT I
2460     DISP J
2470     NEXT J
2480     OUTPUT @File3;T2(*),Power(*)
2490     OUTPUT @File10;T2(*),Powin(*)
2500     OUTPUT @File5;Day$,Tim$,Run$
2510     FOR J=3 TO Nscan
2520     !***** Conversion To Pressure from Volt *****
2530     Volt(J,1)=(Volt(J,1)-V(1))*7.5
2540     Volt(J,2)=(Volt(J,2)-V(2))*7.5
2550     Volt(J,3)=(Volt(J,3)-V(3))*5
2560     Volt(J,4)=(Volt(J,4)-V(4))*3.0
2570     Volt(J,5)=(Volt(J,5)-V(5))*5
2580     Volt(J,6)=(Volt(J,6)-V(6))*3.0

```

```

2590 Volt(J,7)=(Volt(J,7)-V(7))
2600 Volt(J,8)=(Volt(J,8)-V(8))* .5
2610 Volt(J,9)=(Volt(J,9)-V(9))*7.5
2620 Volt(J,10)=(Volt(J,10)-V(10))* .5
2630 Volt(J,11)=(Volt(J,11)-V(11))*3.0
2640 Volt(J,12)=(Volt(J,12)-V(12))* .5
2650 Volt(J,13)=(Volt(J,13)-V(13))
2660 Volt(J,14)=(Volt(J,14)-V(14))* .5
2670 NEXT J
2680 WAIT .1
2690 OUTPUT @File4;T1(*),Volt(*)
2700 IF Ipr=1 THEN PRINT CHR$(12)
2710 PRINT USING ""COUNTERCURRENT EXPERIMENT NUMBER
: "" ,DDD";Ru
2720 PRINT "DATE OF EXPERIMENT   : ",Day$
2730 PRINT "SUMMARY OF PRESSURE DISTRIBUTION DURING THE RUN"
2740 PRINT "NOTE: Last column indicates dP(psi) across the core"
2750 PRINT "-----"
2760 PRINT " "
2770 FOR K=3 TO Nscan
2780 P1(K)=Volt(K,1)+2.0*(Volt(K,1)-Volt(K,2))/11.0
2790 P2(K)=Volt(K,7)-2.0*(Volt(K,6)-Volt(K,7))/11.0
2800 Delp(K)=P1(K)-P2(K)
2810 P2w(K)=Volt(K,9)-13*(Volt(K,11)-Volt(K,9))/36.5
2820 P1w(K)=Volt(K,13)+13*(Volt(K,13)-Volt(K,11))/36.5
2830 Dlpw(K)=P1w(K)-P2w(K)
2840 PRINT USING
"M4D.DD";Volt(K,1),Volt(K,2),Volt(K,3),Volt(K,4),Volt(K,5),Volt(K,6),Volt(K,7),Delp
p(K)
2850 PRINT USING
"M4D.DD";Volt(K,8),Volt(K,9),Volt(K,10),Volt(K,11),Volt(K,12),Volt(K,13),Volt(K,1
4)
2860 NEXT K
2870 BEEP
2880 INPUT "DO YOU WANT HARD COPY PLOT (mW vs X )? 1=YES 0=NO",Ipl
2890 IF Ipl=1 THEN DISP "CHANGE PAPER ON PLOTTER AND HIT CONTINUE"
2900 IF Ipl=1 THEN PAUSE
2910 PEN 1
2920 GINIT
2930 IF Ipl<>1 THEN PLOTTER IS CRT,"INTERNAL"
2940 IF Ipl=1 THEN PLOTTER IS 705,"HPGL"
2950 GRAPHICS ON
2960 X_gdu_max=100*MAX(1,RATIO)
2970 Y_gdu_max=100*MAX(1,1/RATIO)
2980 LOG 6
2990 !FOR I=-.3 TO .3 STEP .1
3000 MOVE X_gdu_max/2,Y_gdu_max
3010 LABEL USING ""mW vs X as Function of t,Countercurrent RUN"" ,3D";Ru
3020 !NEXT I
3030 DEG
3040 LDIR 90
3050 CSIZE 3
3060 MOVE 0,Y_gdu_max/2
3070 LABEL "Power (mW)"

```

```

3080 LORG 4
3090 LDIR 0
3100 MOVE X_gdu_max/2,.07*_gdu_max
3110 LABEL "Length of Core"
3120 VIEWPORT .1*X_gdu_max,.99*X_gdu_max,.15*Y_gdu_max,.9*Y_gdu_max
3130 FRAME
3140 WINDOW 0.,100,0.,MAX(Power(*))
3150 AXES 5.0,.05,0,0,5,5,2
3160 CLIP OFF
3170 CSIZE 2.5,.5
3180 LORG 6
3190 FOR I=0 TO 100 STEP 10
3200 MOVE I -.1
3210 LABEL USING "#,K";I
3220 NEXT I
3230 LORG 8
3240 FOR I=0 TO MAX(Power(*))
3250 MOVE -.2,I
3260 LABEL USING "#,D.5D";I
3270 NEXT I
3280 PENUP
3290 FOR K=3 TO Nscan
3300 FOR L=1 TO 100
3310 PLOT L,ABS(Power(K,L))
3320 NEXT L
3330 PENUP
3340 WAIT .1
3350 NEXT K
3360 GRAPHICS OFF
3370 PEN 0
3380 BEEP
3390 INPUT "WANT HARD COPY PLOT (PRESSURE)? ANSWER 1=YES
0=NO",Ipl1
3400 IF Ipl1=1 THEN
3410 DISP "CHANGE PAPER ON PLOTTER AND HIT CONTINUE"
3420 PAUSE
3430 END IF
3440 PEN 4
3450 GINIT
3460 IF Ipl1<>1 THEN PLOTTER IS CRT,"INTERNAL"
3470 IF Ipl1=1 THEN PLOTTER IS 705,"HPGL"
3480 GRAPHICS ON
3490 X_gdu_max=100*MAX(1,RATIO)
3500 Y_gdu_max=100*MAX(1,1/RATIO)
3510 LORG 6
3520 MOVE X_gdu_max/2,Y_gdu_max
3530 LABEL USING """"Pressure Distribution Along X, Countercurrent RUN""",3D";Ru
3540 DEG
3550 LDIR 90
3560 CSIZE 3.5
3570 max/2
3580 LABEL "Pressure (psi)"
3590 LORG 4
3600 LDIR 0

```

```

3610 MOVE X_gdu_max/2,.07*Y_gdu_max
3620 LABEL "X-ducer Location in Core"
3630 VIEWPORT .1*X_gdu_max,.98*X_gdu_max,.9*Y_gdu_max
3640 FRAME
3650 WINDOW 1.,7,0.,MAX(Volt(*))
3660 AXES 1.0,5.0,0,1,5,5,2
3670 CLIP OFF
3680 CSIZE 2.5,.5
3690 LORG 6
3700 !FOR I=1 TO 7
3710 MOVE I,-.1
3720 LABEL USING "#,K";I
3730 !NEXT I
3740 LORG 8
3750 FOR I=0 TO MAX(Volt(*)) STEP 5
3760 MOVE -.1,I
3770 LABEL USING "#,DDD.DD";I
3780 NEXT I
3790 PENUP
3800 PEN 1
3810 FOR K=3 TO Nscan
3820 PLOT 1,Volt(K,1)
3830 PLOT 2,Volt(K,2)
3840 PLOT 4,Volt(K,4)
3850 PLOT 6,Volt(K,6)
3860 PLOT 7,Volt(K,7),2
3870 PENUP
3880 PEN 4
3890 WAIT 1
3900 PLOT 2,Volt(K,9)
3910 PLOT 4,Volt(K,11)
3920 PLOT 6,Volt(K,13),2
3930 WAIT .1
3940 PENUP
3950 NEXT K
3960 PEN 0
3970 GRAPHICS OFF
3980 BEEP
3990 INPUT "DO YOU WANT HARD COPY PLOT FOR dP? 1=Y 0=N ",Ip2
4000 IF Ip2=1 THEN DISP "CHANGE PAPER ON THE PLOTTER AND HIT
CONTINUE"
4010 IF Ip2=1 THEN PAUSE
4020 PEN 4
4030 GINIT
4040 IF Ip2<>1 THEN PLOTTER IS CRT,"INTERNAL."
4050 IF Ip2=1 THEN PLOTTER IS 705,"HPGL"
4060 GRAPHICS ON
4070 X_max=100*MAX(1,RATIO)
4080 Ymax=100*MAX(1,1/RATIO)
4090 LORG 6
4100 MOVE X_gdu_max/2,Y_gdu_max
4110 LABEL "DIFFERENTIAL PRESSURE = f(TIME)"
4120 DEG
4130 LDIR 90

```

```

4140 CSIZE 3.5
4150 MOVE 0,Y_gdu_max/2
4160 LABEL "Pressure (psi)"
4170 LORG 4
4180 LDIR 0
4190 MOVE X_gdu_n:ax/2,.07*Y_gdu_max
4200 LABEL "Time (sec)"
4210 VIEWPOINT .1*X_gdu_max,.98*X_gdu_max,.15*Y_gdu_max,.9*Y_gdu_max
4220 FRAME
4230 WINDOW 0.,MAX(T1(*)),0.,MAX(Volt(*))
4240 AXES 500.,5.0,0,0,5,5,2
4250 CLIP OFF
4260 CSIZE 2.5,.5
4270 LORG 6
4280 FOR I=0 TO MAX(T1(*)) STEP 2000
4290  MOVE I,-.2
4300  LABEL USING "#,K";I
4310  NEXT I
4320  LORG 8
4330  FOR I=0 TO MAX(Volt(*)) STEP 10
4340  MOVE -.2,I
4350  LABEL USING "#,DDD.D";I
4360  NEXT I
4370  PENUP
4380  PEN 4
4390  FOR K=3 TO Nscan
4400  PLOT T1(K),Delp(K)
4410  NEXT K
4420  PEN 0
4430  GRAPHICS OFF
4440  DISP "YOU ARE DONE WITH THE COUNTERCURRENT FLOW EXPT. "
4450  GOTO 4500
4460  !*****          Creating Storage Files          *****
4470  Createfile:~
4480  CREAT BDAT Name$&Msus$,Size_recrds,No_records
4490  RETURN
4500  END
4510  SUB Zero_meter(@Meter)
4520  Rezero:OUTPUT @Meter;"Z1T"
4530  ENTER @Meter;Power
4540  IF ABS(Power)>2 THEN Rezero
4550  Unzero:OUTPUT @Meter;"3+AI"
4560  ENTER @Meter;Power
4570  IF Power>=84 THEN Unzero
4580  Preset:OUTPUT @Meter;"3A+I"
4590  SUBEND
4600  SUB Read_meter(@Meter,Power)
4610  ENTER @Meter;Power
4620  SUBEND

```

#### A.4: Data Retrieval and Interpretation for Cocurrent Flow Experiments

```

10 ! *****
20 !*
30 !* PROGRAM FOR DATA RETRIEVAL AND ANALYSIS FOR COCURRENT
40 !* FLOW EXPERIMENT.
50 !* DATA FILES ARE RETIEVAL BY CALLING THEIR APPRPRIATE NAMES
50 !* THE PROGRAM IS INTERACTIVE.
60 !* SOME ANALYSES ARE OPTIONAL, AND CAN BE BY-PASSED.
70 !*
80 !*
90 !*
100 !*****      DIMENSIONALISING OF VARIABLES      *****
110 OPTION BASE 1
120 INTEGER I,J,K,N,H,M,L
130 INTEGER Nsat,Nscan,Npoint,Nend,Ipoint,Nbegin,Nhalf
140 DIM Sw(50,100),Aaw(50,100),C(100),B(100)
150 DIM A$(50)|17|
160 DIM Volt(50,14),Akw(50),Ako(50)
170 DIM Perm(50),Permw(50)
180 DIM V(14),Delp(50),P1(50),P2(50),Dlpw(50),P1w(50),P2w(50)
190 DIM T1(50),T2(50),Tp(50),Tm(50),Powin(50,100)
200 DIM Power(50,100),T7(10)
210 DIM T3(50),Pko(50,14),Pk1(50),Pk2(50),Delpk(50),Perm1(50),Perm2(50)
220 INPUT "No. OF SATURATION PROFILES ?",Nsat
230 Nscan=Nsat+2
240 INPUT "IRREDUCIBLE (INITIAL) WATER SATURATION Swi (fraction)?",Swi
250 INPUT "DO YOU WANT HARD COPY PRINTOUT ? ... 1=YES;0=NO",Ipr
260 INPUT "DO YOU WANT HARD COPY PLOT ? ... 1=YES;0=NO",Ipl
270 IF Ipr=1 THEN OUTPUT 701;CHR$(27)&"&11L"
280 !*****RETRIEVINGDATAFROMTHEFILES*****
290 !*
300 INPUT "FILENAME FOR OP POWER @ Sw=1 (OP#S1)",Name$
310 ASSIGN @File11 TO Name$
320 INPUT "FILENAME FOR OP POWER @ Swi (OP#S2)",Name$
330 ASSIGN @File1 TO Name$
340 INPUT "FILENAME FOR IP POWER @ Sw=1 (IP#S1)",Name$
350 ASSIGN @File12 TO Name$
360 INPUT "FILENAME FOR IP POWER @ Swi (IP#S2)",Name$
370 ASSIGN @File2 TO Name$
380 INPUT "FILENAME FOR DATE AND TIME EXPT. STARTED (R#D)",Name$
390 ASSIGN @File5 TO Name$
400 INPUT "FILENAME FOR INPUT MICROWAVE POWER DATA (R#I)",Name$
410 ASSIGN @File10 TO Name$
420 INPUT "ENTER FILENAME OUTPUT POWER METER DATA (R#O)",Name$
430 ASSIGN @File3 TO Name$
440 INPUT "ENTER FILENAME FOR PRESSURE DATA (R#P)",Name$
450 ASSIGN @File4 TO Name$
460 ENTER @File11;Power(*)

```

```

470 ENTER @File1;Power(*)
480 ENTER @File12;Powin(*)
490 ENTER @File2;Powin(*)
500 ENTER @File10;T2(*),Powin(*)
510 ENTER @File7;Tb(*),Wgt(*)
520 ENTER @File3;T2(*),Power(*)
530 ENTER @File4;T1(*),Volt(*)
540 ENTER @File5;Day$,Tim$,Run$
550 Ru=VAL(Run$)
560 Ttime=T1(60)
570 PRINTER IS 1
580 INPUT "OIL FLOWRATE in CC/HR? ",Ro
590 INPUT "WATER FLOWRATE in CC/HR? ",Rw
600 INPUT "TOTAL VOLUME OF OIL PUMPED CC? ",Ov
610 INPUT "TOTAL VOLUME OF WATER PUMPED CC? ",Wv
620 To=Ov/Ro*3600
630 Tw=Wv/Rw*3600
640 IF To>Tw THEN GOTO 670
650 Sati=To/Nsat
660 GOTO 680
670 Sati=Tw/Nsat
680 INPUT "DENSITY OF WATER? ",Rhow
690 INPUT " OIL USED? 1=LAGO,2=MCT5,3=MCT5LAGO,4=MCT10",Ioil
700 IF Ioil=1 THEN
710   Rhoo=.7963
720   Ac=16342.0
730   Visl=4.7
740 END IF
750 IF Ioil=2 THEN
760   Rhoo=.8123
770   Ac=13566.0
780   Visl=30.48
790 END IF
800 IF Ioil=3 THEN
810   Rhoo=.8043
820   Ac=14185.0
830   Visl=11.1
840 END IF
850 IF Ioil=4 THEN
860   Rhoo=.8576
870   Ac=13573.0
880   Visl=60.0
890 END IF
900 Bulkvol=625.0
910 INPUT "ENTER PORE VOLUME OF THE SANDPACK IN CC? ",Pv
920 Por=Pv/Bulkvol
930 ! EXTRAPOLATE INTERNAL PRESSURES TO THE OUTLET ENDS OF THE
COREHOLDER"
940 FOR K=3 TO Nscan
950   P1(K)=Volt(K,1)+2.0*(Volt(K,1)-Volt(K,2))/11.0)
960   P2(K)=(Volt(K,7)-2.0*(Volt(K,6)-Volt(K,7))/11.0)
970   Delp(K)=(P1(K)-P2(K))
980   P1w(K)=(Volt(K,9)-13*(Volt(K,11)-Volt(K,9))/36.5)
990   P2w(K)=(Volt(K,13)-13*(Volt(K,11)-Volt(K,13))/36.5)

```

```

1000  D1pw(K)=(P1w(K)-P2w(K))
1010  NEXT K
1020  A1=1000  ! LENGTH OF THE CORE IN CC
1030  A=6.215  ! CROSS SECTIONAL AREA OF SANDPACK CM**2
1040  Porvol=A1*A*Por
1050  Ros=Ro/3600.0
1060  Rws=Rw/3600.0
1070  IF Ipr=1 THEN PRINTER IS 701
1080  INPUT "ENTER VISCOSITY OF WATER IN CP",Vis
1090  IF Ipr=0 THEN GOTO 1130
1100  DISP "SET PRINTER TO A NEW PAGE i.e. PRESS FF AND THEN HIT
CONTINUE"
1110  PAUSE
1120  IF Ipr=1 THEN PRINTER IS 701
1130  PRINT USING """"EXPERIMENTAL COCURRENT RUN No. """,3A";Run$
1140  PRINT "DATE OF EXPERIMENT  ",Day$
1150  PRINT "TIME EXPT. STARTED  ",Tim$
1160  PRINT "-----"
1170  PRINT " "
1180  PRINT USING """"VISCOSITY OF OIL, CP  """,3D.DD";Vis1
1190  PRINT USING """"VISCOSITY OF WATER, CP  """,3D.DD";Vis
1200  PRINT USING """"DENSITY OF OIL, GM/CC  """,D.4D";Rho0
1210  PRINT USING """"VOLUMETRIC OIL FLOWRATE, CC/SEC  """,D.5D";Ros
1220  PRINT USING """"VOLUMETRIC WATER FLOWRATE, CC/SEC
""",D.5D";Rws
1230  PRINT USING """"LENGTH OF COREHOLDER, CM  """,3D.D";A1
1240  PRINT USING """"RECTANGULAR AREA OF PACK, CM**2  """,3D.DD";A
1250  PRINT USING """"POROSITY  """,D.3D";Por
1260  PRINT USING """"Swi  """,D.3D";Swi
1270  PRINT USING """"OIL FLOWRATE (cc/hr)  """,4D.D";Ros*3600.0
1280  PRINT USING """"WATER FLOWRATE (cc/hr)  """,4D.D";Rws*3600.0
1290  PRINTER IS 1
1300  !
1310  !* FINDING THE MICROWAVE EQUATION'S CONSTANTS (B & C )
1320  FOR I=1 TO 100
1330  B(I)=1./(1.-Swi)*((LOG(ABS(Power(1,I)/Powin(1,I)))-
(LOG(ABS(Power(2,I)/Powin(2,I))))))
1340  C(I)=(LOG(ABS(Power(1,I)/Powin(1,I)))-B(I))
1350  NEXT I
1360  !*
1370  !* CALCULATING WATER SATURAION (Sw )
1380  !*
1390  FOR J=1 TO Nscan
1400  FOR I=1 TO 100
1410  Sw(J,I)=((LOG(ABS(Power(J,I)/Powin(J,I)))-C(I))/B(I))
1420  PRINT J,I,Sw(J,I)
1430  NEXT I
1440  DISP J
1450  NEXT J
1460  PRINTER IS 1
1470  INPUT "WANT INTEGRATION OF SATURATION DATA, 1=YES 0=NO
?",Idsat
1480  IF Idsat=0 THEN GOTO 1920
1490  PRINT "INTEGRATION OF DIMENSIONLESS SATURATION ALONG

```



```

LENGTH "
1500 PRINT "-----"
1510 PRINT "FOR MAXIMUM ACCURACY BOTH SIMPSON 1/3 AND 3/8
RULES ARE APPLIED."
1520 PRINT "COMBINATION OF BOTH RULES ARE REQUIRED IN CASE OF ODD
NUMBER OF INTERVALS."
1530 PRINT "IN CASE OF EVEN NUMBER, 1/3 RULE IS MORE ACCURATE,
WHILE IN CASE OF"
1540 PRINT "ODD INTERVALS, 3/8 RULE IS APPLIED FOR FIRST 3 PANELS
AND 1/3 RULE"
1550 PRINT "FOR THE REST."
1560 !INCREMENT IN DIMENSIONLESS DISTANCE
1570 REAL Hx,Sss(60)
1580 Hx=1
1590 INPUT "ENTER NUMBER OF DATA POINTS i.e. NPOINT",Npoint
1600 Xd=Hx*Npoint
1610 PRINT " "
1620 PRINT " "
1630 PRINT "EXPERIMENTAL COCURRENT RUN NUMBER",Run$
1640 PRINT "DATE OF EXPERIMENT   ",Day$
1650 PRINT "TIME EXPT STARTED   ",Tim$
1660 Ipoint=Npoint-1
1670 Nhalf=Ipoint/2
1680 FOR K=3 TO Nscan
1690 !THE FIRST POINT IS THE POINT @ WHICH COCURRENT STARTED (3rd
SCAN)
1700 Nbegin=3
1710 Ssw=0.
1720 IF (Ipoint-(2*Nhalf))=0 THEN GOTO 1890
1730 !IF No. OF PANELS ODD, USE 3/8 RULE ON FIRST 3 PANELS,
1740 1/3 RULE ON REST OF THEM
1750 Ssw=3.*Hx/8.*(Sw(K,3)+3.0*Sw(K,4)+3.*Sw(K,5)+Sw(K,6))
1760 !THE 4th pt IS ACTUALLY THE 6th pt IN THE SCAN (4+2=6)
1770 Nbegin=6
1780 !NOW APPLY 1/3 RULE - ADD 1st, 2nd AND LAST VALUES
1790 Ssw=Ssw+Hx/3.*(Sw(K,Nbegin)+4.0*Sw(K,Nbegin+1)+Sw(K,Npoint))
1800 Nbegin=Nbegin+2
1810 IF Nbegin=Npoint THEN GOTO 1970
1820 !PATTERN AFTER (Nbegin+2) IS REPETITIVE TILL NEND
1830 Nend=Npoint-2
1840 FOR J=Nbegin TO Nend STEP 2
1850 Ssw=Ssw+Hx/3.0*(2.*Sw(K,J)+4.0*Sw(K,J+1))
1860 NEXT J
1870 PRINT USING "5D.DD,5X,MDD.DDDE";T2(K),Ssw
1880 !CONSIDERING LAST PT OF Sw AS THAT @ THE LAST SCAN @ THE
MIDDLE OF CORE
1890 T2(K)=Rws*T2(K)/(A*A1*Por*(Sw(Nscan,50)))
1900 Sss(K)=Ssw/100.0
1910 NEXT K
1920 PRINTER IS 1
1930 INPUT "WANT TO SMOOTHEN PRESSURE DATA, 1=Y 0=N?",Ipd
1940 IF Ipd=0 THEN GOTO 3610
1950 PRINT "SMOOTHENING OF PRESSURE DATA ALONG DIMENSIONLESS
LENGTH"

```

```

1960 PRINT "-----"
1970 PRINT " "
1980 PRINT " "
1990 REAL X(11),Psi(60,11)
2000 FOR I=3 TO Nscan
2010   Psi(I,1)=P1(I)
2020   Psi(I,2)=Volt(I,1)
2030   Psi(I,3)=Volt(I,2)
2040   Psi(I,4)=Volt(I,4)
2050   Psi(I,5)=Volt(I,6)
2060   Psi(I,6)=Volt(I,7)
2070   Psi(I,7)=P2(I)
2080 NEXT I
2090 GOTO 2170
2100 Psi(Nscan,1)=P1(Scan)
2110 Psi(Nscan,2)=Volt(Nscan,1)
2120 Psi(Nscan,3)=Volt(Nscan,2)
2130 Psi(Nscan,4)=Volt(Nscan,4)
2140 Psi(Nscan,5)=Volt(Nscan,6)
2150 Psi(Nscan,6)=Volt(Nscan,7)
2160 Psi(Nscan,7)=P2(Nscan)
2170 X(1)=0.
2180 X(2)=.0102
2190 X(3)=.12245
2200 X(4)=.50
2210 X(5)=.87755
2220 X(6)=.98979
2230 X(7)=1.0
2240 Np=7
2250 !THIS PART SMOOTHENS PRESSURE DATA WHICH ARE NOT
EQUISPACED i.e. VARIABLE H"
2260 NP=NO. OF DATA PAIRS
2270 MS, MF = RANGE OF DEGREE OF POLYNOMIALS, MAXM DEGREE:=9
2280 AA=AUGMENTED ARRAY OF COEFFICIENT OF NORMAL EQNS
2290 CC=ARRAY OF COEFFS OF LEAST SQUARE POLYNOMIAL
2300 REAL Aa(8,9),Cc(10),Xn(11)
2310 INTEGER Mf,Ms,Mfp1,Mfp2,Msp1,Kk,Ii,J1,Imt,Jm1,Im1,Ipt
2320 INTEGER Icoef,Jcoef,Ia,Ic,Iaa
2330 INPUT "SMALLEST DEGREE OF POLYNOMIAL",Ms
2340 INPUT "GREATEST DEGREE OF POLYNOMIAL",Mf
2350 IF Mf<=(Np-1) THEN GOTO 2380
2360 Mf=Np-1
2370 PRINT "DEGREE OF POLYNOMIAL TOO LARGE. REDUCED TO ",Mf
2380 Mfp1=Mf+1
2390 Mfp2=Mf+2
2400 Kk=1
2410 IF Kk>6 THEN GOTO 3510
2420 FOR Ia=1 TO Mfp1
2430   FOR Iaa=1 TO Mfp2
2440     Aa(Ia,Iaa)=0.
2450   NEXT Iaa
2460 NEXT Ia
2470 PRINT USING """"SCAN""",2D";Kk
2480 FOR I=1 TO Np

```

```

2490 Xn(I)=1.0
2500 NEXT I
2510 FOR J=1 TO Mfp1
2520 Aa(J,1)=0.
2530 Aa(J,Mfp2)=0.
2540 FOR N=1 TO Np
2550 Aa(J,1)=Aa(J,1)+Xn(N)
2560 Aa(J,Mfp2)=Aa(J,Mfp2)+Psi(Kk,N)*Xn(N)
2570 Xn(N)=Xn(N)*X(N)
2580 NEXT N
2590 NEXT J
2600 FOR I=2 TO Mfp1
2610 Aa(Mfp1,I)=0.
2620 FOR J=1 TO Np
2630 Aa(Mfp1,I)=Aa(Mfp1,I)+Xn(J)
2640 Xn(J)=Xn(J)*X(J)
2650 NEXT J
2660 NEXT I
2670 FOR J=2 TO Mfp1
2680 FOR I=1 TO Mf
2690 Aa(I,J)=Aa(I+1,J-1)
2700 NEXT I
2710 NEXT J
2720 PRINT "THE MATRIX OF NORMAL EQUATIONS"
2730 PRINT "-----"
2740 PRINT " "
2750 PRINT " "
2760 FOR J1=1 TO Mfp1
2770 PRINT USING
"S5D.4D";Aa(J1,1),Aa(J1,2),Aa(J1,3),Aa(J1,4),Aa(J1,5),Aa(J1,6),Aa(J1,7),Aa(J1,8),A
a(J1,9)
2780 NEXT J1
2790 PRINT " "
2800 PRINT " "
2810 !L-U DECOMPOSITION OF MATRIX AA IS OBTAINED. IT FORMS L-U
EQUIVALENT
2820 !OF SQUARE COEFFICIENT MATRIX, AA.
2830 FOR I=1 TO Mfp1
2840 FOR J=2 TO Mfp1
2850 Sumb1=0.
2860 IF J>I THEN GOTO 2930
2870 Jm1=J-1
2880 FOR K=1 TO Jm1
2890 Sumb1=Sumb1+Aa(I,K)*Aa(K,J)
2900 NEXT K
2910 Aa(I,J)=Aa(I,J)-Sumb1
2920 GOTO 3100
2930 Im1=I-1
2940 IF Im1=0 THEN GOTO 3080
2950 FOR K=1 TO Im1
2960 Sumb1=Sumb1+Aa(I,K)*Aa(K,J)
2970 NEXT K
2980 IF ABS(Aa(I,I))<1.0E-10 THEN GOTO 3030
2990 Aa(I,J)=(Aa(I,J)-Sumb1)/Aa(I,I)

```

```

3000 NEXT J
3010 NEXT I
3020 GOTO 3140
3030 PRINT "REDUCTION INCOMPLETE DUE TO SMALL DIVISOR VALUE IN
ROW ",I
3040 Msp1=Ms+1
3050 FOR Ii=Msp1 TO Mfp1
3060 FOR J=1 TO Ii
3070 Cc(J)=Aa(J,Mfp2)
3080 NEXT J
3090 Cc(1)=Cc(1)/Aa(1,1)
3100 FOR I=2 TO Ii
3110 Imp=I-1
3120 Sumb2=0.
3130 FOR K=1 TO Imp
3140 Sumb2=Sumb2+Aa(I,K)*Cc(K)
3150 NEXT K
3160 Cc(I)=(Cc(I)-Sumb2)/Aa(I,I)
3170 NEXT I
3180 FOR J=2 TO Ii
3190 Nmjp2=Ii-J+2
3200 Nmjp1=Ii-J+1
3210 Sumb2=0.
3220 FOR K=Nmjp2 TO Ii
3230 Sumb2=Sumb2+Aa(Nmjp1,K)*Cc(K)
3240 NEXT K
3250 Cc(Nmjp1)=Cc(Nmjp1)-Sumb2
3260 NEXT J
3270 Imt=Ii-1
3280 PRINT USING ""COEFFICIENTS FOR DEGREE ="";DD";Imt
3290 FOR Ih=1 TO Ii
3300 PRINT USING "DD,3X,S6D.8D";Ih-1,Cc(Ih)
3310 NEXT Ih
3320 Beta=0.
3330 Sumb=0.
3340 FOR Ipt=1 TO Np
3350 FOR Icoef=2 TO Ii
3360 Jcoef=Ii-Icoef+2
3370 Sumb=(Sumb+Cc(Jcoef))*X(Ipt)
3380 NEXT Icoef
3390 Sumb=Sumb+Cc(1)
3400 Beta=(Psi(Kk,Ipt)-Sumb)^2
3410 NEXT Ipt
3420 Beta=Beta/(Np-Ii)
3430 PRINT " STATISTICAL VARIANCE, BETA^2",Beta
3440 FOR Ic=1 TO Ii
3450 Cc(Ic)=0.
3460 NEXT Ic
3470 NEXT Ii
3480 PRINT "PICK THE COEFFICIENTS WITH LEAST BETA FOR CURVE
FITTING"
3490 Kk=Kk+1
3500 GOTO 2410
3510 DISP "PLOT BEGINS, "

```

```
3520 BEEP
3530 DISP "NOW OBATIN DIFF. PRESS. AS FUNCTION OF TIME PLOT, WHEN
READY HIT CONTINUE"
3540 PAUSE
3550 PEN 4
3560 GINIT
3570 PEN 4
3580 IF Ipl=1 THEN PLOTTER IS 705, "HPGL"
3590 IF Ipl<>1 THEN PLOTTER IS CRT, "INTERNAL"
3600 GRAPHICS ON
3610 X_max=100*MAX(1,RATIO)
3620 Y_max=100*MAX(1,1/RATIO)
3630 LORG 6
3640 MOVE X_gdu_max/2,Y_gdu_max
3650 LABEL USING """"DIFF PRESSURE AS FUNCTION OF TIME, RUN""",3D";Ru
3660 DEG
3670 LDIR 90
3680 CSIZE 3.5
3690 MOVE 0,Y_gdu_max/2
3700 LABEL USING """"PRESSURE (psi), dPmax=""",3D.2D";MAX(Delp(*))
3710 LORG 4
3720 LDIR 0
3730 MOVE X_gdu_max/2,.07*Y_gdu_max
3740 LABEL USING """"TIME (SECONDS), Tmax=""",6D.D";MAX(T1(*))
3750 VIEWPORT .1*X_gdu_max,.98*X_gdu_max,.15*Y_gdu_max,.9*Y_gdu_max
3760 FRAME
3770 WINDOW 0.,T1(Nscan),0.,MAX(Delp(*))
3780 AXES 2000.,10.0,0.0,5,5,2
3790 CLIP OFF
3800 CSIZE 2.5,.5
3810 LORG 6
3820 FOR I=0 TO T1(Nscan) STEP Sati
3830 MOVE I,-2
3840 LABEL USING "#,K";I
3850 NEXT I
3860 LORG 8
3870 FOR I=0 TO MAX(Delp(*))
3880 MOVE -.2,I
3890 LABEL USING "#,DDD.DD";I
3900 NEXT I
3910 PENUP
3920 PEN 4
3930 FOR K=3 TO Nscan
3940 PLOT T1(K),Delp(K)
3950 NEXT K
3960 PEN 0
3970 GRAPHICS OFF
3980 BEEP
3990 PRINTER IS 1
4000 DISP "OBTAIN SATURATION PROFILES, WHEN READY HIT CONTINUE"
4010 BEEP
4020 PAUSE
4030 PEN 4
4040 GINIT
```

```
4050 PEN 4
4060 IF Ipl=1 THEN PLOTTER IS 705,"HPGL"
4070 IF Ipl<>1 THEN PLOTTER IS CRT,"INTERNAL"
4080 GRAPHICS ON
4090 X_gdu_max=100*MAX(1,RATIO)
4100 Y_max=100*MAX(1,1/RATIO)
4110 LORG 6
4120 !FOR I=-.3 TO .3 STEP .1
4130 MOVE X_gdu_max_/2,Y_gdu_max
4140 LABEL USING ""Sw PROFILES VS. TIME,COCURRENT RUN "" ,DDD";Ru
4150 !NEXT I
4160 DEG
4170 LDIR 90
4180 CSIZE 3
4190 MOVE 0,Y_gdu_max/2
4200 LABEL "WATER SATURATION, Sw (%)"
4210 LORG 4
4220 LDIR 0
4230 MOVE X_gdu_max/2,.07*Y_gdu_max
4240 LABEL "CORE LENGTH"
4250 VIEWPORT .1*X_gdu_max,.99*X_gdu_max,.15*Y_gdu_max,.9*Y_gdu_max
4260 FRAME
4270 WINDOW 0.,100,0.,100.0
4280 AXES 10,10,0,0,5,5,2
4290 CLIP OFF
4300 CSIZE 2.5,.5
4310 LORG 6
4320 FOR I=0 TO 100 STEP 10
4330 MOVE I,-.2
4340 LABEL USING "#,K";I
4350 NEXT I
4360 LORG 8
4370 FOR I=0 TO 100 STEP 10
4380 MOVE -.2,I
4390 LABEL USING "#,DDD.D";I
4400 NEXT I
4410 PEN 1
4420 FOR K=3 TO Nscan
4430 FOR L=1 TO 100
4440 PLOT L,Sw(K,L)*100
4450 NEXT L
4460 PENUP
4470 NEXT K
4480 GRAPHICS OFF
4490 PEN 0
4500 BEEP
4510 DISP "OBTAIN SCAN PROFILES ALONG THE CORE, WHEN READY HIT
CONTINUE"
4520 PAUSE
4530 PEN 1
4540 GINIT
4550 PEN 1
4560 IF Ipi=1 THEN PLOTTER IS 705,"HPGL"
4570 IF Ipl<>1 THEN PLOTTER IS CRT,"INTERNAL"
```

```
4580 GRAPHICS ON
4590 X_gdu_max=100*MAX(1,RATIO)
4600 Y_max=100*MAX(1,1/RATIO)
4610 LORG 6
4620 !FOR I=-.3 TO .3 STEP .1
4630 MOVE X_gdu_max/2,Y_gdu_max
4640 LABEL USING """"SCAN PROFILES OF RUN,COCUPRENT RUN""",DDD":Ru
4650 !NEXT I
4660 DEG
4670 LDIR 90
4680 CSIZE 3
4690 MOVE 0,Y_gdu_max/2
4700 LABEL USING """"Power (mW), Max. """,M2D.4D";MAX(Power(*))
4710 LORG 4
4720 LDIR 0
4730 MOVE X_gdu_max/2,.07*Y_gdu_max
4740 LABEL "Length of Core (X)"
4750 VIEWPORT .1*X_gdu_max,.99*X_gdu_max,.15*Y_gdu_max,.9*Y_gdu_max
4760 FRAME
4770 WINDOW 0.,100,0.,MAX(Power(*))
4780 AXES 5.0,.1,0,0,5,5,2
4790 CLIP OFF
4800 CSIZE 2.5,.5
4810 LORG 6
4820 FOR I=0 TO 100 STEP 10
4830 MOVE I,-.1
4840 LABEL USING "#,K";I
4850 NEXT I
4860 LORG 8
4870 FOR i=0 TO MAX(Power(*))
4880 MOVE -.2,I
4890 LABEL USING "#,DD.DD";I
4900 NEXT I
4910 PENUP
4920 FOR K=1 TO Nscan
4930 FOR L=1 TO 100
4940 PLOT L,Power(K,L)
4950 NEXT L
4960 PENUP
4970 NEXT K
4980 WAIT .1
4990 GRAPHICS OFF
5000 PEN 0
5010 BEEP
5020 DISP "YOU ARE DONE WITH THE COCURRENT EXPT. ANALYSIS"
5030 STOP
5040 END
```

### A.5: Data Retrieval and Interpretation for Countercurrent Flow Experiments

```

10 ! ***** COUNTERCURRENT.INT *****
20 !*
30 !* PROGRAM FOR DATA RETRIEVAL AND ANALYSIS FOR
40 !* COUNTERCURRENT FLOW EXPERIMENT.
50 !* DATA FILES ARE RETRIEVAL BY CALLING THEIR APPROPRIATE NAMES
50 !* THE PROGRAM IS INTERACTIVE.
60 !* SOME ANALYSES ARE OPTIONAL, AND CAN BE BY-PASSED.
70 !*
80 !*
90 !*
100 !***** DIMENSIONALISING OF VARIABLES *****
110 OPTION BASE 1
120 INTEGER I,J,K,N,H,M,L
130 DIM Nsat,Nscan,Npoint,Nend,Ipoint,Nbegin,Nhalf
140 DIM S(50,100),Aaw(50,100),C(100),B(100)
150 DIM AS(17)
160 DIM Voh(50,14),Akw(50),Ako(50)
170 DIM Perm(50),Permw(50)
180 DIM V(14),Delp(50),P1(50),P2(50),Dlpw(50),P1w(50),P2w(50)
190 DIM T1(50),T2(50),Tp(50),Tm(50),Powin(50,100)
200 DIM Power(50,100),T7(10)
210 DIM T3(50),Pko(50,14),Pk1(50),Pk2(50),Delpk(50),Perm1(50),Perm2(50)
220 INPUT "No. OF SATURATION PROFILES ?",Nsat
230 Nscan=Nsat+2
240 INPUT "IRREDUCIBLE (INITIAL) WATER SATURATION Swi (fraction)?",Swi
250 INPUT "DO YOU WANT HARD COPY PRINTOUT ? ... 1=YES;0=NO",lpr
260 INPUT "DO YOU WANT HARD COPY PLOT ? ... 1=YES;0=NO",lpl
270 IF lpr=1 THEN OUTPUT 701;CHR$(27)&"&11L."
280 !*****RETRIEVING DATA FROM THE FILES *****
290 !*
300 INPUT "FILENAME FOR OP POWER @ Sw=1 (OP#S1)",Name$
310 ASSIGN @File11 TO Name$
320 INPUT "FILENAME FOR OP POWER @ Swi (OP#S2)",Name$
330 ASSIGN @File1 TO Name$
340 INPUT "FILENAME FOR IP POWER @ Sw=1 (IP#S1)",Name$
350 ASSIGN @File12 TO Name$
360 INPUT "FILENAME FOR IP POWER @ Swi (IP#S2)",Name$
370 ASSIGN @File2 TO Name$
380 INPUT "FILENAME FOR DATE AND TIME EXPT. STARTED (R#D)",Name$
390 ASSIGN @File5 TO Name$
400 INPUT "FILENAME FOR INPUT MICROWAVE POWER DATA (R#I)",Name$
410 ASSIGN @File10 TO Name$
420 INPUT "ENTER FILENAME OUTPUT POWER METER DATA (R#O)",Name$
430 ASSIGN @File3 TO Name$
440 INPUT "ENTER FILENAME FOR PRESSURE DATA (R#P)",Name$
450 ASSIGN @File4 TO Name$
460 ENTER @File11;Power(*)

```



```

470 ENTER @File1;Power(*)
480 ENTER @File12;Powin(*)
490 ENTER @File2;Powin(*)
500 ENTER @File10;T2(*),Powin(*)
510 ENTER @File7;Tb(*),Wgt(*)
520 ENTER @File3;T2(*),Power(*)
530 ENTER @File4;T1(*),Volt(*)
540 ENTER @File5;Day$,Tim$,Run$
550 Ru=VAL(Run$)
560 Time=T1(60)
570 PRINTER IS 1
580 INPUT "OIL FLOWRATE in CC/HR? ",Ro
590 INPUT "WATER FLOWRATE in CC/HR? ",Rw
600 INPUT "TOTAL VOLUME OF OIL PUMPED CC? ",Ov
610 INPUT "TOTAL VOLUME OF WATER PUMPED CC? ",Wv
620 To=Ov/Ro*3600
630 Tw=Wv/Rw*3600
640 IF To>Tw THEN GOTO 670
650 Sati=To/Nsat
660 GOTO 680
670 Sati=Tw/Nsat
680 INPUT "DENSITY OF WATER? ",Rhow
690 INPUT " OIL USED? 1=LAGO,2=MCT5,3=MCT5LAGO,4=MCT10",Ioil
700 IF Ioil=1 THEN
710   Rhoo=.7963
720   Ac=16342.0
730   Vis1=4.7
740 END IF
750 IF Ioil=2 THEN
760   Rhoo=.123
770   Ac=13566.0
780   Vis1=30.48
790 END IF
800 IF Ioil=3 THEN
810   Rhoo=.8043
820   Ac=14185.0
830   Vis1=11.1
840 END IF
850 IF Ioil=4 THEN
860   Rhoo=.8576
870   Ac=13573.0
880   Vis1=60.0
890 END IF
900 Bulkvol=625.0
910 INPUT "ENTER PORE VOLUME OF THE SANDPACK IN CC? ",Pv
920 Por=Pv/Bulkvol
930 ! EXTRAPOLATE INTERNAL PRESSURES TO THE OUTLET ENDS OF THE
CORFHOLDER"
940 FOR K=3 TO Nscan
950   P1(K)=(Volt(K,1)+2.0*(Volt(K,1)-Volt(K,2))/11.0)
960   P2(K)=(Volt(K,7)-2.0*(Volt(K,6)-Volt(K,7))/11.0)
970   Delp(K)=(P1(K)-P2(K))
980   P2w(K)=(Volt(K,9)-13*(Volt(K,11)-Volt(K,9))/36.5)
990   P1w(K)=(Volt(K,13)+13*(Volt(K,13)-Volt(K,11))/36.5)

```

```

1000 Dlpw(K)=ABS(P1w(K)-P2w(K))
1010 NEXT K
1020 A1=100.0 !LENGTH OF THE CORE IN CM
1030 A=6.215 ! CROSS SECTIONAL AREA OF SANDPACK CM**2
1040 Porvol=A1*A*Por
1050 Ros=Ro/3600.0
1060 Rws=Rw/3600.0
1070 IF Ipr=1 THEN PRINTER IS 701
1080 INPUT "ENTER VISCOSITY OF WATER IN CP",Vis
1090 IF Ipr=0 THEN GOTO 1130
1100 DISP "SET PRINTER TO A NEW PAGE i.e. PRESS FF AND THEN HIT
CONTINUE"
1110 PAUSE
1120 IF Ipr=1 THEN PRINTER IS 701
1130 PRINT USING """"EXPERIMENTAL COUNTERCURRENT RUN No.
"",3A";Run$
1140 PRINT "DATE OF EXPERIMENT: " Day$
1150 PRINT "TIME EXPT. STARTED: " Tim$
1160 PRINT "-----"
1170 PRINT " "
1180 PRINT USING """"VISCOSITY OF OIL, CP """,3D.DD";Vis1
1190 PRINT USING """"VISCOSITY OF WATER, CP """,3D.DD";Vis
1200 PRINT USING """"DENSITY OF OIL, GM/CC """,D.4D";Rho0
1210 PRINT USING """"VOLUMETRIC OIL FLOWRATE, CC/SEC """,D.5D";Ros
1220 PRINT USING """"VOLUMETRIC WATER FLOWRATE, CC/SEC
"",D.5D";Rws
1230 PRINT USING """"LENGTH OF COREHOLDER, CM """,3D.D";A1
1240 PRINT USING """"RECTANGULAR AREA OF PACK, CM**2 """,3D.DD";A
1250 PRINT USING """"POROSITY """,D.3D";Por
1260 PRINT USING """"Swi """,D.3D";Swi
1270 PRINT USING """"OIL FLOWRATE (cc/hr) """,4D.D";Ros*3600.0
1280 PRINT USING """"WATER FLOWRATE (cc/hr) """,4D.D";Rws*3600.0
1290 PRINTER IS 1
1300 !
1310 !* FINDING THE MICROWAVE EQUATION'S CONSTANTS (B & C )
1320 FOR I=1 TO 100
1330 B(I)=1./(1.-Swi)*((LOG(ABS(Power(1,I)/Powin(1,I))))-
(LOG(ABS(Power(2,I)/Powin(2,I))))
1340 C(I)=(LOG(ABS(Power(1,I)/Powin(1,I))))-B(I)
1350 NEXT I
1360 !*
1370 !* CALCULATING WATER SATURAION (Sw )
1380 !*
1390 FOR J=1 TO Nscan
1400 FOR I=1 TO 100
1410 Sw(J,I)=((LOG(ABS(Power(J,I)/Powin(J,I))))-C(I))/B(I)
1420 PRINT J,I,Sw(J,I)
1430 NEXT I
1440 DISP J
1450 NEXT J
1460 PRINTER IS 1
1470 INPUT "WANT INTEGRATION OF SATURATION DATA, 1=YES 0=NO
?" ,Idsat
1480 IF Idsat=0 THEN GOTO 1920

```

```

1490 PRINT "INTEGRATION OF DIMENSIONLESS SATURATION ALONG
LENGTH"
1500 PRINT "-----"
1510 PRINT "FOR MAXIMUM ACCURACY BOTH SIMPSON'S 1/3 AND 3/8
RULES ARE APPLIED."
1520 PRINT "COMBINATION OF BOTH RULES ARE REQUIRED IN CASE OF ODD
NUMBER OF INTERVALS."
1530 PRINT "IN CASE OF EVEN NUMBER, 1/3 RULE IS MORE ACCURATE,
WHILE IN CASE OF"
1540 PRINT "ODD INTERVALS, 3/8 RULE IS APPLIED FOR FIRST 3 PANELS
AND 1/3 RULE"
1550 PRINT "FOR THE REST."
1560 !INCREMENT IN DIMENSIONLESS DISTANCE
1570 REAL Hx,Sss(60)
1580 Hx=1
1590 INPUT "ENTER NUMBER OF DATA POINTS i.e. NPOINT",Npoint
1600 Xd=Hx*Npoint
1610 PRINT " "
1620 PRINT " "
1630 PRINT "EXPERIMENTAL COUNTERCURRENT RUN NUMBER",Run$
1640 PRINT "DATE OF EXPERIMENT  ",Day$
1650 PRINT "TIME EXPT STARTED  ",Tim$
1660 Ipoint=Npoint-1
1670 Nhalf=Ipoint/2
1680 FOR K=3 TO Nscan
1690 !THE FIRST POINT IS THE POINT @ WHICH COUNTERCURRENT
STARTED (3rd SCAN)
1700 Nbegin=3
1710 Ssw=0.
1720 IF (Ipoint-(2*Nhalf))=0 THEN GOTO 1890
1730 !IF No. OF PANELS ODD, USE 3/8 RULE ON FIRST 3 PANELS,
1740 1/3 RULE ON REST OF THEM
1750 Ssw=3.*Hx/8.*(Sw(K,3)+3.0*Sw(K,4)+3.*Sw(K,5)+Sw(K,6))
1760 !THE 4th pt IS ACTUALLY THE 6th pt IN THE SCAN (4+2=6)
1770 Nbegin=6
1780 !NOW APPLY 1/3 RULE - ADD 1st, 2nd AND LAST VALUES
1790 Ssw=Ssw+Hx/3.*(Sw(K,Nbegin)+4.0*Sw(K,Nbegin+1)+Sw(K,Npoint))
1800 Nbegin=Nbegin+2
1810 IF Nbegin=Npoint THEN GOTO 1970
1820 !PATTERN AFTER (Nbegin+2) IS REPETITIVE TILL NEND
1830 Nend=Npoint-2
1840 FOR J=Nbegin TO Nend STEP 2
1850 Ssw=Ssw+Hx/3.0*(2.*Sw(K,J)+4.0*Sw(K,J+1))
1860 NEXT J
1870 PRINT USING "5D.DD,5X,MDD.DDDE";T2(K),Ssw
1880 !CONSIDERING LAST PT OF Sw AS THAT @ THE LAST SCAN @ THE
MIDDLE OF CORE
1890 T2(K)=Rws*T2(K)/(A*A1*Por*(Sw(Nscan,50)))
1900 Sss(K)=Ssw/100.0
1910 NEXT K
1920 PRINTER IS 1
1930 INPUT "WANT TO SMOOTHEN PRESSURE DATA, 1=Y 0=N?",Ipd
1940 IF Ipd=0 THEN GOTO 3610
1950 PRINT "SMOOTHENING OF PRESSURE DATA ALONG DIMNESIONLESS

```

```

LENGTH"
1960 PRINT "-----"
1970 PRINT " "
1980 PRINT " "
1990 REAL X(11),Psi(60,11)
2000 FOR I=3 TO Nscan
2010 Psi(I,1)=P1(I)
2020 Psi(I,2)=Volt(I,1)
2030 Psi(I,3)=Volt(I,2)
2040 Psi(I,4)=Volt(I,4)
2050 Psi(I,5)=Volt(I,6)
2060 Psi(I,6)=Volt(I,7)
2070 Psi(I,7)=P2(I)
2080 NEXT I
2090 GOTO 2170
2100 Psi(Nscan,1)=P1(Scan)
2110 Psi(Nscan,2)=Volt(Nscan,1)
2120 Psi(Nscan,3)=Volt(Nscan,2)
2130 Psi(Nscan,4)=Volt(Nscan,4)
2140 Psi(Nscan,5)=Volt(Nscan,6)
2150 Psi(Nscan,6)=Volt(Nscan,7)
2160 Psi(Nscan,7)=P2(Nscan)
2170 X(1)=0.
2180 X(2)=.0102
2190 X(3)=.12245
2200 X(4)=.50
2210 X(5)=.87755
2220 X(6)=.98979
2230 X(7)=1.0
2240 Np=7
2250 !THIS PART SMOOTHENS PRESSURE DATA WHICH ARE NOT
EQUISPACED i.e. VARIABLE H"
2260 NP=NO. OF DATA PAIRS
2270 MS, MF = RANGE OF DEGREE OF POLYNOMIALS, MAXM DEGREE 9
2280 AA=AUGMENTED ARRAY OF COEFFICIENT OF NORMAL EQNS
2290 CC=ARRAY OF COEFFS OF LEAST SQUARE POLYNOMIAL
2300 REAL Aa(8,9),Cc(10),Xn(11)
2310 INTEGER Mf,Ms,Mfp1,Mfp2,Msp1,Kk,Ii,J1,Imt,Jm1,Im1,Ipt
2320 INTEGER lcoef,Jcoef,Ia,lc,laa
2330 INPUT "SMALLEST DEGREE OF POLYNOMIAL",Ms
2340 INPUT "GREATEST DEGREE OF POLYNOMIAL",Mf
2350 IF Mf<=(Np-1) THEN GOTO 2380
2360 Mf=Np-1
2370 PRINT "DEGREE OF POLYNOMIAL TOO LARGE. REDUCED TO ",Mf
2380 Mfp1=Mf+1
2390 Mfp2=Mf+2
2400 Kk=1
2410 IF Kk>6 THEN GOTO 3510
2420 FOR Ia=1 TO Mfp1
2430 FOR Iaa=1 TO Mfp2
2440 Aa(Ia,Iaa)=0.
2450 NEXT Iaa
2460 NEXT Ia
2470 PRINT USING """"SCAN""",2D";Kk

```

```

2480 FOR I=1 TO Np
2490  Xn(I)=1.0
2500 NEXT I
2510 FOR J=1 TO Mfp1
2520  Aa(J,1)=0.
2530  Aa(J,Mfp2)=0.
2540  FOR N=1 TO Np
2550    Aa(J,1)=Aa(J,1)+Xn(N)
2560    Aa(J,Mfp2)=Aa(J,Mfp2)+Psi(Kk,N)*Xn(N)
2570    Xn(N)=Xn(N)*X(N)
2580  NEXT N
2590 NEXT J
2600 FOR I=2 TO Mfp1
2610  Aa(Mfp1,I)=0.
2620  FOR J=1 TO Np
2630    Aa(Mfp1,I)=Aa(Mfp1,I)+Xn(J)
2640    Xn(J)=Xn(J)*X(J)
2650  NEXT J
2660 NEXT I
2670 FOR J=2 TO Mfp1
2680  FOR I=1 TO Mf
2690    Aa(I,J)=Aa(I+1,J-1)
2700  NEXT I
2710 NEXT J
2720 PRINT "THE MATRIX OF NORMAL EQUATIONS"
2730 PRINT "-----"
2740 PRINT " "
2750 PRINT " "
2760 FOR J1=1 TO Mfp1
2770  PRINT USING
"S5D.4D";Aa(J1,1),Aa(J1,2),Aa(J1,3),Aa(J1,4),Aa(J1,5),Aa(J1,6),Aa(J1,7),Aa(J1,8),A
a(J1,9)
2780 NEXT J1
2790 PRINT " "
2800 PRINT " "
2810 !L-U DECOMPOSITION OF MATRIX AA IS OBTAINED. IT FORMS L-U
EQUIVALENT
2820 !OF SQUARE COEFFICIENT MATRIX, AA.
2830 FOR I=1 TO Mfp1
2840  FOR J=2 TO Mfp1
2850    Sumb1=0.
2860    IF J>I THEN GOTO 2930
2870    Jm1=J-1
2880    FOR K=1 TO Jm1
2890      Sumb1=Sumb1+Aa(I,K)*Aa(K,J)
2900    NEXT K
2910    Aa(I,J)=Aa(I,J)-Sumb1
2920    GOTO 3100
2930    Im1=I-1
2940    IF Im1=0 THEN GOTO 3080
2950    FOR K=1 TO Im1
2960      Sumb1=Sumb1+Aa(I,K)*Aa(K,J)
2970    NEXT K
2980    IF ABS(Aa(I,I))<1.0E-10 THEN GOTO 3030

```

```

2990  Aa(I,J)=(Aa(I,J)-Sumb1)/Aa(I,I)
3000  NEXT J
3010  NEXT I
3020  GOTO 3140
3030  PRINT "REDUCTION INCOMPLETE DUE TO SMALL DIVISOR VALUE IN
ROW ",I
3040  Msp1=Ms+1
3050  FOR Ii=Msp1 TO Mfp1
3060  FOR J=1 TO Ii
3070  Cc(J)=Aa(J,Mfp2)
3080  NEXT J
3090  Cc(1)=Cc(1)/Aa(1,1)
3100  FOR I=2 TO Ii
3110  Imp=I-1
3120  Sumb2=0.
3130  FOR K=1 TO Imp
3140  Sumb2=Sumb2+Aa(I,K)*Cc(K)
3150  NEXT K
3160  Cc(I)=(Cc(I)-Sumb2)/Aa(I,I)
3170  NEXT I
3180  FOR J=2 TO Ii
3190  Nmjp2=Ii-J+2
3200  Nmjp1=Ii-J+1
3210  Sumb2=0.
3220  FOR K=Nmjp2 TO Ii
3230  Sumb2=Sumb2+Aa(Nmjp1,K)*Cc(K)
3240  NEXT K
3250  Cc(Nmjp1)=Cc(Nmjp1)-Sumb2
3260  NEXT J
3270  Imt=Ii-1
3280  PRINT USING """"COEFFICIENTS FOR DEGREE =""",DD";Imt
3290  FOR Ih=1 TO Ii
3300  PRINT USING "DD,3X,S6D.8D";Ih-1,Cc(Ih)
3310  NEXT Ih
3320  Beta=0.
3330  Sumb=0.
3340  FOR Ipt=1 TO Np
3350  FOR Icoef=2 TO Ii
3360  Jcoef=Ii-Icoef+2
3370  Sumb=(Sumb+Cc(Jcoef))*X(Ipt)
3380  NEXT Icoef
3390  Sumb=Sumb+Cc(1)
3400  Beta=(Psi(Kk,Ipt)-Sumb)^2
3410  NEXT Ipt
3420  Beta=Beta/(Np-Ii)
3430  PRINT " STATISTICAL VARIANCE, BETA^2",Beta
3440  FOR Ic=1 TO Ii
3450  Cc(Ic)=0.
3460  NEXT Ic
3470  NEXT Ii
3480  PRINT "PICK THE COEFFICIENTS WITH LEAST BETA FOR CURVE
FITTING"
3490  Kk=Kk+1
3500  GOTO 2410

```

```

3510 DISP "PLOT BEGINS, "
3520 BEEP
3530 DISP "NOW OBATIN DIFF. PRESS. AS FUNCTION OF TIME PLOT,WHEN
READY HIT CONTINUE"
3540 PAUSE
3550 PEN 4
3560 GINIT
3570 PEN 4
3580 IF Ipl=1 THEN PLOTTER IS 705,"HPGL"
3590 IF Ipl<>1 THEN PLOTTER IS CRT,"INTERNAL"
3600 GRAPHICS ON
3610 X_max=100*MAX(1,RATIO)
3620 Y_max=100*MAX(1,1/RATIO)
3630 LORG 6
3640 MOVE X_gdu_max/2,Y_gdu_max
3650 LABEL USING """"DIFF PRESSURE AS FUNCTION OF TIME, RUN""",3D";Ru
3660 DEG
3670 LDIR 90
3680 CSIZE 3.5
3690 MOVE 0,Y_gdu_max/2
3700 LABEL USING """"PRESSURE (psi), dPmax=""",3D.2D";MAX(Delp(*))
3710 LORG 4
3720 LDIR 0
3730 MOVE X_gdu_max/2,.07*Y_gdu_max
3740 LABEL USING """"TIME (SECONDS), Tmax=""",6D.D";MAX(T1(*))
3750 VIEWPORT .1*X_gdu_max,.98*X_gdu_max,.15*Y_gdu_max,.9*Y_gdu_max
3760 FRAME
3770 WINDOW 0.,T1(Nscan),0.,MAX(Delp(*))
3780 AXES 2000.,10.0,0,0,5,5,2
3790 CLIP OFF
3800 CSIZE 2.5,.5
3810 LORG 6
3820 FOR I=0 TO T1(Nscan) STEP Sati
3830 MOVE I,-.2
3840 LABEL USING "#,K";I
3850 NEXT I
3860 LORG 8
3870 FOR I=0 TO MAX(Delp(*))
3880 MOVE -.2,I
3890 LABEL USING "#,DDD.DD";I
3900 NEXT I
3910 PENUP
3920 PEN 4
3930 FOR K=3 TO Nscan
3940 PLOT T1(K),Delp(K)
3950 NEXT K
3960 PEN 0
3970 GRAPHICS OFF
3980 BEEP
3990 PRINTER IS 1
4000 DISP "OBTAIN SATURATION PROFILES, WHEN READY HIT CONTINUE"
4010 BEEP
4020 PAUSE
4030 PEN 4

```

```
4040 GINIT
4050 PEN 4
4060 IF Ipl=1 THEN PLOTTER IS 705,"HPGL"
4070 IF Ipl<>1 THEN PLOTTER IS CRT,"INTERNAL"
4080 GRAPHICS ON
4090 X_gdu_max=100*MAX(1,RATIO)
4100 Y_max=100*MAX(1,1/RATIO)
4110 LORG 6
4120 !FOR I=-.3 TO .3 STEP .1
4130 MOVE X_gdu_max/2,Y_gdu_max
4140 LABEL USING ""Sw PROFILES VS. TIME,COUNTERCURRENT RUN
"";D;D";Ru
4150 !NEXT I
4160 DEG
4170 LDIR 90
4180 CSIZE 3
4190 MOVE 0,Y_gdu_max/2
4200 LABEL "WATER SATURATION, Sw (%)"
4210 LORG 4
4220 LDIR 0
4230 MOVE X_gdu_max/2,.07*Y_gdu_max
4240 LABEL "CORE LENGTH"
4250 VIEWPORT .1*X_gdu_max,.99*X_gdu_max,.15*Y_gdu_max,.9*Y_gdu_max
4260 FRAME
4270 WINDOW 0.,100,0.,100.0
4280 AXES 10,10,0,0,5,5,2
4290 CLIP OFF
4300 CSIZE 2.5,.5
4310 LORG 6
4320 FOR I=0 TO 100 STEP 10
4330 MOVE I,-.2
4340 LABEL USING "#,K";I
4350 NEXT I
4360 LORG 8
4370 FOR I=0 TO 100 STEP 10
4380 MOVE -.2,I
4390 LABEL USING "#,DDD.D";I
4400 NEXT I
4410 PEN 1
4420 FOR K=3 TO Nscan
4430 FOR L=1 TO 100
4440 PLOT L,Sw(K,L)*100
4450 NEXT L
4460 PENUP
4470 NEXT K
4480 GRAPHICS OFF
4490 PEN 0
4500 BEEP
4510 DISP "OBTAIN SCAN PROFILES ALONG THE CORE, WHEN READY HIT
CONTINUE"
4520 PAUSE
4530 PEN 1
4540 GINIT
4550 PEN 1
```



```
4560 IF Ipl=1 THEN PLOTTER IS 705,"HPGL"  
4570 IF Ipl<>1 THEN PLOTTER IS CRT,"INTERNAL"  
4580 GRAPHICS ON  
4590 X_gdu_max=100*MAX(1,RATIO)  
4600 Y_max=100*MAX(1,1/RATIO)  
4610 LORG 6  
4620 !FOR I=-.3 TO .3 STEP .1  
4630 MOVE X_gdu_max/2,Y_gdu_max  
4640 LABEL USING """"SCAN PROFILES OF RUN,COUNTERCURRENT  
RUN""",DDD";Ru  
4650 !NEXT I  
4660 DEG  
4670 LDIR 90  
4680 CSIZE 3  
4690 MOVE 0,Y_gdu_max/2  
4700 LABEL USING """"Power (mW), Max. """,M2D.4D";MAX(Power(*))  
4710 LORG 4  
4720 LDIR 0  
4730 MOVE X_gdu_max/2,.07*Y_gdu_max  
4740 LABEL "Length of Core (X)"  
4750 VIEWPORT .1*X_gdu_max,.99*X_gdu_max,.15*Y_gdu_max,.9*Y_gdu_max  
4760 FRAME  
4770 WINDOW 0.,100,0.,MAX(Power(*))  
4780 AXES 5.0.,1,0,0,5,5,2  
4790 CLIP OFF  
4800 CSIZE 2.5,.5  
4810 LORG 6  
4820 FOR I=0 TO 100 STEP 10  
4830 MOVE I,-.1  
4840 LABEL USING "#,K";I  
4850 NEXT I  
4860 LORG 8  
4870 FOR I=0 TO MAX(Power(*))  
4880 MOVE -.2,I  
4890 LABEL USING "#,DD.DD";I  
4900 NEXT I  
4910 PENUP  
4920 FOR K=1 TO Nscan  
4930 FOR L=1 TO 100  
4940 PLOT L,Power(K,L)  
4950 NEXT L  
4960 PENUP  
4970 NEXT K  
4980 WAIT .1  
4990 GRAPHICS OFF  
5000 PEN 0  
5010 BEEP  
5020 DISP "YOU ARE DONE WITH THE COUNTERCURRENT EXPT. ANALYSIS"  
5030 STOP  
5040 END
```

## **APPENDIX B: Data Conditioning Procedure and Some Experimental Results and Figures**

Data conditioning was carried out to include all the data points in the analysis. The conditioning was done keeping in mind that the sum of or the difference between two straight lines results in another straight line. Data conditioning was done in two ways. For the case of cocurrent experiments, all the data (from transducers which measured the pressure in the oil phase and from those which measured the pressure in the water phase) were fitted to create the best straight lines of pressure versus dimensionless distance. This was accomplished by first obtaining the best straight line for the pressure in the oil phase and the best straight line for the pressure in the water phase (Figures 6.5 and 6.6). Then the resulting equations were used to estimate the pressure in the oil phase at dimensionless distances (2 points) corresponding to the two points on the water phase pressure line where the pressure in the water phase was experimentally measured and at which the pressure measurement in the oil phase was not available. The same was done for the water phase and the pressure in the water phase was estimated at three different dimensionless distances (corresponding to dimensionless distances where pressure in the oil phase was experimentally measured). Then the pressure in the oil phase was added to that in the water phase and the best straight line was obtained. The pressure in the water phase was also subtracted from the pressure in the oil phase and the difference in pressure was plotted versus dimensionless distance to obtain another straight line (samples of such lines are shown in Figures B.1 and B.2 in Appendix B). The average of the two slopes was used for the pressure gradient in the oil phase while the difference between the slopes divided by 2 was used for the pressure gradient in the water phase. For the case of countercurrent flow, pressure data versus distance for each phase were fitted (Figures 6.7 and 6.8); then the pressure in the water phase versus distance was added to the corresponding point on the best straight line of pressure in the oil phase (Figures B.3 and B.4).

Table B.1: Results of Cocurrent Flow Experiments ( Set I )

Experiment No.	$q_w$ (cc/hr)	$q_o$ (cc/hr)	$q_w/q_o$ (-)	$S_w$ (%)	Raw		Conditioned	
					$\Delta P_w/L$ (psi/cm)	$\Delta P_o/L$ (psi/cm)	$\Delta P_w/L$ (psi/cm)	$\Delta P_o/L$ (psi/cm)
1	8.75	40	0.21875	14.25	0.05585	0.05865	0.05585	0.05863
2	16	25	0.64	23.75	0.06273	0.05999	0.06003	0.06002
3	20	20	1	28.00	0.05729	0.06010	0.05729	0.06010
4	30	16	1.875	35.50	0.05765	0.05999	0.05765	0.05999
5	40	12.5	3.2	37.75	0.05794	0.06000	0.05794	0.06001
6	50	10	5	41.00	0.05812	0.05971	0.05812	0.05971
7	80	7.5	10.67	49.00	0.05836	0.06000	0.05836	0.06000
8	100	5	20	53.75	0.05842	0.05970	0.05842	0.06546
9	120	4	30	57.75	0.05888	0.05999	0.05888	0.05999
10	140	3.125	44.80	61.53	0.05871	0.06021	0.05871	0.06021
11	180	2.5	72	67.50	0.05900	0.06003	0.05899	0.06003
12	200	2	100	70.01	0.05945	0.05987	0.05945	0.05987

Table B.2: Results of Countercurrent Flow Experiments ( Set I )

Experiment No.	$q_w^*$ (cc/hr)	$q_o^*$ (cc/hr)	$-q_w^*/q_o^*$ (-)	$S_w$ (%)	$\frac{\Delta P_w^* / L}{(\text{psi/cm})}$ Raw	$\frac{\Delta P_o^* / L}{(\text{psi/cm})}$ Raw	$\frac{\Delta P_w^* / L}{(\text{psi/cm})}$ Conditioned	$\frac{\Delta P_o^* / L}{(\text{psi/cm})}$ Conditioned
13	2	35	0.057	12.25	0.05756	0.06585	0.05620	0.06574
14	3.75	30	0.125	14.75	0.05562	0.06404	0.06162	0.06538
15	6.25	25	0.25	18.75	0.06160	0.06809	0.06356	0.06786
16	7.5	24	0.3125	20.50	0.06199	0.06996	0.06583	0.06983
17	10	20	0.5	24.10	0.05400	0.06139	0.05712	0.06049
18	16	16	1	29.50	0.05663	0.06443	0.06189	0.06459
19	24	12.5	1.920	35.03	0.05287	0.05955	0.05727	0.05961
20	30	10	3	38.25	0.05257	0.05920	0.05993	0.06203
21	40	4	5	43.02	0.05200	0.05686	0.05492	0.05681
22	50	6.25	8	47.01	0.05099	0.05564	0.05401	0.05560
23	60	5	12	50.25	0.05154	0.05586	0.05429	0.05581
24	80	3.75	21.333	56.04	0.05306	0.05749	0.05437	0.05741
25	100	3	33.333	60.51	0.05282	0.05533	0.05419	0.05542
26	120	2	60	64.52	0.052067	0.05396	0.05358	0.05462

Table B.3: Results of Cocurrent Flow Experiments ( Set II )

Experiment No.	$q_w$ (cc/hr)	$q_o$ (cc/hr)	$q_w/q_o$ (-)	$S_w$ (%)	Raw		Conditioned	
					$\Delta P_w/L$ (psi/cm)	$\Delta P_o/L$ (psi/cm)	$\Delta P_w/L$ (psi/cm)	$\Delta P_o/L$ (psi/cm)
27	7.5	40	0.1875	14.53	0.05545	0.05965	0.05543	0.05966
28	12	35	0.3429	17.25	0.05636	0.05999	0.05636	0.06000
29	20	30	0.6667	21.50	0.05830	0.06041	0.05830	0.06041
30	25	25	1.	24.25	0.05666	0.05999	0.05665	0.05999
31	30	24	1.25	26.11	0.05811	0.06002	0.05811	0.06002
32	40	20	2.	29.75	0.05862	0.05984	0.05861	0.05984
33	60	16	3.75	35.50	0.05624	0.05894	0.05624	0.05894
34	80	12.5	6.4	40.74	0.05867	0.05982	0.05866	0.05985
35	100	10	10	45.52	0.05900	0.06001	0.05900	0.06002
36	120	8	15	50.25	0.05930	0.06053	0.05930	0.06053
37	140	6.25	22.4	55.04	0.05874	0.05997	0.05873	0.05998
38	160	5	32	59.12	0.05966	0.06000	0.05966	0.06000
39	200	2.5	80	67.03	0.05933	0.05996	0.05932	0.05997

Table B.4: Results of Countercurrent Flow Experiments ( Set II )

Experiment No.	$q_w^*$ (cc/hr)	$q_o^*$ (cc/hr)	$-q_w^*/q_o^*$ (-)	$S_w$ (%)	$\frac{\Delta P_w^* / L}{(\text{psi/cm})}$ Raw	$\frac{\Delta P_o^* / L}{(\text{psi/cm})}$ Raw	$\frac{\Delta P_w^* / L}{(\text{psi/cm})}$ Conditioned	$\frac{\Delta P_o^* / L}{(\text{psi/cm})}$ Conditioned
40	2	35	0.057	11.75	0.05535	0.06611	0.05644	0.06617
41	6	30	0.2	16.03	0.05932	0.06534	0.06103	0.06627
42	12.5	24	0.521	21.74	0.06160	0.06409	0.06155	0.06531
43	20	20	1.	26.76	0.05976	0.06210	0.05974	0.06195
44	35	16	2.1875	32.75	0.06359	0.06621	0.06361	0.06602
45	50	12.5	4.	38.00	0.06396	0.06545	0.06402	0.06607
46	80	8	10	46.73	0.06437	0.06603	0.06602	0.05961
47	100	6	16.667	52.25	0.06455	0.06582	0.06608	0.06203
48	120	4	30	57.51	0.06469	0.06608	0.06467	0.06598
49	140	2.5	56	62.52	0.06481	0.06599	0.06605	0.05560

**Table B.5: Relative Permeabilities and Inlet Capillary Pressure for Cocurrent Flow (Set I)**

Experiment No.	$S_w$ (%)	$k_{rw}$ (-)	$k_{ro}$ (-)	$P_{cin}$ (psi)
1	14.25	0.0052	0.6545	0.594
2	23.75	0.0091	0.4091	0.341
3	28.00	0.107	0.3276	0.280
4	33.50	0.0161	0.2628	0.235
5	37.75	0.0214	0.2044	0.206
6	41.00	0.0272	0.1658	0.189
7	49.00	0.0437	0.1249	0.155
8	53.75	0.0544	0.0820	0.141
9	57.75	0.0658	0.0663	0.130
10	61.53	0.0753	0.0512	0.121
11	67.50	0.09 <sup>3</sup>	0.0415	0.109
12	70.01	0.1097	0.0332	0.085

**Table B.6: Relative Permeabilities and Inlet Capillary Pressure for Cocurrent Flow (Set II)**

Experiment No.	$S_w$ (%)	$k_{rw}$ (-)	$k_{ro}$ (-)	$P_{cin}$ (psi)
27	14.53	0.0046	0.6560	0.620
28	17.25	0.0070	0.5790	0.483
29	21.50	0.0113	0.2350	0.380
30	24.25	0.0146	0.4243	0.334
31	26.11	0.0170	0.3931	0.309
32	29.75	0.0228	0.3345	0.267
33	35.50	0.0336	0.2615	0.221
34	40.74	0.0448	0.2081	0.190
35	45.52	0.0555	0.1678	0.168
36	50.25	0.0665	0.1315	0.152
37	55.04	0.0776	0.1028	0.137
38	59.12	0.0872	0.0809	0.127
39	67.03	0.1100	0.0442	0.079



**Table B.7: Relative Permeabilities and Inlet Capillary Pressure for  
Countercurrent Flow (Set I)**

Experiment No.	$S_w$ (%)	$k_{rw}^*$ (-)	$k_{ro}^*$ (-)	$P_{cn}^*$ (psi)
13	12.25	0.0011	0.5226	0.954
14	14.75	0.0020	0.4500	0.522
15	18.75	0.0033	0.3701	0.431
16	20.50	0.0039	0.3570	0.400
17	24.10	0.0055	0.3009	0.337
18	29.50	0.0089	0.2400	0.269
19	35.03	0.0142	0.2048	0.234
20	38.25	0.0182	0.1493	0.210
21	43.02	0.0244	0.1275	0.189
22	47.01	0.0310	0.1103	0.160
23	50.25	0.0372	0.0879	0.151
24	56.04	0.0471	0.0584	0.138
25	60.51	0.0509	0.0492	0.124
26	64.52	0.0612	0.0301	0.104

**Table B.8: Relative Permeabilities and Inlet Capillary Pressure for  
Countercurrent Flow (Set II)**

Experiment No.	$S_w$ (%)	$k_{rw}^*$ (-)	$k_{ro}^*$ (-)	$P_{cin}^*$ (psi)
40	11.75	0.0011	0.5232	0.973
41	16.03	0.0032	0.4484	0.524
42	21.74	0.0065	0.3588	0.376
43	26.76	0.0103	0.2991	0.221
44	32.75	0.0178	0.2391	0.241
45	38.00	0.0253	0.1869	0.205
46	46.73	0.0402	0.1196	0.164
47	52.25	0.0501	0.0897	0.145
48	57.51	0.0600	0.0620	0.131
49	62.52	0.0700	0.0410	0.119

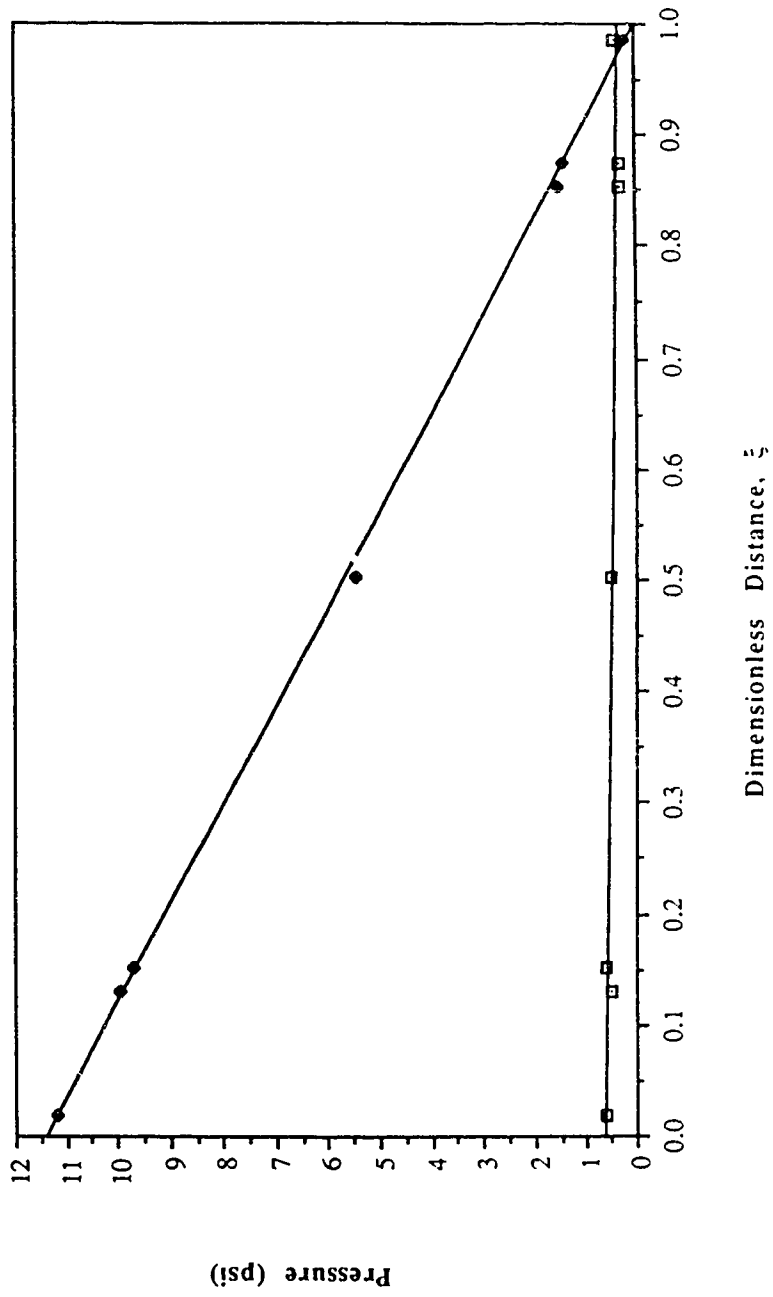


Figure B.1: Conditioned Pressure Profiles during Cocurrent Flow (Experiment No. 1)

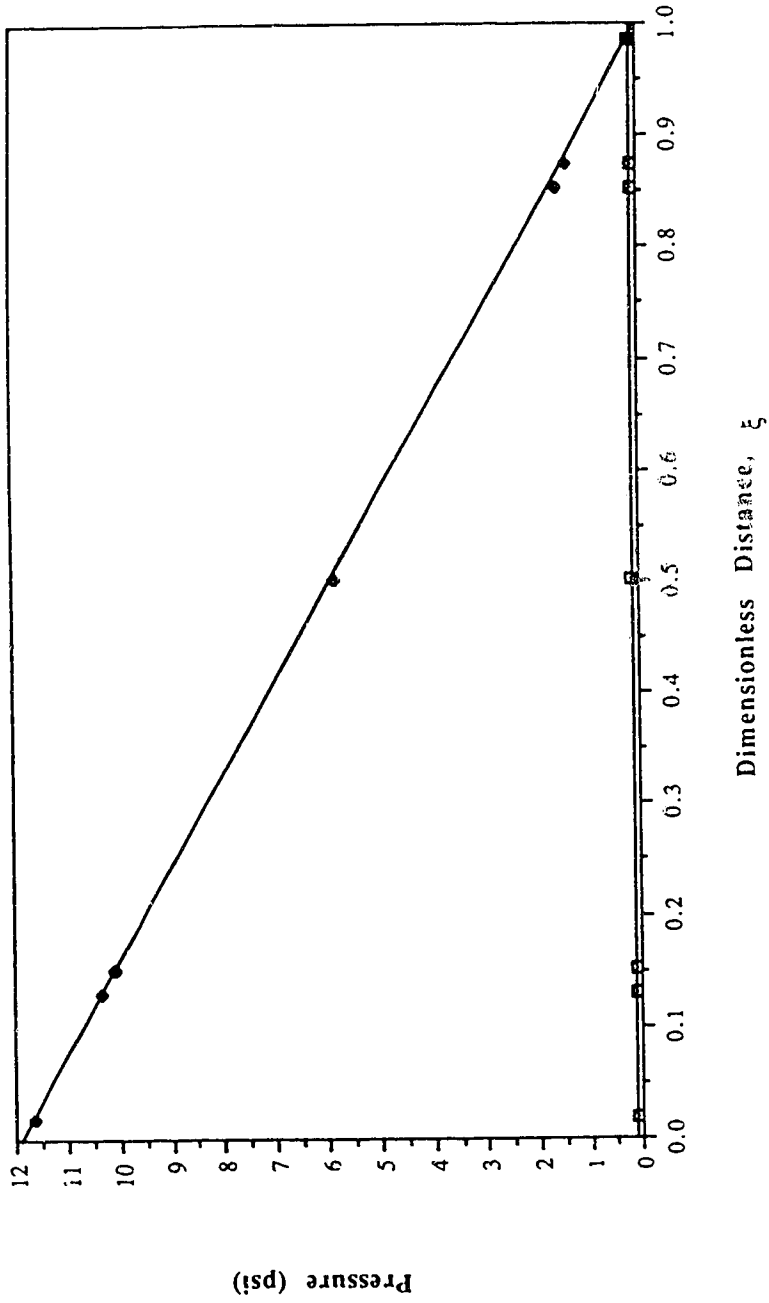


Figure B.2: Conditioned Pressure Profiles during Cocurrent Flow (Experiment No. 2)

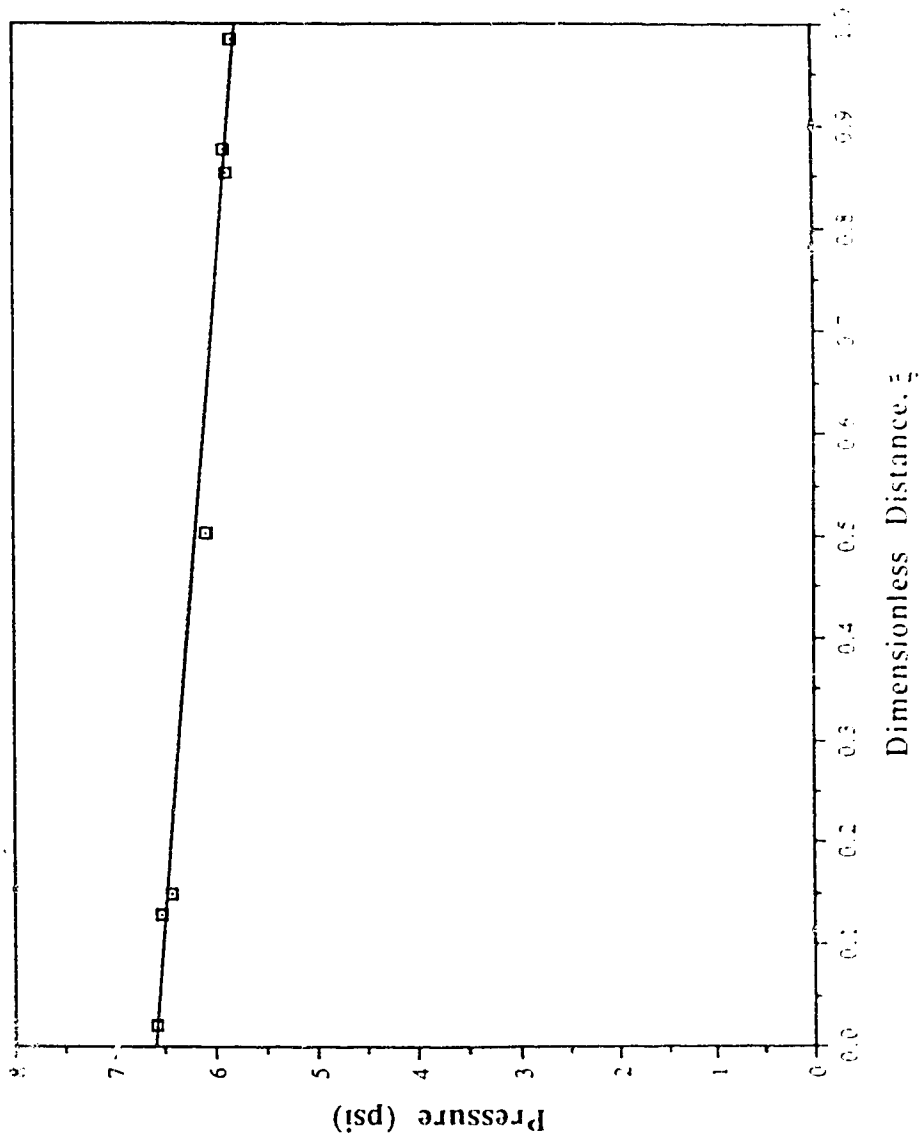


Figure B.3 : Conditioned Pressure Profile during Countercurrent Flow (Experiment No. 13)

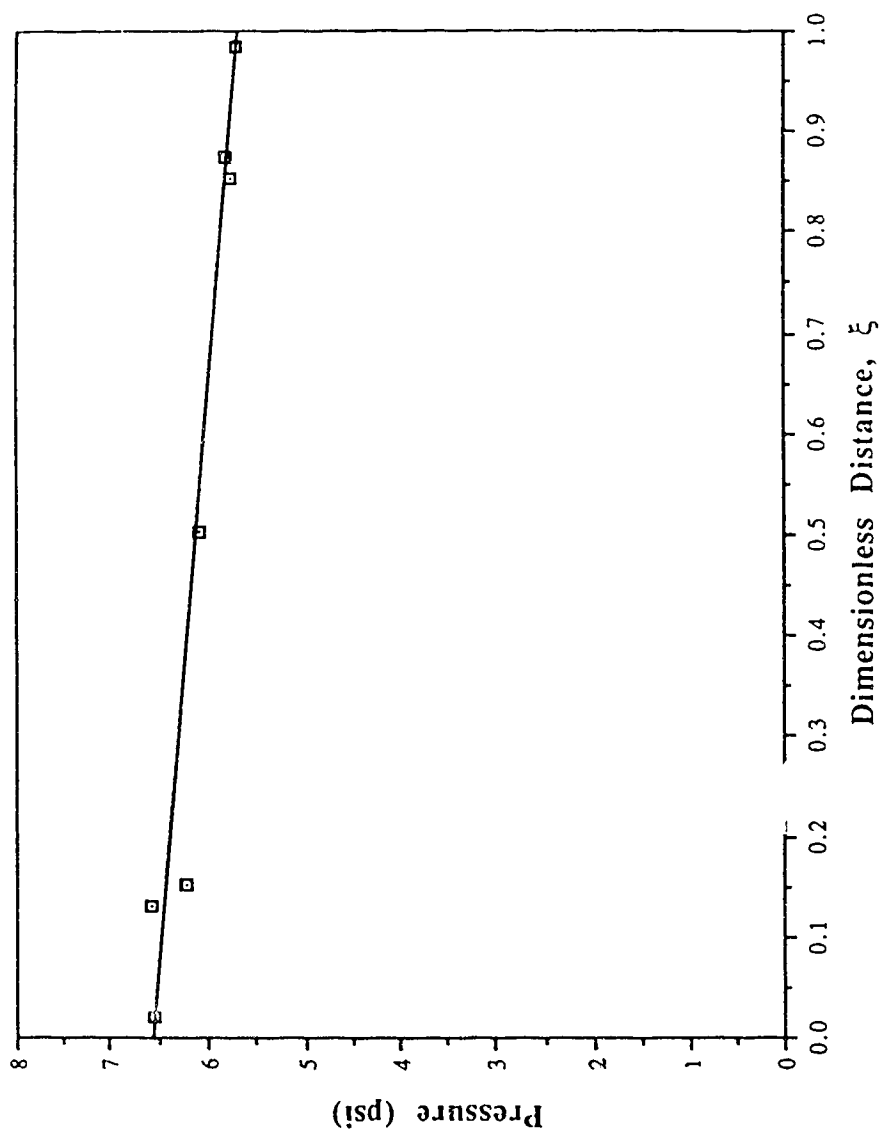


Figure B.4 : Conditioned Pressure Profile during Countercurrent Flow (Experiment No. 14)

**APPENDIX C: Typical Routines for Fitting of Experimental Data and Values of Parameters Obtained from Fitting the Data.**

**C1: Typical BMDP Routine for Fitting of Water Relative Permeability.**

```

/PROBLEM TITLE='FITTING OF REL. PERM. OF WATER'.
/INPUT FILE='DATAFILE'.
  VARIABLES=2.
  FORMAT=FREE.
/VARIABLE NAMES=SW,KW.
/REGRESS DEPENDENT=KW.
  INDEPENDENT=SW.
  PARAMETERS=3.
  ITERATIONS=25.
/PARAMETER NAMES=A1,B1,C1.
  MAX="maximum value".
  MIN="minimum value".
  INITIAL="initial value of A1","initial value of B1","initial value of C1".
/FUNCTION F=A1*(SW-SWI)+B1*((SW-SWI)**2)+C1*((SW-SWI)**3).
/PLOT VARIABLE=SW.
  RESID.
  NORM.
  DNORM.
/END

```

*Note:* SWI denotes initial water saturation. Exact numerical value of initial water saturation must be used when running the program. Moreover, exact numerical values of initial values of the different parameters, maximum, and minimum must be used.

**C2: Typical BMDP Routine for Fitting of Oil Relative Permeability.**

```

/PROBLEM TITLE='FITTING OF REL. PERM. OF OIL'.
/INPUT FILE='DATAFILE'.
  VARIABLES=2.
  FORMAT=FREE.
/VARIABLE NAMES=SW,KO.
/REGRESS DEPENDENT=KO.
  INDEPENDENT=SW.
  PARAMETERS=3.
  ITERATIONS=25.
/PARAMETER NAMES=A2,B2,C2.
  MAX="maximum".
  MIN="minimum".
  INITIAL="initial value of A2","initial value of B2","initial value of C2"..
/FUNCTION F=A2*(1-SOR-SW)+B2*((1-SOR-SW)**2)+C2*((1-SOR-SW)**3).
/PLOT VARIABLE=SW.
  RESID.
  NORM.
  DNORM.
/END

```

*Note:* Sor denotes residual oil saturation. Exact numerical value of residual oil saturation must be used when running the program. Moreover, exact numerical values of initial values of the different parameters, maximum, and minimum must be used.



**C3: Typical SPSSX Routine for Fitting of Ratio of Flow Rates.**

```

$create spss.out
$empty spss.out ok
$run *spssx sprint=spss.out
TITLE 'Fitting of Ratio of Flow Rates'.
DATA LIST FILE='DATAFILE' FREE
  /SW QR
LIST
MODEL PROGRAM
  A3="initial" B3="initial" C3="initial" A4="initial" B4="initial" C4="initial"
COMPUTE PRED=
  (A*(SW-SWI)/(1-SOR-SWI)+1-A)*MUR*(A4*(SW-SWI)+B4*((SW-SWI)**2)
  +C4*((SW-SWI)**3))/(A5*(1-SOR-SWI)+B5*((1-SOR-SWI)**2)+C5*((1-SOR-
SW)**3))
CNLR QR WITH SW
/BOUNDS
  "minimum" < A3 < "maximum";
  "minimum" < B3 < "maximum";
  "minimum" < C3 < "maximum";
  "minimum" < A4 < "maximum";
  "minimum" < B4 < "maximum";
  "minimum" < C4 < "maximum";
/SAVE PRED RESID
LIST
PLOT FORMAT=OVERLAY/PLOT=QR PRED WITH SW
PLOT FORMAT=OVERLAY/PLOT=QR WITH PRED RESID
PLOT /PLOT=RESID WITH SW

```

**Note:** SWI denotes initial water saturation, SOR denotes residual saturation and MUR denotes viscosity ratio. Exact numerical values of these variables must be used when running the program. Moreover, exact numerical values of initial values of the different parameters, maximum, and minimum must be used.

**C4: Typical SPSSX Routine for Fitting of Inlet Capillary Pressure.**

```
$create spss.out
$empty spss.out ok
$run *spssx sprint=spss.out
'TITLE 'Fitting of Inlet Capillary Pressure'.
DATA LIST FILE='DATAFILE' FREE
  /S PCIN
LIST
MODEL PROGRAM
  A5="initial" B5="initial" C5="initial" D5="initial"
COMPUTE PRED=
  (A5+B5-A5*S-B5*S**2)/(1+C5*S+D5*S**2)
CNLR PC WITH S
/BOUNDS
  "minimum" < A5 < "maximum";
  "minimum" < B5 < "maximum";
  "minimum" < C5 < "maximum";
  "minimum" < D5 < "maximum";
/SAVE PRED RESID
LIST
PLOT FORMAT=OVERLAY/PLOT=SPC WITH PRED RESID
PLOT /PLOT=RESID WITH S
```

**Table C.1: Parameters Obtained From Fitting of Water Cocurrent Relative Permeability**

Set	$a_1$	$b_1$	$c_1$	Residual Sum of Squares	Estimated Mean-Square Error
I	0.028000000	0.034253014	0.400000000	5.49203E-04	4.99276E-05
II	0.080000000	0.077959288	0.260645472	2.223161E-04	1.8526E-05

**Table C.2: Parameters Obtained From Fitting of Water Countercurrent Relative Permeability**

Set	$a_1^*$	$b_1^*$	$c_1^*$	Residual Sum of Squares	Estimated Mean-Square Error
I	0.013019531	0.103391053	0.110695138	9.89652E-06	7.61270E-07
II	0.037000000	0.159670881	0.050231717	1.03299E-05	1.14777E-06

**Table C.3: Parameters Obtained From Fitting of Oil Cocurrent Relative Permeability**

Set	$a_2$	$b_2$	$c_2$	Residual Sum of Squares	Estimated Mean-Square Error
I	0.150000000	0.010000000	1.778697581	6.23711E-03	5.67009E-05
II	0.220000000	0.010000000	1.583233445	4.22899E-03	3.52416E-04

**Table C.4: Parameters Obtained From Fitting of Oil Countercurrent Relative Permeability**

Set	$a_2^*$	$b_2^*$	$c_2^*$	Residual Sum of Squares	Estimated Mean-Square Error
I	0.120000000	0.02917365	1.20000000	2.52032E-03	1.93871E-05
II	0.116205352	0.32183123	0.78568883	1.39483E-04	1.54985E-05

**Table C.5: Parameters Obtained From Fitting of Ratio of Cocurrent Flow Rates**

Parameter	Set I	Set II
$a_3$	-0.179921235	0.004262611
$b_3$	1.144813793	0.193301170
$c_3$	-2.46261280	-0.355556636
$a_4$	-0.95184440	-0.047263499
$b_4$	3.210830121	0.316779037
$c_4$	-4.269238637	0.316779037
Residual Sum of Squares	0.2216713	0.1035900
Estimated Mean-Square Error	0.0316673	0.0129500

**Table C.6: Parameters Obtained From Fitting of Ratio of Countercurrent Flow Rates**

Parameters	Set I	Set II
$a_3^*$	0.119145376	-0.014599715
$b_3^*$	-2.180098123	-2.309927896
$c_3^*$	3.73408938	2.652774308
$a_4^*$	-0.279234097	-0.351519141
$b_4^*$	-0.483060017	4.99990071
$c_4^*$	8.884278267	0.789242842
Residual Sum of Squares	0.48310	0.11201
Estimated Mean-Square Error	0.05368	0.02240

**Table C.7: Parameters Obtained From Fitting Cocurrent Ratio of Pressure Gradients**

Set	a	Residual Sum of Squares	Estimated Mean-Square Error
I	0.056074054	9.65686E-03	8.77897E-04
II	0.054390898	1.78727E-03	1.48939E-04

**Table C.8: Parameters Obtained From Fitting Countercurrent Ratio of Pressure Gradients**

Set	a*	Residual Sum of Squares	Estimated Mean-Square Error
I	-0.07928671	6.57327E-03	5.05636E-04
II	-0.04678441	7.66600E-02	8.51736E-03

**Table C.9: Parameters Obtained From Fitting Inlet Capillary Pressure**

Set	$a_s$	$b_s$	$c_s$	$d_s$	Residual Sum of Squares	Estimated Mean- Square Error
I	-53.83612	63.87292	313.53826	-169.635	6.19632E-03	2.81651E-04
II	-5.216245	7.296876	43.077211	-24.1575	1.19575E-03	6.29342E-05